Development of tools to investigate resistance of HCV genotype 3 to NS5A inhibitors

Lorna Jane Kelly

Submitted in accordance with the requirements for the degree of Doctor of Philosophy

The University of Leeds

Faculty of Biological Sciences

School of Molecular and Cellular Biology

July 2017

The candidate confirms that the work submitted is her own, except where work which has formed part of jointly-authored publications has been included. The contribution of the candidate and the other authors to this work has been explicitly indicated below. The candidate confirms that appropriate credit has been given within the thesis where reference has been made to the work of others.

The chapter within this thesis that has been based on work from jointly-authored publication is chapter 3:

Manipulation of both virus- and cell-specific factors are required for robust transient replication of a hepatitis C virus genotype 3a sub-genomic replicon. Lorna Kelly, Anjna Badhan, Jean Lutamyo Mbisa and Mark Harris. Journal of General Virology, 2017 (In revision)

- Lorna Kelly performed all experiments with the except of the next-generation sequencing which was performed by Anjna Badhan.
- Claire Courtney under the supervision of Stephen Griffin (acknowledged in the publication) produced the Huh7.5 cells expressing PIV5 V protein.
- Jean Lutamyo Mbisa and Mark Harris co-authored the publication.

Acknowledgements

I'm incredibly grateful to my supervisor, Mark Harris, for his guidance, support and patience. Thank you so much for giving me the chance. I'm also grateful to my secondary supervisor, Tamyo, for his invaluable input on all aspects of my work.

Thank you to all those who have helped with the direction of the project with big ideas and small suggestions, especially Ste**ph**en Griffin, Nicola Stonehouse, David Rowlands and Hazel Stewart. Thank you so much to Jack Silberrad for his enthusiasm, and for his help.

To everyone inside and outside virology 8.61 who has offered support, technical help and encouragement. You know who you are but a special mention to Carsten Zothner, Nnenna Nwogu, Rachel Dods, Vikki Easton, Patrick Knight and Michael Day. Thanks especially to Eleni-Anna Loundras for keeping me sane.

An especial thank you to Doug Ross-Thriepland, for his attentive help during the first few months, when I know for a fact that there were a million other things he should've (and would rather have) been doing.

To John McLaughlan and the HCVRUK board, and PHE, for funding: There are no words to describe the difference that extra six months made. Without that I'm not entirely sure there would've been a thesis at all!

And last, but certainly not least, to my parents and Suzanne – the unshakeable, formidable Team Kelly. Thank you for keeping me going at every stage and for rallying round when I needed it most. And especially to my amazing, wonderful Nick. With you by my side I can do anything. Thank you for everything.

Abstract

HCV infection leads to liver failure. Genotype 3 (GT3) is known to respond poorly to newly-developed direct-acting antivirals, especially inhibitors of the multifunctional NS5A protein.

This work reports the establishment of efficient transient replication of the S52 GT3 sub-genomic replicon (SGR) by further culture adaptation of S52 in the context of an optimised luciferase reporter. Also documented is the development of hepatoma cells with immune-attenuating modifications and expressing the lipid binding factor hSEC14L2 to support transient replication of S52. In parallel, stable replication of S52 in SGR-harbouring cells was used to investigate the differences between early and established replication.

Differences in sensitivity to the NS5A inhibitor Daclatasvir (DCV) in both transient and stable S52 were observed compared to other genotypes, and between transient and stable replication. In addition, it is shown here that the resistance-associated substitution (RAS) Y93H conferred a significant fitness cost which is not apparent for stable S52 selected with DCV, despite this RAS being detected. This thesis explores the molecular basis of such an observation and highlights a potential mechanism which warrants further research.

The role of RAS in the development of resistance is still unclear though this work reports that the presence of a RAS within a mixed population greatly influenced the development of resistance to DCV *in vitro*.

Moreover, this work identified that a cellular metabolism-regulating factor, AMP-mediated protein kinase (AMPK), may be differentially regulated during GT3 infection compared to other GTs. This thesis presents the hypothesis that AMPK regulation by HCV may contribute to hepatic steatosis as a direct consequence of viral infection, which is unique to GT3.

More insight into the propensity of GT3 to develop resistance can aid further antiviral design, and an understanding of the molecular basis of steatosis offers a rationale for treating the symptoms of HCV in addition to direct targeting of the virus.

Table of contents

Table of figures

Table of tables

Abbreviations

A	Alanine
A	Adenine
ACC	Acetyl CoA carboxylase
AMPK	AMP-mediated protein kinase
BCA	Bioinchionic acid assay
BMI	Body mass index
BODIPY	Boron dipyrrhomethene
C	Cysteine
C	Cytosine
CAS	Culture-adaptive substitution
CC_{50}	50% cytotoxic concentration
CD81	Cluster of differentiation 81
D	Aspartic acid
DAA	Direct-acting antiviral
DAPI	4',6-diamidino-2-phenylindole
DAS	Dasabuvir
DCV	Daclatasvir
DEPC	Diethyl pyrocarbonate
DMEM	Dulbecco-modified Eagle's medium
DMSO	Dimethyl sulphoxide
DNA	Deoxyribonucleic acid
E	Glutamic acid
EAP	Early Access Program

EC_{50}	50% effective concentration
EGFR	Epithelial growth factor receptor
eIF4	Eukaryotic initiation factor 4
EMCV	Encephalomyocarditis virus
EqHV	Equine Hepacivirus
ER	Endoplasmic reticulum
ERK	Extracellular signal-related kinase
EVR	Early virological response
F	Phenylalanine
FAS	Fatty acid synthase
FBS	Foetal bovine serum
FDA	Food and Drug Administration
FFU	Focus-forming units
FMDV	Foot and mouth disease virus
G	Guanine
GAPDH	Glyceraldehyde phosphate dehydrogenase
GLB	Glasgow lysis buffer
GT	Genotype
h	Hours
H	Histidine
HAV	Hepatitis A virus
HBV	Hepatitis B virus
HCC	Hepatocellular carcinoma
HCV	Hepatitis C virus
HCVRUK	HCV Research UK

HEPES	4-(2-Hydroxyethyl)piperazine-1-ethanesulfonic acid
HIV	Human Immunodeficiency virus
HRQL	Health-related quality of life
I	Isoleucine
IDU	Intravenous drug user
IFNα	Interferon alpha
IFN-λ3	Interferon lambda-3
IRES	Internal ribosome entry site
IRRDR	Interferon/Ribavirin resistance determining region
ISDR	Interferon sensitivity determining region
ISG	Interferon-stimulated genes
K	Lysine
kDa	kilodaltons
LB	Lysogeny broth
LC3BII	lipidated microtubule associated protein 1 light chain 3 β-I
LCS	Low-complexity sequence
LD	lipid droplet
LDLr	Low-density lipoprotein receptor
LDV	Ledipasvir
LXRα	Liver X receptor alpha
M	Methionine
MAPK	Mitogen-activated protein kinase
miRNA	Micro-RNA
MLK3	Mixed-lineage protein kinase 3
MOI	Multiplicity of infection

MOPS	Morpholinepropanesulfonic acid
MTT	3-(4,5-dimethylthiazol-2-yl)-2,5-diphenyltetrazolium bromide
MW	Molecular weight
MWM	Molecular weight marker
N	Asparagine
NANBH	Non-A, non-B hepatitis
NASH	Non-alcoholic steatohepatitis
NGS	Next-generation sequencing
NHS	National Health Service
Nluc	Nanoluciferase
non-nuc	Non-nucleotidic
NPT	Neomycin phosphotransferase
NS	Non-structural protein
NS5A	Non-structural protein 5A
NS5B	Non-structural protein 5B
NTC	No template control
nuc	Nucleotidic
OLT	Orthotic liver transplant
ORF	Open reading frame
P	Proline
PBS	Phosphate-buffered saline
PCR	Polymerase chain reaction
PFA	Paraformaldehyde
PHH	Primary human hepatocytes
PI3K	Phosphotidylinositol-3-kinase

PI4KIIIα	Phosphotidylinositol-4-kinase type 3 alpha
PI4P	Phosphotidylinositol-4-phosphate
PIV-5	Parainfluenza virus 5
PKB	Protein kinase B (Akt)
PLB	Passive lysis buffer
PPARγ	Peroxisome proliferator-activated receptor gamma
Q	Glutamine
qRT-PCR	quantitative real-time PCR
R	Arginine
RAS	Resistance-associated substitution
RBV	Ribavirin
RdRP	RNA-dependent RNA polymerase
RIG-I	Retinoic acid-inducible gene I
RLU	Relative light units
RNA	Ribonucleic acid
ROS	Reactive oxygen species
RVR	rapid virological response
S	Serine
SAR	Structure-activity relationship
SCID	Severe combined immunodeficient
SDM	Site-directed mutagenesis
SDS-PAGE	Sodium dodecyl sulphate-polyacrylamide gel electrophoresis
SGR	Sub-genomic replicon
SNP	Single nucleotide polymorphism
SOF	Sofosbuvir

SP	Signal peptidase
SPP	Signal peptidase peptidase
SR-BI	Scavenger receptor class B member 1
SREBP	Sterol regulatory element binding protein
SVR	Sustained virological response
T	Threonine
T	Thymine
TAP1	Tocopherol activated protein 1
TBS	Tris-buffered saline
TGFα	Transforming growth factor alpha
U	Uracil
UTR	Untranslated region
V	Valine
VEL	Velpatasvir
VLDL	Very low-density lipoprotein
vRNA	virus RNA
Y	Tyrosine
YB1	Yellow box 1

Chapter 1: General Introduction

1.1 Hepatitis C virus

During the 1970s the term non-A, non-B hepatitis (NANBH) was used to describe the transfusion-associated disease of patients which was not attributable to hepatitis A or B viruses (HAV, HBV). 50% of patients who were infected went on to develop chronic hepatitis with virus antigen detectable in their sera (Vitvitski et al., 1979; Seeff, 2009). Using an antibody capture approach the causative agent was identified and named hepatitis C virus (HCV) (Choo et al., 1990). HCV is the type member of the hepacivirus genus, one of three genera within the Flaviviridae (Smith et al., 2014). The classification of the hepacivirus genus has recently been updated, and includes viruses with non-human tropism such as Equine Hepacivirus (EqHV) and the primate virus GBV-B. The Flaviviridae contains related Pegiviruses as well as the Flavivirus genus, which includes a number of important arthropod-borne human pathogens such as Dengue, West Nile virus, Tick-borne encephalitis virus and the recently re-emerged Zika virus which is the subject of considerable research, reviewed recently (Wang et al., 2017).

HCV infects an estimated 170 million individuals worldwide and is distributed globally, affecting between 0.9 and 14.7% of the population in different countries worldwide, depending on region. The average global seroprevalence is 2.5% (Petruzziello et al., 2016).

1.1.1 HCV genotypes

The Nonstructural protein 5B (NS5B) RNA-dependent RNA polymerase of HCV is highly error-prone, making an error in each cycle of genome replication (Martell et al., 1992; Powdrill et al., 2011). As a result of this the genetic diversity of HCV is extremely high and the virus exists as a quasispecies within the infected individual. As a result of this diversity, seven genotypes and over 65 subtypes have diverged, each with a different geographical distribution (Messina et al., 2015). The most prevalent worldwide is genotype 1 (GT1), responsible for 49% of HCV infections worldwide. The graphic in Figure 1-1 shows the distribution of each genotype in distinct geographical locations. Genotype 2 (GT2) is primarily distributed in Asia, genotype 5 (GT5) is most prevalent in sub-Saharan Africa and genotype 4 (GT4) in northern Africa and the Middle East. Indeed, approximately 15% of the Egyptian population are infected with HCV GT4 after a treatment program for schistosomiasis involving tartar emetic injections from the 1950s to 1980s, in which needles were not properly sterilised (Elgharably et al., 2017).

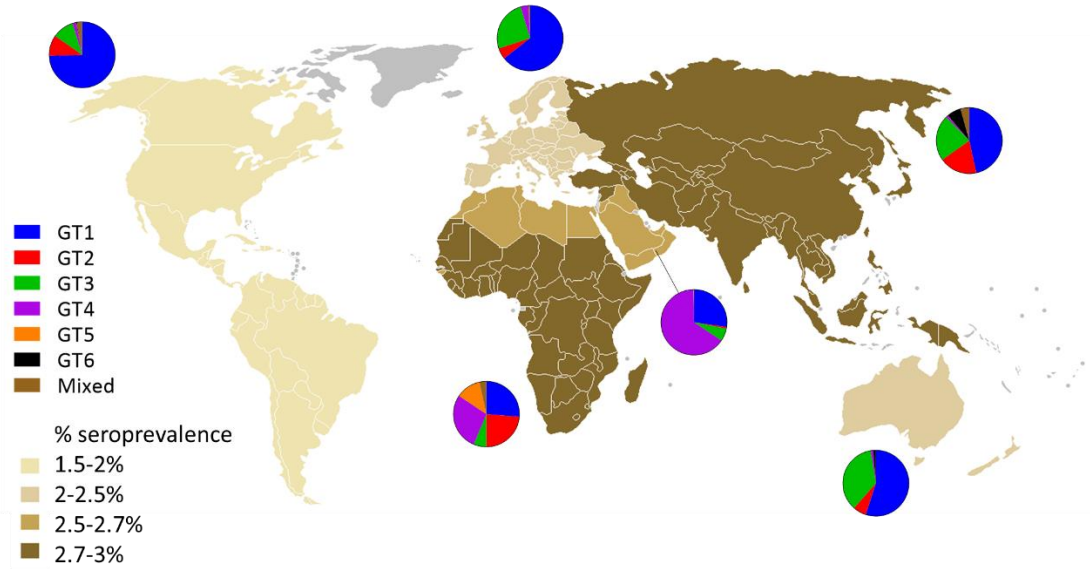

Figure 1-1. Worldwide geographical distribution of HCV genotypes. Graphic made using data from (Petruzziello et al., 2016) and creative commons image.

1.1.1.1 Genotype 3

Genotype 3 (GT3) is increasing in prevalence in the UK and northern Europe and is currently the second most prevalent genotype worldwide. GT3 is estimated to have diverged as a genotype around 460 years ago and a GT3a common ancestor is dated around 78 years (Chunhua Li et al., 2014). It is responsible for approximately 80% of cases in the Middle East, India, Syria and Pakistan, and is thought to be increasing in worldwide prevalence due to high levels of migration from these regions. Accordingly, GT3 was estimated, using Bayesian evolutionary reconstruction, to have originated in the Indian subcontinent (Choudhary et al., 2014).

However, a different study concluded that the increase in GT3 may not be wholly due to recent immigration increases. A greater consensus is that genotype divergence occurred prior to the African slave trade establishment and that spread of GT3 occurred during this period (May et al., 2015).

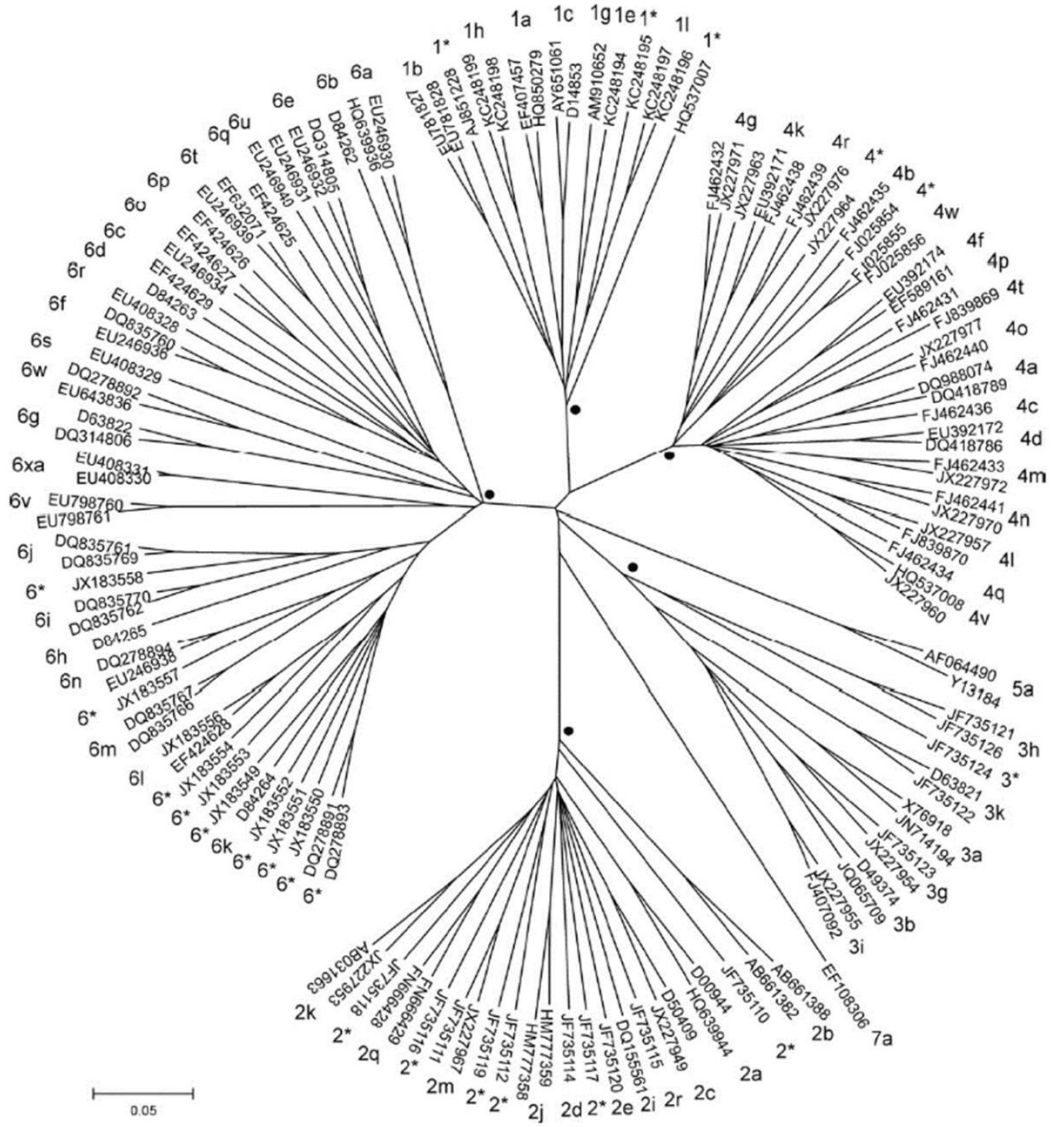

Figure 1-2. Phylogenetic analysis of HCV genotypes and subtypes from 129 complete genome sequences. Image from (Smith et al., 2014)

A great number of clinical studies have used histopathological techniques to document an increased prevalence of hepatic steatosis in patients with GT3. HCV infection is not normally a causative agent of hepatic steatosis in the absence of other contributing factors such as alcohol abuse and high Body Mass Index (BMI) (Rubbia-Brandt et al., 2004). However, infection with GT3 is commonly associated with hepatic steatosis in the absence of these major risk factors. Severity of hepatic steatosis in GT3 patients correlates with viral load and is reversed by successful treatment of the virus (Mihm et al., 1997; Rubbia-Brandt et al., 2000; Nkontchou et al., 2011). Work to identify a molecular mechanism for this difference is not

extensive, and some minor differences in lipid metabolism and phospholipid signalling have been identified which likely combine to produce the hepatic steatosis observed, though these may be complemented by an as yet un-identified additional mechanism. These are discussed in more detail in chapter 5.

1.1.2 Transmission routes

Transmission of HCV is largely lateral. Historically, before the identification of the infectious agent (as well as the HIV epidemic in the 1980s) led to screening of blood products, infections were transfusion-associated. A cohort of Irish women who were exposed to GT1b from infusion of contaminated anti-D immunoglobulin identified during a voluntary screening program in 1994 have shown fascinating differences in pathology, thought to be due to the young age of infection, which have provided an opportunity to study novel aspects of viral pathology (Fanning, 2002). In addition, improper sterilisation of equipment during vaccinations has contributed to spread of HCV (Gürtler and Eberle, 2017). Modern HCV infections are occasionally associated with contaminated blood products, tattoos and intravenous drug use (IDU) (Pybus et al., 2005; Magiorkinis et al., 2009; Mokhtari et al., 2017). IDU is the main transmission route of GT3 (Pawlotsky et al., 1995).

Vertical transmission of mother to child (MTCT) is rare, accounting for 5% of cases, with a higher risk for the infants of HIV-positive mothers. Suppression of the HIV viral load reduces the risk of MTCT (Tovo et al., 2016). Sexual transmission is also rare, but is of concern as transmission rates are higher amongst HIV-positive men who have sex with men (MSM), reviewed by (Chan et al., 2016). A study found that HCV prevalence in MSM who are beginning pre-exposure prophylaxis (PrEP) for HIV is higher than previously reported, and suggests that this may lead to an increase in transmission between MSM (Hoornenborg et al., 2017).

1.1.3 Disease progression

Infection with HCV is frequently chronic, with only 20% of those exposed to the virus estimated to spontaneously clear, by an unknown mechanism thought to be related to host factors (Gauthiez et al., 2017). Disease progression rates were reviewed recently (Thrift et al., 2017) and the reported values are summarised in Figure 1-3.

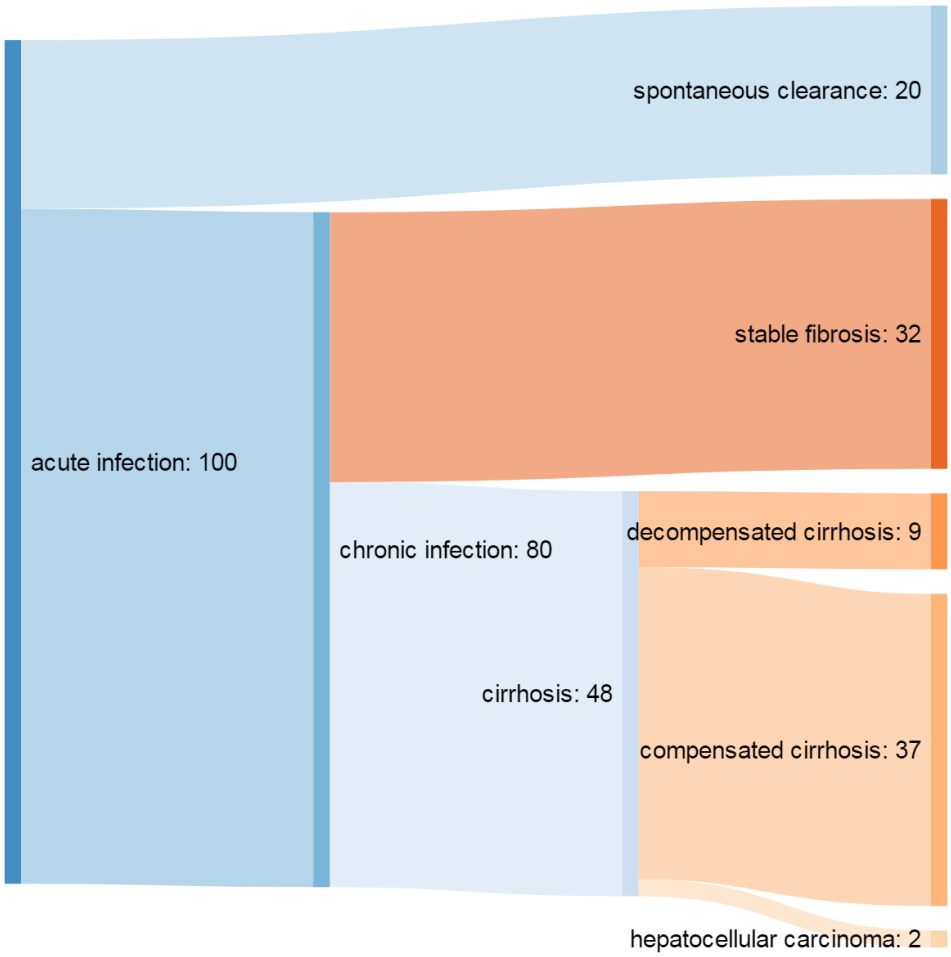

Figure 1-3. Disease progression rates after infection with HCV. Sankey diagram generated using Sankeymatic Beta (sankeymatic.com) and using data from (Thrift et al., 2017)

Of the 80% of infected individuals who develop chronic hepatitis, progressive fibrosis and cirrhosis is the most common cause of death with a survival after 35 years of 84%, compared to 91-95% for the uninfected population. Hepatocellular carcinoma is the third leading cause of cancer related death worldwide, and occurs at a rate of 1-3% amongst the HCV-infected population; HCV infection increases the risk of HCC 10-fold above the uninfected population. The annual rate of HCC amongst patients with cirrhosis rises to 8% (Thrift et al., 2017)

The classic hypothesis of HCV-induced HCC states that HCV infection causes inflammation of the liver and tissue damage, leading to fibrosis and, ultimately, cirrhosis. Over time this tissue is regenerated and transformations of progenitor cells during this process lead to malignancy and HCC (Okada et al., 1997; Chen et al., 2014; Pezzuto et al., 2016). This was recently reviewed (Takeda et al., 2017). Indeed, treatment with direct-acting antivirals (DAAs)

(summarised in section 1.3.2) does not reduce the risk of HCC (Reig et al., 2016; Strazzulla et al., 2016; Conti et al., 2016; Thrift et al., 2017).

However, there is a growing body of evidence that the virus causes direct transformation events, including the upregulation of NANOG by core, enhancing cell growth and cell cycle progression (Zhou et al., 2014); upregulation of OCT4 by core, resulting in increased proliferation (Zhou et al., 2016); NS4B interaction with Scribble, a tumour suppressor, inducing its degradation (Hu et al., 2016); and induction of TLR4 by NS5A, resulting in upregulation of NANOG (Machida et al., 2009).

Non-hepatic manifestation of HCV disease is usually linked to the propensity of the virus to modulate host cell lipids during the course of infection. Insulin resistance is common (Caronia et al., 1999; Gastaldi et al., 2017), mediated by HCV infection and may be a direct effect of core upregulating SOCS-3 which causes proteosomal degradation of two proteins involved in the insulin response, IRS1 and IRS2. Alternatively, an indirect pathway has been proposed, involving reactive oxygen species (ROS) generated by HCV infection triggering the NFκB response. These have been reviewed by (Douglas and George, 2009; Abenavoli et al., 2014). There is also evidence to support an association with carotid atherosclerosis (Ishizaka et al., 2002; Petta, 2017) due to immune reaction to the circulation of the virus in serum complexed with very low-density lipoproteins (VLDLs), lipid and protein complexes which accumulate to cause blockages of blood vessels. Like other aspects of HCV disease this is likely to persist in some form after treatment (Bassendine et al., 2017).

HCV infection has also been linked to systemic health problems which are collectively known as CHASM (C Hepatitis Associated Systemic Manifestations) and include diseases of the thyroid, eye, kidney, skin and immune system (such as cryoglobulinaemia and lymphoma), which are reviewed by (Sherman and Sherman, 2015).

1.1.4 Molecular biology and replication

The full life cycle of HCV is not fully defined, though substantial work has implicated host lipids and lipoproteins in multiple stages of the replication cycle, discussed in **Chapter 5:** and reviewed by (Alvisi et al., 2011; Popescu et al., 2014; Grassi et al., 2016).

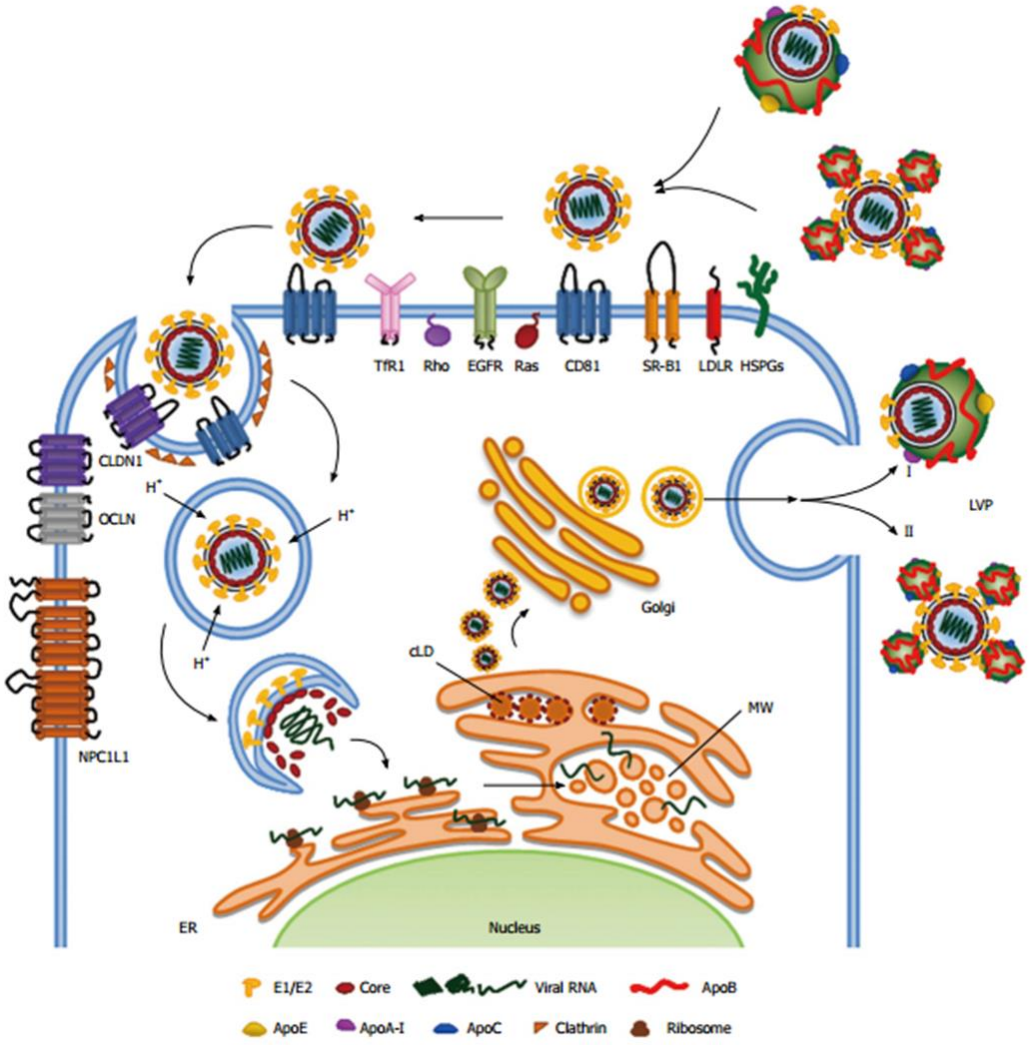

Figure 1-4. The HCV replication cycle, taken from (Grassi et al., 2016)

The HCV particle circulates in the blood of the infected individual complexed with lipoproteins, cholesterol and triglycerides as a virolipoprotein, closely resembling a VLDL (Falcón et al., 2017). The virus particle is approximately 40-70 nm in diameter and exists as a mixture of infectious and non-infectious particles (Zhong et al., 2005; Gastaminza et al., 2010); infectivity correlates negatively with buoyant density with the most infectious particles having a very low buoyant density of 1.03-1.2 g/cm^3. The complex with lipoproteins and lipids is thought to contribute to immune evasion by shielding neutralising epitopes on E1 and E2 glycoproteins (Vercauteren et al., 2014b). HCV is hepatotropic, as evidenced by its reliance upon the hepatocyte-specific miRNA-122 for replication (Jopling et al., 2005; Wilson and Huys, 2013), and utilisation of hepatocyte-specific entry factors for its ability to gain access to the cell. A great number of cell surface markers have been implicated as entry factors including CD81,

Occludin, Claudin, SR-BI, EGFR and the low-density lipoprotein receptor (LDLr) (Lindenbach and Rice, 2013; Ding et al., 2011). Binding of these to HCV triggers activation of Ras and Rho GTPase pathways which results in movement of the CD81-HCV complex towards the tight junctions for interaction with Claudin, followed by clathrin-mediated endocytosis and endosomal fusion (Brazzoli et al., 2008; Lupberger et al., 2011; Farquhar et al., 2012; Zona et al., 2013).

The 9.6kb single-stranded, positive-sense RNA genome is released into the cytoplasm where it undergoes direct translation on the ribosome as a single open reading frame (ORF) (Hijikata et al., 1991). The coding region of the virus genome is flanked by untranslated regions (UTRs); both are highly structured and the 5' UTR has been shown to have internal ribosome entry site (IRES) activity (Tsukiyama-Kohara et al., 1992; Tanaka et al., 1995; Tanaka et al., 1996; Kolykhalov et al., 1996; Hwang et al., 1998; Tang et al., 1999). RNA structures in the IRES are crucial for binding to eIF protein complexes and the ribosome, initiating translation (Lukavsky, 2009). The genome is translated as a single polyprotein which is post-translationally cleaved by host and viral proteases to liberate the 3 structural and 7 non-structural proteins: the functions of these will be discussed in greater detail in sections 1.1.4.2.1 and 1.1.4.2.2 (Bartenschlager et al., 1995; Shimotohno et al., 1995; Agapov et al., 1999). The 3 structural proteins – core, E1 and E2 – are translocated to sites of assembly and 5 of the 7 nonstructural proteins – NS3, NS4A, NS4B, NS5A and NS5B – assemble into the replication complex to replicate the viral RNA. The remaining proteins – p7 and NS2 – have roles in the organisation of assembly (Jones et al., 2007; Steinmann et al., 2007; Ma et al., 2011).

Replication of the genome occurs upon lipid-enriched membranes in a complex structure of single-, double- and multi-membrane vesicles derived from the ER and mitochondria. These are induced by the NS3-5B non-structural proteins but primarily by NS4B and NS5A; this structure is termed the membranous web (Egger et al., 2002; Romero-Brey et al., 2012). Sites of replication and assembly are separated and translocation between the two is likely controlled by NS5A, which shuttles around the cytoplasm using the trans-Golgi network and microtubules to deliver the newly-synthesised positive-sense genomes to lipid droplets, where core accumulates (Eyre et al., 2014). Assembly is triggered by the displacement of ADRP by core, leading to its degradation and, subsequently, trafficking of cellular components to aid the recruitment of other viral and cellular components, including E1 and E2 to ER membranes through which nascent particles bud (Boulant et al., 2008; Eggert et al., 2014; Syed et al.,

2017). Particles exit via the secretory pathway in a process which is highly dependent on the VLDL/LDL transport pathway (Benedicto et al., 2015; Takacs et al., 2017; Syed et al., 2017).

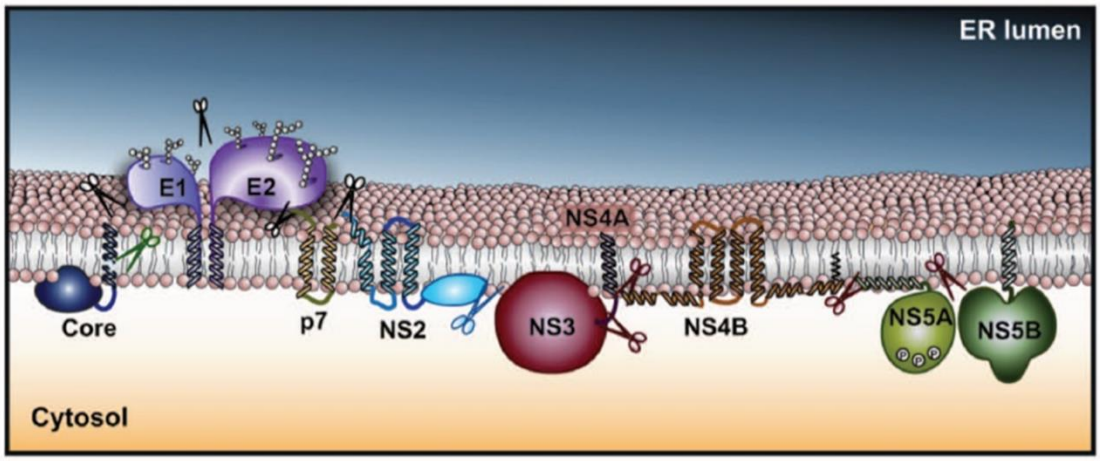

Figure 1-5. The replication complex, taken from (Alvisi et al., 2011). The HCV structural and non-structural proteins are indicated in genome order, with scissors indicating cleavage sites (black and green represent SP and SPP respectively, blue represents NS2 protease, red indicates NS3 protease). Glycosylation sites in E1 and E2 are shown as sugar chain symbols. NS5A is shown with P symbols representing phosphorylation

1.1.4.1 Relationship with host lipids

HCV replication is closely linked to cellular lipids and lipid membranes at every stage of the replication cycle (Alvisi et al., 2011). Proteomic analyses have shown that HCV causes differential expression of lipid metabolism and distribution-associated genes, favouring energy conservation, and the cell is reprogrammed to favour the pathways required for the virus life cycle such as glycolysis as a means of energy production (Diamond et al., 2010). The virus particle resembles a VLDL (Merz et al., 2011) and uses VLDL receptors and Apolipoproteins as well as a number of other surface receptors to gain entry into the cell (Agnello et al., 1999). The membranous web, at which RNA genome replication occurs, is enriched with cellular lipids and lipoproteins (Egger et al., 2002), as outlined in section 1.1.4.2.2. HCV infection has been shown to activate the autophagy response whilst inhibiting maturation of autophagic vesicles into autolysosomes where the cargo is degraded, potentially to increase the number of double-membrane vesicles as sites of replication (Linya Wang et al., 2015). Genomes are directed to the surfaces of lipid droplets where they associate with core (Barba et al., 1997), which is sufficient to cause lipid accumulation *in vitro* (Abid et al., 2005); virion assembly takes

place at lipid-enriched membranes containing Apolipoproteins as well as the envelope proteins E1 and E2; and trafficking to the cell surface utilises the VLDL pathway (Appel et al., 2008; Merz et al., 2011). Interestingly, these processes are not likely to cause non-alcoholic steatohepatitis (NASH) in the absence of high BMI and other risk factors in HCV GT1 infections (Rogers et al., 1992; Rubbia-Brandt et al., 2000).

1.1.4.2 Encoded proteins

1.1.4.2.1 Structural proteins

The core protein is a 177-amino acid nucleocapsid protein with a primary role in forming a complex with the viral RNA for packaging into the virus particle. It is released from the polyprotein by signal peptidase (SP) and matured by SP peptidase (SPP). The structure is not known but it has a positively-charged N-terminal domain and a hydrophobic C-terminal domain for membrane anchorage (Santolini et al., 1994). Core has been shown to bind to 5' RNA fragments *in vitro*, suppressing translation (Shimoike et al., 1999; Tanaka et al., 2000). It is for this purpose that the processes of RNA replication and virus assembly should be separated in the cell, and the former compartmentalised in membrane structures. In addition, core was shown to recognise RNA stem loop structures throughout the genome which are suggested to be packaging signals to selectively package virus RNA (Stewart et al., 2016), though core is also capable of binding non-specifically to ribosomal RNA (Santolini et al., 1994).

Core also has well documented roles in immune modulation and oncogenesis. Examples of the former include attenuation of JAK/STAT signalling and blocking ISG induction by IFN treatment (de Lucas et al., 2005). The role of core protein in oncogenesis is reviewed (Koike, 2007). It has been shown to modulate the MAPK and AP1 pathways which are involved in cell cycle control (Tsutsumi et al., 2003; Katsarou et al., 2010); and to activate NFκB and TGFα leading to increased proliferation (Sato et al., 2006). Although, interestingly, core was also shown to activate p53 to suppress cell growth (Lu et al., 1999). In a parallel mechanism, it has been shown to induce oxidative stress leading to the activation of the antioxidant response element by NRF2 (Ivanov et al., 2011; Smirnova et al., 2016) and inducing inflammation (Pal et al., 2010), though core is also capable of blocking apoptosis caused by this same pathway (Seo et al., 2015). This inflammation and resulting tissue damage is considered to lead to development of HCC when substitutions in key oncogenes are accumulated during accelerated tissue regeneration. Core protein is widely implicated in pathogenesis due to its ability to cause lipid accumulation in the absence of other HCV proteins and to perturb insulin pathways and cause insulin sensitivity in transgenic mice (Hui-Chun Li et al., 2014).

E1 and E2 are envelope glycoproteins with a pivotal role in cell entry; both are necessary to mediate cell entry. Their structure and function were reviewed by (Tarr et al., 2015). E2 binds to CD81 and SR-BI and both have fusion peptides, mediating the release of viral RNA into the cytoplasm to initiate translation (Pileri et al., 1998; Scarselli et al., 2002; Drummer et al., 2007; Li et al., 2009). The receptor binding regions are highly conserved yet structure analysis has demonstrated that the CD81 binding face of E2 is conformationally flexible (Meola et al., 2015). Broadly-neutralising antibodies to E2 usually target the hypervariable regions which explains the difficulty in achieving an effective humoral immune response (Farci et al., 1996). Little is known about E1 due to the difficulty in expressing this protein in isolation, but both are known to be required for cell entry (Bartosch et al., 2003; Hsu et al., 2003).

1.1.4.2.2 Nonstructural proteins

The p7 protein (Madan and Bartenschlager, 2015) is a 63-amino acid protein with two transmembrane spanning regions which localises to and forms an ion channel in ER and mitochondrial membranes as a multimeric structure (Carrère-Kremer et al., 2002; Griffin et al., 2003; Clarke et al., 2006; Haqshenas et al., 2007; Wozniak et al., 2010; Foster et al., 2014). Its function is hypothesised to be the increase in pH of acidic membrane compartments (Steinmann et al., 2007; Bentham et al., 2013), contributing to viral maturation and egress in a mechanism which is not fully understood, but is suggested to involve the prevention of premature fusion of membranes by the E1 and E2 glycoproteins in acidic conditions (Wozniak et al., 2010). P7 has an additional role in virus entry, functioning as a signal peptide for endocytic fusion (Griffin et al., 2005) and assembly by functioning as a signal peptide to recruit NS2 (Boson et al., 2011; Tedbury et al., 2011).

NS2 has a cysteine protease function to release itself from NS3 and the remainder of the polyprotein (Hijikata et al., 1993; Grakoui et al., 1993; Welbourn and Pause, 2007). It is dispensable for RNA replication (Lohmann et al., 1999) and inclusion of NS2 in SGRs lowers replication efficiency. NS2 is known to be capable of inserting into ER membranes and colocalises with the ER, and has been implicated in the modulation of cellular gene expression in such examples as NFκB and TNFα (Dumoulin et al., 2003). Aside from its autoprotease activity, NS2 primarily functions as a director of the initial stages of virus assembly, with interactions with p7, E2 and NS3/4A reported in numerous studies (Jirasko et al., 2010; Stapleford and Lindenbach, 2011; Tedbury et al., 2011).

NS3 possesses serine protease and helicase activities in a single protein as two distinct domains separated by a linker (Kim et al., 1996; Kim et al., 1998). The purpose of the two

functions existing as domains of a single protein is not known, but the linker between the two is involved in functionality (Aydin et al., 2013). The N terminal domain consists of a hydrophobic membrane anchor which dictates localisation of the protein (He et al., 2012) followed by a serine protease domain which contains a zinc-binding active site. The NS3 protease is responsible for the cleavage of itself from NS4A and then separation of the NS4B, NS5A and NS5B nonstructural proteins, leading to the formation of the replication complex for RNA replication (Bartenschlager et al., 1994; Bartenschlager et al., 1995). The NS3 protease active site is dependent on NS4A, which acts as a cofactor, having a hydrophobic membrane anchor domain of its own (Failla et al., 1994). Substitutions destabilising the interaction with NS4A impair protease function. The helicase domain, which also contains ATPase activity, participates in assembly through a mechanism which is not fully understood; culture adaptive substitutions (CAS) in this region improve particle production whilst having no effect on RNA replication efficiency. Nucleic acid binding to the helicase domain induces a structural change in one of the helices of the protein which is likely to be involved in the coordination of multiple modes of action (Gu and Rice, 2016). ATPase and helicase activities are dependent on low pH which causes a change in the stability to induce an open conformation for substrate binding (Ding et al., 2011; Ventura et al., 2014).

NS4B is a highly hydrophobic protein of 261 amino acids with a primary role in the formation of the membranous web as sites of genome replication (Egger et al., 2002; Gouttenoire et al., 2009; Cho et al., 2010; Li et al., 2012). Expression of NS4B alone has been shown to induce membrane curvature and the formation of single-membrane vesicles (Egger et al., 2002; McMahon and Gallop, 2005; Romero-Brey et al., 2012; Eyre et al., 2014) but requires the addition of NS5A to cause membrane rearrangements more similar to the membranous web. It has been shown to cause ER stress and activate the NFκB pathway, by interaction with CREBP (an ER stress response protein) (Tong et al., 2002; Welsch et al., 2007); ER stress is a trigger of autophagy which is induced by viral infection and is thought to increase the pool of double- and multi-membrane vesicles as sites of replication (Dreux and Chisari, 2011). It also plays a role in the modulation of lipid metabolism, stimulating the PI3K-Akt pathway leading to the upregulation of SREBPs and fatty acid synthase (FAS) (Horton et al., 2002; Waris et al., 2007; Park et al., 2009).

NS5A will be discussed in section 1.1.4.2.3.

NS5B is the RNA-dependent RNA polymerase (Behrens et al., 1996; Sesmero and Thorpe, 2015). The structure is of a typical polymerase with fingers and thumb subdomains, though

unique amonst RdRPs they encircle the active site (Lesburg et al., 1999). Binding to RNA is thought to induce a conformational change in the protein (Shatskaya and Dmitrieva, 2013). The RNA binding capability of NS5B has been demonstrated, with an affinity for the 3' UTR and highly structured regions of RNA (Lohmann et al., 1997; Yamashita et al., 1998; Cheng et al., 1999; Gouklani et al., 2012; Haqshenas, 2012). The RdRP function of NS5B is highly error-prone with a high mutation rate of between $2.7x10^{-3}$ and $8.7x10^{0}$ errors per genome (depending on template base). This leads to the quasispecies nature within an infected individual with a variability within a patient of approximately 2.7%, and has given rise to the great number of genoytypes and subtypes in circulation. The polymerase has a propensity to make G:U mismatches most frequently, and transitions more commonly occurring than transversions (Martell et al., 1992; Powdrill et al., 2011). NS5B stimulates the helicase activity of NS3 within the replication complex (Jennings et al., 2008) and recruits the eIF4 complex to the IRES to initiate translation (Kyono et al., 2002; Lourenço et al., 2008). NS5B has been demonstrated to play a role in virus assembly by its interaction with p7 and mutagenic analysis shows regions with a role in morphogenesis of virions (Aligeti et al., 2015).

1.1.4.2.3 NS5A

NS5A is a multifunctional protein with roles at various stages of the virus life cycle including modification of the host cell environment, assembly of the replication complex and assembly of new virus particles (Ross-Thriepland et al., 2015).

It is a phosphoprotein, composed of three distinct domains, separated by serine-rich low complexity sequences (LCS). Domains II and III are highly flexible, though the structure of domain I has been solved by different groups with a consensus on this single structure and the identification of a metalloprotein function, with a zinc binding site being crucial for replication (Tellinghuisen et al., 2004; Love et al., 2009; Lambert et al., 2014). NS5A is known to form a homodimer and, though the structure of the domain I monomer is agreed the dimer conformation has been differentially reported (shown in Figure 1-6). It is thought that the two dimer conformations are both important in the different functions of NS5A in the virus life cycle. The "open" conformation (Love et al., 2009) reveals a positively-charged groove which has been postulated as an RNA binding region (Ascher et al., 2015). Two populations of NS5A exist in the cell - large, static structures and smaller, more motile ones (Eyre et al., 2014). Both associate with VAP-A and Rab5A, with smaller ones shuttling across the surface of LDs. Only a

small amount of NS5A colocalises with core at a time, and at LD cap-like structures. Motility and trafficking are dependent on the microtubule network (Eyre et al., 2014).

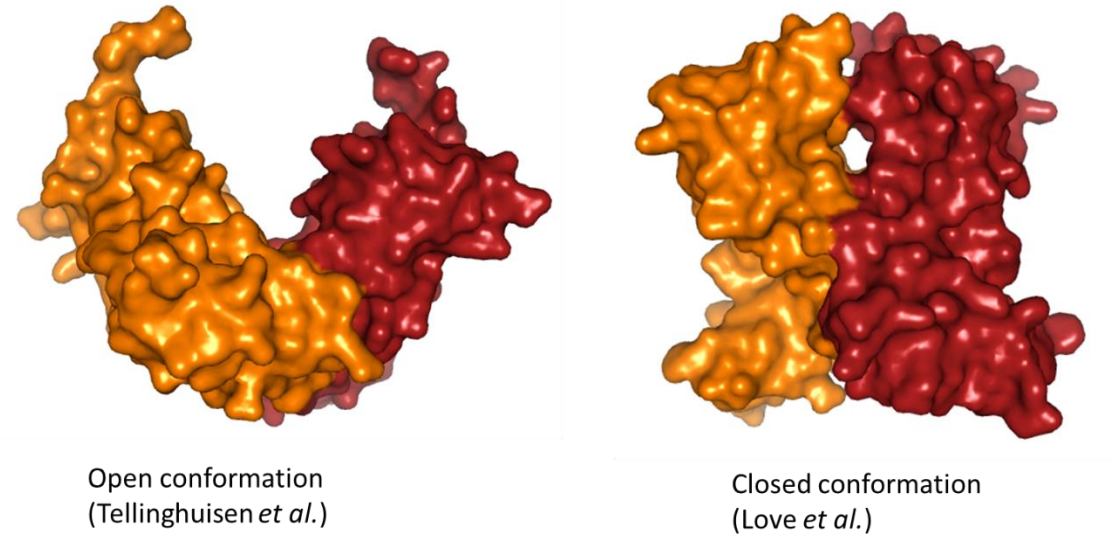

Figure 1-6. NS5A dimer structures. Images created using Pymol software from PDB files 1ZH1 and 3FQM respectively (Tellinghuisen et al., 2004; Love et al., 2009)

NS5A has been implicated in the direct oncogenesis of HCV due to its effect on the EGFR-Ras-ERK signalling cascade, affecting control of cell cycle regulation. The inhibitory effect on EGFR internalisation contributes to entry of new virus, since EGFR is a known entry factor for HCV (Lupberger et al., 2011).

NS5A reacts with DDX3, an oncogene, and Y box binding protein 1 (YB1) which is a DDX3 interacting protein; both have roles in control of cellular proliferation (Wei-Ting Wang et al., 2015). The relationship with YB1 is linked to Akt phosphorylation which is in turn associated with control of proliferation and apoptosis (Street et al., 2005; Street et al., 2004). A recent proteomics study identified 132 proteins that interact with NS5A, including proteins in pathways previously linked to pathogenesis of HCV and other viral pathogens in addition to several novel interacting partners (Tripathi et al., 2013). Roles in cell signalling modulation have also been identified: it has been shown that NS5A arrests host cells in G1 phase by inhibiting the Ras-ERK-MAPK pathway to favour replication (Street et al., 2004; Kannan et al., 2011). NS5A may also interact with mixed lineage kinase 3 (MLK3), which activates MAPK, to block apoptosis (Amako et al., 2013).

NS5A is crucial in the formation of the membranous web in combination with NS4B. Expression of NS5A in the absence of other viral proteins induced multi-membrane vesicles in a fashion similar to the redistribution of membranes and the formation of single, double and multi-membrane vesicles of ER origin by HCV infection. NS4B expression alone induced single membrane vesicles, indicating a cooperative role (Romero-Brey et al., 2012; Eyre et al., 2014). A siRNA screen of the human kinome identified PI4K as an interacting partner. PI4K silencing inhibits replication and stable knockdown inhibits the formation of multi-membrane vesicles. NS5A domain I is the region responsible for upregulation of PI4P by activation of PI4K (Reiss et al., 2011; Harak et al., 2016).

NS5A has been shown to interact with TIP47 and Rab18, components of lipid droplets, to target the replication complex to these (Salloum et al., 2013; Vogt et al., 2013).

A further key function of NS5A is its interaction with lipid metabolism and biosynthesis pathways. Increases in lipid droplet formation in cells displaying transient expression of NS5A (Parvaiz et al., 2014) and replication of a sub-genomic replicon (SGR) (Qadri et al., 2012) have been shown. HCV NS5A upregulation of key lipid biosynthesis pathway members is well characterised, including upregulation of peroxisome proliferator-activated receptor γ (PPARγ), sterol regulatory element-binding protein 1c (SRBP1c), fatty acid synthase (FAS) and, indirectly through the PI3K pathway, Liver X receptor α (LXRα) (García-Mediavilla et al., 2012).

NS5A is an RNA binding protein; indeed, all three domains possess RNA binding function (Foster et al., 2010). Domain II has been shown to be required for RNA replication: A study identified a number of residues in the C-terminal region of domain II that are required for RNA replication but not virus assembly. The LCS-II contains two polyproline motifs, the first of which is required for replication of GT1 but not 2, and the second is not essential for replication or assembly. Mutagenic studies of these motifs highlight roles at different stages of the virus life cycle (Appel et al., 2005; Hughes et al., 2009a; Hughes et al., 2009b; Ross-Thriepland et al., 2013).

NS5A has a well-defined role in virus assembly, a function which is mostly performed by domain III and which is closely linked to its role in earlier stages of replication rather than an isolated function (Hughes et al., 2009b). Deletion of domain III is not lethal to replication but does prevent assembly of virus (Hughes et al., 2009b; Appel et al., 2008). This mutant does not colocalise with core and does not release infectious virus; it accumulates intracellular core on lipid droplets but not infectious virus, which illustrates a defect in packaging rather than release. In addition, GT2 isolates contain a 19 amino acid insertion in domain III, the deletion

of which delays replication and assembly (Hughes et al., 2009b). NS5A colocalises with core and has been implicated in targeting the core protein and other non-structural proteins of the replication complex to lipid droplets (Masaki et al., 2008; Boson et al., 2017)

The various functions of NS5A have been shown to be controlled by phosphorylation, since the protein has no enzymatic function (Appel et al., 2005; Ross-Thriepland and Harris, 2014; Ross-Thriepland et al., 2015; Eyre et al., 2016; Chong et al., 2016; Lee et al., 2016). The protein exists in two distinct phosphorylated forms, which resolve as two species by SDS-PAGE – basally phosphorylated p56 (apparent M.W. 56 kDa) and hyperphosphorylated p58 (58 kDa). It has been hypothesised that the pattern of phosphorylation of key serine residues in the LCS 1 exerts an effect on the protein's function, with hyperphosphorylation causing a switch from RNA replication to virion assembly (Appel et al., 2005; Ross-Thriepland and Harris, 2014). Serines in the LCS-I are phosphorylated by CKIa in a manner controlled by PI4KIIIa, allowing downstream phosphorylation of residues in the LCS-II and domains II and III (Eyre et al., 2016; Chong et al., 2016). Serines 146 and 235 have been suggested to form these master controls, with downstream phosphorylation controlling motility and distribution of NS5A and other replication complex proteins, colocalization of dsRNA and virus assembly. Phosphomimetic substitutions at S225 and S235 both restrict distribution of NS5A to a perinuclear region. Similarly, deletion of serines in domain II which are involved in RNA replication abrogates hyperphosphorylation (Appel et al., 2005). Mutation of a serine cluster in domain III impairs basal phosphorylation and reduces assembly, with phosphomimetic substitutions capable of partly rescuing this phenotype. Similarly, phosphoablatant substitutions suppress the core-RNA interaction. The NS5A at ER membranes is predominately basally phosphorylated (Qiu et al., 2011). It was demonstrated that substitutions which are culture-adaptive abrogate hyperphosphorylation of NS5A, and NS4B CAS can also abrogate hyperphosphorylation (Harak et al., 2016). This led to the hypothesis that phosphorylation forms a molecular switch between replication and assembly.

1.2 In vitro models of HCV

1.2.1 Sub-genomic replicons

The numerous tools for basic research of HCV have been reviewed in detail (Bukh, 2016; Ortega-Prieto and Dorner, 2016).

The development of the SGR system for studying HCV provided a novel *in vitro* culture model, allowing the non-structural proteins to be characterised, and their roles in RNA replication to be determined. Lohmann *et al* demonstrated in 1999 that a bicistronic construct containing the NS3-5B coding regions from the HCV GT1b genome under the control of an EMCV internal ribosome entry site (IRES) and a neomycin phosphotransferase gene under the control of the HCV IRES can be assembled and transfected into cultured cells. Cells supporting the replication of this construct could be selected with a neomycin analogue (G418), forming clonal colonies of cells able to survive in the presence of G418, after those unable to support replication of the SGR had died. After subsequent replication cycles these SGR constructs had obtained a number of CAS, which were identified and cloned back into the original construct, giving one capable of greater colony-forming efficiency than the wild-type sequence (Lohmann et al., 1999). The functions of CAS are rarely explored in the studies which report their phenotype, but suggested mechanisms for the culture adaption phenotype of NS3 substitutions involve the altered localisation of NS3 to the ER (Murayama et al., 2017; Yan et al., 2017). However, the S2204I culture adaptive mutation which was identified in Con1 through the approach described above, located in the NS5A domain I coding region, abrogates hyperphosphorylation of NS5A (a subject described in detail in section 1.1.4.2.3) and the enhanced replication capacity it confers is dependent on PI4K function (Harak et al., 2016).

As well as allowing the identification of culture-adaptive substitutions these selected cells which stably harbour the HCV SGR are of great importance in their own right, in the development of therapies and investigation of the functions of non-structural proteins (Bukh, 2016).

Following this breakthrough, SGR have now been developed for genotypes 2-6 (Kato et al., 2003; Saeed et al., 2012; Saeed et al., 2013; Yu et al., 2013; Wose Kinge et al., 2014; Yu et al., 2014; Camus et al., 2018). The GT2a SGR developed by Kato *et al* in 2003 was of critical importance; this was developed from a clinical isolate from a Japanese patient with fulminant hepatitis (termed JFH-1) and was capable of very high levels of transient replication. This SGR was also able to replicate in the absence of CAS, though presence of these did increase replication. These SGRs primarily utilise consensus sequences from databases or from sequencing of patient-derived virus isolates, however several groups have demonstrated the ability to construct an SGR directly from a clinical isolate, paving the way for investigation of particular sequences within a virus quasispecies – a possibility which is of particular use when

exploring the relationship between resistance-associated substitutions (RAS) and treatment response (further discussed in section 1.3.2.3) (Rajyaguru et al., 2013; Lu et al., 2014).

Recent work has focussed on the further development of SGRs using further culture adaptation or modification of the host cell environment. SGR experiments are primarily carried out in Huh7 cells, an immortalised line of hepatoma cells. SGR harbouring cells were selected and the SGR was subsequently eradicated; it was discovered that the resulting cell line, termed Huh7.5, was more permissible to SGR replication (Blight et al., 2002). Characterisation revealed that the cells had acquired a mutation in the RIG-I gene, which is responsible for intracellular sensing of double-stranded RNA, an intermediate of virus replication (Foy et al., 2005; Sumpter et al., 2005). In addition, the cells have an IFN-L3 locus rs12979860 single nucleotide polymorphism (SNP) of CT, which is more commonly associated with GT1 infected patients than the general population who more commonly have CC at this locus (Rojas et al., 2014)– this is associated with spontaneous clearance of HCV (Rauch et al., 2010). This concept has been replicated several times to generate more permissible cell lines for SGR-based research (Blight et al., 2002; Zhong et al., 2005; Yu et al., 2013). Recently a cellular gene was identified that increased permissibility of host cells to replication of an unadapted SGR or clinical virus isolates – hSEC14L2. This was found in a cDNA library screen and was suggested to assist in the protection of SGRs from lipid peroxidation (Saeed et al., 2015).

Genotype-chimeric or hybrid SGRs have been used in a number of studies involving development of DAAs and investigation into the functions of NS5A. In 2006, Lanford *et al* showed that a hybrid SGR could be constructed containing amino acids 87 to 429 of GT3a NS5A in a Con1 (GT1b) backbone; this was able to replicate efficiently in a transient system, but the study was not able to show a differential sensitivity to pegylated interferon alpha (IFNα), leading them to conclude that IFN sensitivity is not determined by the region included in the hybrid SGR (Lanford et al., 2006). Hernandez *et al* developed a partial hybrid containing the first 429 amino acids of a consensus sequence of GT3a NS5A and residues 430-471 from JFH-1 NS5A in a JFH-1 SGR backbone. They used this system to investigate the effect of a number of NS5A inhibitor RAS which have been reported for GT1, as well as determining the frequency of these substitutions in patients (Hernandez et al., 2013).

Another partial NS5A-JFH-1 hybrid using the same region of GT3a NS5A from three clinical isolates was assembled and used in a study to identify potentially novel RAS in GT3a NS5A following selection with an NS5A inhibitor, and to compare the effect of these substitutions on

50% effective concentrations (EC_{50}) in a transient system (Wang et al., 2013). The effects of these substitutions beyond conferring drug resistance were not reported. In addition, a NS5A-5B hybrid replicon in a Con1 backbone was reported, showing robust transient expression with a wild-type sequence, and the Y93H NS5A inhibitor RAS (Kylefjord et al., 2014).

1.2.2 Infectious virus culture systems

Development of a full-length JFH-1 infectious clone has allowed the *in vitro* observation of the full virus life cycle (Lindenbach et al., 2005; Wakita et al., 2005). Since then, chimera viruses have been reported for a range of different genotypes. Jens Bukh and colleagues have been instrumental in the development of a number of GT3a chimera viruses. J6/JFH-1 viruses (both GT2a) with NS5A from GT1-7 were constructed initially, and tested for differential sensitivity to a NS5A inhibitor (Scheel et al., 2011). Subsequently, chimera viruses containing NS3 and NS5A from GT1a and 3a, with the rest of the viral genome from JFH-1 were used to test a combination therapy (Gottwein et al., 2013). Ultimately a GT3a virus was reported, containing only the NS5B and 3' UTR regions of JFH-1 (termed 5-5A), which showed a good correlation of treatment response to clinical observations for GT3a for NS5A and NS3 inhibitors (Yi-Ping Li et al., 2014). More recently, however, the same group constructed a full-GT3 virus with efficient replication capacity based on the DBN clinical isolate (using the UTRs from S52) and they used this to investigate resistance of GT3 to the NS5B inhibitor Sofosbuvir (Ramirez et al., 2016).

1.2.3 Additional model systems

The initial identification of HCV as the causative agent of NANB Hepatitis was heavily reliant on chimpanzees as an animal model. Chimpanzees are used for studying particle composition and in some infection studies with clinical isolates but the immune composition of the chimpanzee host is too different as indicated by the knowledge that HCV does not establish chronic infection in chimpanzees (Walker, 1997; MacArthur et al., 2012). Non-human primate research is also limited in scale due to the ethics and cost of using these animals.

HCV has a narrow tissue tropism and host range and so does not readily infect species other than humans, although some work has explored the use of humanised chimeric mice (Bukh, 2012; MacArthur et al., 2012; Tesfaye et al., 2013; Vercauteren, de Jong, et al., 2014). Immunodeficient (SCID) mice can be xenotransplanted with human hepatocytes and these can

support HCV infection. In addition, adenoviral delivery of human surface receptors allows the investigation of entry inhibitors in rodent models, though the full replication cycle does not take place.

The potential to use primate-tropic GBV-B as a model system has been suggested, since GBV-B can form either acute or chronic infection in primates, similar to HCV (Manickam and Reeves, 2014). The potential of EqHV in horses has also been suggested due to the similarity of EqHV to HCV, but not explored due to conflicting evidence as to whether this virus causes chronic disease in its host (Reuter et al., 2014; Pfaender et al., 2015).

A number of studies have explored the use of primary human hepatocytes (PHH), or hepatocytes derived from induced pluripotent or embryonic stem cells (Cheng et al., 2015). Recently, it was demonstrated that foetal liver tissue can support the entire replication cycle of different genotypes of HCV (Guo et al., 2017). However due to the ethical and technical limitations in handling of these cells and tissues they do not provide a high-throughput platform for experimentation or drug discovery. In addition, PHH are limited in the timescale of experiments due to extremely rapid dedifferentiation, and hepatocyte-like cells from stem cells rarely progress beyond a progenitor stage and may not express mature cell markers required to study replication fully.

1.3 Treatment of HCV

1.3.1 Historic treatment of HCV

Treatment for chronic HCV has been in the form of IFNα and Ribavirin (IFN/RBV). This regimen is effective in achieving a sustained virological response at 24 weeks following cessation of treatment (SVR24) in approximately 40% of patients with HCV GT1 and up to 80% in patients with HCV GT2a or 3a (Manns et al., 2001). Treatment success rates with IFN/RBV are strongly influenced by host factors such as age and gender, with older patients and men less likely to respond; race, with African populations less likely to achieve SVR12 than European populations; higher levels of ISGs at baseline and presence of cirrhosis (Ge et al., 2009; Cavalcante and Lyra, 2015; Enomoto et al., 2015; Yu, 2017).

A region of the NS5A protein which became known as the Interferon sensitivity determining region, ISDR, was found to be associated with response to treatment to IFN: sequences with higher rates of mutation at this position are associated with a higher probability of achieving

SVR (Enomoto et al., 1996; Frangeul et al., 1998; Pascu et al., 2004; Fukuhara et al., 2010; Akuta et al., 2012; Mansoor et al., 2013). In addition, two residues of core are also found to be more frequently mutated in patients who achieved SVR12 and presence of these substitutions increases the likelihood of having more substitutions in the ISDR, which increases the probability of achieving SVR (Akuta et al., 2007; Abe et al., 2010; Akuta et al., 2012). A further region of NS5A known as the IFN/RBV resistance determining region, IRRDR, dictates response to the combination therapy of IFN and RBV and has been shown to have the same pattern of higher mutation rates correlating with treatment outcome (El-Shamy et al., 2008; Qashqari et al., 2013). The ISDR of GT3 sequences is reported as being more conserved than for other genotypes, and the ability of substitutions in this region to predict an increased likelihood of achieving SVR12 is debated (Bittar et al., 2010; Frangeul et al., 1998; McKechnie et al., 2000; Knolle et al., 1998; Yokozaki et al., 2011).

An additional host factor has been extensively studied and its effect on SVR12 rates is well studied. A single nucleotide polymorphism (SNP) in either of the rs12979860 locus from major CC allele to heterozygous CT or homozygous TT, and the rs8099917 locus from major TT allele to heterozygous TG or homozygous GG are both associated with lower success rates with IFN-based therapy. Interestingly, it has been observed that GT3 patients have a higher incidence of a favourable IFN λ genotype whereas GT1b patients have higher incidences of CT or TT genotypes (Kadjbaf et al., 2016; Peiffer et al., 2016). This may contribute to the higher efficacy of IFN against GT3, but this is not known. Similarly unknown is the reason for the link between GT3 and CC genotype; it is of note that the CC genotype is more frequent in European populations than in African ones, which explains the differential response rates by race, however the origin of GT3 has been estimated as the African continent (Chunhua Li et al., 2014; May et al., 2015).

The mechanism of action of RBV is highly contentious, and a number of parallel mechanisms have been proposed and investigated. It is thought that, rather than a single mechanism being responsible for the efficacy of RBV there may be a combination of effects which exert minimal effects in isolation but coordinate to produce an antiviral response. These have been reviewed (Thomas et al., 2012; Nakatsuka et al., 2015). RBV is a nucleoside analogue of guanosine and has hence been postulated to function as a chain terminator, inhibiting the function of the NS5B polymerase. However, once incorporated, RBV can base-pair with either Cytosine or Uracil, causing high frequencies of mutations leading to error catastrophe. It also functions as an inhibitor of inosine monophosphate dehydrogenase (IMPDH), which catalyses the rate-

limiting step in guanosine biosynthesis; this results in a reduction in GTP levels. It has been suggested that the reduction in GTP biosynthesis may work in combination with the error catastrophe mechanism, reducing the available GTP pool in the cell so that other bases are incorporated instead.

RBV has been shown to have an effect on the immune response to HCV, following observations that it is most effective when administered in combination with IFN. RBV is known to increase type 1 and/or type 2 cytokine production which supports helper T cell type 1 (Th1) activity. RBV may also have an effect on ISG activation, which concurs with its synergistic effect with IFN.

IFN/RBV is also associated with a substantial side effects profile: including flu-like symptoms, headaches and skin rash in over half of patients; anaemia, neutropenia; and psychiatric events in up to 30% such as depression, lethargy, suicide ideation and attempt and even homicidal tendencies. IFN/RBV cannot be given to patients who are pregnant or who will not adhere to strict contraceptive measures as it is associated with foetal abnormalities, and cannot be given to patients with major psychiatric disorders and renal or vascular problems (Ghany et al., 2009).

1.3.2 Development of Direct-acting antivirals

Numerous reviews have been published which explore the scale of DAAs now available to treat HCV; almost all stages of the virus life cycle have been explored as potential antiviral targets though compounds targeted to a small number of the non-structural proteins (NS3, NS5A, NS5B) have been the most successful (Griffin, 2010; Rice, 2011; Pawlotsky, 2013; Colpitts and Baumert, 2016; Taherkhani and Farshadpour, 2017). The first of these compounds were a number of NS3 protease inhibitors, licenced in 2011. These demonstrated excellent potency in treating HCV *in vitro* and were better tolerated by patients than IFN and RBV (Manzano-Robleda et al., 2015). Discovered using peptide-based functional screens and refined by structure-activity relationship (SAR) analysis, these compounds were targeted to NS3 protease activity which is essential for cleavage of the HCV polyprotein and assembly of the replication complex (Elbaz et al., 2015; Götte and Feld, 2016; McCauley and Rudd, 2016). Analysis of resistance demonstrated a number of residues which reduce efficacy by reducing affinity of the drug with minimal effect on substrate binding (Pawlotsky, 2016; Premoli and Aghemo, 2016). However, the first such NS3 protease inhibitors (PI), Telaprevir and Boceprevir were

withdrawn for commercial reasons due to their inability to compete with newer therapies. Second-generation PIs such as Asunaprevir and Simeprevir are widely used in the United States and Japan and have a higher barrier to resistance (a consequence of RAS to these compounds being associated with a more severe fitness cost), though are associated with higher incidences of adverse events than other classes of DAA (Banerjee and Reddy, 2016; Pawlotsky, 2016). Until recently they were not licenced to treat GT3 due to almost complete inefficacy (Moreno et al., 2012; Ampuero et al., 2014), however a number of combination therapies now exist which are effective against GT3.

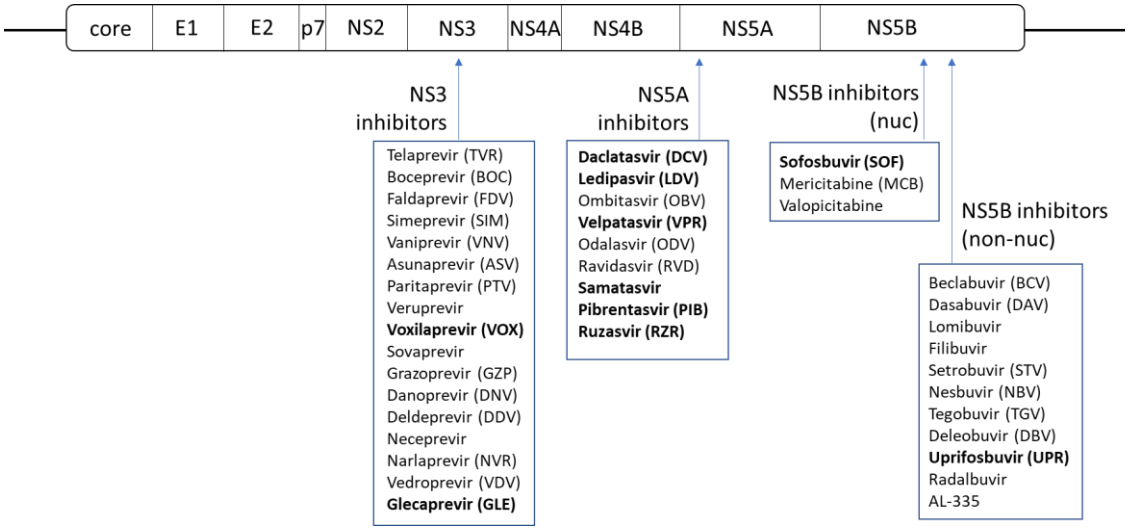

Figure 1-7. A recent summary of direct-acting antivirals against HCV. Schematic diagram of the HCV genome populated with information from (Taherkhani and Farshadpour, 2017). Compounds in bold type are stated in the review as being effective against genotype 3.

A parallel approach of in-silico docking screens led to the development of NS5B inhibitors, of which there are two types: Nucleoside analogs (nuc) such as Sofosbuvir (SOF) and non-nucleoside (non-nuc) compounds such as Dasabuvir. SOF, developed by Gilead and licenced in 2014, is a chain terminator which is delivered as a prodrug and as such requires conversion into the active compound in hepatocytes (Zeng et al., 2013; Kirby et al., 2015; Yang and Choi, 2017). RAS for SOF have been reported *in vitro,* including S282T, but are rarely identified in clinical studies, and SOF exhibits pan-genotypic activity. The smallest class of DAA, non-nuc NS5B inhibitors such as Dasabuvir (Mantry and Pathak, 2016), bind to the palm region of the NS5B protein and cause allosteric inhibition by inducing a conformational change to the active site of the enzyme. These have been little explored due to the extraordinary efficacy of SOF and the NS5A inhibitors described below.

Due to the propensity of each of these classes of inhibitor to be susceptible to resistance, they are almost exclusively used in combination therapies. A great number of these include RBV for increased efficacy, however and increasing number do not include IFN; these are known as all-oral. A recent summary of the currently-licenced combination therapies with their respective marketing names is shown in Table 1-1.

Combination of compounds	Targets	Trade name
Paritaprevir, Ombitasvir, Ritonavir, Dasabuvir, Ribavirin	NS3, NS5A, NS5B	Viekira Pak (Abbvie)
Grazoprevir, Elbasvir	NS3, NS5A	Zepatier (Merck, Sharpe & Dohme)
Daclatasvir, Sofosbuvir, Ribavirin	NS5A, NS5B	Sovodak (Beacon Pharmaceuticals)
Ledipasivr, Sofosbuvir, Ribavirin	NS5A, NS5B	Harvoni (Gilead)
Ombitasvir, Ritonavir, Paritaprevir	NS3, NS5A	Technivie (Abbvie)
Velpatasvir, Sofosbuvir, Ribavirin	NS5A, NS5B	Epclusa (Gilead)
Glecaprevir, Pibrentasvir	NS3, NS5A	Maviret (Abbvie)

Table 1-1. A summary of the HCV DAA combination therapies in current use. This list is not exhaustive as there are combinations that have been tested for many compounds that are not currently marketed under a brand name.

1.3.2.1 NS5A inhibitors – structure and proposed function

NS5A has proven to be an attractive target for development of DAAs, due to the extensive interactions with host cell processes and multiple putative functions in viral replication. A number of NS5A inhibitors have been developed, all with a symmetrical structure, identified during high-throughput replication assays and blind docking screens (Gao et al., 2010; Link et al., 2014; Vince et al., 2014; Gao et al., 2016). The first such inhibitor is Daclatasvir (DCV), previously known as BMS-790052, although a great many NS5A inhibitors are now in use with increased potency and higher genetic barrier to resistance (a subject discussed in 1.3.2.3). A

recent list of NS5A inhibitors is shown in Figure 1-7 (Taherkhani and Farshadpour, 2017). DCV was identified by performing structure-activity relationship (SAR) analysis on an initial hit compound identified in a high-throughput library screen of a million molecules. The improved efficacy of the lead compound, DCV, was reported alongside the prediction that it is an inhibitor of NS5A based on two pieces of evidence: the selection of resistance which was located in domain I of NS5A and the demonstration that DCV binds to NS5A. No hypothesis as to the mechanism of action was initially presented (Gao et al., 2010). During the following years a great number of studies have begun to elucidate the mechanism of action of NS5A inhibitors, a question with numerous answers because of the variety of roles that NS5A plays in the infected cell. DCV is widely used in mechanistic studies as a model compound. Initially the greatest effect of DCV is on assembly of virus particles (Guedj et al., 2013; McGivern et al., 2014; Nettles et al., 2014; Boson et al., 2017), with short treatments causing a block in the delivery of viral genomes from replication complexes to sites of assembly where it would associate with core. This bottleneck causes the accumulation of core, E2 and NS5A within punctate structures which are likely failed sites of assembly, from which the accumulating structural proteins were never successfully released (Boson et al., 2017). There is also evidence that DCV causes an accumulation of viral RNA for the same reason (Guedj et al., 2013), and sequesters NS5A in lipid droplets to also prevent particle formation (Nettles et al., 2014).

In addition to the effect on assembly NS5A inhibitors have also been shown to inhibit RNA replication in SGR assays, which have no assembly pathway. HCV RNA declines quickly after DCV treatment with a half-life of 45 minutes (Guedj et al., 2013). DCV has also been demonstrated to affect the cellular distribution of NS5A, unrelated to protein level and any effect upon RNA replication (Lee et al., 2011; Qiu et al., 2011; Chukkapalli et al., 2015; Boson et al., 2017). It has been shown to alter the association of NS5A with Golgi membranes, affecting the association of NS5A with trans-Golgi but not ER membranes (Qiu et al., 2011) and altering distribution from a cytoplasmic to a perinuclear distribution (Boson et al., 2017). An effect upon replication complex formation has also been demonstrated, with DCV treatment inhibiting the redistribution of PI4P which NS5A mediates, but only in a system in which the full polyprotein was expressed rather than NS5A alone, suggesting that its effect in this regard is upon a cooperative function with another non-structural protein, most likely NS4B (Chukkapalli et al., 2015). The effect of DCV upon replication complex formation, linked to its distribution, was demonstrated in a number of other studies (Lee et al., 2011; McGivern et al., 2014; Nettles et al., 2014), and the hypothesis that DCV treatment acts upon an early stage of

polyprotein processing and replication complex formation followed the observation that DCV causes the accumulation of an NS4B-5A polyprotein precursor (Lee et al., 2011; Qiu et al., 2011; McGivern et al., 2014). It is accepted that the most pronounced effect of DCV is upon the formation of new replication complexes rather than those which are already formed, and this hypothesis is further supported by *in vitro* data suggesting that the efficacy of DCV upon transient replication is greater than in stable SGR harbouring cells (Fridell et al., 2010).

These effects are likely to be mediated by the nature in which DCV binds to NS5A. DCV binding is thought to over-stabilise a weak homodimer and preventing the dissociation and reformation of dimers of different conformations which are likely to be crucial to the multiple functions of NS5A. It has been demonstrated that the dimeric compound can crosslink two NS5A molecules into a more stable dimer and the "half" form of the compound can bind but is not sufficient to inhibit (Gao et al., 2010; O'Boyle Ii et al., 2013; Lambert et al., 2014). In addition, the compound has been shown in multiple studies to abrogate or completely inhibit hyperphosphorylation, which is also known to be crucial (Lemm et al., 2010). Abrogation of hyperphosphorylation of NS5A at S225 (Ross-Thriepland and Harris, 2014; Goonawardane et al., 2017) reduces distribution of NS5A to a perinuclear region; inhibitor treatment, which also abrogates hyperphosphorylation (Qiu et al., 2011) has the same phenotype (Boson et al., 2017) and affects the association of NS5A with trans-Golgi but not ER membranes. The NS5A at ER membranes is predominately basally phosphorylated (Qiu et al., 2011) which supports these findings.

The working biochemical hypothesis for DCV and other NS5A inhibitors is that these symmetrical compounds bind in a groove formed by the head-to-head conformation of the NS5A homodimer and can over-stabilise a weak structure to prevent dissociation between different conformations (Lambert et al., 2014; Barakat et al., 2015). Binding of DCV may reduce affinity for RNA by allosterically changing the dimer structure (Ascher et al., 2015). Compound and RNA binding sites are in different locations of the protein structure, suggesting that binding of an inhibitor molecule induces a conformational change which prohibits binding of RNA to its own site on the protein (Targett-Adams et al., 2011).

1.3.2.2 Efficacy of NS5A inhibitors in clinical trials

NS5A inhibitors have displayed extraordinary efficacy in clinical trials. For GT1a patients without evidence of cirrhosis or experience of prior treatment failure the inclusion of an NS5A inhibitor improves treatment outcomes to 95-100% efficacy, represented as SVR12 (Pol et al., 2016). However, it is widely reported that GT3 is much less responsive to DAAs of all classes,

to a greater or lesser extent (Ampuero et al., 2014; Pol et al., 2016; Johnson et al., 2017). Protease inhibitors, the first HCV DAA class to be licenced, are no longer used to treat GT3 due to almost complete inefficacy. NS5B inhibitors such as SOF are slightly less effective against GT3, though still effective in clinical trials giving SVR12 rates of over 90% when used in combination with RBV and another DAA of a different class (Nelson et al., 2015; Leroy et al., 2016; Poordad et al., 2016).

The studies which have recruited GT3 patients for trials of all-oral treatment regimens (excluding IFN) are summarised in Table 1-2.

Single DAAs of any class as a monotherapy, except for phase I dose-escalation studies of new compounds, are not widely used in clinical trials due to the risk of treatment failure and resistance. Instead, combination therapies are widely used. The combination of SOF and RBV is associated with SVR12 rates of 30-67% in non-cirrhotic, treatment-naïve GT3 patients treated for 12 weeks, increasing to 94% after 24 weeks' treatment (Jacobson et al., 2013; Sulkowski et al., 2014a; Sulkowski et al., 2014b; Zeuzem et al., 2014; Molina et al., 2015; Nelson et al., 2015; Wyles et al., 2015; Leroy et al., 2016; Poordad et al., 2016). Combination treatment of DCV and SOF leads to SVR12 rates of 89% (Nelson et al., 2015; Wyles et al., 2015) and 91% SVR12 rates were reported for the triple combination of DCV, SOF and RBV (Leroy et al., 2016).

Clinical trials often include a number of patients with compensated cirrhosis, defined as cirrhosis without a decompensation or liver failure event. Patients with cirrhosis are commonly reported to have a lesser response rate, with a decrease in SVR12 from 68-92% down to 21-83%, depending on the treatment durations and regimens used for the study. In addition, prior treatment failure with IFN/RBV or a DAA is associated with a similar decrease in SVR12 rate, from 90-92% down to 86-88%, again depending on the conditions of the trial. Patients who have failed therapy with a particular class of DAA are often excluded from a subsequent trial which uses that class of compound. The combination of cirrhosis and treatment experience is an especially difficult to treat patient group, with SVR12 rates of 62% with 16 weeks' treatment with SOF and RBV (Zeuzem et al., 2014). Recently a novel NS5A inhibitor, Velpatasvir (VEL) was reported by Gilead, with pangenotypic activity and SVR12 rates (as a combination with SOF) of 95% in healthy, treatment-naïve patients, with 89% in patients with compensated cirrhosis and prior treatment experience (Foster et al., 2015).

Adverse events are usually either related to RBV treatment with some discontinuations or reductions, or not sufficiently severe (headache, fatigue, nausea) and usually identical to

placebo groups, where a placebo arm was included in the trial design. These are likely to be symptoms of liver disease rather than directly related to treatment. There was some concern following a FDA report that the combination Viekira Pak (Paritaprevir/ritonavir, Ombitasvir and Dasabuvir) might be associated with an increase in hepatic decompensation events and impairment in renal function (US FDA communication, 2015), but this has not been verified in a trial designed to test this observation (Butt et al., 2017). Factors influencing response in addition to genotype are usually presence of cirrhosis, treatment experience, male gender, older age, high baseline viral load and high body mass index (BMI). Early virological response (EVR) or rapid virological response (RVR), defined as a reduction in HCV RNA to below the limit of quantification of the assays used in the study at 4 weeks after the start of treatment, often correlate with treatment response.

Compounds used	**SVR12 rates in all patients (averages)**	**SVR12 rates in patients with cirrhosis & treatment experience (averages)**	**References**
SOF + RBV	61-94%	21-86%	(Jacobson et al., 2013; Sulkowski et al., 2014b; Zeuzem et al., 2014; Molina et al., 2015)
SOF + DCV	72.8-90%	63-86%	(Nelson et al., 2015; Wyles et al., 2015; Foster et al., 2016)
SOF + DCV + RBV	88-91%	83-88%	(Sulkowski et al., 2014a; Leroy et al., 2016; Poordad et al., 2016)
SOF + LDV	61.2-64%	73-82% (with RBV)	(Gane et al., 2015; Foster et al., 2016)
VEL + SOF + RBV	85-95% (50% without RBV)	89-91%	(Curry et al., 2015; Gane et al., 2015; Foster et al., 2015)

Table 1-2. Summary of clinical trials inclusive of GT3 patients from 2013 – 2017. Ranges calculated from data taken from the clinical studies referenced**.**

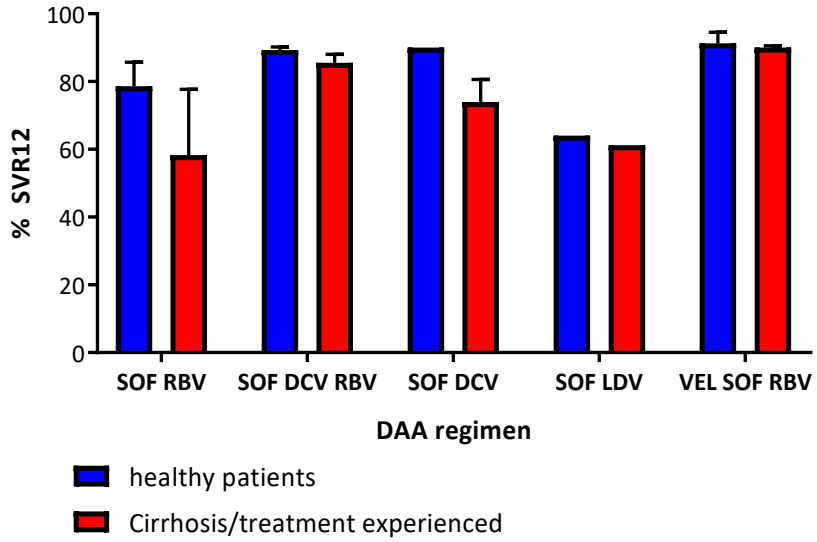

Figure 1-8. Comparison of combination DAA regimens efficacy against GT3. Graphic produced using data from Table 1-2

The careful design of clinical trials to exclude high numbers of cirrhotic patients, those with HCC or who have undergone an orthotic liver transplant (OLT), coinfections with human immunodeficiency virus (HIV) or hepatitis B virus (HBV) functions as a pure assessment of the efficacy of a particular treatment regimen without added complication for data analysis. However, it is emerging from cohort based studies that the real-world usage of DAAs is likely to report a different outcome (Younossi et al., 2014; Foster et al., 2016), and highly controlled clinical trials have provided an unrealistic image of the efficacy of these compounds. There are a number of important social factors which will affect real-world efficacy of DAAs, including treatment adherence (Younossi et al., 2015). Studies using patient reported outcomes (PROs) report that health-related quality of life (HRQL) is higher in patients receiving all-oral treatment regimens, though all patients who achieve SVR12 have an equal overall HRQL score at the end of follow-up regardless of treatment regimen. In addition, cirrhosis, previous experience of an adverse event and baseline mental health scores were shown to negatively impact HRQL and as such are likely to affect treatment adherence (Younossi et al., 2014; Younossi et al., 2015).

Cohort studies are currently rare, but are increasingly reporting that real-world use of DAAs is resulting in lower SVR12 rates than their clinical trials would suggest. The NHS early access programme (EAP), a compassionate use program designed to treat patients at high risk of

death or serious liver damage with DAAs, showed that lower proportions of people in the clinic responded to treatment than clinical trials would predict – 72.8% of patients treated with the triple DCV/SOF/RBV combination achieved SVR12 – and that treatment of the virus did not necessarily reverse the liver damage or development of HCC though most patients reported an increase in MELD score as a representation of improvement of liver function (Cheung et al., 2016; Foster et al., 2016). Indeed, 7 patients died during treatment or follow-up. However, it should be noted that the patients included in this study were those with severe liver disease, extrahepatic manifestations or a previous decompensation event, which are often excluded from clinical trials, and hence healthier patients would be predicted to respond to a higher degree. A cohort study in Germany (Steinebrunner et al., 2015) also found lower SVR rates than reported in clinical trials when treating patients with SOF/RBV and IFN. SVR rates for GT3 were reported as 92%, which exceeds those from the EAP, however this is expected due to the inclusion of IFN which is more effective against GT3 infection. The study reported that 69% and 58% of relapsers were cirrhotic and treatment-experienced, respectively.

1.3.2.3 Resistance to NS5A inhibitors

Despite showing excellent potency in replicon-based screens with EC_{50} ranging from 5-50pM in GT1 (Fridell et al., 2010; Gao et al., 2010), resistance develops readily. A number of NS5A inhibitor RAS have been identified in GT1a, 1b and 3a clinical isolates from treatment failure and relapse patients and from *in vitro* selection assays, clustering around residues 28-31 and 93 of NS5A domain I, and these have been corroborated in a great number of studies. The key RAS identified during *in vitro* studies using GT1a, 1b and 3a SGRs and associated culture systems is shown in Table 1-3, Table 1-4 and Table 1-5 respectively. References are contained therein. It is interesting to note that RAS in GT1a and 3a confer a lesser degree of resistance to DCV as a fold-change over wild-type, and a much greater degree of resistance in GT1b. Fold changes in resistance for GT3a are much lower than for GT1 which potentially reflects baseline resistance. A double mutation at residue 30 or 31, with a polymorphism at Y93, is associated with the greatest degree of resistance, between 4000 (Q30R-Y93C in GT1a to DCV) and over 500,000 (L31V-Y93H in GT1b to LDV).

As expected for inhibitors within the same class, RAS which were selected by DCV are cross-resistant to LDV, but no cross-resistance has been observed for other classes of DAA, IFN or RBV. Indeed, RAS may be slightly more sensitive to IFN than wild-type sequences though the reason for this is not known.

The prevalence of each RAS is also a popular research area, with a consensus that NS5A RAS exist in the population at low frequencies, with some variation based on genotype and geographical location, contributing to low-level resistance. High-level RAS such as Y93H vary widely in prevalence based on study up to 31% for a Y93 polymorphism in GT1b (Suzuki et al., 2012; Paolucci et al., 2013; Miura et al., 2014; Walker et al., 2015; Patiño-Galindo et al., 2016; Uchida et al., 2016; Eltahla et al., 2017); combinations of RAS which confer the highest levels of resistance such as a double substitution at residues 30 or 31, and 93 – the natures of which differ greatly by genotype – found rarely (usually <5%) in untreated populations (Miura et al., 2014). Where pre-existing in the population NS5A RAS are stable, while a study found that NS3 and NS5B RAS fluctuate over time, emerging and disappearing at different time points (Eltahla et al., 2017; Kai et al., 2017).

Substitution	**Average EC_{50} fold change [standard deviation] (drug)**	**Fitness (% of wild-type) [standard deviation]**	**References**
Q30R	860 [470] (DCV). 630 (LDV)	41.7 [1.2]	(Gao et al., 2010; Fridell et al., 2011; Sun et al., 2012; Wang et al., 2012; Wang et al., 2013)
Q30E	25,000 (DCV). 950 (LDV)	130	(Wang et al., 2013; Cheng et al., 2016)
L31V	2500 [1700] (DCV)	98 [38]	(Gao et al., 2010; Fridell et al., 2011; Wang et al., 2012; Wang et al., 2013; Liu et al., 2015)
L31M	200 (DCV). 550 (LDV)		(Wang et al., 2013)
Y93H	3400 [2300] (DCV). 2500 [1200] (LDV)	12 [10]	(Fridell et al., 2011; Scheel et al., 2011; Wang et al., 2012; Wang et al., 2013; Liu et al., 2015; Cheng et al., 2016)
Y93C	1900 (DCV)	211	(Gao et al., 2010)
Q30R-L31M	200,000	54	(Wang et al., 2013)
Q30R-Y93H	57,000	6	(Fridell et al., 2011; Wang et al., 2012)
Q30D-Y93N	22,000	15	(Liu et al., 2015)
Q30R-Y93C	4200 (DCV). 1000 (LDV)		(Wang et al., 2013)

Table 1-3. Effect of resistance-associated substitutions in GT1a on NS5A inhibitor efficacies

Substitution	Average EC_{50} fold change [standard deviation] (drug)	Fitness (% of wild-type) [standard deviation]	refs
L31F	15 (DCV)	0.1	(Liu et al., 2015)
L31V	26 [2.3] (DCV). 490 (LDV)	151 [7.5]	(Fridell et al., 2010; Gao et al., 2010; Fridell et al., 2011; Wang et al., 2012; Nitta et al., 2016)
Y93H	30 [22] (DCV). 3500 [3133] (LDV)	22 [13]	(Fridell et al., 2010; Gao et al., 2010; Lemm et al., 2010; Fridell et al., 2011; Wang et al., 2012; Liu et al., 2015; Nitta et al., 2016)
L31V-Y93H	22,000 [18,000] (DCV). 540,000 (LDV)	40 [14]	(Fridell et al., 2010; Nitta et al., 2016)

Table 1-4. Effect of resistance-associated substitutions in GT1b on NS5A inhibitor efficacies

Substitution	Average EC_{50} fold change [standard deviation] (drug)	Fitness (% of wild-type) [standard deviation]	Refs
A30K	52 [11] (DCV). 12 (LDV)	14	(Hernandez et al., 2013; Wang et al., 2013)
L31F	230 [130] (DCV)	152	(Wang et al., 2013)
Y93H	1800 [881] (DCV). 30 (LDV)	33 [15]	(Scheel et al., 2011; Hernandez et al., 2013; Wang et al., 2013; Kylefjord et al., 2014; Liu et al., 2015)

Table 1-5. Effect of resistance-associated substitutions in GT3a on NS5A inhibitor efficacies

The locations of these residues have been mapped onto putative homodimer structures for NS5A domain I, and amino acids 28-30 may form a binding groove into which DCV is predicted to bind (Lambert et al., 2014; Barakat et al., 2015), as shown in Figure 1-9. The precise location of the proposed binding groove so as to include the Y93 residue is not universally agreed, though Barakat and colleagues predicted using a molecular dynamics simulation that DCV binds in the interface contacted by Y93 and R30. Mutation of residues 27 and 28 would change the conformation of the R30 side chain and Y93H would displace the hydrophobic linker of DCV and preclude formation of the hydrogen bond with R30. A different study suggests that this residue does not bind directly to the drug but instead is involved in a communication link with the residues at locations 28-30, and a change of this residue results in

a downstream effect in the ability of the drug to bind to its putative binding site (Lambert et al., 2014). This is in agreement with observations that DCV and similar compounds still bind to a resistant variant and that binding of drug to protein is not sufficient for inhibition (Sun et al., 2015; O'Boyle et al., 2016).

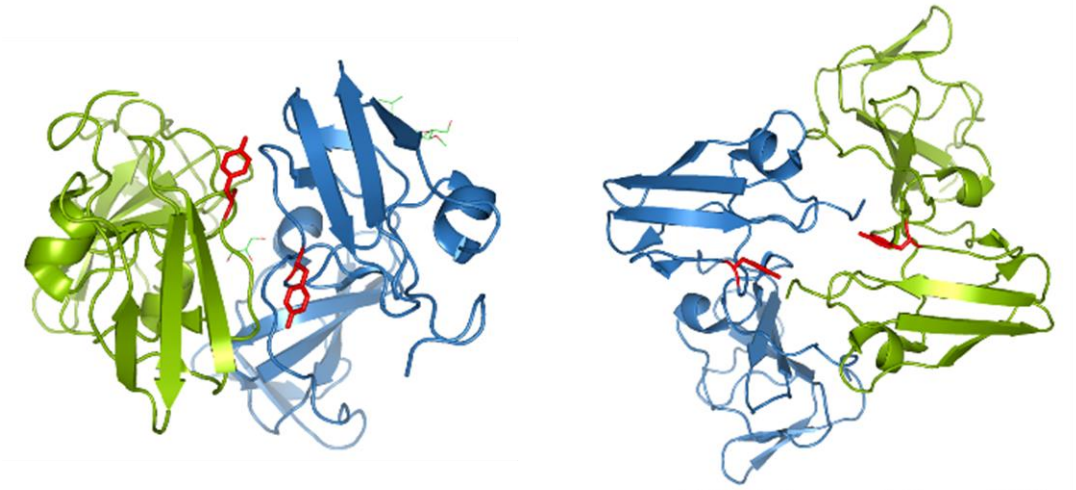

Love *et al; J Virol 2009* Tellinghuisen *et al; Nature 2005*

Figure 1-9. NS5A dimer structures with Y93 shown in red. PDB structures 3FQM and 1ZH1 respectively

There is increasing evidence that NS5A RAS can be associated with a fitness cost to replication which is not apparent in the presence of the drug but results in a decrease in replication capacity in the absence of the drug. *In vitro* studies frequently show that such a fitness cost is only associated with substitutions of Y93H, with RAS at L31 to V in GT1 increasing replication capacity (summarised in Table 1-3, Table 1-4 and Table 1-5 and references therein). Y93H is associated with approximately 20-30% replication capacity of the wild-type, though a single study using infectious virus showed that Y93H mutants have a greater infectivity (Nitta et al., 2016). Given the effects of RAS on the structure of NS5A which was described above a fitness cost is to be expected, however it has also been shown that RAS which emerge on treatment are stable after the cessation of therapy for several years (Yoshimi et al., 2015). A mechanism for the stabilisation of RAS in the absence of selection pressure has not been suggested, though double combinations of Y93H with a L31 or Q30 RAS tend to have a slightly increased replicative fitness compared to the Y93, and a multiple combination of three NS5A RAS identified in the BOSON trial was recently demonstrated to have wild-type replication capacity (personal communication). In addition, it has been suggested that the persistence of RAS could be linked to the immunological selection pressure within the infected patient (Eltahla et

al., 2017). This is of especial interest following a number of studies which highlight an association between Y93H prevalence at baseline and IFNλ4 SNP genotype. Patients with a major genotype (TT at the rs8099917 locus), which is indicative of a favourable response to IFN treatment, are more likely to have a Y93H mutation at baseline, and with this a higher baseline viral load (Miura et al., 2014; Akamatsu et al., 2015; Peiffer et al., 2016; Uchida et al., 2016).

Given the quasispecies nature of a HCV population within an infected cell, substitutions which confer resistance to NS5A inhibitors will naturally occur within the population, and are amplified when the selection pressure of the drug is applied. The genetic barrier to resistance refers to the number of nucleic acid substitutions which results in a RAS, or combination of RAS: the barrier to resistance for NS5A inhibitors such as DCV is very low. For NS5A inhibitors, combinations are possible which confer a high level of resistance but the single Y93H mutation, generated by a single codon change from TAC to CAC, gives a change in EC_{50} of several thousand-fold. In addition to being generated by a single nucleic acid substitution, the Y93H RAS requires a mismatch of U:G, which is the mismatch made most frequently by the NS5B polymerase, resulting in the T to C change – a transition, also more frequently made by the NS5B polymerase than a transversion (Powdrill et al., 2011). Thus, this single RAS has a lower genetic barrier than one which would require a less readily-made mismatch of the polymerase.

The role of these RAS in treatment response is complex. Clinical trials frequently show that prevalence of a RAS reduces the likelihood of achieving SVR though the link is not a causal one. Patients without a RAS are capable of developing one, or a combination, during therapy and patients with a RAS at baseline, including Y93H, have been shown to achieve SVR (Pawlotsky, 2016). A study of the role of emergence of resistance and pre-existence demonstrated that there are two distinct populations of RAS which occur at the end of treatment – those who have a RAS at baseline are likely to maintain it and may acquire additional substitutions, all of which are largely stable. In contrast RAS which emerge on treatment are likely to be more transient in nature, and do not persist to the same extent (Kai et al., 2017). The correlation is doubtless complicated by patient factors which are known to affect treatment response such as presence of cirrhosis, baseline viral load (though this could be linked to a RAS, as described), BMI, gender and race. However, the reason for the inability of *in vitro* inhibitor sensitivity data to recapitulate clinical trial efficacy is not known, nor is it known whether baseline sequencing of patients is of greatest benefit to predict treatment responses. Also of interest in this respect is a study which showed that the passage of HCV 100 times in Huh7.5 cells, in the

absence of DAAs, increasing the replication capacity, induced resistance to multiple classes of DAA in the complete absence of any RAS (Sheldon et al., 2014).

During the investigation of RAS and their phenotype an interesting observation was made, linked to the demonstration that binding to NS5A is not sufficient to cause inhibition. A pair of studies have identified that the resistant phenotype can be reversed by adding a second compound to DCV, one which does not have a pharmacological effect of its own; this is suggested to resensitise the RAS (Sun et al., 2015; O'Boyle et al., 2016). The model for this proposed by the authors is that DCV binding to a multi-NS5A structure induces a conformation change, inhibiting replication. Resistant NS5A is not sensitive to this change but the addition of the synergistic compound acts with DCV to enhance the effect.

1.4 Thesis aims

The aim of this project was to use *in vitro* tools to consider the profound differences which exist between GT3 and other genotypes of HCV, primarily where such differences are involved in the response to NS5A inhibitors. This work intended to investigate such differences in NS5A inhibitor sensitivity in the hope of identifying why the treatment efficacy against GT3 is so profoundly different. In addition, this work aimed to investigate the molecular mechanisms underpinning the development of hepatic steatosis in GT3-infected patients using these *in vitro* tools. To achieve this, the intention was to exploit and develop existing *in vitro* culture systems, primarily the S52 SGR but also involving full-virus culture systems, where available.

The initial purpose of the project was to utilise the wealth of resources in the HCV Research UK biobank to apply any findings as to the nature of such genotype differences in an epidemiological approach. The quasispecies nature of the infected individual could be translated into this *in vitro* system in the form of chimera SGR and virus constructs to investigate the role of genetic diversity in the degree of response to antiviral therapy and to begin to address the complexity of NS5A inhibitor resistance and how it impacts treatment response. It is feasible that further insight into the role of RAS could allow the prediction of patients who are more likely to respond to treatment, and use this information to guide treatment regimens in a personalised approach. In a similar vein, insight into the molecular nature of hepatic steatosis in GT3-infected patients could provide avenues for therapeutic intervention, to treat the symptoms in parallel with treatment of the cause.

Chapter 2: Materials and methods

2.1 Materials

2.1.1 Plasmids

S52 feo (both AII and SHI variants) SGRs were obtained from C. Rice (Saeed et al., 2012). Con1 SGRs with wild-type or CpG/UpA-low luciferase were obtained from P. Simmonds (Witteveldt et al., 2016). Insertion of CpG/UpA-low luciferase into S52 feo required mutation of the last three residues of the 19-residue section of core protein, immediately upstream of the luciferase start codon, from RRP to RRA to introduce a unique AscI restriction site; translation of the reporter was not compromised. Primer sequences available on request. Plasmid containing hSEC14L2 for lentiviral transduction was obtained from P. Simmonds.

2.1.2 Cell lines and reagents

Huh7.5 cells (Blight et al., 2002) were maintained in DMEM containing 4.5g/L glucose, 2mM glutathione and sodium pyruvate (Lonza) supplemented with 10% FBS (Sera laboratories international), penicillin/streptomycin (Sigma) and non-essential amino acids (Lonza) in a humidified 37^{o}C, 5% CO_2 incubator. Huh7.5 cells stably transfected with Parainfluenza virus 5 (PIV-5) V protein (Huh7.5-V) were obtained from S. Griffin. Huh7.5-V cells were maintained in DMEM as described above with 50 ng/mL G418 (neomycin).

2.1.3 Antibodies

Antibodies used for immunoblot and immunofluorescence assays, with corresponding concentrations, are shown in Table 2-1.

Primary antibody	Dilution used	Corresponding secondary antibody	Dilution used
Anti-NS5A serum	1:5000	Anti-sheep 800	1:15,000
Anti-β-actin (Abcam)	1:20,000	Anti-mouse 680	1:15,000
Anti-V5 tag (Cell Signalling Technologies)	1:1000	Anti-rabbit 800	1:15,000
Anti-AMPK-T172(Cell Signalling Technologies)	1:1000	Anti-rabbit 800	1:15,000
Anti-ACC (Cell Signalling Technologies)	1:1000	Anti-rabbit 800	1:15,000
Anti-EGFR (Santa Cruz Biotechnology)	1:500	Anti-mouse 680	1:15,000
Anti-LC3BII (Abcam)	1:1000		
Anti-Akt (Cell Signalling Technologies)	1:1000	Anti-rabbit 800	1:15,000
Anti-GAPDH	1:10,000	Anti-mouse 680	1:15,000

Table 2-1. Antibodies used for immunoblot assays

2.1.4 Clinical isolates

Samples from were obtained from the HCV Research UK Biobank. Patients with HCV GT3 were enrolled in the NHS Extended Access Program (Foster et al., 2016).

2.2 Methods

2.2.1 DNA and RNA manipulation methods

2.2.1.1 Plasmid DNA manipulation

2.2.1.1.1 Amplification and purification of plasmid DNA

Plasmid DNA was transformed into z-competent DH5α *E. coli* cells and recovered for 1h at 37°C in LB medium before being plated onto agar plates containing the appropriate selection antibiotic before being cultured for two days at 30°C. Single colonies were picked into LB medium containing the appropriate antibiotic and cultured overnight at 30°C with 200 rpm

agitation. Cultures were centrifuged at 4000 xg for 15 minutes at 4°C to pellet cells and extracted using the GeneJET plasmid miniprep/midiprep alkaline lysis and purification kit (Thermo Fisher). Plasmid DNA was stored as glycerol preparations in 20% (v/v) glycerol in LB medium at 80°C, or in water at -20°C.

2.2.1.1.2 Site-directed mutagenesis

Site directed mutagenesis (SDM) was performed using the QuickChange protocol from Stratagene. Briefly, 25 ng plasmid DNA was amplified using complimentary primers designed to anneal at the mutation site and containing the mutated nucleotide. Amplifications were performed using Pfu Ultra (Agilent) according to the manufacturers' instructions with the following exception: an annealing temperature of 55°C was used for the first five cycles followed by 58°C for the following 13 cycles. The PCR product was digested with DpnI to degrade the methylated input DNA and transformed into DH5α cell for screening on antibiotic agar plates. More recently, SDM was performed using the Q5 kit (NEB) according to the manufacturer's instructions. This involved the design of primers that amplified a linear product which was then ligated before DpnI digestion and transformation as described above.

2.2.1.1.3 Molecular subcloning

Molecular subcloning was carried out according to standard techniques. Plasmid DNA was digested using NEB restriction enzymes according to the manufacturer's instructions, with a ratio of 2 units of enzyme per 1 µg DNA and digested for 1h for diagnostic digests and 2h for subcloning applications. Digested DNA was resolved on 0.7% agarose gel and DNA fragments were purified from excised bands using a commercial kit (Qiagen). DNA fragments were ligated at a 3:1 molar ratio of insert to vector using T4 DNA ligase (NEB). Ligation reactions were transformed into DH5α for screening by antibiotic agar plates as described. Modified SGRs were verified by sequence analysis from Beckman Coulter genomics.

2.2.1.2 RNA synthesis and SGR electroporation in cultured cells

SGR plasmids were linearised with XbaI (New England Biolabs) and linear SGR DNA was transcribed using a T7 transcription kit (Promega) according to the manufacturer's instructions. Integrity and concentration of RNA transcripts was verified using 1% MOPS-agarose-formaldehyde gel. 2 µg RNA transcripts were transfected into $2x10^6$ cells in diethyl pyrocarbonate (DEPC)-phosphate-buffered saline (PBS) by electroporation using a square-wave protocol at 260 V for 25 ms.

2.2.1.3 RNA extraction from cells and non-quantitative PCR

Cells were harvested in TRIZol (Invitrogen Life Technologies) and RNA purified according to manufacturers' instructions. 1 µg RNA was reverse-transcribed using Superscript II (Invitrogen) and random hexamer primers. 2 µL of this cDNA was used as a template for PCR amplification using Vent polymerase according to the manufacturers' instructions. DNA fragments were resolved on 1% agarose gel.

2.2.1.3.1 PCR sequencing of SGR RNA

For Sanger sequencing of SGR RNA, primer pairs (Table 2-4) were designed to amplify 800-900 bp overlapping fragments which were sequenced as a single consensus by Beckman Coulter Genomics (Genewiz) then aligned on DNA Dynamo (Blue Tractor Software) using the S52 SGR sequence as a reference.

2.2.1.3.2 PCR amplification of NS5A domain I coding region from patient serum samples

Virus RNA from HCV-infected patient serum samples (outlined in 2.1.4) was extracted using the Qiagen QIAmp Virus RNA kit, according to the manufacturers' instructions. Briefly, 140 µL serum was extracted and eluted twice in 30 µL elution buffer. 12 µL of this eluate was reverse transcribed using Superscript III (Invitrogen) and gene-specific reverse primer (NS5A_Nest_R, detailed in Table 2-2). 2 µL cDNA was used as a template for the first step of a nested PCR using Vent polymerase according to the manufacturers' instructions with the addition of 2 mM $MgCl_2$, using the Nest_F and Nest_R PCR primers detailed in Table 2-2. 2 µL of this first-step cDNA was used as a template for the second step of nested PCR without the addition of $MgCl_2$, using the NS5A_Bsu_F and NS5A_Psp_R primers.

2.2.1.4 Preparation of shuttle vector for insertion of NS5A domain I from patient sequences

The S52 SGR was modified to contain a pair of unique restriction sites, Bsu36I and PspXI, flanking the NS5A domain I coding region to allow insertion of the corresponding sequence amplified from patient serum samples detailed in 2.1.4. The experimental strategy required the expansion of SGR DNA containing NS5A from patient sequences as a mixture to maintain the quasispecies nature of the clinical NS5A sequence. To ensure that any carry-over of vector from the ligation was not replication competent a short stuffer fragment was inserted. To achieve this, short, complimentary oligonucleotides were designed (Table 2-3), to anneal together with overhanging sequences at either end corresponding to the restriction sites at the 5' and 3' ends of NS5A domain I: Bsu36I and PspXI respectively. Oligonucleotides were

diluted to 50 µM in T4 DNA ligase buffer, mixed in a 1:1 ratio and heated to 95°C in a heat block. The heat block insert was removed from the heating module and left to cool for approximately 60 minutes until it had reached room temperature, after which it was ligated into the S52 SGR.

Primer name	Sequence	T_m (°C)
NS5A_Nest_F	CGCCATACTATCTCCGGGGC	60
NS5A_Nest_R	CCTTCACCCTAGAC	44
NS5A_Bsu_F	CACAAGTCTCCTCAGGCGGTTACACAAG	62
NS5A_Psp_R	GGAGGGGACCCTCGAGCAAGGCGGCGC	73

Table 2-2. Primer sequences for reverse-transcription and amplification of NS5A from patient serum samples

Olio name	Sequence	T_m (°C)
Stuffer_frag_F	TCAGGGCGATACGCCGAACGATCGCAC	68
Stuffer_frag_R	TCGAGTGCGATCGTTCGGCGTATCGCCC	68

Table 2-3. Sequences of oligonucleotides to produce the stuffer fragment to replace NS5A domain I.

Primer name	Sequence	T_m (°C)
NS3-5B_1F	TGCTTTACATGTGTTTAGTCGAGGTTAAAAAAACG	59
NS3-5B_1R	GGTCGGGGCATGAAGGTACCCTACTTGAT	62
NS3-5B_2F	CAGCGGTAAGAGCACAAAGGTCCCGGCCGC	69
NS3-5B_2R	CCCGTACGGCCACGACGTTGGCTGCGGGAAA	71
NS3-5B_3F	TACCGATATGTTGCCCCGGGTGAAAGACC	63
NS3-5B_3R	CCTTGAACTGGTGGGCGATTGCCTGAGC	65
NS3-5B_4F	TAGGACTGCTGCAGCGAGCCACCCAGCAAC	69
NS3-5B_4R	CCGCCGGAGCAGACTTGTGACAGTTAGAGAAC	65
NS3-5B_5F	GAAGACTACCCAAGCCCTTGCAGCGGCGATTGG	68
NS3-5B_5R	GCCGTCTCGGCGGTGATATGAGAAGGGTCTCTC	67
NS3-5B_6F	TCCCCTCCATCAGAGGCAAGCTCATCCGCC	68
NS3-5B_6R	CCCGGCTCTCCCTCGAGAGGAGGCATGG	68
NS3-5B_7F	TCGACACACAGTCCAGCACTACCTCCAGG	64
NS3-5B_7R	CCCCCAGATCAGGGTACACAATGAGGCGA	64
NS3-5B_8F	TGGCGAAGAACGAGGTGTTTTGTGTGGACC	64
NS3-5B_8R	CGTGCTACGGAGACGTTAGAGGAGCAAGATG	63
NS3-5B_9F	GACCAGGTACTCTGCTCCACCCGGAGATGC	66
NS3-5B_9R	GGAGTGTTATCCTACCAGCTCACCGAGCTGGC	66

Table 2-4. PCR amplification primers for Sanger sequencing of the S52 SGR. F and R refer to forward and reverse primers to be used in pairs.

2.2.1.5 Next generation sequencing (NGS)

Viral RNA was extracted from cells stably expressing S52 SGR using the RNeasy plus mini kit (Qiagen). PCR amplification and NGS was performed as previously described (Thomson et al., 2016) with modifications. Briefly, the SGR was amplified using HCV gt3a genotype specific primers for four overlapping amplicons spanning the HCV gt3a non-structural genes. The forward primers for the NS3_4A fragment were redesigned to be complimentary to the EMCV IRES region of the SGR (supplementary table – for primers). SGR RNA was amplified by single-step RT-PCR (Superscript III Reverse Transcriptase, Invitrogen), followed by nested or semi-nested PCR. PCR products were purified using the QIAQuick kit (QIAGEN) and quantified by Qubit® dsDNA Broad Range and High Sensitivity Assay Kits and the Qubit® 2.0 Fluorometer (Life Technologies). Alternate amplicons were pooled in two reactions of equimolar amounts and 1

ng/µl of the pooled DNA was used for library preparation (Nextera XT DNA sample preparation kit; Illumina) according to manufacturer's instructions. Indexed libraries were sequenced using Illumina MiSeq deep sequencing reagent kit v2 (Illumina).

2.2.1.6 Quantitative PCR

Following extraction and quantification of RNA from SGR-harbouring cells, 200 ng was used as a template for a Taqman probe-based, one-step qRT-PCR assay as described previously (Takeuchi et al., 1999). A standard curve of *in vitro*-transcribed S52 SGR RNA, with a concentration verified by MOPS-agarose-formaldehyde gel, was used to convert cycle threshold values (Ct) to relative RNA copies; normalised to the amount of input RNA.

2.2.2 Cell culture methods

2.2.2.1 Selection of stable SGR-harbouring cells

Selection of stable, SGR-harbouring cells, 10^6 electroporated cells were seeded into 10 cm^2 dishes and selected with 50 ng/mL G418 (neomycin) from 48 hours post-electroporation. Surviving cells were pooled into polyclonal popluations for further analysis.

2.2.2.2 Transient replication assays

Electroporated cells were seeded in white 96-well plates at a density of 10,000 cells per well in 4 assay replicates for each. Following incubation cells were washed with PBS and lysed in 30µL passive lysis buffer (PLB, Promega). Luciferase activity was measured on a FLUROstar Optima plate reader (BMG Labtech) primed with Luciferase Assay Reagent I (LAR I, Promega).

2.2.2.3 Colony formation assay

For colony formation assays, $1x10^5$ electroporated cells were seeded in 6-well plates and selected with G418 as described above from 48 hours post-electroporation. After three weeks surviving cells were stained with crystal violet (10% crystal violet with 4% PFA in PBS) and counted manually.

2.2.2.4 Lentiviral transduction and maintenance of modified cell lines

Lentiviruses were generated using a containing hSEC14L2 as reported by (Witteveldt et al., 2016) and both Huh7.5 and Huh7.5-V cell lines were separately transduced. Transduced Huh7.5 cells were selected with 2 µg/mL puromycin; surviving cells were pooled into a polyclonal population and were termed Huh7.5-SEC14 cells. Transduced Huh7.5-V cells were selected with both G418 and puromycin; cells surviving double selection were pooled into a

polyclonal population and termed VSEC cells. Huh7.5-SEC14 cell lines were maintained in 1 µg/mL puromycin and VSEC cells were maintained in 50 ng/mL G418 and 1 µg/mL puromycin.

2.2.2.5 Antiviral treatment

2.2.2.5.1 Antiviral treatment of stable, SGR-harbouring cells

$8x10^3$ cells of each type were seeded into white 96-well plates and treated with indicated concentrations of Daclatasvir, Ledipasvir (both SelleckChem), Sofosbuvir (Gilead) or RBV (fluorochem ltd) in duplicate with 0.25% (v/v) final DMSO for 48 hours before being harvested for luciferase as described above.

2.2.2.5.2 Antiviral treatment of transiently-replicating SGR

VSEC cells (described above) were electroporated with 2 µg SGR RNA transcripts and 10^4 electroporated cells were seeded into white 96-well plates. Cells electroporated with Con1 and JFH-1 were treated with indicated concentrations of each compound in duplicate with 0.25% (v/v) final DMSO at 4 hours post-electroporation for 72 hours. Cells electroporated with S52 wild-type and Y93H were treated at 24 hours post-electroporation for 72 hours, following preliminary observation that replication is not reliably detected until 96 hours post-electroporation. This allowed a constant treatment duration of 72 hours for all electroporated cells. Cells were harvested for luciferase after 72 hours treatment as described above.

2.2.2.6 MTT assay

Electroporated or stable SGR-harbouring cells were seeded into clear 96-well plates for antiviral treatment as described above. Following the indicated incubation periods drug media were aspirated and replaced with MTT reagent (3-(4,5-dimethylthiazol-2-yl)-2,5-diphenyltetrazolium bromide) at 1 mg/mL (w/v) in serum-free DMEM. Plates were incubated at 37°C for one hour; after this period the MTT reagent was aspirated and cells lysed in 100 µL DMSO to dissolve the formazan pigment. Absorbance was measured at 570 nm.

2.2.2.7 Treatment with AMPK inhibitors

SGR-harbouring cells were seeded at a density of $2x10^5$ cells per well of a 6-well plate and serum-starved for 24h in DMEM supplemented with penicillin/streptomycin and non-essential amino acids. Cells were then treated with 0, 1 or 10 mM metformin (Sigma) for 48 hours before being harvested for western blotting in 200 µL PLB supplemented with protease and phosphatase inhibitors. Western blotting was carried out as described below and luciferase activity was measured in 20 µL of the PLB lysate.

2.2.2.8 Cell growth assay

Cells were seeded at a density of $1x10^5$ cells per well of a 6-well plate and cultured for 24, 48 or 72 hours before being trypsinised from the well and counted using trypan blue exclusion.

2.2.3 Protein detection and visualisation methods

2.2.3.1 Immunoblotting

Cells were washed twice in PBS and lysed in Glasgow Lysis Buffer (GLB; 1% [vol/vol] Triton X-100, 120 mM KCl, 30 mM NaCl, 5 mM MgCl2, 10% [vol/vol] glycerol, 10 mM PIPES [piperazine-*N*,*N*'-bis(2-ethanesulfonic acid)]-NaOH, pH 7.2, with protease and phosphatase inhibitors), and clarified by centrifugation at 2,800 × *g* for 5 min at 4°C. Protein concentration was measured for normalisation by bicinchoninic acid assay (BCA, Pierce). Proteins were resolved on 7.5% polyacrylamide gel before being transferred to polyvinylidene difuoride (PVDF) membrane. Membranes were blocked in 50% (v/v) Odyssey blocking buffer (LI-COR) in Tris-buffered saline (TBS) and incubated in primary antibodies overnight at 4˚C and infra-red tagged secondary antibodies (LI-COR) at room temperature for one hour. Membranes were imaged using a LI-COR Odyssey infra-red imaging system.

2.2.3.2 Immunofluorescence

Cells were washed once in PBS, fixed for 10 minutes in 4% (w/v) paraformaldehyde (PFA) and permeabilised in 0.1% (v/v) Triton X-100 in PBS. Fixed cells were immunostained with anti-NS5A (as described above) at 1:2000 or BODIPY at 1:5000, washed three times in PBS, then subjected to a secondary stain of anti-sheep (488 nm, AlexaFluor) before being washed three times more. Cells were mounted using Prolong Gold antifade mountant with DAPI and imaged using a Carl Zeiss LSM 700 inverted microscope and Zeiss Zen 2012 software.

2.2.3.3 Flow cytometry

Cells were washed once in PBS by centrifugation, fixed for 10 minutes in 4% (w/v) paraformaldehyde (PFA) and permeabilised in 0.1% (v/v) Triton X-100 in PBS. Fixed cells were washed in PBS then immunostained with anti-NS5A or BODIPY (as described above) at 1:2000 and 1:5000 respectively followed by anti-sheep (488 nm, AlexaFluor). All incubation and wash steps were carried out in suspension followed by centrifugation at 1000x G for three minutes. Stained cells, and appropriate unstained and monostained controls, were resuspended in PBS and analysed using a BD LSR Fortessa flow cytometer. Cells were gated based on forward and side scatter, to eliminate excessively large or small objects, and sensitivity parameters were optimised for each cell type using the unstained and monostained controls. Data were analysed using DiVa6 software

2.2.4 Infectious virus methods

2.2.4.1 Culture of infectious virus

Huh7.5 or VSEC cells were electroporated with 10 µg RNA transcribed from infectious virus plasmid DNA as described above. Electroporated cells were resuspended in 10 mL complete DMEM supplemented with 2.5 mM HEPES and virus supernatants were aspirated every 48 hours for titration.

2.2.4.2 Titration of infected cells

Huh7.5 cells were seeded at a density of $8x10^3$ cells in each well of a clear, 96-well plate and left to settle for 15 hours. Virus supernatants were serially diluted 1/2 and 100 µL of each dilution including undiluted supernatant was added to the seeded Huh7.5 cells before being incubated for 48 hours. Infected cells were washed with PBS, fixed with 4% paraformaldehyde and permeabilised with 0.1% Triton-X 100. Fixed cells were immunostained with anti-NS5A (as described above) at 1:2000 and anti-sheep (594 nm, AlexaFluor) at 1:500. Immunostained cells were imaged using the Incucyte ZOOM system (Essen Bioscience) using a 10x objective and the Incucyte software was used to calculate the number of red fluorescent objects from an average of four non-overlapping fluorescent images. This was extrapolated to calculate the number of red fluorescent objects in each well and hence as the number of focus forming units (ffu) per 100 µL diluted supernatant. FFU/mL of each undiluted supernatant was calculated by adjusting for dilution and calculating an average of each dilution.

Chapter 3: Development of Cell Culture Systems for HCV Genotype 3

3.1 Introduction

Development of new therapies has relied upon the sub-genomic replicon (SGR) system which was first reported for GT1b (Lohmann et al., 1999). Subsequently the efficiently-replicating GT2a isolate JFH-1 (Kato et al., 2003) has become widely used throughout the field of HCV research. Initially the SGR constructs contained a neomycin phosphotransferase selectable marker allowing the establishment of stable cell lines harbouring the SGR. However, critical for the development of DAAs was the availability of a transient, luciferase-based, SGR. Such a system does not yet exist for GT3. Three separate GT3 SGRs derived from two different patient isolates have been reported but none of these show robust levels of replication in short-duration, transient experiments. The S52 SGR replicates to high levels during selection and generates levels of HCV RNA comparable to JFH-1 but has not been demonstrated to robustly replicate transiently using a luciferase reporter (Bukh et al., 1993; Saeed et al., 2012). The S310/A SGR has been shown to replicate transiently but luciferase levels were several orders of magnitude lower than the input translation (Saeed et al., 2013), and another S52-based SGR which was culture-adapted in Lunet cells showed detectable levels of replication at 7 days post-transfection (Yu et al., 2013).

The majority of studies with GT3 have thus far used chimeric SGRs, in which fragments of GT3 isolates or consensus sequences were used to replace the corresponding coding regions in efficiently-replicating GT1 or GT2 backbones. These have been used to show differential sensitivity to NS5A and NS5B inhibitors *in vitro* of GT3 sequences compared to wild type controls (Lanford et al., 2006; Wang et al., 2013; Kylefjord et al., 2014). Chimera SGRs are limited in that they do not allow study of the cognate interactions between viral proteins in the replication complex and this may provide a hindrance to development of combination therapies. An intact (non-chimeric) GT3 SGR that replicates transiently would be of benefit to understand the baseline resistance of GT3 to the DAAs, and for development of new DAAs with efficacy against GT3.

Infectious virus systems are immensely important in translating the findings of experiments using SGRs into a more clinically relevant format. SGRs allow the study of genome replication in a non-infectious system but cannot take into account the entry, genome uncoating, genome delivery, assembly and egress stages of the virus life cycle. The relationship between HCV and host cell lipids, notably the organisation of the membranous web, lipid accumulation and influence in autophagy pathways (discussed in chapter 5) is tightly associated with cellular lipids (Alvisi et al., 2011). Though the non-structural proteins play roles in these pathways, it is

reported that accumulation of lipids in infected cells requires the core protein, which SGRs lack (Barba et al., 1997; Jhaveri et al., 2009; Kim et al., 2009).

Infectious virus systems for GT3 almost exclusively consist of chimeras, with the GT3 structural and nonstructural proteins expressed in various combinations with the remaining genome regions from JFH-1, which replicates to much higher levels. The first of these contained the core, E1, E2, p7 and NS2 of S52, to investigate genome differences in protease inhibitor efficacies, and was gradually developed to contain all but NS5B and 3' UTR from S52 (Gottwein et al., 2007). However, the recent DBN3a virus, the first fully GT3 infectious virus, replicates to comparable levels to JFH-1 (Ramirez et al., 2016). This chapter details the work to develop one such GT3 virus for use in inhibitor sensitivity studies.

3.2 Results

3.2.1 Establishment of a transient replication assay for HCV GT3a.

3.2.1.1 The S52 SGR

The S52 GT3a SGR (Saeed et al., 2012) was assembled from a consensus full-length DNA clone of the S52 clinical isolate (Gottwein et al., 2010) and consists of a bicistronic construct containing a neomycin phosphotransferase/firefly luciferase (Feo) reporter under the translational control of the HCV internal ribosome entry site (IRES) together with the NS3-5B coding region under the control of an EMCV IRES. Two variants were received, with different CAS: The AII variant contains (by H77 numbering) T1056A, T1429I, and SHI contains P1220S and D1430H, all within NS3. In addition, both SGR variants contain the S2204I NS5A culture-adaptive mutation which has shown to be crucial to replication.

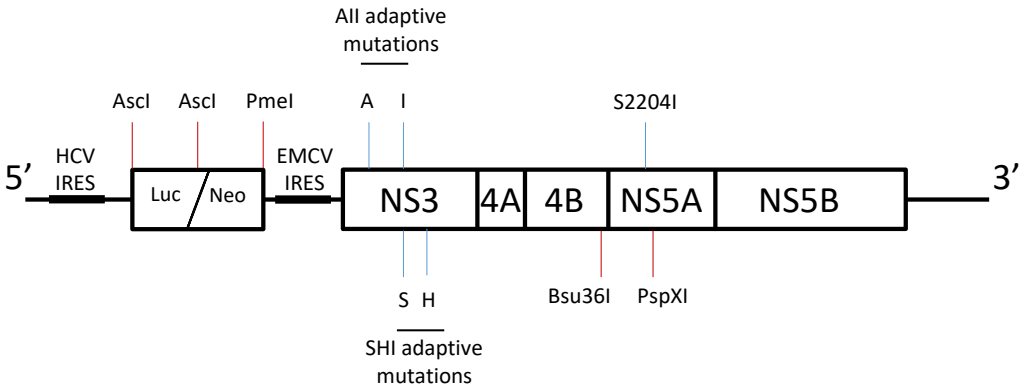

Figure 3-1. Diagram of the S52 SGR.

Features of the SGR are labelled: Luc/Neo (luciferase-neomycin phosphotransferase fusion) and HCV non-structural proteins (NS3, NS4A, NS4B, NS5A, NS5B). AII (T1056A, T1429I) and SHI (P1220S, D1430H) CAS labelled with blue lines, restriction sites labelled with red lines. S2204I adaptive substitutions and restriction sites common to both variants

3.2.1.2 Transient replication of the S52 SGR

To test for transient replication of the S52 SGR, RNA transcribed *in vitro* from DNA of both variants of the S52 SGR was transfected into Huh7.5 cells, which have a defect in innate immune sensing due to a mutation in the RIG-I cytosolic sensor (Sumpter et al., 2005; Foy et al., 2005). Replication was compared to the positive control of transient replication, JFH-1 which replicates efficiently (Kato et al., 2003), and a negative control of JFH-1 and S52 SGR with a triple point mutation at the active site of the RdRP of GDD to GNN to render it inactive.

Cells were electroporated with *in vitro*-transcribed RNA and harvested for luciferase assay. Luciferase was measured at 4 hpe to assay translation of the transfected RNA and at 48 and 72 hpe to assay replication. As shown in Figure 3-2 the S52 SGRs were translated but neither were able to replicate to detectable levels in Huh7.5 cells.

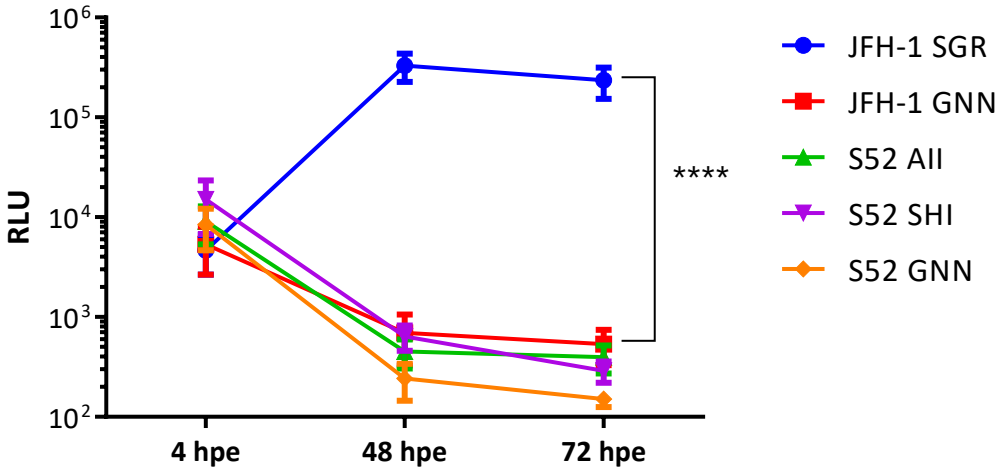

Figure 3-2. The S52 SGR does not replicate in transient assays. 2 µg of the indicated RNAs were electroporated into Huh7.5 cells and harvested for luciferase at the indicated time points. Error bars show standard error of the mean of three experimental repeats. ****p≤0.0001

3.2.1.3 Construction and application of a GT3a NS5A chimera SGR

A fully GT3 (non-chimeric), transiently-replicating SGR was of the greatest use to my project. Nevertheless, a number of additional approaches were explored to establish a functional replication assay in the event that the full-length S52 SGR was unable to replicate. The first of these was a chimeric construct with S52 NS5A in a JFH-1 backbone, unique BamHI and AfeI restriction sites were engineered flanking the NS5A coding region. These modifications have previously been shown to have no effect on replication of the SGR, which was termed mSGR (Hughes et al., 2009b). Primers were designed to amplify the S52 NS5A coding region as well as introduce flanking BamHI and AfeI restriction sites. The amplified NS5A fragment was subcloned into the mJFH-1. The chimera SGR, named mJFH-1/S52-5A, was confirmed by DNA sequencing analysis.

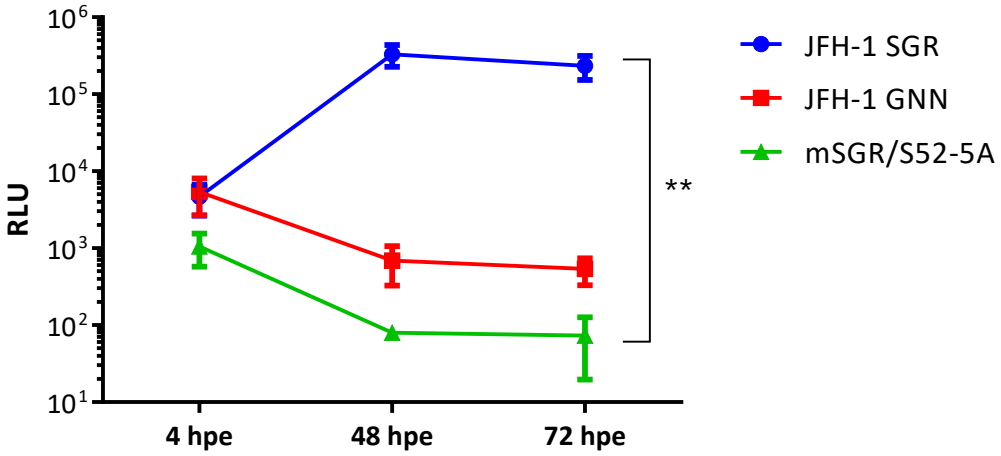

Figure 3-3. A GT3 NS5A chimera SGR does not replicate transiently. 2 µg of the indicated RNAs were electroporated into Huh7.5 cells and harvested for luciferase at the indicated time points. Error bars show standard error of the mean of two experimental repeats. **p≤0.01

In vitro transcribed RNA from this SGR was electroporated into Huh7.5 cells and cells were harvested for luciferase assay at 4, 48 and 72 hpe. As shown in Figure 3-3 luciferase was detected at 4 hpe indicating that the transcript was translated successfully, but no signal at 48 or 72 hpe was detected indicating that the chimera SGR was not able to replicate transiently.

3.2.1.4 Colony formation assay to quantify replication

The other such approach was a colony formation experiment. The initial replication assays of HCV SGRs were in the form of a colony formation assay using the antibiotic resistance marker NPT (Lohmann et al., 1999). This technique was used to assay S52 SGR replication using a S52 NPT-only SGR (termed S52 neo). This experiment was carried out as a proof-of-concept using the S52 AII SGR only. To construct this SGR, a second AscI restriction site was inserted to accompany the site already present between the luciferase and NPT coding regions of the feo reporter. This required mutation of the last of the 19 residues of core which the SGR contains (because the first few residues of core form part of the IRES). The ability of the reporter to be translated in light of this change was ensured using the modified luciferase reporter which was inserted for the purposes of the work in 3.2.1.5 and Figure 3-5. The two AscI restriction sites were used to excise the luciferase coding region from the feo SGR. 2µg of RNA transcribed from S52 neo was electroporated into Huh7.5 cells and selected with G418 for three weeks.

Surviving colonies were fixed and counted and this data is shown in Figure 3-4. As the data shows quantification of replication of the S52 neo SGR was possible using this approach.

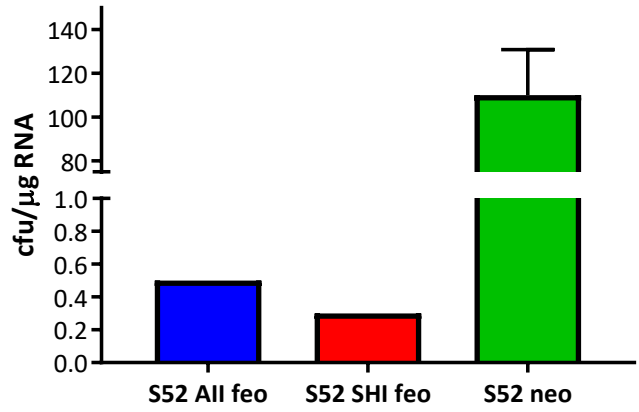

Figure 3-4. Colony-formation assay for replication of S52 SGR. 2 µg of the indicated RNAs were electroporated into Huh7.5 cells and seeded at a density of $1x10^5$ in a 6-well plate. 48 hours after electroporation the cells were selected with 50ng/mL G418 for three weeks, re-treating with G418 every 48 hours. Following selection, colonies were fixed and stained with 10% PFA in crystal violet, then counted manually and expressed as colony forming units per 100 ng RNA electroporated.

3.2.1.5 CpG/UpA dinucleotide frequency optimisation

Luciferase is an insect-derived gene and as such has a higher frequency of CpG/UpA dinucleotides than mammalian genes or viruses with mammalian hosts. It has been previously shown (Atkinson et al., 2014; Tulloch et al., 2014) that reduction of the CpG/UpA dinucleotide frequency of the luciferase reporter can improve replication efficiency. The low CpG/UpA luciferase reporter (CpGluc) was obtained from P. Simmonds and was inserted into the S52 SGRs using flanking AscI/PmeI restriction sites matching those inserted at the 5' end of the firefly luciferase coding region and already present at the 3' end of the NPT coding region, respectively. Replication of these modified SGRs was compared to the GT1b SGR Con1, replication of which is significantly increased by the presence of the CpGluc reporter. As evident in Figure 3-5 the CpGluc reporter significantly enhanced replication of Con1 in Huh7.5 cells but did not exert this same effect on S52.

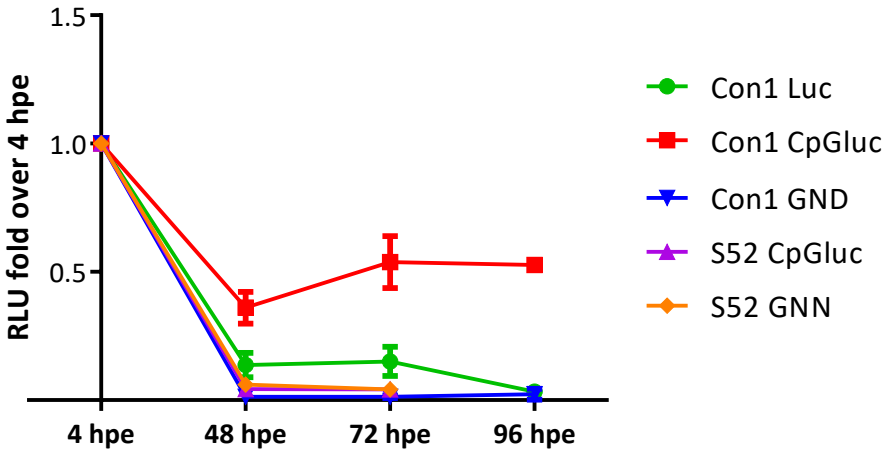

Figure 3-5. The low CpG/UpA dinucleotide luciferase reporter increases Con1 but not S52 SGR replication. The low CpG/UpA dinucleotide luciferase (CpGluc) coding region was inserted into the S52 SGR in place of the feo cassette. 2 µg of *in vitro*-transcribed RNA from this construct and Con1 CpGluc controls were electroporated into Huh7.5 cells and harvested for luciferase at the indicated time points. Relative luciferase units are expressed as the ratio to 4 hpe. Error bars show standard error of the mean of two experimental repeats.

3.2.1.6 Modification of the host cell environment

An alternative approach to establish transient replication of the S52 SGR was to modify the host cell environment in order to increase the permissibility of the host cell for viral genome replication. To achieve this, two approaches were evaluated: firstly, expression of the V protein from parainfluenza virus type 5 (PIV5) – a well characterised interferon antagonist (Poole et al., 2002; Andrus et al., 2011). Secondly, expression of the host cell protein SEC14L2 or Tocopherol-associated protein, TAP1 (Saeed et al., 2015). SEC14L2 has been reported to enable replication of non-culture adapted SGRs.

Therefore, Huh7.5 cells expressing the PIV5 V protein were obtained from S. Griffin, which were transfected with an expression plasmid containing the PIV5 V protein coding region (Poole et al., 2002) under the control of G418 selection. In parallel, Huh7.5 cells were transduced with SEC14L2 using a lentiviral vector under the control of puromycin selection. In addition, Huh7.5V cells were also transduced with SEC14L2 – these were termed VSEC cells. To verify the presence of the respective transfected or transduced genes each cell line was analysed by immunoblot for PIV5 V protein expression and RT-PCR for SEC14L2 RNA (due to

the lack of a suitable antibody for SEC14L2. In addition, the additional effect of the PIV5 V protein on attenuation of IFN signalling was verified using an IFN-inducible system; this was suggested by the reviewers of the publication which reports the work of this chapter to address a concern that, since the Huh7.5 cells already have an impaired innate immune response, the additional presence of the V protein may not attenuate this further. The experiment was carried out by another author of the publication. The effect of these two proteins on transient replication of a GT1b (Con1) SGR was investigated (Kelly et al., 2017).

As expected (Witteveldt et al., 2016), the Con1 CpGluc SGR replicated better than a wildtype luciferase version in Huh7.5 cells. In addition, the presence of either PIV5 V or SEC14L2 enhanced replication of both the wildtype and Con1 CpGluc, and the presence of both proteins had an additive effect. However, the presence of PIV5 V, SEC14L2 or both were not sufficient to support replication of the S52 CpGluc SGR.

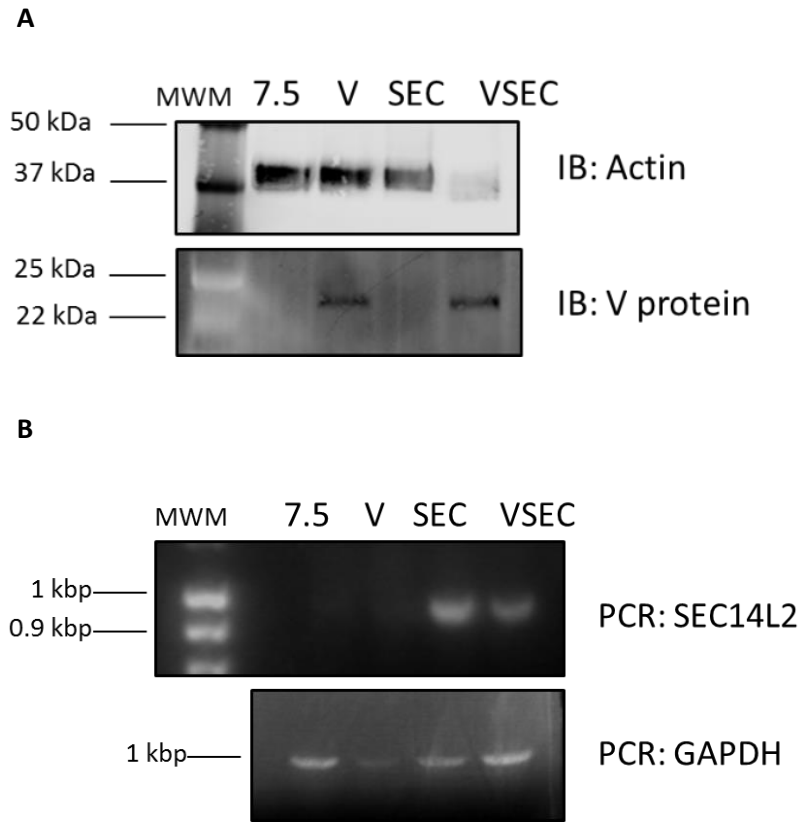

Figure 3-6. Huh7.5 V, Huh7.5 SEC14L2 and VSEC cells express the corresponding transgenes. (A) Protein lysate from all four cell lines was immunoblotted for V protein and β-actin. (B) RNA extracted from all four cell lines was reverse transcribed and used as a template for PCR amplification of SEC14L2 or GAPDH cDNA.

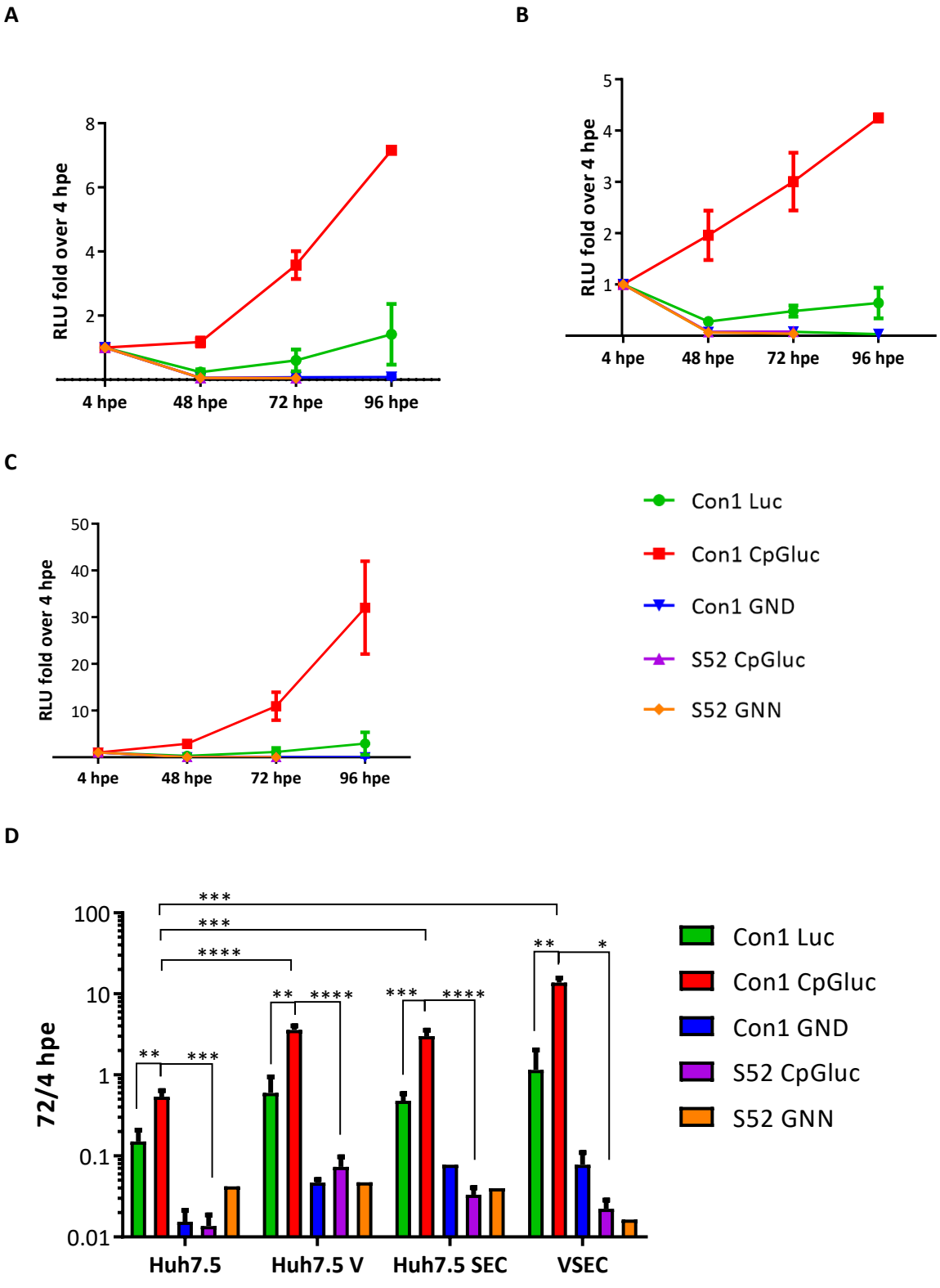
A
B
C
D
RLU fold over 4 hpe
4 hpe
48 hpe
72 hpe
96 hpe
Con1 Luc
Con1 CpGluc
Con1 GND
S52 CpGluc
S52 GNN
72/4 hpe
Huh7.5
Huh7.5 V
Huh7.5 SEC
VSEC

Figure 3-7. PIV5, SEC14L2 and the combination thereof improve replication of Con1 but not S52 SGR. (A). 2 μg of the indicated SGR RNA transcripts were electroporated into Huh7.5 expressing PIV V protein, (B) Huh7.5 transduced with SEC14L2, and (C) Huh7.5 both expressing PIV V protein and transduced with SEC14L2 (termed VSEC cells). (D) For comparative purposes, all data were combined on to a single graph. Cells were harvested for luciferase assay at the indicated time points. Relative luciferase units are expressed as the ratio to 4 hpe. Error bars represent the standard error of the mean of 4 experimental repeats. *p≤0.05; **p≤0.01; ***p≤0.001; ****p≤0.0001.

3.2.2 Selection and characterisation of S52 feo SGR-harbouring cells

3.2.2.1 Selection of S52 feo SGR harbouring cells

The S52 SGR contains a NPT antibiotic resistance marker which permits the selection of stable, SGR-harbouring cell lines. It was hypothesised that the S52 SGR might undergo further adaptation when SGR-harbouring cells were selected, and additional mutations occurring in these stably-replicating SGRs may permit transient replication of the SGR.

Both S52 feo SGRs were *in vitro*-transcribed and 10 μg of these transcripts were electroporated into Huh7.5 cells. Electroporated cells were seeded at a density of $1x10^6$ cells in each well of a 10 cm dish and selected with G418 from 48 hpe for three weeks. Surviving colonies were pooled into a polyclonal population; five colonies survived of S52 AII-electroporated cells, and three colonies of S52 SHI-electroporated cells, giving an estimated colony-formation efficiency of 0.5 and 0.3 cfu/μg RNA respectively.

To confirm that the selected cell population were harbouring the S52 SGR, luciferase activity was evaluated in a population of these cells (Figure 3-8). The S52 AII SGR harbouring cells express a slightly higher luciferase level than S52 SHI, though this is not significant.

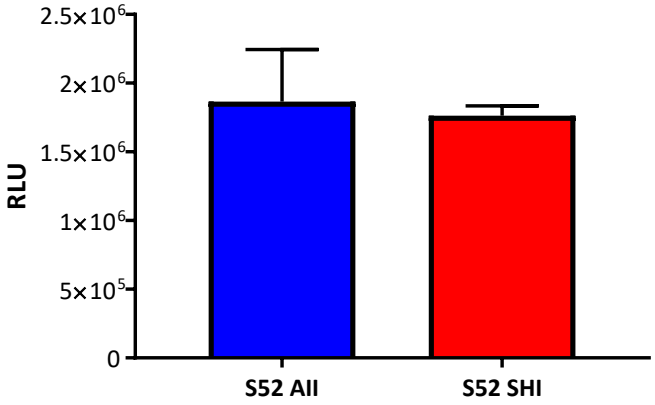

Figure 3-8. Selected, putative SGR-harbouring cell lines possess luciferase activity. 10 µg S52 SGR RNA was electroporated into Huh7.5 cells and selected with 0.5 mg/ml G418 from 48 hpe. Surviving colonies were pooled into a polyclonal population of SGR-harbouring cells. Luciferase activity was measured in $1.1x10^4$ cells.

3.2.3 Characterisation of SGR replication in SGR-harbouring cells

Due to the higher colony formation efficiency of S52 AII compared to SHI, and the higher luciferase expression, it was decided to focus on this variant of the S52 SGR. This decision was also based on an observation that the RNA extracted from S52 AII SGR harbouring cells replicates transiently, whereas S52 SHI RNA does not, detailed in Figure 3-13 and section 3.2.3.2. The SGR harbouring cells were characterised to quantify the levels of SGR RNA and proteins, shown in Figure 3-9. Luciferase levels were measured and compared to the same number of Con1 and JFH-1 SGR-harbouring cells. Luciferase in S52 SGR-harbouring cells was significantly higher than that in JFH-1 cells and approximately 100-fold higher than Con1 SGR-harbouring cells.

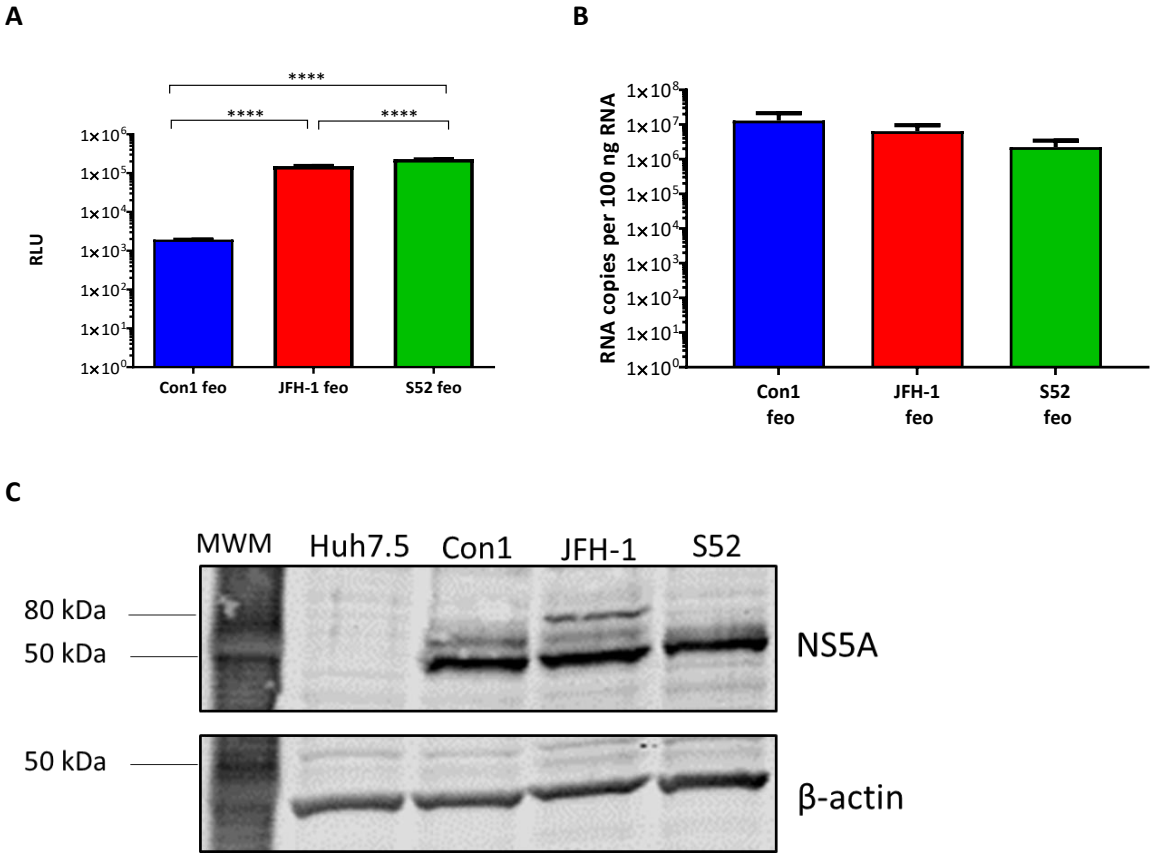

Figure 3-9. S52 SGR harbouring cells express luciferase and NS5A and contain HCV SGR RNA. (A) Assay for luciferase in SGR harbouring cells. Luciferase activity was measured in $8x10^3$ cells and compared to Con1 and JFH-1 SGR-harbouring cell lines. Error bars show the standard error of five experimental repeats. ****p≤0.0001. (B) Quantification of HCV SGR RNA in SGR harbouring cell lines. Total cell RNA was extracted from SGR-harbouring cells and quantified. 200 ng of total RNA from each cell line was used as a template in a one-step RT qPCR reaction and expressed as genome copies per 100ng using an *in vitro*-transcribed SGR RNA as a standard curve. Error bars show the standard error of three experimental repeats. (C) Western blot analysis of NS5A in SGR-harbouring cells. 15 µg of the indicated SGR-harbouring cell lysates were resolved on 7.5% polyacrylamide and stained with sheep polyclonal anti-NS5A serum, anti-β actin and respective Infra-red-tagged secondary antibodies. Membranes were visualised using the LiCor Infra-red scanner system

NS5A protein expression and distribution patterns were analysed in these cells, to compare to that already known for other genotypes. NS5A protein, visualised by western blot resolves as a single band of approximately 50 kDa. This is likely to correspond to the p56 species of NS5A, since the S52 SGR contains the S2204I culture-adaptive mutation that abrogates

hyperphosphorylation. NS5A expression is similar to that of JFH-1 which indicates that the translation efficiency of these two SGRs is broadly similar. Interestingly, despite such a marked difference in luciferase activity between Con1 and S52 SGR-harbouring cells, NS5A protein level of Con1 is similar to the other two SGRs.

HCV SGR RNA was quantified in SGR harbouring cell lines by qPCR. The data show that the SGR RNA level in S52 SGR harbouring cells is lower than for Con1 and JFH-1. It is noteworthy that the abundance of SGR RNA, luciferase activity and NS5A protein expression do not correlate between the different genotypes.

NS5A protein distribution was also visualised using immunofluorescence. Figure 3-10 shows that NS5A protein has a similar distribution to JFH-1 and Con1 as punctate structures throughout the cytoplasm of the transfected cell. As before, the intensity of NS5A within all three types of SGR-harbouring cell is broadly similar, and does not seem to correlate to SGR RNA copies as quantified by qPCR.

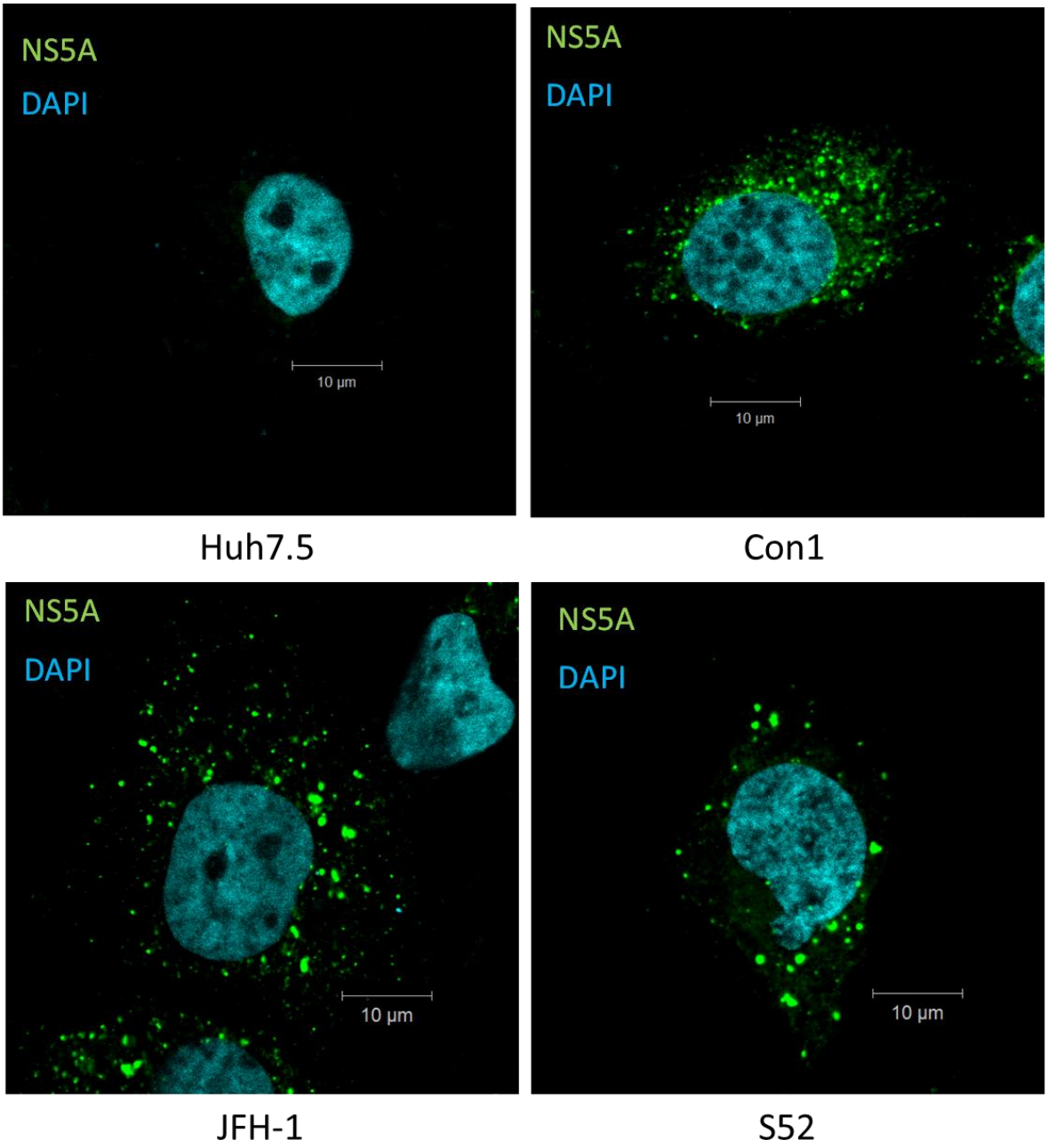

Figure 3-10. SGR-harbouring cell lines have a similar distribution of NS5A to JFH-1. S52, Con1 and JFH-1 SGR-harbouring cells were imaged by immunofluorescence for NS5A (green) using a sheep polyclonal anti-NS5A serum and nuclei using DAPI. Images are the same as those used in **Figure 5-1**)

The effect of the SGR's presence on proliferation of the host cell line was measured using a cell growth assay. Cells from each line were seeded in 6-well plates and counted after 24, 48 and

72 hours' growth under standard conditions. As shown in Figure 3-11 the presence of the SGR did not significantly inhibit growth of the S52 harbouring cells, compared with Con1 or JFH-1.

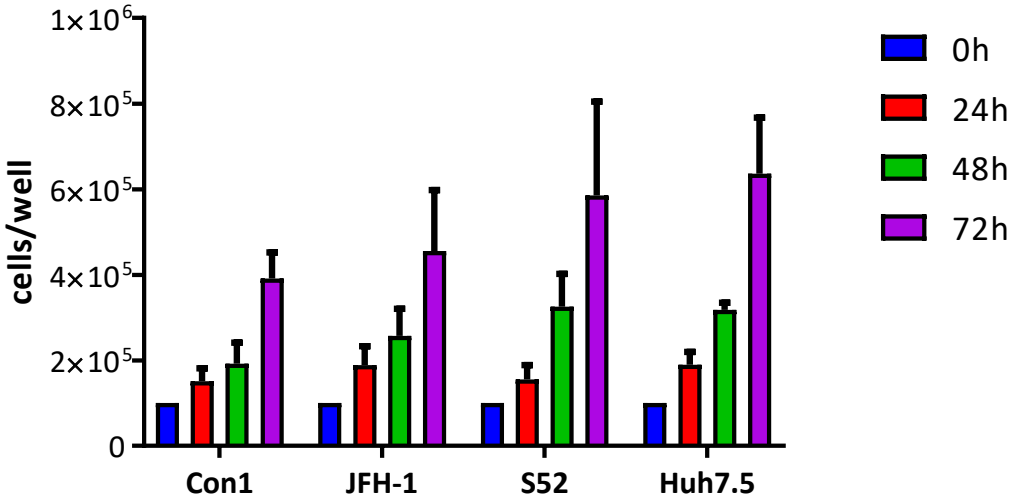

Figure 3-11. SGR-harbouring cell lines have a higher growth rate than other SGR-harbouring cell lines. $1x10^5$ of the indicated cell lines were seeded in 6-well plates. Following the indicated culture periods the cells were removed from the well and counted using trypan blue exclusion. Error bars show the standard error of three experimental repeats.

3.2.3.1 Assay for replication in cured cell lines

It was plausible that, instead of selecting a population of adapted SGR sequences, the G418 selection has instead resulted in a population of cells which was better able to support replication of the SGR. A population of SGR cells were treated with 190 nM of the NS5A inhibitor DCV and 110 nM of the NS5B inhibitor SOF (both 100-fold EC_{50} calculated for the SGR harbouring cells, detailed in chapter 4) to eradicate the SGR; complete loss of luciferase activity to baseline levels confirmed that the SGR was eradicated. 2 µg of the indicated RNAs were electroporated into these cells and harvested for luciferase at the indicated time points (Figure 3-12). As the data show, the cured S52 AII cell line was not capable of supporting replication of the S52 SGR. However, interestingly the S52 AII SGR showed a very low replication signal in the S52 SHI cured cell line.

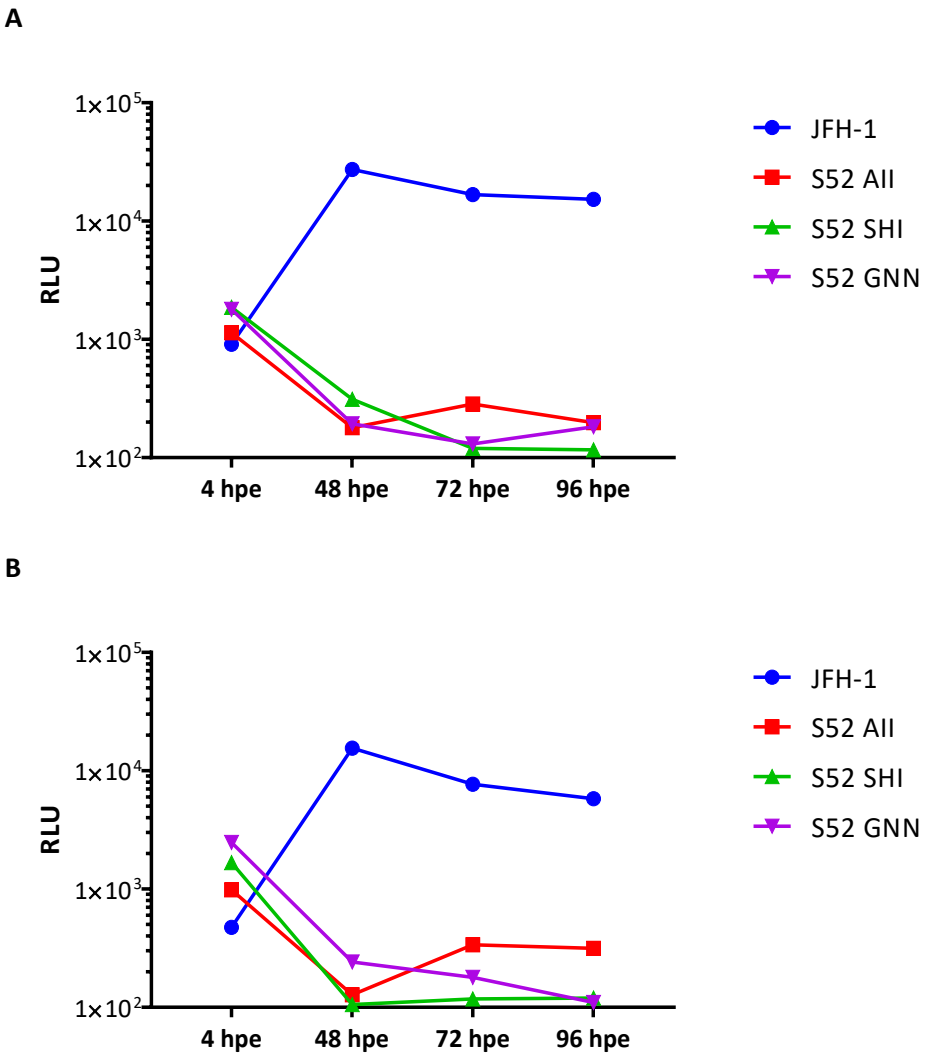

Figure 3-12. S52 SGR does not replicate in cured SGR-harbouring cell lines. S52 SGR harbouring cells were cured with 190 nM and 110 nM DCV and SOF respectively, and re-electrporated with 2 µg of the indicated RNAs. (A) S52 AII. (B) S52 SHI. Cells were harvested for luciferase at the indicated time points.

3.2.3.2 Transient replication of SGR feo cell RNA

It was hypothesised that, if the SGR within S52 SGR harbouring cells had undergone further culture adaptation then the RNA extracted from these cells should be capable of transient replication. To test this, RNA was extracted from S52 SGR-harbouring cells and purified. 10 µg of this extracted, total cell RNA was electroporated into Huh7.5 cells and harvested for luciferase at the indicated time points. As the data in Figure 3-13 show, the S52 SGR within total RNA extracted from SGR-harbouring cells was capable of replication in naïve Huh7.5 cells.

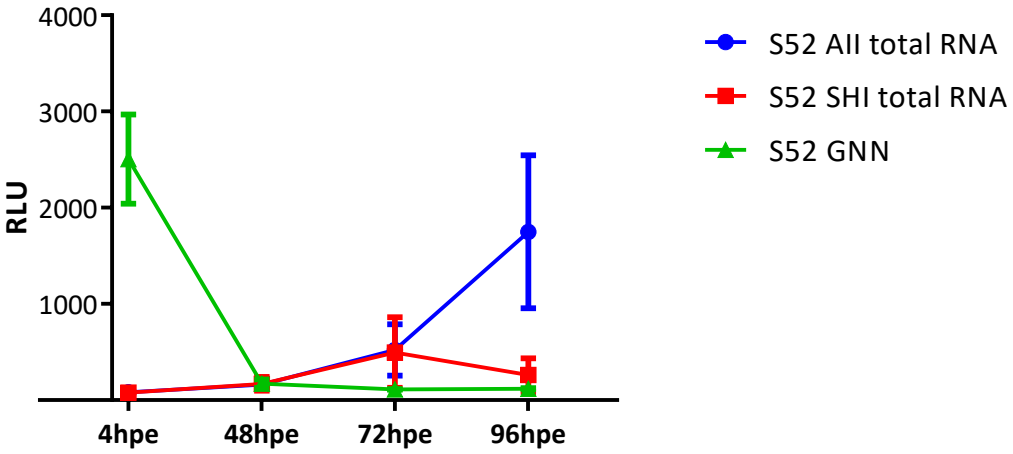

Figure 3-13. Extracted S52 SGR harbouring cell RNA replicates transiently. Total cell RNA was extracted from SGR-harbouring cells. 10 µg of this total RNA was electrporated into Huh7.5 cells and harvested for luciferase at the indicated time periods. Error bars show the standard error of three experimental repeats**.**

3.2.4 Identification of putative culture-adaptive substitutions (CASs)

The observation that S52 replicates efficiently following selection (Figure 3-9); that SGR RNA within these cells replicates transiently (Figure 3-13); and that replication is not as a result of selection of a population of cells more permissible for SGR replication indicate that culture adaptation has occurred. In order to identify any other CAS that have arisen, RNA from both S52 SGR-harbouring cells was amplified by RT-PCR and subjected to amplicon-based next-generation sequencing (NGS). Analysis of the data revealed the presence of nine single nucleotide substitutions at greater than 20% variant frequency. Seven of these were non-synonymous and are detailed in Table 3-1. CAS present in the input S52 SGR sequence at the time of electroporation were maintained following selection at frequencies of 100%.

Nucleotide substitution	Amino acid substitution (individual protein numbering)	Amino acid substitution (polyprotein numbering) [H77 polyprotein numbering]	% variant frequency	Location	Residue in JFH-1	Residue in Con1
G340C	VII3L	V1145L [1139]	24	NS3	V	V
A1143C	K380N	K1412N [1406]	25	NS3	A	K
C1940T	A15V	A1678V [1672]	33	NS4A	A	A
C1978T	H28Y	H1691Y [1685]	70	NS4A	R	R
A2114G	E19G	E1736G [1730]	34	NS4B	S	Q
T3048A	N69K	N2047K [2041]	41	NS5A	L	N
A3998G	Q386R	Q2364R [absent in H77]	24	NS5A	S	absent

Table 3-1. Substitutions found by next-generation sequencing.

3.2.4.1 Identification of linkage of culture-adaptive substitutions

Due to the lack of linkage of the short reads obtained by NGS, and the fact that the substitutions observed were not present in all reads, it was not possible to determine which combination(s) of substitutions might result in enhanced replication. However, it was hypothesised that, since the SGR within SGR harbouring cell RNA can replicate at 96 hpe, the most abundant SGR RNA within these electroporated cells should be the combination which is best able to replicate transiently. To test this, further NGS was performed using RNA extracted from S52 SGR harbouring cell RNA and harvested at 96 hpe. However, SGR RNA was not sufficiently abundant in these cells to allow sequencing analysis. Therefore, the naïve Huh7.5 cells electroporated with S52 SGR harbouring cell RNA were selected once more with G418 and pooled into a population of SGR harbouring cells which were termed second selection cells. The only substitutions which were detected in this second round of sequencing were K1406N in NS3 and A1672V/H1685Y (all by H77 numbering) in NS4A.

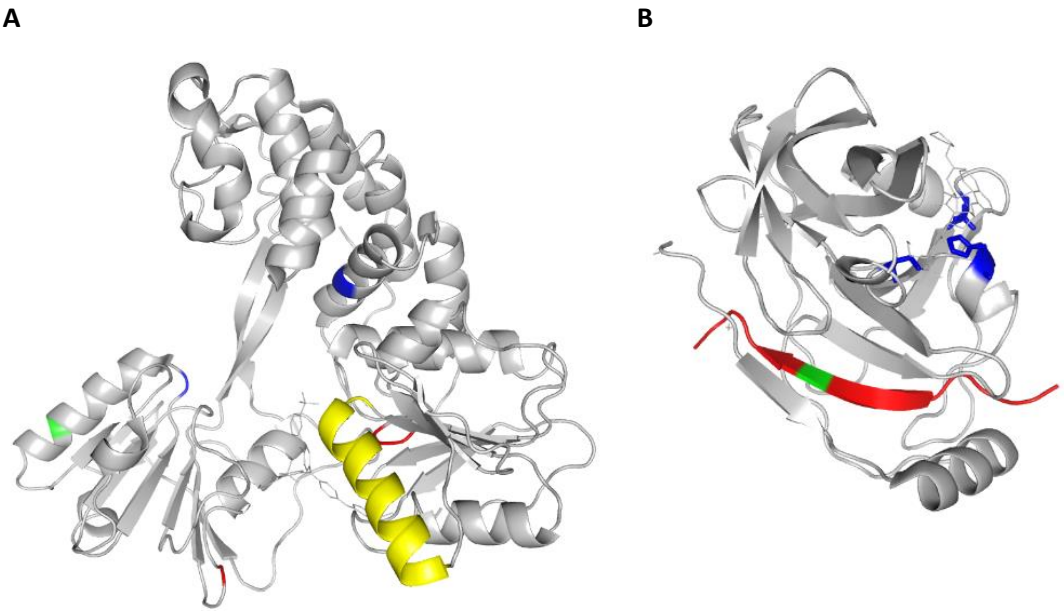

Figure 3-14. Location of putative culture-adaptive substitutions on three-dimensional structures of NS3 helicase (A) (Kim et al., 1998) and NS4A shown as a complex with NS3 protease (B) (Kim et al., 1996). In (A) K1406 is shown in green within NS3 helicase. Proposed spring helix shown in yellow, nucleic acid binding cleft in blue and ATP binding cleft shown in red. In (B) H1685 shown in green within NS3-binding region of the NS4A peptide (red) with NS3 protease active site shown in blue. A1672 is within the hydrophobic N terminus (not shown on crystal structure).

Figure 3-14 shows the location of these putative CAS in the three-dimensional structures of the NS3 helicase and NS4A cofactor peptide bound to the active site of NS3 protease. The location of K1406N within the NS3 helicase domain and H1685Y within the NS4A cofactor peptide are highlighted in green; it was not possible to model A1672V as it is within the hydrophobic N-terminal domain. It was considered that these CAS might enable higher levels of transient replication of the S52 SGR.

3.2.4.2 Effect of putative culture-adaptive substitutions on S52 transient replication

To test this hypothesis, the three substitutions described above were introduced into the S52 CpGluc SGR by site-directed mutagenesis singly and in each combination of two or three mutations. The putative CAS were then screened using the transient replication assay described previously and the data are shown in Figure 3-15. In panel A, the A1672V substitution replicated to a very low level in Huh7.5 cells whereas the other substitutions gave a replication signal which was indistinguishable from baseline. However, panel B shows that

K1406N and A1672V mutants, and a double mutant of A1672V and H1685Y gave a luciferase signal in VSEC cells which, for A1672V, was significantly higher than the signal observed at 4 hpe corresponding to translation of the input RNA.

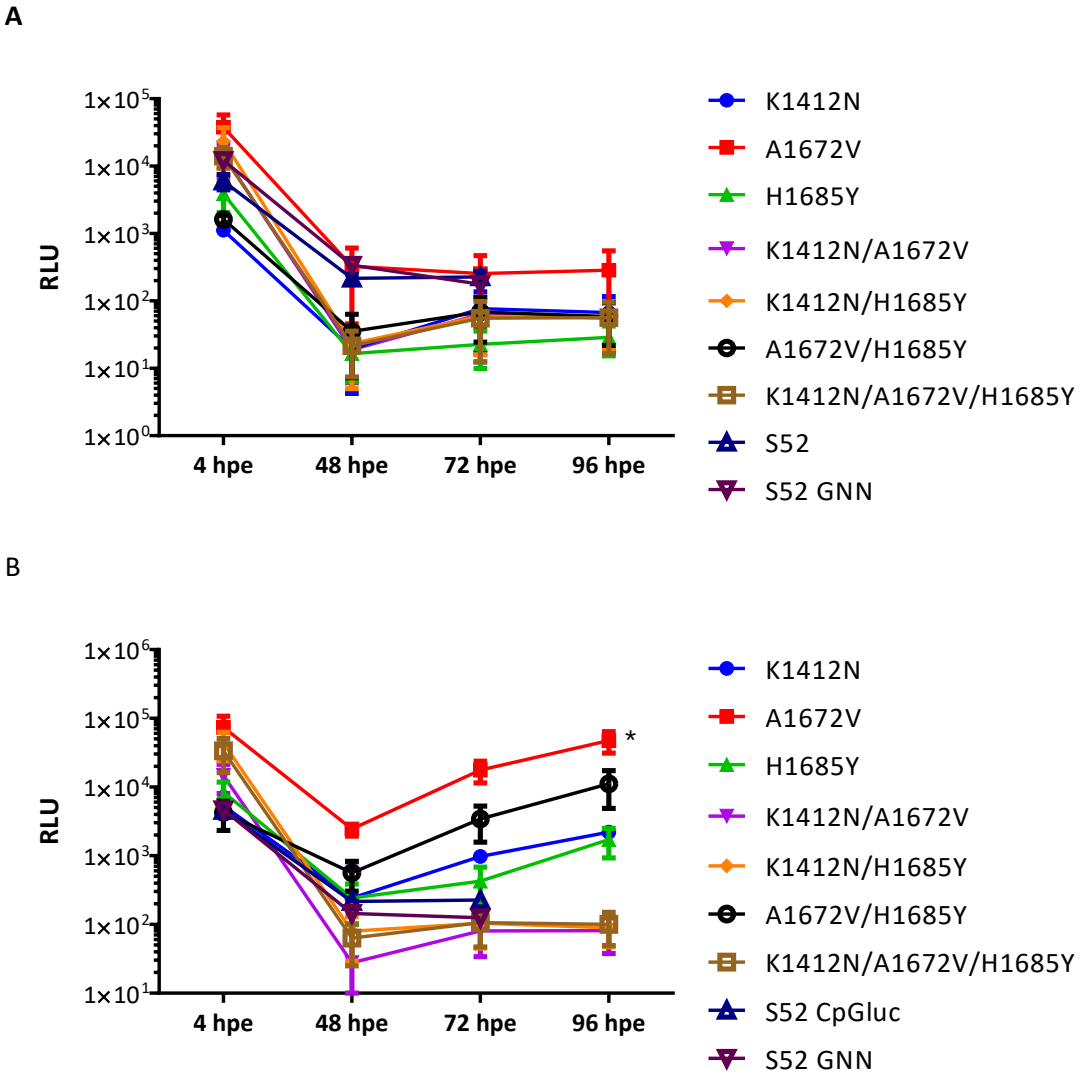

Figure 3-15. Putative culture-adaptive substitutions confer transient replication ability upon S52 SGR. The indicated substitutions were introduced back into S52 SGR by molecular subcloning, 2 µg RNA transcripts were electroporated into Huh7.5 cells (A) and VSEC cells (B) and harvested for luciferase assay. Error bars show the standard error of the mean of 3 experimental repeats. Statistical analyses were carried out compared to the non-replicating control and those not shown are not significant. *$p<0.05$

3.2.5 Optimisation of culture of full-length GT3 infectious clone

The chimera S52 virus reported by (Yi-Ping Li et al., 2014) was donated by Jens Bukh. This untagged GT3 virus consists of the 5' UTR, structural proteins and non-structural proteins of S52 up to NS5A, recombined with the NS5B and 3' UTR of JFH-1. The virus contains seven CAS: The combination of LSG (F1416L/A1672S/D2929G) within NS3, NS4A and NS5B respectively, was found to be effective across all genotypes. The two variants contain additional CAS in p7 and NS4B (GR virus), with an additional pair in the GERA virus in NS3 and NS5A.

Construct code	**Transfection**		**Second Passage**	
	Day with >80% cells infected	**Peak log_{10} FFU/mL (day)**	**Peak log_{10} FFU/mL (days)**	**Peak log_{10} IU/mL**
S52 LSG GR *(F1416L/A1672S/D2929G/ D871G/H1819R)*	13	3.3 (13)	3.7 (8)	8.9
S52 LSG GERA *(F1416L/A1672S/D2929G/ D871G/V1612E/H1819R/V2417A)*	7	4.0 (11)	4.3 (12)	7.2

Table 3-2. S52 virus constructs received from Jens Bukh, adapted from (Yi-Ping Li et al., 2014)**.**

3.2.5.1 Baseline replication of full-length clone

Replication of the S52 full virus construct was measured using the Incucyte system developed in-house for titration of infectious virus in cell supernatants. Cells electroporated with S52 virus RNA were cultured for fourteen days with supernatants harvested for titration every 48 hours. In concurrence with the original study which reported this virus, peak infectivity was detected approximately 12 dpe, with a peak titre of $5x10^5$ IU/mL.

3.2.5.2 Characterisation of S52-infected cells

A preliminary experiment was performed to infect naïve cells with MOI=1 S52 virus supernatant and detect NS5A protein by immunofluorescence; this is shown in Figure 3-16. As the immunofluorescence shows, the distribution of NS5A in this infected cell is different to that observed for SGR-transfected cells and the JFH-1 virus. NS5A signal intensity in this

infected cell was significantly lower than for JFH-1, which correlates with the observation that released titres were significantly lower.

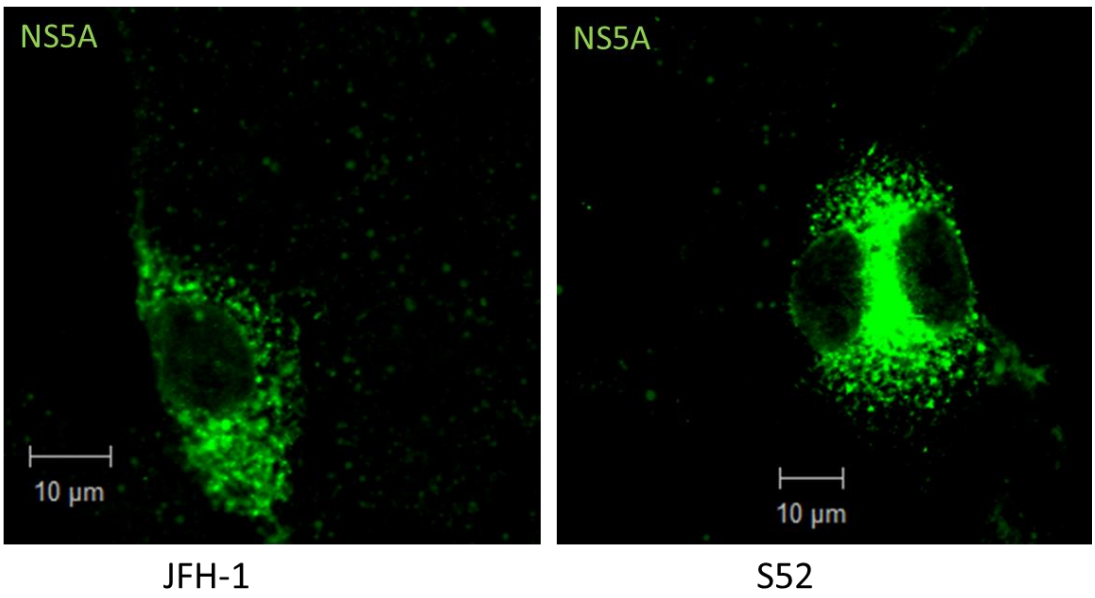

Figure 3-16. NS5A distribution in S52 infected cells is similar to JFH-1. Huh7.5 cells were infected at MOI=1 with S52 virus supernatant for 48 hours before being fixed with 4% PFA. Cells were imaged by immunofluorescence for NS5A (green) using a sheep polyclonal anti-NS5A serum**.**

S52 virus-infected cells were also treated with increasing concentrations of the NS5A inhibitors, as a proof-of concept to determine if this system can be used for inhibitor sensitivity studies. Huh7.5 cells were seeded in 96-well plates and infected with S52 supernatant at an approximate MOI=1 (due to low titres higher MOI was not possible) for 48 hours before being treated with the indicated concentrations of DCV and LDV for a further 48 hours. Following this treatment period infected cells were fixed and stained for detection using the Incucyte instrument. As the data in Figure 3-17 show, infectivity was very low and a reliable 50% effective concentration (EC_{50}) cannot be calculated, however there is an indication of a reduction in replication of the S52 virus at higher concentrations of both inhibitor.

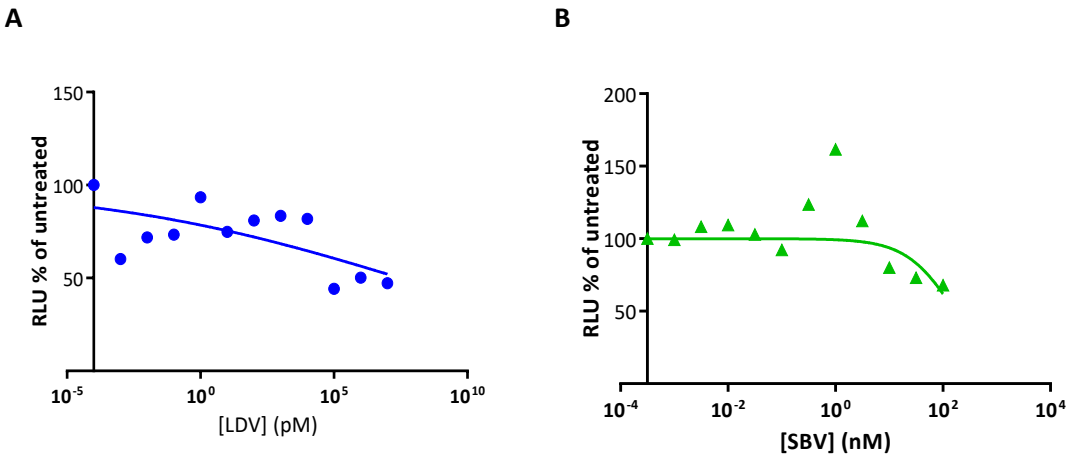

Figure 3-17. S52 virus replication can be inhibited using HCV inhibitors. $8x10^3$ Huh7.5 cells were infected with S52 at an MOI of 1 for 48 hours before being treated with the indicated concentrations of LDV (A) and SOF (B) for a further 48 hours. Cells were then fixed and stained with polyclonal sheep anti-NS5A serum and 594nm fluorescent secondary antibody. Stained cells were imaged using the Incucyte system and associated software.

3.2.5.1 Construction of Nluc reporter virus

Following this preliminary experiment, the possibility of inserting a reporter into the S52 virus to enable more sensitive detection of infected cells for the purpose of conducting inhibitor sensitivity studies was explored. Previously a JC1 virus construct, a GT2a chimera of the J6/CF and JFH-1 isolates with 100- to 1000-fold higher infectious titres than either parental strain (Pietschmann et al., 2006), was modified to insert Nanoluc, a smaller luciferase subunit from a deep-sea shrimp species with 100-fold greater bioluminescence (England et al., 2016), between the p7 and NS2 coding region (Amako et al., 2015). A similar approach was utilised to insert the Nanoluc gene into the S52 virus, at the same location. A diagram of the geneblock constructed to insert into the S52 genome is shown in Figure 3-18. Briefly, the first four residues of NS2, to allow recognition by virus-specific proteases, were followed by the Nanoluc gene and the Foot and Mouth Disease Virus (FMDV) 2A coding region, which has been shown to be an efficient separator of protein coding regions, causing the ribosome to skip the formation of a peptide bond during translation of a single polyprotein and allowing equal translation of the two coding regions which it separates, an established technique reviewed in (Luke et al., 2010). This was then followed by the NS2 coding region as normal.

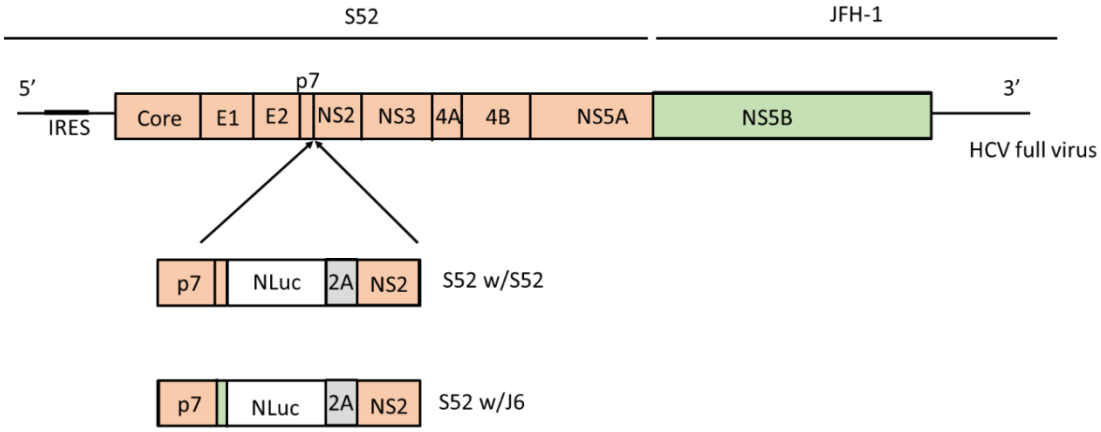

Figure 3-18. Schematic diagram of the Nanoluc insert for the S52 virus.

However, as the diagram shows, two variants of this geneblock were synthesised: The NS2 protease recognition sequence upstream of the Nanoluc was either that of S52 or JC1 in the two variants. The reason for this is that the JC1 sequence is known to function as a cleavage site, whereas the S52 sequence maintains the GT3 homology of the majority of the virus. Genotype-specific sequence specificity may be important for proper cleavage in the context of the GT3 virus.

These two reporter viruses were constructed and *in vitro*-transcribed RNA was electroporated into VSEC cells, with the results shown in Figure 3-19a.

A

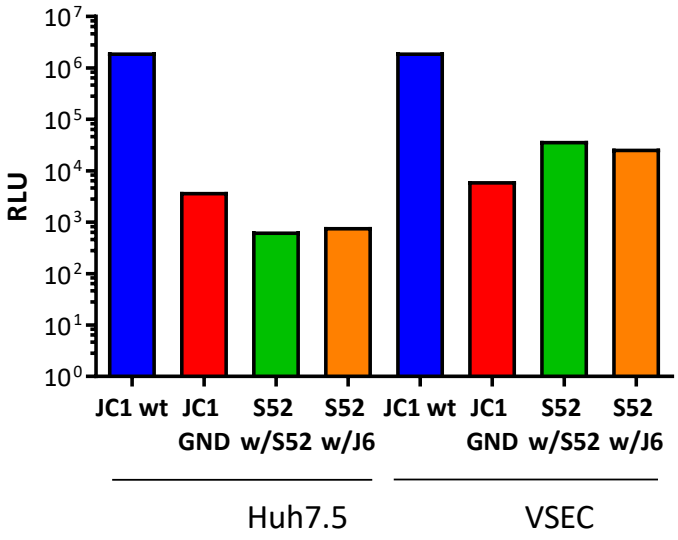

B

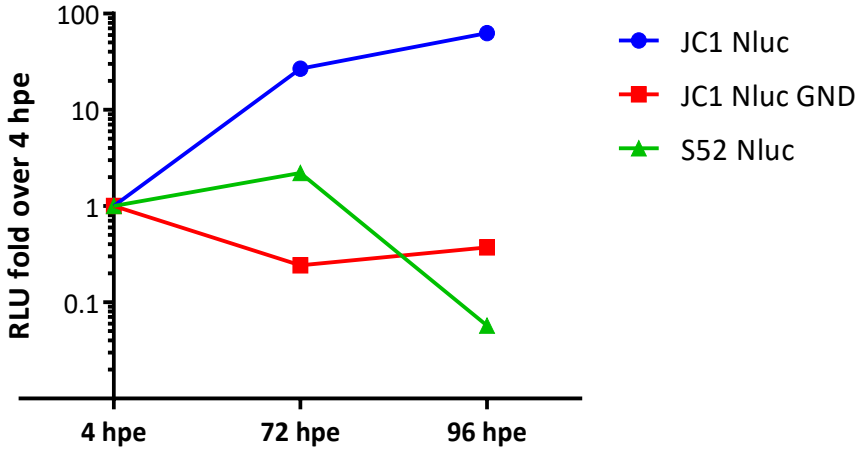

Figure 3-19. S52 Nluc reporter viruses express luciferase. 10 µg of the indicated *in vitro*-transcribed virus RNAs were electrporated into Huh7.5 cells and cultured for 72 and 96 hours before being harvested for luciferase. (A) $2x10^5$ electroporated cells were seeded in a 6-well plate and harvested in 200 µL PLB after 72 hours. Nanoluc was measured in 20 µL of this lysate. (B) Nanoluc activity was measured in $8x10^3$ cells as a proof-of-concept for inhibitor sensitivity studies

As the data show, luciferase activity can be detected in infected cell lysates at 72 hpe of the Nanoluc reporter viruses, and slightly higher for the reporter virus which was constructed

using the genotype-specific p7/NS2 cleavage site (Nluc w/ S52). However, this was a fraction of the signal observed for the JC1 Nanoluc positive control virus. Indeed the difference cannot be reliably calculated since the two samples had to be quantified using different parameters of the luciferase activity measurement instrument. This was to be expected, however it was not known whether this difference would prohibit comparison of the JC1 and S52 viruses in inhibitor sensitivity assays.

To test this, VSEC cells were electroporated with JC1 and S52 Nanoluc virus RNAs and assayed for luciferase at 72 and 96 hpe. As shown in Figure 3-19b, luciferase activity in the S52 virus was too low to be detected in the number of cells seeded in 96-well plate format for inhibitor sensitivity assays.

In addition, the effect of the Nanoluc gene insertion on S52 replication and release was explored. Insertion of a reporter or tag at this position is tolerated by JC1 (Amako et al., 2015), however replication of JC1 is sufficiently high that a reduction in titre of released particles is not likely to be severely detrimental. S52 replicates to much lower levels, so a defect in replication of the virus caused by the Nanoluc insert may be more apparent. Figure 3-21 shows the titres of released virus over time in culture, and a reduction in released virus can be observed with the S52 Nanoluc virus, likely corresponding to a defect in replication capacity.

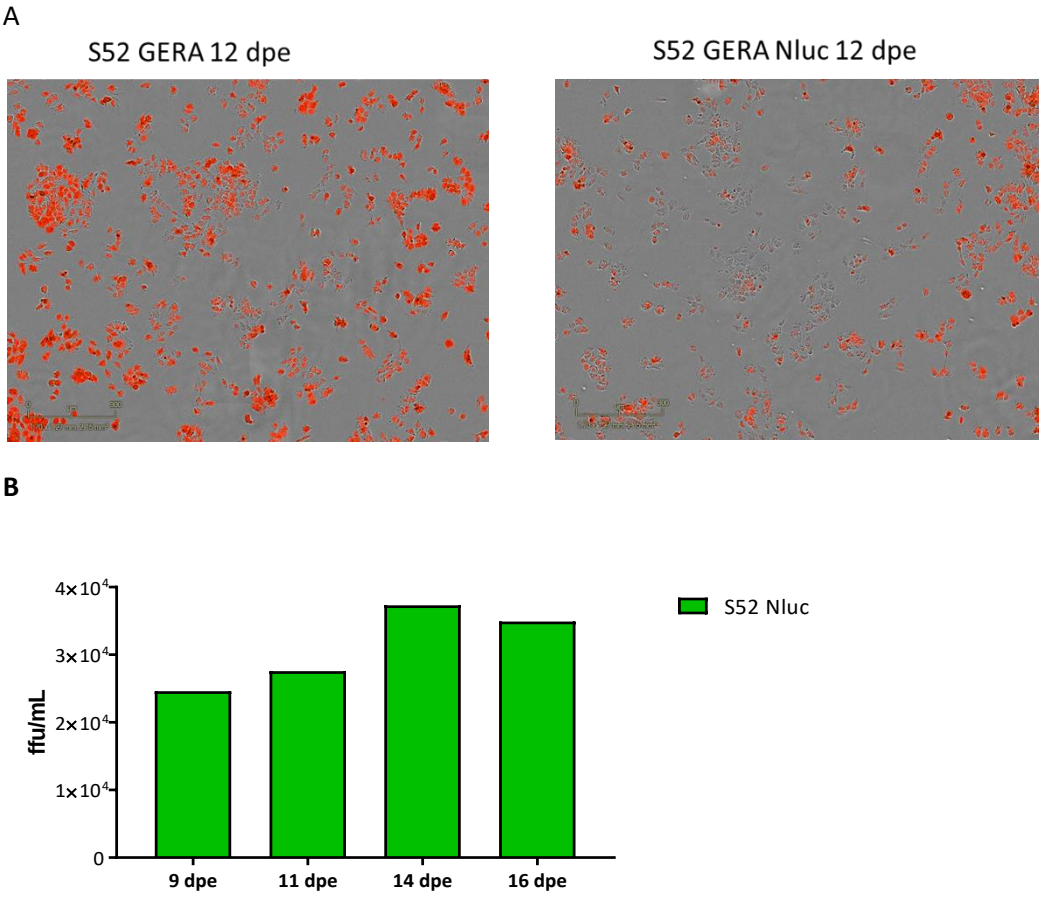

Figure 3-20. Virus replication in S52 Nluc-electroporated cells is lower than S52 without Nluc. 10 µg of the indicated *in vitro*-transcribed virus RNAs were electroporated into Huh7.5 cells and cultured for 14 days, with supernatants harvested for titration of infectious virus approximately every 48 hours. S52 Nluc virus supernatants were serially-diluted two-fold and applied to naïve Huh7.5 cells for 48 hours. Following this period infected cells were fixed with 4% paraformaldehyde and stained with polyclonal sheep anti-NS5A serum and 594nm fluorescent secondary antibody. Stained cells were imaged using the Incucyte system and associated software. (A) NS5A stain in electroporated cells. (B) Calculated ffu/mL of released S52 Nluc virus using Incucyte software

3.3 Discussion

Transiently-replicating SGRs have been instrumental in the elucidation of the functions of the HCV non-structural proteins, mechanisms of genome replication and development of DAAs. The three SGRs which have so far been reported for GT3, derived from two different isolates, are limited in their ability to replicate efficiently in a transient system and only replicate efficiently following selection with G418 (Saeed et al., 2012). Transient replication of S310 was measured but only showed luciferase levels of several orders of magnitude lower than input translation at 4 hpe, and replication of the S52 SGR which was culture-adapted in transfected-and-cured Lunet cells did not replicate efficiently until 7 days post-transfection (Saeed et al., 2013; Yu et al., 2013).

The S52 SGR did not replicate transiently within this project when compared to JFH-1, the GT2a SGR which is widely used in HCV research. In concurrence with the original study which reported this SGR, the S52 SGR only replicates detectably following selection with G418. This work has relied upon the luciferase reporter for quantification of replication, however the authors of the original publication used quantitative PCR, colony formation and western blotting to characterise the SGR. Luciferase assay is a high-throughput, sensitive detection method which would be of greater benefit to drug discovery than the other characterisation techniques reported in this thesis and in the 2012 study.

Stable, SGR-harbouring cells are useful tools in basic research but the effect of the SGR and its reporter in a single cell population over an extended period must be considered. For instance, it has been reported (Volker Lohmann, personal communication) that the luciferase reporter is toxic to cells. Indeed, it was observed that the ability of the S52 SGR to form colonies during selection with G418 was enhanced by the removal of the luciferase coding region of the feo reporter cassette, with a colony-formation efficiency of the S52 feo SGR of 0.5 cfu/µg RNA, compared to 110 for S52 neo SGR. Similarly, the reduction in growth rate of cell populations harbouring different HCV SGRs compared to Huh7.5 cells indicates that the presence of the SGR has a deleterious effect on growth rates of the host cell, an observation made previously (Igloi et al., 2015). It may be that this effect is partly a consequence of the presence of G418 and the NPT resistance gene product, which has a metabolic effect on the cell (Yallop and Svendsen, 2001). This effect is, naturally, not a concern over short-term experiments. In addition, stable replicon-harbouring cells are of limited use for development of DAAs and do not allow investigation into mechanisms of resistance since the most widely reported RAS for

NS5A – Y93H – is associated with a fitness cost (Lemm et al., 2010; Kylefjord et al., 2014). They are not able to model initiation of infection and, as such, are a less representative model of HCV replication *in vivo*.

Prior to the successful establishment of transient replication of S52 two additional approaches were considered to overcome the problem and allow further investigation of unexplored aspects of GT3 replication. The first of these was the colony formation assay which was employed as a means of quantifying HCV replication when the SGR was first developed (Lohmann et al., 1999). This allowed quantification of the earlier stages of replication, albeit the first three weeks, but is subject to some of the same problems as SGR-harbouring cells, such as the effects of G418 and NPT expression on the host cell. The second approach was the use of a chimera SGR containing the NS5A coding region of the S52 SGR in place of that of JFH-1, within a JFH-1 backbone. The use of chimera SGRs in drug discovery for GT3 has been documented (Lanford et al., 2006; Wang et al., 2013; Kylefjord et al., 2014) and, as a result, the inclusion of this work in this thesis is primarily an attempt at the technique rather than to report a novel cell culture system for GT3.

This work shows that, unique for GT3, substantial modification of the host cell environment as well as modification of the SGR reporter and additional culture adaptation are crucial for efficient transient replication. A number of approaches were investigated to increase the replication fitness of the SGR or to modulate the host cell environment to increase permissibility to SGR replication. DNA from different types of organism differs in CpG and UpA dinucleotide frequency, in particular as luciferase is insect-derived it contains a higher frequency than mammalian genes. Optimisation of CpG and UpA dinucleotide frequency increases replication capacity of a number of viruses (Tulloch et al., 2014). This effect is thought to be mediated by avoiding a yet uncharacterised innate immune recognition of high-CpG/UpA sequences (Atkinson et al., 2014). This work demonstrated that replacement of the feo reporter cassette with a CpG/UpA-low luciferase does not by itself allow detectable replication of S52, despite conferring a 4-fold increase in replication on Con1 SGR.

The parainfluenza virus type 5 (PIV5) V protein blocks STAT1-mediated immune activation by binding directly to STAT1 and inhibiting downstream interferon-α activation (He et al., 2002; Poole et al., 2002; Lu et al., 2008). It has been shown that stable expression of the V protein enhances replication of HCV in human foetal liver cells (Andrus et al., 2011). Recently, the host cell protein SEC14L2 or Tocopherol-associated protein, TAP1, was found to allow replication of an unadapted SGR or isolates from patient samples including GT3. This is thought to work by

accumulation of vitamin E, which provides protection against lipid peroxidation (Saeed et al., 2015). It was demonstrated that expression of either the V protein or SEC14L2 did not allow detectable replication of either Feo (with unmodified luciferase) or CpG/UpA-low luciferase containing wild-type S52 SGRs. In addition, a potential additive or synergistic effect of V protein and SEC14L2 was investigated (these cells were termed VSEC) and identified an additive effect on replication of Con1 CpG/UpA-low luciferase, but no effect on the inability of S52 CpG/UpA-low luciferase to replicate. It would likely be beneficial to combine the PIV5 V and SEC14L2 transgenes within a single lentiviral vector, separated by the FMDV 2A coding region (as used in the Nanoluc geneblock described in 3.2.5.1), to ensure equal expression of both transgenes under the control of a single puromycin resistance marker to eliminate the problems with cell growth rate and potential variable expression associated with double resistance to both puromycin and G418. This would also give a user of these cells the option of selecting stable SGR to identify culture adaptation.

Only after selection of stable SGR using G418 did S52 show robust levels of luciferase activity, with a slight, albeit significant, increase over JFH-1 SGR harbouring cells. The SGR RNA, when extracted from these cells, was capable of detectable replication at 96 hpe, strongly indicating that the SGR within them had undergone further culture adaptation. This was supported by an inability of the S52 SGR to replicate in Huh7.5 cells which were cured of the SGR they had previously supported; the selection of a supportive cell line in addition to an adapted SGR is well documented, including the development of Huh7.5 cells (Blight et al., 2002; Yu et al., 2013).

Two of the substitutions identified in stably replicating SGR by next-generation sequencing conferred the ability to replicate upon the SGR when introduced to the CpGluc SGR. The A1672V substitution, which conferred the greatest levels of replication, is located in the hydrophobic N-terminal, membrane anchoring domain of NS4A (Kim et al., 1996). It is not clear why a substitution to a broadly similar amino acid side chain in this region proves to be so beneficial to replication. There was no correlation between my CAS and the corresponding residues in JFH-1 which replicates at much greater levels, however this substitution site was reported by Li and colleagues as a culture adaptive mutation in the chimera S52 virus (Yi-Ping Li et al., 2014). Interestingly, the authors report that a substitution to a polar residue at this position confers culture adaptation. The exact roles of culture adaptive substitutions in promoting HCV replication is rarely explored, with the exception of a link between the S2204I substitution within NS5A, which the S52 SGR carries, and PI4K activity (Harak et al., 2016).

The difference in replication efficiency between the A1672V mutant and the SGR within stable SGR-harbouring cells is profound: it may be that additional CASs which were not screened in this the course of this work may further enhance replication of the A1672V mutant. The other combinations of two and three mutations did not confer high levels of transient replication on the S52 SGR which potentially indicates that these mutations are not linked. The fact that none of the mutations are present as majority populations indicates that there may be two or more variants containing different combinations of substitutions that complement each other. The identification of these would require long-read NGS or single-genome sequencing. It may also be worthwhile to assess replication of the A1672V culture adaptive mutation in the SGR-harbouring cells which were cleared, described above. The adaptation of the A1672V mutant may be specific to an additional change in the host cell which was selected for by G418 and the presence of the SGR, a combination which was reported by Yu and colleagues (Yu et al., 2013).

I was unable to make sufficient progress with the infectious S52 virus to enable application of any result obtained using the SGR system. There is a utility for the Nanoluc reporter in full-virus inhibitor sensitivity studies and characterisation of resistance, however replication of the S52 virus is not sufficiently high enough. Attenuation of the virus by the insertion of the Nanoluc reporter reduced replication and infectious virus production to below a level which is practical. The full-GT3 virus reported recently (Ramirez et al., 2016) may well better tolerate the insertion of a Nanoluc reporter.

This work reports on the modifications necessary to confer a transient replication phenotype on the S52 SGR in order to develop an efficient assay. The S52 SGR requires additional culture adaptation as well as a modified luciferase reporter, coupled with modification of the host cell environment to perturb the innate immune response and alteration of lipid metabolism pathways. A transient replication assay has utility in basic research to investigate genotype differences in replication and host cell interaction, and in drug discovery to function as a high-throughput assay for compound screening.

Chapter 4: Functional analysis of resistance to HCV NS5A inhibitors

4.1 Introduction

Recent years have seen the development of a great number of direct-acting antivirals (DAAs) to treat HCV, with vastly improved efficacy over IFN/RBV standard therapy, depending on genotype. Treatment of GT1 infection with these compounds is effective at producing a sustained virological response (SVR) in 95-100% of patients in clinical trials (Pol et al., 2016). However outside of the highly-regulated, controlled environment of the clinical trial, cohort studies are beginning to show different results (Steinebrunner et al., 2015; Foster et al., 2016), with real-life use likely to follow suit. GT3 is widely reported as being more difficult to treat with DAAs and patients with cirrhosis and previous experience of treatment failure are less likely to achieve SVR. Given that GT3 patients progress quicker through disease states due to higher incidences of hepatic steatosis (described in chapter 5), this pattern is of increasing concern. Patients with GT3 respond better to IFN- and RBV-containing regimens than GT1, and to 24 weeks of all-oral therapy containing RBV instead of 12 (Table 1-2 on page 29). However, as well as having strict exclusion criteria for its use, the inclusion of IFN in combination therapies and the longer treatment duration with RBV affects health-related quality of life for these patients. This is likely to severely affect adherence to treatment, providing the circumstances for the emergence and propagation of resistant strains (Younossi et al., 2014; Younossi et al., 2015). Hence, refinement of all-oral therapies for treatment of GT3 is of great importance.

Resistance to NS5A inhibitors has been well characterised, and substitutions at residues 28-31 and 93 being implicated in treatment failure in clinical trials and *in vitro* studies of resistance. Y93H in particular is associated with between 30- and 3000-fold changes in EC_{50} of DCV depending on genotype (Table 1-3, Table 1-4, Table 1-5 and references therein). The mechanism of resistance is not known, but as inhibitor binding is thought to involve the dimer interface (discussed in chapter 1) it is proposed that mutations in the inhibitor binding region itself (Lambert et al., 2014; Ascher et al., 2015; Barakat et al., 2015) or in regions that are involved in crosstalk with the dimer interface (Ascher et al., 2015) preclude inhibitor binding. It was recently suggested that the Y93H RAS inhibits the ability of DCV binding to cause a conformational change, affecting multi-order structures of NS5A (Sun et al., 2015).

RAS exist in the population at proportions depending on genotype (Suzuki et al., 2012; Paolucci et al., 2013; Miura et al., 2014; Walker et al., 2015; Uchida et al., 2016; Patiño-Galindo et al., 2016) and have a correlative association with treatment response. Pre-existence of a RAS is associated with a lesser chance of achieving SVR but the relationship is correlative rather than

causative, as patients with a pre-existing RAS can achieve SVR whereas patients with no pre-existing RAS can fail treatment (Poveda et al., 2014; Cento et al., 2015; Chayama and Hayes, 2015). Pre-existing RAS can expand upon treatment and lead to resistance; conversely RAS can arise *de novo* during treatment (Eltahla et al., 2017; Kai et al., 2017). The demonstration that RAS are common and that the relationship between RAS occurrence and treatment outcome is not a causative one adds weight to the complexity of DAA resistance.

The development of the transient replication assay and stable SGR harbouring cell lines from the S52 SGR has afforded the opportunity to investigate NS5A inhibitor resistance in two parallel systems. Stably-replicating S52 SGR within SGR harbouring cells provides insight into the maintenance of persistent replication and provides a forward genetic system for selecting resistance. The transient replication assay allows the exploration of early replication events and provides a reverse genetic system for assessing the phenotype of any changes identified. The aim of the work in this chapter was to apply the parallel systems of transient and stable S52 replication to that which is already known about NS5A inhibitor resistance using DCV as a model compound. Initially the work aimed to validate the S52 SGR and its utility in the investigation of resistance and to explore the resistance phenotype further in a GT3-specific manner.

4.2 Results

4.2.1 Use of stable SGR harbouring cells to investigate efficacy of HCV inhibitors

The relative efficacies of clinically available NS5A inhibitors have been documented for GT1, and for GT3 using chimera SGRs; the consensus shows a significant degree of resistance for GT3 in the absence of RAS. The utility of the S52 SGR harbouring cells in DAA sensitivity studies as a culture system comprised entirely of GT3 sequence was explored, as a proof-of-concept to show a similar pattern of DAA efficacy. Sensitivity of S52, Con1 (GT1b) and JFH-1 (GT2a) SGRs to NS5A inhibitors was measured and used to calculate the 50% effective concentration (EC_{50}). SGR harbouring cells were treated with increasing concentrations of DCV, LDV (both NS5A inhibitors), SOF (NS5B inhibitor) and RBV (nucleotidic chain terminator causing mutation error catastrophe) for 48h prior to harvest for luciferase activity assay, or MTT assay for cell viability, which was used to calculate the 50% cytotoxic concentration (CC_{50}). The data in Figure 4-1 show the concentration-response curves for the four compounds, with the corresponding cell toxicity data shown in Figure 4-2.

As expected there was a difference in sensitivity to NS5A inhibitors, with an increase in EC_{50} of 200-fold for DCV between Con1 and S52. LDV was significantly more effective against Con1 than DCV, and significantly less effective against S52, corresponding to a change in EC_{50} of 140,000-fold between Con1 and S52. SOF was approximately 5-fold less effective against S52 than Con1. There was no difference in sensitivity to RBV for any of the SGR harbouring cell lines. A summary of the calculated EC_{50} and CC_{50} for each SGR harbouring cell line and each compound is summarised in Table 4-1.

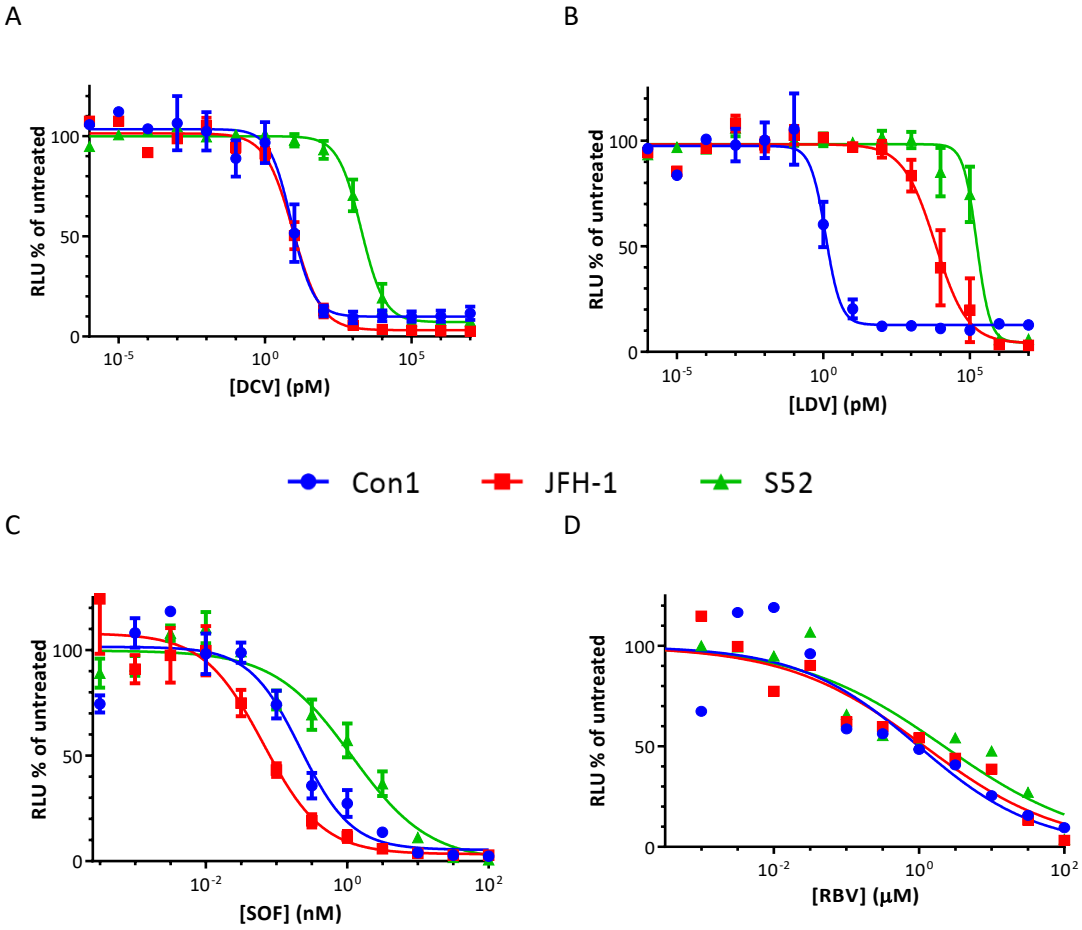

Figure 4-1. Stably-replicating S52 SGR within SGR harbouring cells is less sensitive to DAAs than other genotypes. $8x10^3$ of the indicated SGR harbouring cell lines were seeded in white, 96-well plates and treated with the indicated concentrations of DCV (a), LDV (b), SOF (c) or RBV (d) for 48 hours before being harvested for luciferase assay. Relative light units were expressed relative to a 0.25% DMSO vehicle control. EC_{50} values were calculated using Graphpad Prism 7 software. Error bars represent the standard error of the mean of five experimental repeats.

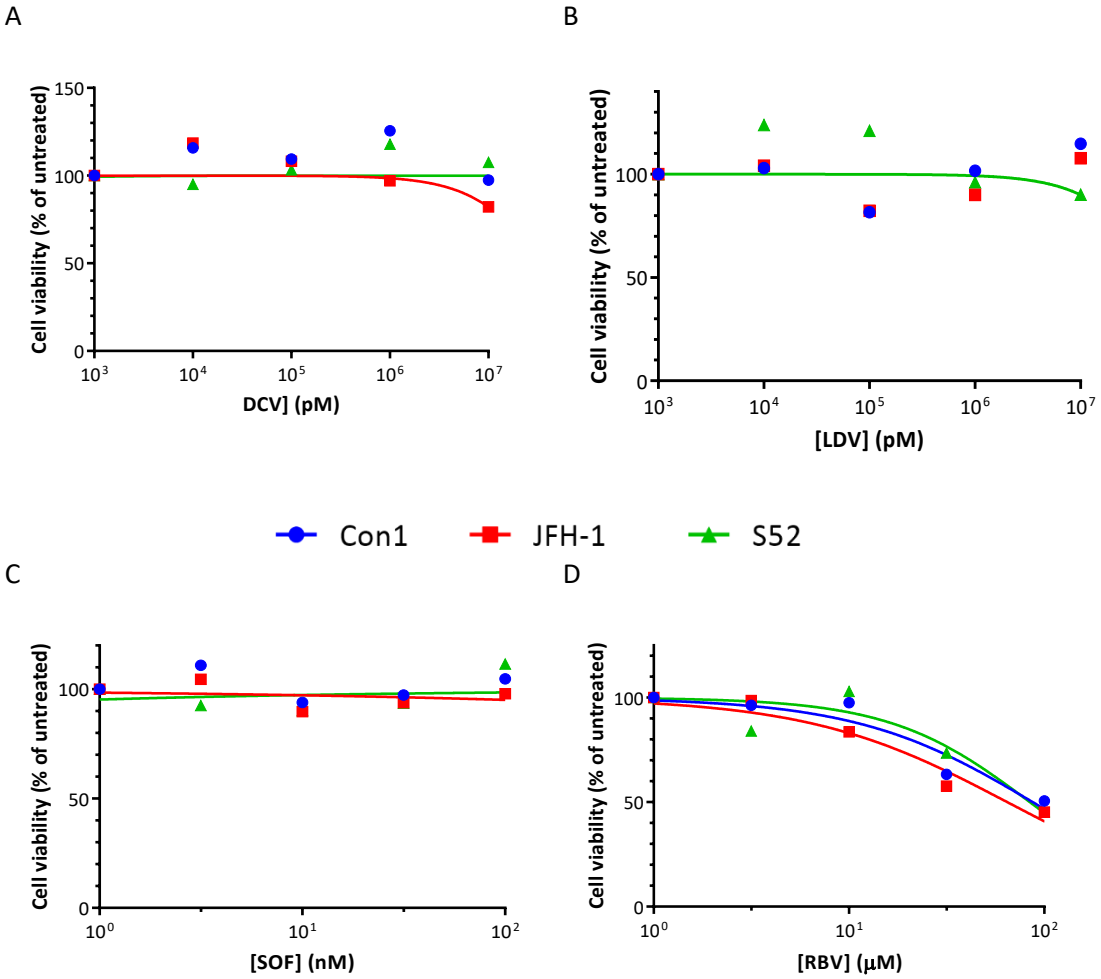

Figure 4-2. DAAs are not cytotoxic except at the highest concentrations. $8x10^3$ of the indicated SGR harbouring cell lines were seeded in 96-well plates and treated with the indicated concentrations of DCV (a), LDV (b), SOF (c) or RBV (d) for 48 hours before being assayed for cell viability using the MTT assay. Absorbance values were expressed relative to a 0.25% DMSO vehicle control.

There was a slight difference in sensitivity to SOF between all three SGR types, indicative of the pan-genotypic nature of SOF. There was no difference in sensitivity to RBV. Cell viability assays indicate that the effect on the SGR is not due to toxicity; indeed, there was no toxicity observed at the concentrations used for either DCV, LDV or SOF at the concentrations at which antiviral affect was observed. The 50% cytotoxic concentration (CC_{50}) calculated for RBV was 80 µM.

SGR harbouring cell line		DCV	LDV	SOF	RBV
Con1	EC_{50}	8.1 pM	1.7 pM	0.2 nM	0.99 µM
	Fold over Con1	n/a	n/a	n/a	n/a
	CC_{50}	>10 µM	>10 µM	>100 nM	87.3 µM
	Therapeutic window	$>1x10^6$	$>5x10^6$	$>1x10^6$	88.18
JFH-1	EC_{50}	9.2 pM	8.1 nM	0.1 nM	1.19 µM
	Fold over Con1	1.1	5500****	0.5	1.2
	CC_{50}	>10 µM	>10 µM	>100 nM	64.6 µM
	Therapeutic window	$>1x10^6$	>1000	>1000	54.29
S52	EC_{50}	1.9 nM	172 nM	1.1 nM	2.21 µM
	Fold over Con1	230****	140,000****	5.5	2.2
	CC_{50}	>10 µM	>10 µM	>100 nM	84.4 µM
	Therapeutic window	>5000	>50	>90	38.18

Table 4-1. Comparison of calculated EC_{50} and CC_{50} values for DAA treatment of HCV SGR harbouring cell lines. Fold changes to two significant figures. Statistical significance was calculated where sufficient data was available (****p<0.0001, **p<0.005)

4.2.2 Use of SGR cell lines to study development of NS5A inhibitor resistance.

4.2.2.1 Selection of NS5A inhibitor resistance

Resistance to NS5A inhibitors by GT3 in clinical studies and *in vitro* using chimera SGRs has implicated two RAS with several thousand-fold resistance when compared to the wild-type SGR. However, there is much that is not known about the development of resistance, the role of RAS and the phenotype of RAS in a full-GT3 system. Thus, the utility of S52 SGR harbouring cells in inhibitor resistance characterisation was also explored. Following calculation of the EC_{50} for each compound (Table 4-1), S52 SGR harbouring cells were selected with DCV at a concentration equivalent to 100x EC_{50} whilst maintaining G418 selection. After an initial

period of cell death most cells survived and the remaining were pooled into a polyclonal population which was termed S52 DCV. These SGR harbouring cell lines were characterised and compared to the pre-selection SGR harbouring cells which are wild-type with respect to NS5A inhibitor resistance. As expected the S52 DCV SGR within SGR harbouring cells exhibited a decrease in sensitivity to NS5A inhibitors, shown in Figure 4-3. Selection with DCV increased the EC_{50} of DCV 480-fold, and of LDV 5-fold. A degree of cross-resistance to LDV was expected following DCV selection as these compounds have similar structures and are predicted to work by a similar mechanism due to the characterisation of resistance (Table 1-3, Table 1-4, Table 1-5 and references therein). It is interesting to note that there is a slight increase in sensitivity to both SOF and RBV in the S52 DCV SGR harbouring cells when the data are compared; this is not significant, indicating that resistance has been selected rather than altering the cells or the SGR.

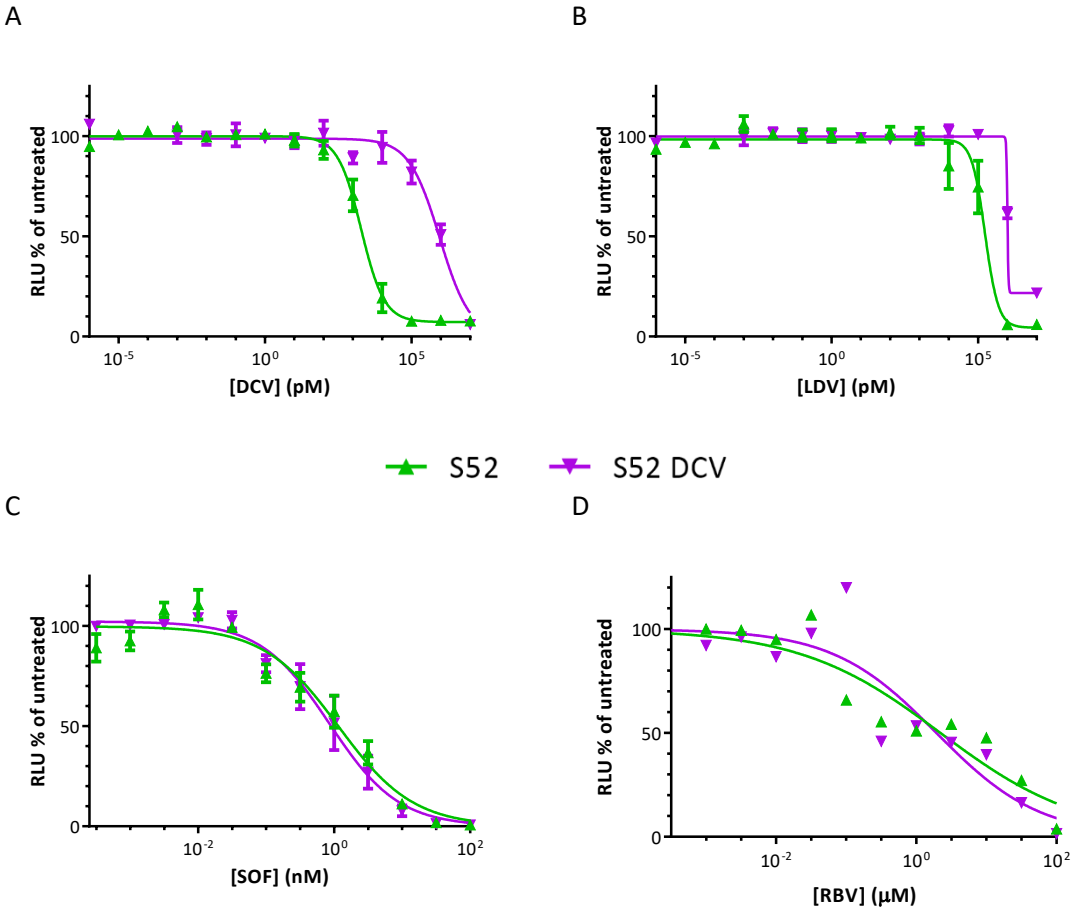

Figure 4-3. Selection of S52 SGR harbouring cells with DCV generates resistance to NS5A inhibitors. S52 SGR harbouring cells were selected with 100-fold the calculated EC_{50} of DCV whilst maintaining G418 selection for approximately two weeks until cell death was no longer occurring. Surviving cells were pooled into a polyclonal population and termed S52 DCV. $8x10^3$ of these S52 DCV SGR harbouring cells were seeded in white, 96-well plates and treated with the indicated concentrations of DCV (a), LDV (b), SOF (c) and RBV (d) for 48h before being harvested for luciferase assay. Relative light units were expressed relative to a 0.25% DMSO vehicle control. EC_{50} values were calculated using Graphpad Prism 7 software. Error bars represent the standard error of five experimental repeats.

	DCV	LDV	SOF	RBV
EC_{50}	910 nM	1 µM	0.8 nM	1.93 µM
Fold over wild-type	480****	5.8****	0.7	0.87
CC_{50}	>10 µM	>10 µM	>100 nM	77.63
Therapeutic window	n/a	n/a	n/a	89.22

Table 4-2. Comparison of calculated EC_{50} and CC_{50} values for DAA treatment of S52 DCV SGR harbouring cell lines. Fold changes to two significant figures. Statistical significance was calculated where sufficient data was available (****p<0.0001, **p<0.005)

4.2.2.2 Characterisation of resistance following selection

The effect of resistance selection on the SGR and the cells was calculated using assays described in chapter 3. Figure 4-4 and Figure 4-5C show NS5A expression by western blot and distribution by immunofluorescence respectively. The western blot in the figure is the same blot as shown in Figure 3-9. Interestingly, both are similar to wild-type S52; it has been suggested in multiple studies that the resistant phenotype of HCV to NS5A inhibitors is associated with a fitness cost which is not apparent in the presence of the compound but manifests as an impairment of replication in its absence (Table 1-3, Table 1-4, Table 1-5 and references therein). Accordingly, no such fitness cost was observed in the luciferase activity of S52 DCV SGR harbouring cells (Figure 4-5A). In addition, there was a similar amount of SGR RNA detected by qPCR (Figure 4-5B)

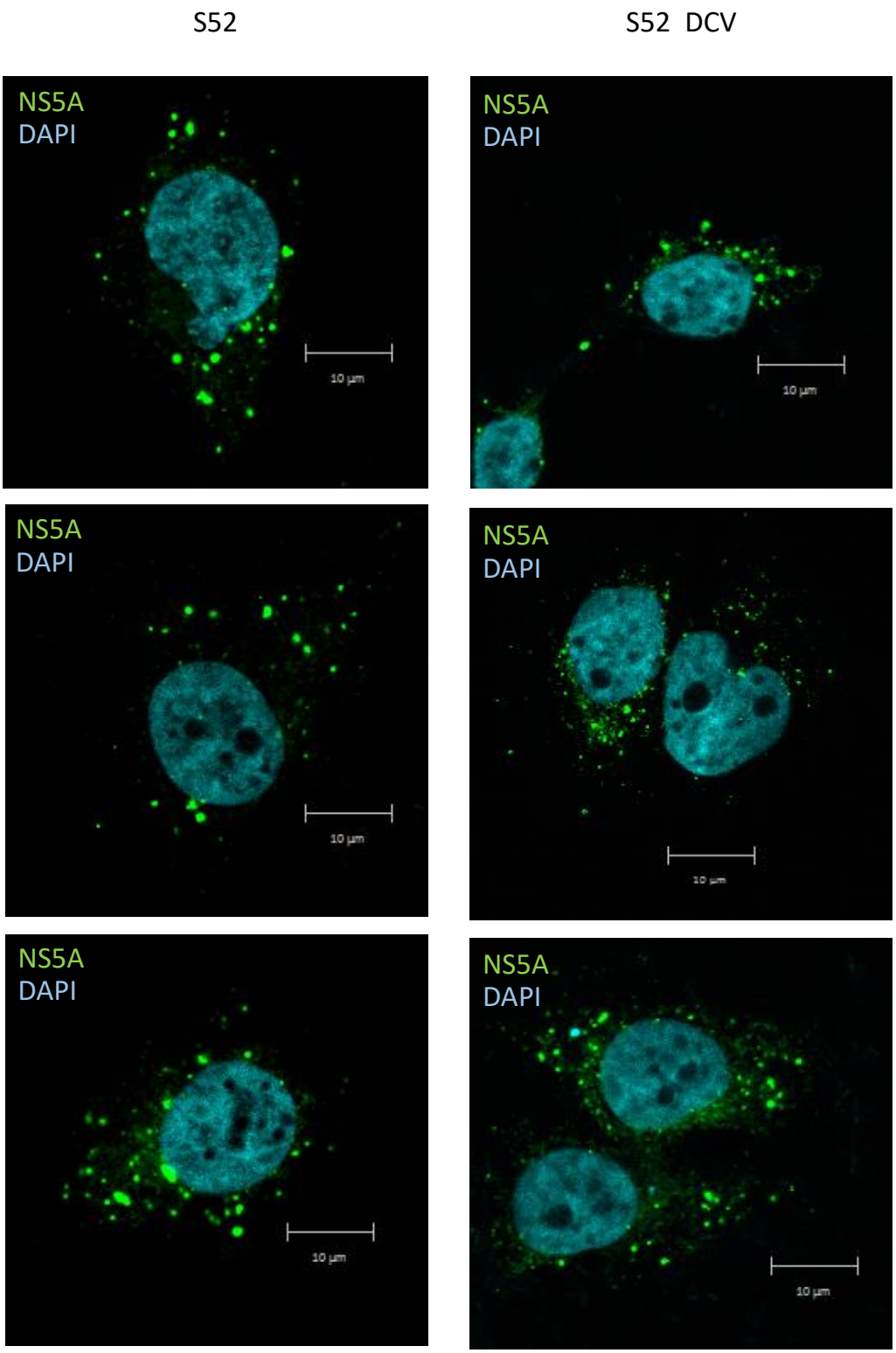

Figure 4-4. DCV selection of S52 SGR harbouring cells does not alter NS5A distribution. S52 and S52 DCV SGR-harbouring cells were immunostained for NS5A (green) using a sheep polyclonal anti-NS5A serum and nuclei using DAPI. Multiple images shown for each cell type.

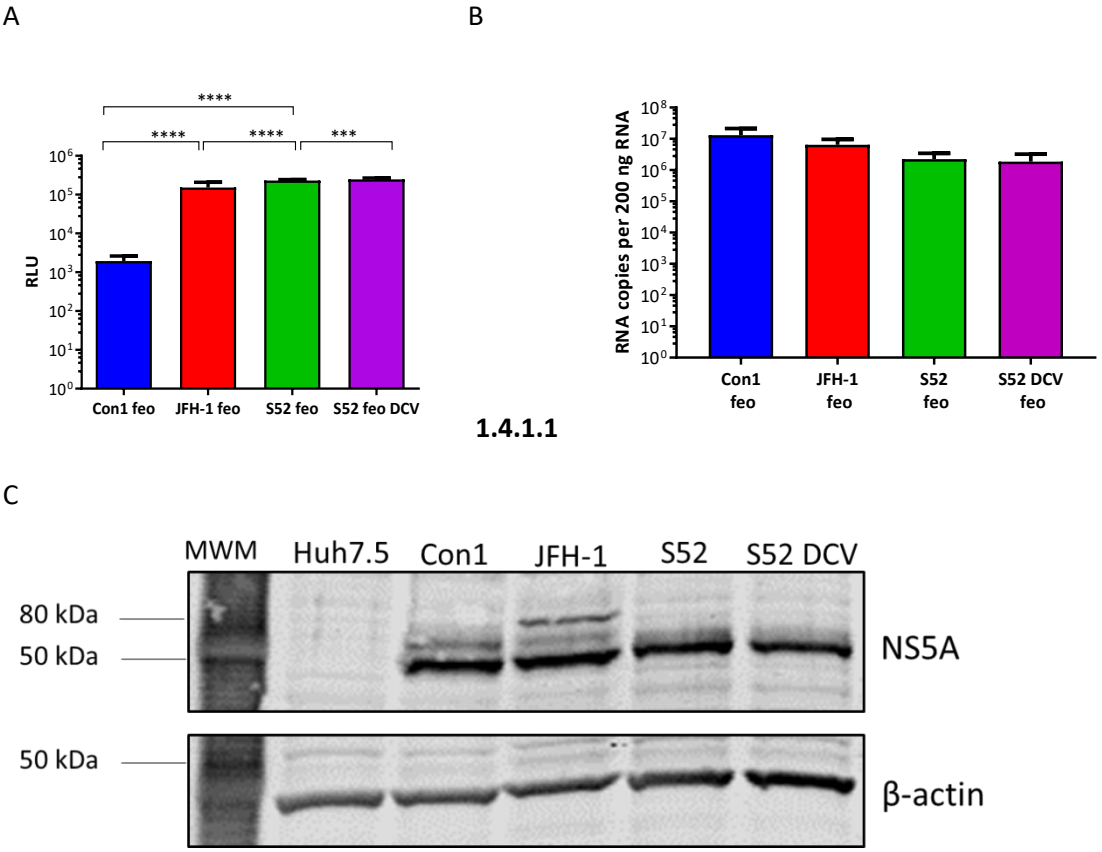

Figure 4-5. DCV selection of S52 SGR harbouring cells does not alter luciferase activity, SGR RNA or NS5A protein levels. (A) Assay for luciferase activity in SGR harbouring cells. Luciferase activity was measured in $8x10^3$ cells and compared to Con1 and JFH-1 SGR-harbouring cell lines. Error bars show the standard error of five experimental repeats. ****p≤0.0001. ***p≤0.001. (B) Quantification of HCV SGR RNA in SGR harbouring cell lines. Total cell RNA was extracted from SGR-harbouring cells and quantified. 200 ng of total RNA from each cell line was used as a template in a one-step RT qPCR reaction and expressed as genome copies per 200ng using an *in vitro*-transcribed SGR RNA as a standard curve. Error bars show the standard error of three experimental repeats. (C) Western blot analysis of NS5A in SGR-harbouring cells. 15 µg of the indicated SGR-harbouring cell lysates were resolved on 7.5% polyacrylamide and stained with sheep polyclonal anti-NS5A serum, anti-β actin and respective Infra-red-tagged secondary antibodies. Membranes were visualised using the LiCor Infra-red scanner system.

4.2.2.3 Investigation of the synergistic effect of multiple NS5A inhibitors

A series of studies by Bristol Myers Squibb, the pharmaceutical company who developed DCV, suggest that NS5A inhibitors may act synergistically. Therefore, a structurally similar compound with the capacity to bind to the same region of NS5A but which individually lacks therapeutic activity can, when used in combination with one which is pharmacologically active such as DCV, resensitise a resistant SGR or virus to that combination (Sun et al., 2015; O'Boyle et al., 2016).

As a proof-of-concept of the utility of the S52 SGR harbouring cell line and its DCV-resistant counterpart in the investigation of the activity of NS5A inhibitors this work was reproduced using DCV and LDV, the latter of which has a greatly reduced therapeutic activity against S52. This data is shown in Figure 4-6. S52 DCV cells were treated with a concentration of DCV that would have no inhibitory effect, together with increasing concentrations of LDV, to identify a difference in EC_{50} for the resistant S52 SGR due to the presence of the second inhibitor. The single concentrations were chosen to have a maximum difference between wild-type and DCV-selected: 50 nM for DCV and 500 nM for LDV. However, as the data show, the presence of LDV had no effect on DCV sensitivity. Inhibition was only observed when LDV was present at 1 µM, consistent with the calculated EC_{50} for LDV. This experiment was not able to show that the combination of NS5A inhibitors increased sensitivity beyond an additive effect of the two concentrations administered together.

A

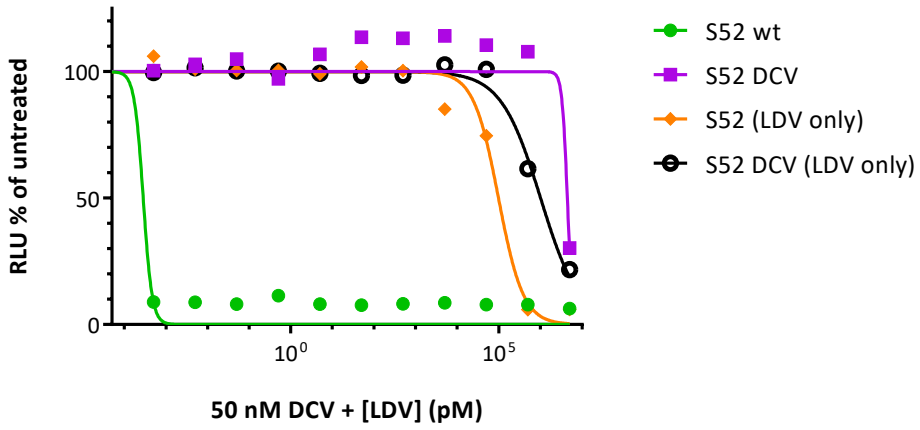

B

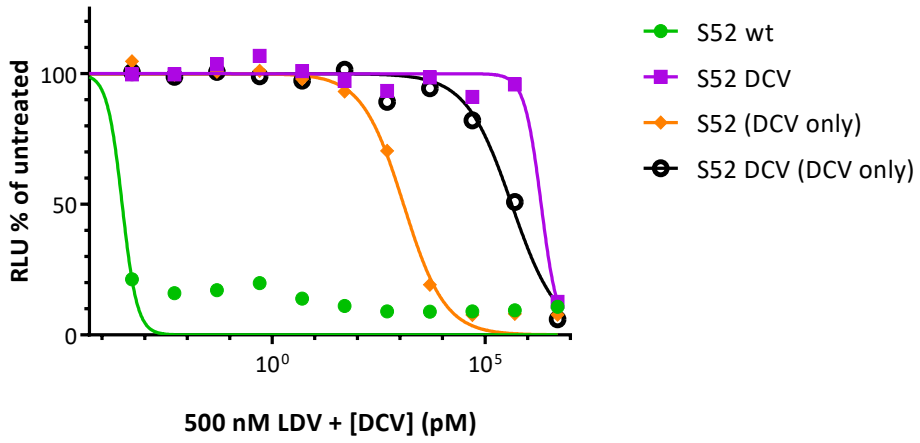

Figure 4-6. NS5A inhibitors DCV and LDV do not synergise. S52 wild-type and S52 DCV SGR harbouring cells were treated with: 50 nM DCV and the indicated concentrations of LDV (A); or 500 nM LDV as a single concentration and the indicated concentrations of DCV (B) for 48 hours before being harvested for luciferase assay. RLU values were expressed as a percentage of an untreated control.

4.2.2.4 Identification of resistance-associated substitutions

Resistance to NS5A inhibitors has been well characterised in most GTs, with a cluster of substitutions at residues 28-31 and a single substitution at Y93 giving several thousand-fold resistance depending on compound and genotype (Table 1-3, Table 1-4, Table 1-5 and references therein). In order to determine what changes were driven by DCV selection of S52, sequencing analysis was carried out on RNA extracted from S52 and S52 DCV SGR harbouring

cells. Extracted RNA was reverse transcribed to cDNA, which was then used as a template for PCR amplification. Amplified DNA fragments were analysed by Sanger sequencing and aligned to a reference sequence. Substitution sites were identified by manual identification of mixed sequencing traces, however consensus-based Sanger sequencing does not allow analysis of the relative proportions of mixed sequences within the population. Relative heights of the two peaks at a particular site are not representative of the proportion of the different nucleotides.

Figure 4-7 shows the sequence traces at the position corresponding to L31 and Y93. As the image shows a mixed population is visible at both of these locations, with the predominant sequence at residue 93 being His rather than Tyr. As described earlier the relative proportions of His and Tyr at this position cannot be accurately inferred, however the dominance of the mutation at this position is indicative that the proportion is sufficiently high to be assigned as a mutation by the data analysis software. This indicates that the selection of resistance has resulted in the emergence of RAS which are consistent with NS5A resistance in GT3.

A


CTC/TTC
L/F
Reference
Forward PCR fragment
Reverse PCR fragment
S52 Forward PCR fragment
S52 Reverse PCR fragment
S52 DCV Forward PCR fragment
S52 DCV Reverse PCR fragment

B

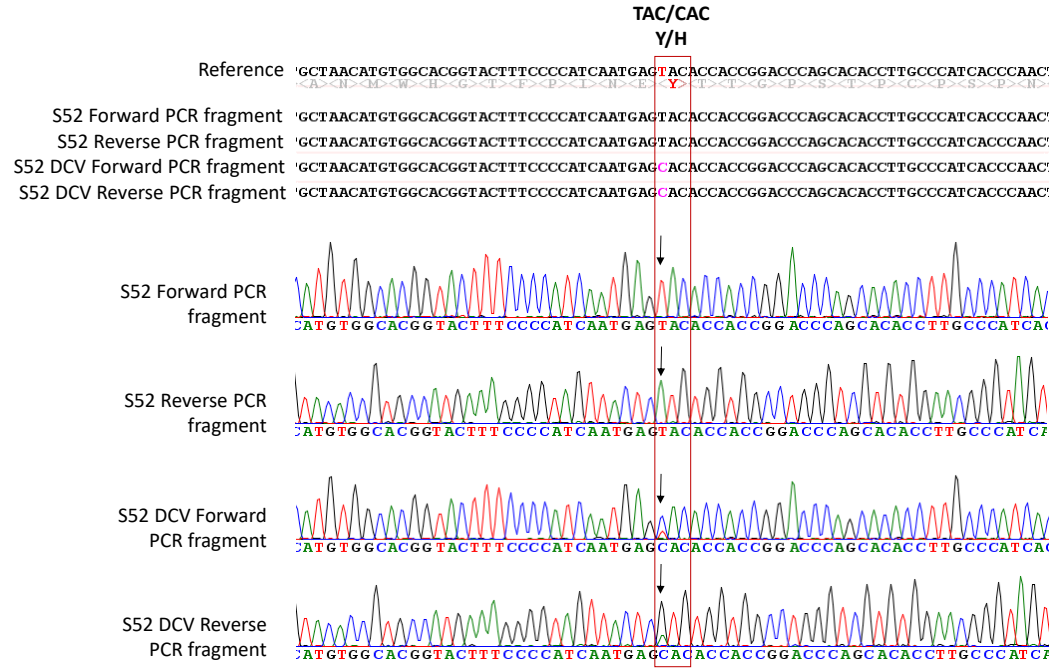
TAC/CAC
Y/H
Reference
S52 Forward PCR fragment
S52 Reverse PCR fragment
S52 DCV Forward PCR fragment
S52 DCV Reverse PCR fragment

Figure 4-7. S52 DCV SGR harbouring cells have acquired resistance-associated substitutions. RNA was extracted from S52 and S52 DCV SGR harbouring cells using TRIzol and reverse-transcribed to cDNA. cDNA was used as a template for PCR amplification of the NS5A region and PCR products were subjected to Sanger sequencing. Sequences were aligned to a reference sequence of S52 SGR. (A) The genome position corresponding to L31. (B) The genome position corresponding to Y93. The first base of the mutated codon is highlighted with a black box.

4.2.2.5 Sensitivity of transiently-replicating SGRs to NS5A inhibitors

The proposed mechanisms of action of DCV as an inhibitor of genome replication are the inhibition of NS5A trafficking through the cell and the formation of new replication complexes during the early stages of infection. SGR harbouring cells have proved useful in selection of resistance, however they are likely to exhibit different results based on the fact that replication has already been established. Thus, development of DAAs usually involves transient replication data. To evaluate the effects of NS5A inhibitors upon transient replication of full-GT3 (as opposed to chimera SGRs which most data on inhibitor efficacy and RAS is generated from) DAA sensitivity studies were carried out in the transiently-replicating full-GT3 S52 SGR described in Chapter 3, with CpGluc and a single point mutation of A1672V (by H77 polyprotein numbering) in NS4A conferring efficient transient replication ability on the SGR when electroporated into VSEC cells. In addition, since the resistance study using SGR harbouring cells identified that the Y93H point mutation confers significant DCV resistance upon S52, a Y93H (by NS5A numbering, Y2065H by H77 polyprotein numbering) single point mutant was constructed by site-directed mutagenesis to screen alongside.

As shown in Figure 4-8 the S52 SGR was less sensitive than Con1 and JFH-1 to both DCV and LDV, consistent with observations using SGR harbouring cell lines. The Y93H point mutant was highly resistant to both NS5A inhibitors, with a difference in EC_{50} of 70,000-fold for DCV; EC_{50} could not be extrapolated for LDV.

The data in Figure 4-9 also show that (as expected) stably-replicating S52 wild-type is much more resistant to DCV than transiently-replicating S52. In addition, wild-type transiently-replicating S52 Y93H is more resistant to DCV than stably-replicating S52 DCV; these data could be indicative of a difference in the mechanism of action of DCV at different stages of replication.

Interestingly, transiently-replicating S52 seems to be more sensitive to SOF than JFH-1; S52 Y93H also seems to be slightly resistant (2-fold) to SOF when compared to wild-type, though this was not statistically significant. Moreover, there was a difference in sensitivity to RBV between S52 and Con1 of 4-fold for which statistical significance was not able to be calculated due to the high variability of replication signal for Con1. There was also a slight difference between S52 wt and S52 Y93H (1.7-fold).

EC_{50} values for transiently-replicating SGRs and fold changes are shown in Table 4-3.

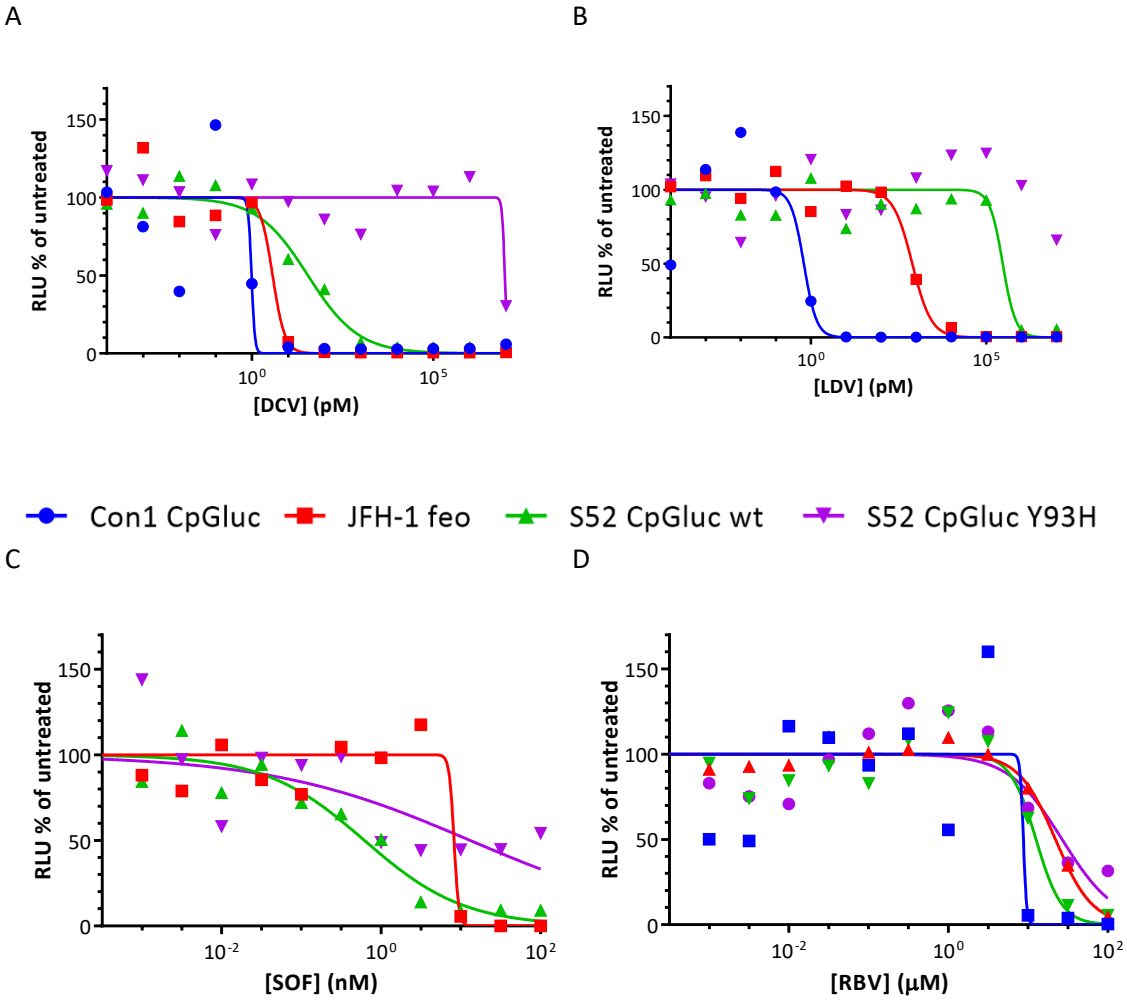

Figure 4-8. Transiently-replicating S52 SGR is less sensitive to NS5A inhibitors than other genotypes. $8x10^3$ of VSEC cells electroporated with the indicated SGRs were seeded in white, 96-well plates and treated at 4 hpe (Con1, JFH-1) or 24 hpe (S52, S52 Y93H) with the indicated concentrations of DCV (a), LDV (b), SOF (c) or RBV (d) for 72 hours before being harvested for luciferase assay. Relative light units were expressed relative to a 0.25% DMSO vehicle control. EC_{50} values were calculated using Graphpad Prism 7 software.

SGR harbouring cell line		DCV	LDV	SOF	RBV
Con1	EC_{50}	0.98 pM	0.32 pM		8.7 uM
	Fold over Con1				
JFH-1	EC_{50}	3.9 pM	0.98 nM	51.2 nM	22.9 uM
	Fold over Con1	4	3040		6.3
S52	EC_{50}	63 pM	0.2 uM	6.3 nM	12.6 uM
	Fold over Con1	64**	610,000		4.3
S52 Y93H	EC_{50}	4.5 uM		22.7 nM	23.9 uM
	Fold over Con1	4,600,000			7.2
	Fold over wild-type	72,000****		3.63	1.7

Table 4-3. Comparison of calculated EC_{50} and CC_{50} values for DCV treatment of HCV SGR harbouring cell lines. Fold changes to two significant figures. Statistical significance was calculated where sufficient data was available (****p<0.0001, **p<0.005)

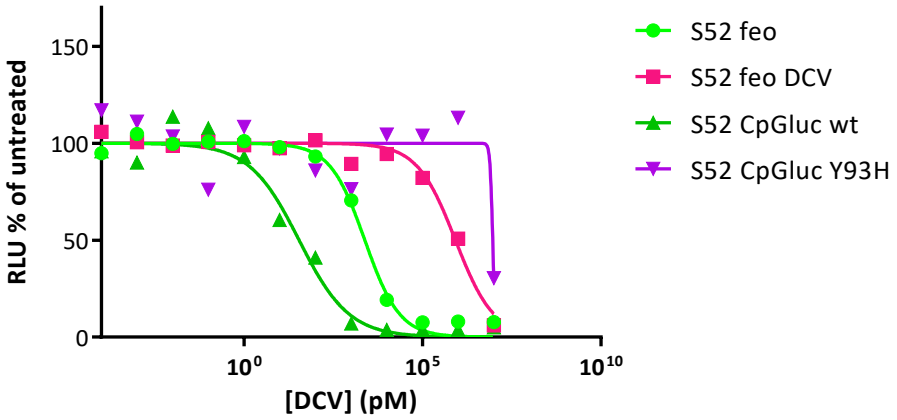

Figure 4-9. Stably-replicating wild-type S52 is less sensitive to DCV than transiently-replicating wild-type S52. The chart shows sensitivity of stably replicating S52 (S52 feo and S52 feo DCV) from Figure 4-1; and transiently-replicating S52 (S52 CpGluc and S52 CpGluc Y93H) from Figure 4-8 as a comparison.

4.2.2.6 Analysis of fitness cost of NS5A inhibitor resistance

Whilst conducting the concentration-response experiments with transiently-replicating S52 SGRs it was observed that the level of replication of the S52 Y93H mutant was significantly lower than the wild-type SGR, shown in Figure 4-10. This is consistent with reports that NS5A inhibitor resistance was associated with a fitness cost to replication (section 1.3.2.3). However, as shown in Figure 4-5 and Figure 4-10B no such fitness cost was observed in the stable SGR harbouring cell lines. There was no decrease in HCV RNA, luciferase activity or NS5A protein expression levels in the DCV-selected S52 SGR harbouring cells. This implies that the stably-replicating, resistant SGR is capable of similar levels of translation and replication to the wild-type.

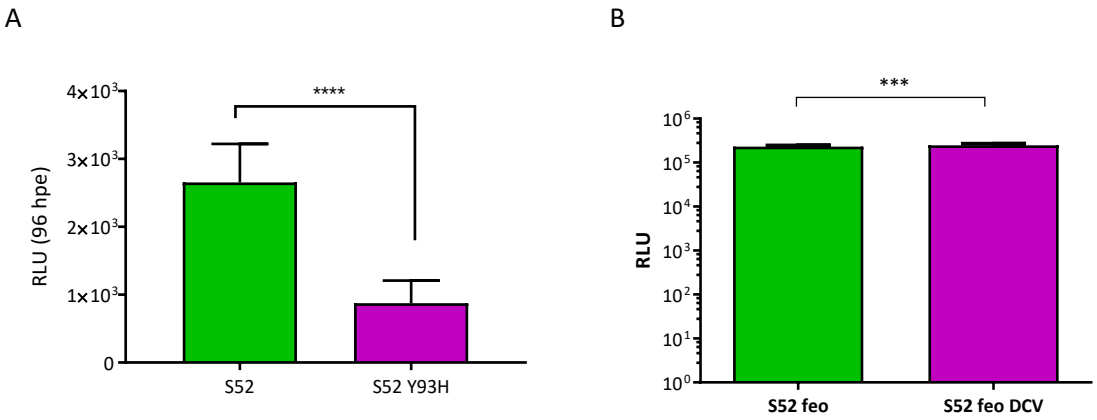

Figure 4-10. DCV-resistance of S52 SGR is associated with a fitness cost in transient assay. (A) 2 µg of the indicated RNAs were electroporated into VSEC cells and harvested for luciferase assay at 96 hpe. Error bars show standard error of the mean of five experimental repeats. (B) $8x10^3$ of the indicated SGR harbouring cell lines were harvested for luciferase assay. Error bars show standard error of the mean of five experimental repeats. ****p≤0.0001. ***p≤0.001

A consequence of a fitness cost would be that, in the absence of DAA selection, the RAS would revert to wild-type. To test this, the persistence was investigated of the RAS which were identified through sequencing of the DCV-selected S52 SGR. DCV selection pressure was removed from a population of the S52 DCV SGR harbouring cells and these were cultured in the presence of G418 to maintain the selection of the SGR itself whilst no longer selecting for DCV resistance. As described in Figure 4-7, a mixed sequence at the genome position corresponding to the Tyr93 residue can be identified. If there was indeed a fitness cost to replication then it would only be apparent in the absence of the selecting drug; in the presence of the selecting drug then the wild-type sequence would be incapable of replication to any level, and the mutant would remain the dominant sequence. The cells were passaged at 1:3 and after ten passages, approximately 30 days, there was no evidence of reversion of the resistant mutant as evident from the sequence traces shown in Figure 4-11.

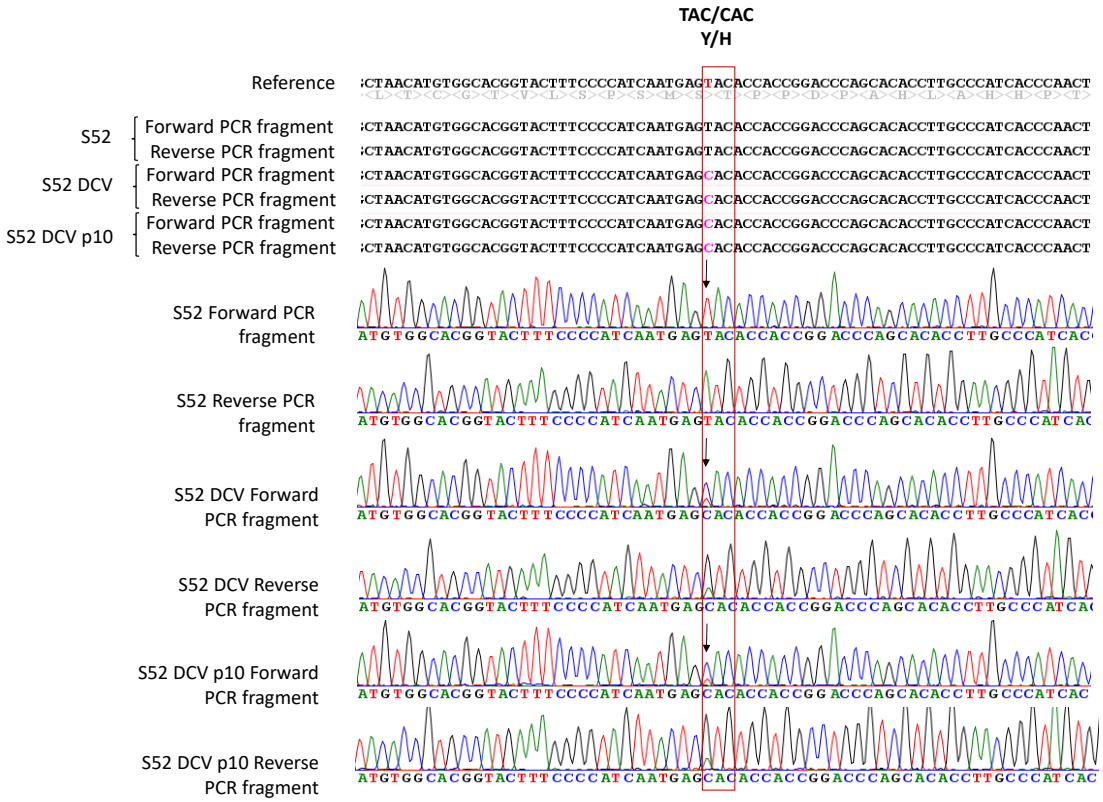

Figure 4-11. The Y93H RAS persists following removal of the selection pressure. RNA was extracted from S52 and S52 DCV SGR harbouring cells using TRIzol and reverse-transcribed to cDNA. cDNA was used as a template for PCR amplification of the NS5A region and PCR products were subjected to Sanger sequencing. Sequences were aligned to a reference sequence of S52 SGR. Images show forward and reverse sequences (reverse sequences are generated as reverse-complemented which are automatically aligned by the analysis software. This results in the colours used to designate individual bases being reversed).

The observation that RAS are stable in the absence of the selection pressure as shown in Figure 4-11 highlighted a further difference between transient and stable replication of S52.

4.2.2.7 Evidence for compensatory mutation in resistance

One explanation was that the fitness cost of Y93H might be compensated for by additional mutation(s). This was explored using two parallel experiments. Initially, PCR sequencing data were reanalysed to identify any additional mixed sequences which are not present in the wild-type sequencing traces. A single additional mutation was identified which showed no evidence of a mixed sequence in any wild-type sequencing traces. This mutation was also identified in

the S52 DCV SGR harbouring cells which had been removed from DCV selection (labelled DCV -10). This was K41R: close to the cluster of residues at M28-L31; it has not been mentioned in *in vitro* or clinical studies as being a RAS.

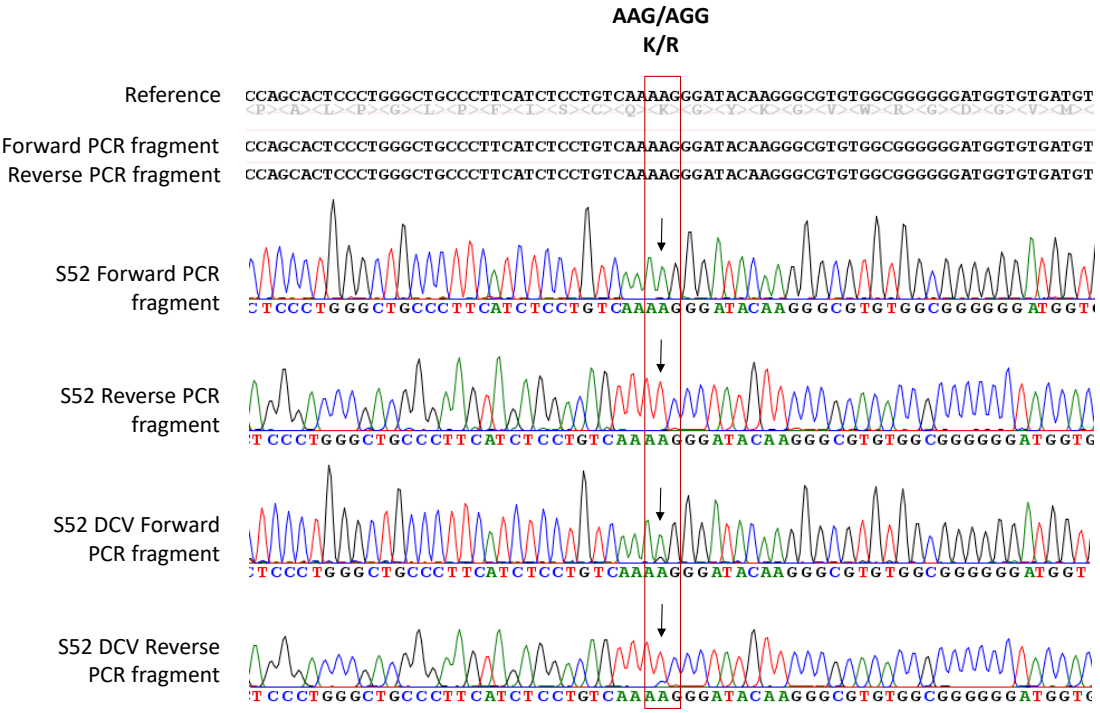

Figure 4-12. An additional substitution. K41R, was selected with DCV resistance. RNA was extracted from S52 and S52 DCV SGR harbouring cells using TRIzol and reverse-transcribed to cDNA. cDNA was used as a template for PCR amplification of the NS5A region and PCR products were subjected to Sanger sequencing. Sequences were aligned to a reference sequence of S52 SGR.

This mutation was introduced into the S52 wild-type and Y93H transiently-replicating SGRs by site-directed mutagenesis and was screened for a potential phenotype as a stabilising mutation. As the data in Figure 4-13 show the combination of K41R and Y93H, far from restoring replication to wild-type levels, is lethal to the SGR.

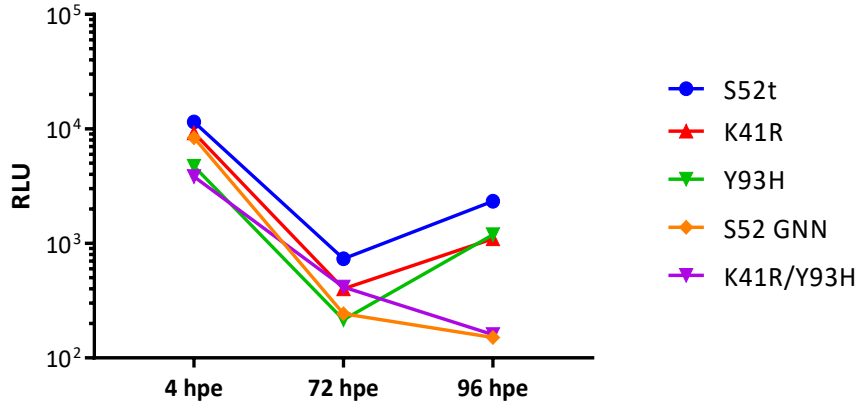

Figure 4-13. K41R does not confer a stabilising phenotype on S52 Y93H SGR. 2 µg of the indicated SGRs were electroporated into VSEC cells and harvested for luciferase assay at the indicated time points.

A parallel experiment to investigate the presence of resistance-stabilising mutations within the S52 DCV SGR involved re-electroporation of SGR harbouring cell RNA. As presented in chapter 3, RNA extracted from SGR harbouring cells will replicate transiently when electroporated into naïve Huh7.5 cells (Figure 3-13). Previously in this chapter it has been shown (Figure 4-5) that S52 wild-type and DCV SGR harbouring cells show no difference in the replication and expression of SGR-encoded proteins, whereas transient replication of DCV-resistant S52 Y93H is subject to a significant fitness cost (Figure 4-10). The SGR RNA within SGR harbouring cells before and after selection with DCV is identical except for a small number of RAS and other mutations which are not characterised as RAS (such as K41R, described above). Hence, if the phenotype difference resulted from mutations within the SGR then these two should replicate to similar levels when electroporated transiently into Huh7.5 cells. The results of this experiment are shown in Figure 4-14.

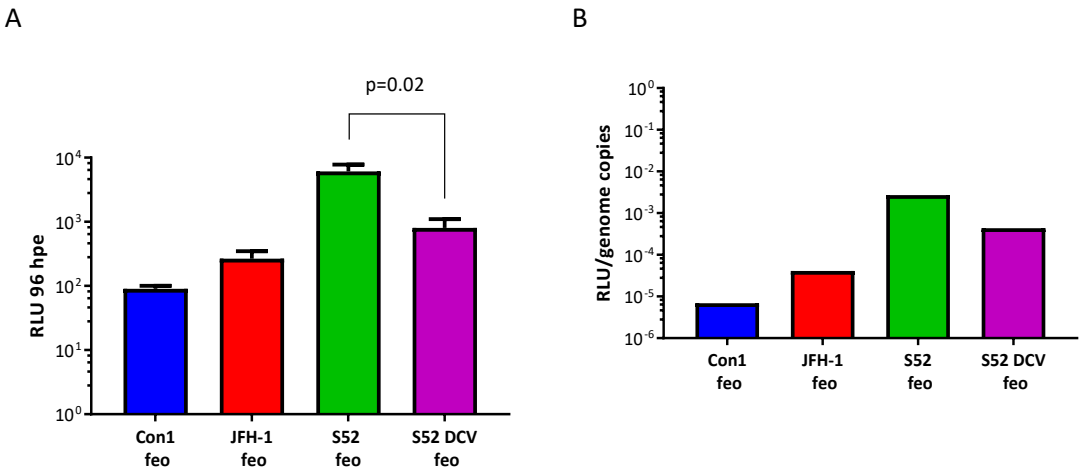

Figure 4-14. Transient replication of SGR harbouring cell RNA is subject to a fitness cost. Total cytoplasmic RNA was extracted from the indicated cell lines using TRIzol. 10 µg of total RNA was electroporated into Huh7.5 cells and harvested for luciferase assay at 96 hpe (A). Average relative light units (RLU) was normalised to average SGR RNA quantified by qPCR (B)

As the data show there is a defect in transient replication of the S52 DCV SGR. This difference is only slightly significant (P=0.02) but the trend was preserved in multiple experimental repeats. This indicates that the difference in phenotype between transient and stable S52 DCV-resistant replication is not solely due to the presence of resistance-stabilising mutations which arise upon selection and rescue replication of the resistant SGR. Indeed, no such evidence was observed that any of these mutations exist, as the only other mutation which is not a RAS did not confer this phenotype (Figure 4-13).

4.2.2.8 Transcomplementation between late and early replication

The fitness cost phenotype difference between transient and stable replication of DCV-resistant S52 could instead be linked to the different functions of NS5A in different stages of replication. NS5A domain I has been shown to adopt different homodimer configurations (Tellinghuisen et al., 2004; Love et al., 2009; Lambert et al., 2014). Although the physiological role of these alternative dimers is not clear it is likely that the NS5A homodimer conformations are linked to the phosphorylation state of the protein to effect different stages of replication (1.1.4.2.3). In each of these structures Tyr93 is predicted to be close to the dimer interface, and may have a crucial role in the switch between the two. Hence, it is possible that Tyr93

may play different roles in the initiation stage of replication and the later stages, once replication has already been established. Therefore, the hypothesis considered is that the Y93H RAS fitness cost is no longer apparent once the role of the region containing this residue in the initiation of replication is complete.

To test whether the differential phenotype in transiently-replicating S52 is affected by the presence of a stably-replicating SGR, a transcomplementation experiment was carried out. Functional NS5A is known to be able to transcomplement non-functional NS5A, and rescue replication in a cell which is transfected with both (Appel et al., 2005). For the purposes of this experiment, if a stably-replicating Y93H-containing SGR has overcome the fitness cost by establishing stable replication, then it will be able to transcomplement a transiently-replicating SGR with the same mutation and restore replication of the latter towards wild-type levels. S52 neo Y93H SGR harbouring cells were selected as described previously (section 3.2.2); the experiment was designed so as to compare the result of wild-type with Y93H SGR harbouring cells, however the S52 neo wild-type cells did not survive in selection and sufficient time to complete the experiment before completion and submission of this thesis had passed. Presence of the SGR was verified by western blot for NS5A and qPCR to detect the SGR RNA as shown in Figure 4-15. The western blot in this figure is the same shown in Figure 3-9 and Figure 4-5. These do not express luciferase, allowing the electroporation of a luciferase-only SGR (S52 CpGluc and S52 CpGluc Y93H) – any resulting luciferase activity is directly as a result of transcomplementation of the transient SGR.

When the S52 CpGluc and S52 CpGluc Y93H was electroporated into these cells, luciferase activity was detected as shown in Figure 4-16. Therefore, transcomplementation must have occurred since these SGR harbouring cells are derived from Huh7.5 and not VSEC cells; S52CpGluc does not replicate in Huh7.5 cells and requires the expression of PIV5 V protein and SEC14L2 (discussed in chapter 3). However, as the data show, the stably-replicating Y93H mutant SGR was able to transcomplement the transiently-replicating Y93H mutant to a lesser extent. It is clear that the interpretation of this experiment requires comparison to the wild-type SGR harbouring cells, which was not possible in the time available – further exploration of this result should involve this as a priority.

A

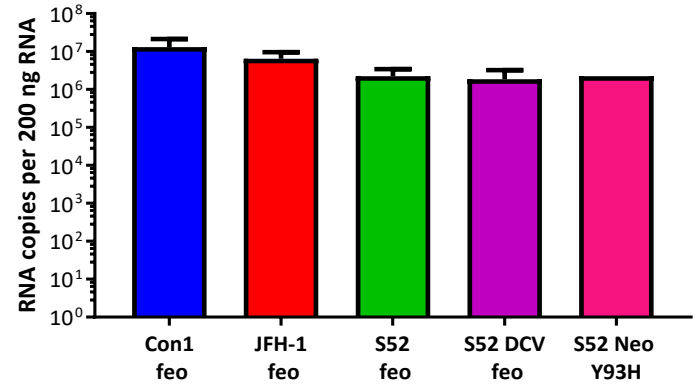

B

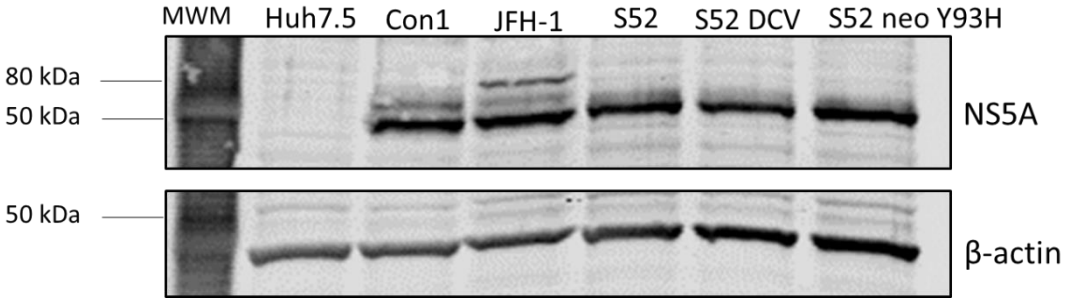

Figure 4-15. S52 neo SGR harbouring cells express NS5A protein and contain SGR RNA. (A) Quantification of HCV SGR RNA in SGR harbouring cell lines. Total cell RNA was extracted from SGR-harbouring cells and quantified. 200 ng of total RNA from each cell line was used as a template in a one-step RT qPCR reaction and expressed as genome copies per 200ng using an *in vitro*-transcribed SGR RNA as a standard curve. Error bars show the standard error of three experimental repeats. (B) Western blot analysis of NS5A in SGR-harbouring cells. 15 µg of the indicated SGR-harbouring cell lysates were resolved on 7.5% polyacrylamide and stained with sheep polyclonal anti-NS5A serum, anti-β actin and respective Infra-red-tagged secondary antibodies. Membranes were visualised using the LiCor Infra-red scanner system.

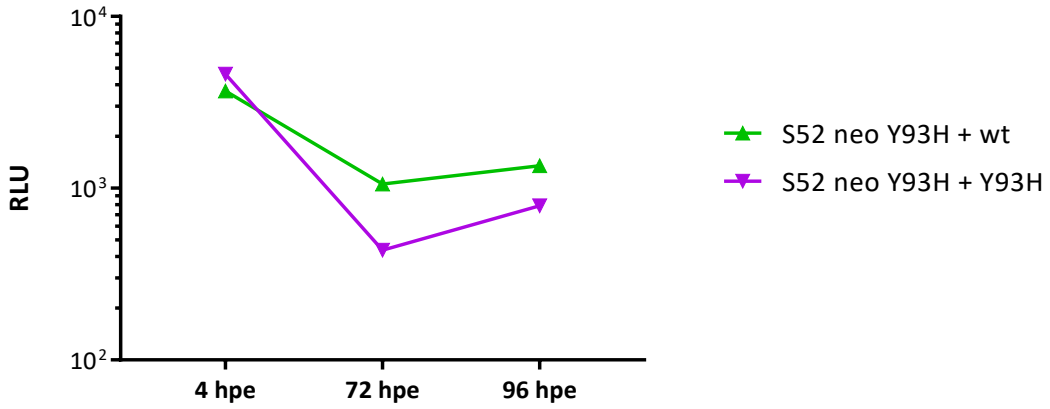

Figure 4-16. Stably-replicating S52 Y93H only partially transcomplements transiently-replicating S52 Y93H. 2 µg of the indicated RNAs were electroporated into S52 Neo Y93H SGRs and harvested for luciferase assay at the indicated time points.

4.2.2.9 Selection of double resistance to Harvoni treatment

The current clinically-licenced therapy for HCV in the United States, which is dominated by GT1 at 75% (Figure 1-1), is the Harvoni combination therapy licenced by Gilead. This is a combination of LDV and SOF and is licenced for GT1 only. Clinical use of LDV to treat GT3 is not extensive following initial reports that it is less effective against GT3, which was confirmed in the NHS EAP (Foster et al., 2016). Despite the addition of SOF which is effective against GT3, Harvoni is not recommended for GT3 patients.

To investigate whether resistance to SOF/LDV combination therapy can be selected, S52 and JFH-1 SGR harbouring cells were selected with 100x the calculated EC_{50} values of LDV and SOF: 17.2 µM and 440 nM respectively. Cells were treated with the aforementioned concentrations of HCV inhibitors without G418 for an initial 48 hours to allow resistance mutations to begin to accumulate, before G418 selection was reintroduced. A population of cells survived this selection and were termed S52 SOF/LDV. These cells grew poorly due to the high concentrations of inhibitor and characterisation was limited. However, analysis of resistance using concentration-response curves, shown in Figure 4-17, showed that a small degree of resistance was selected.

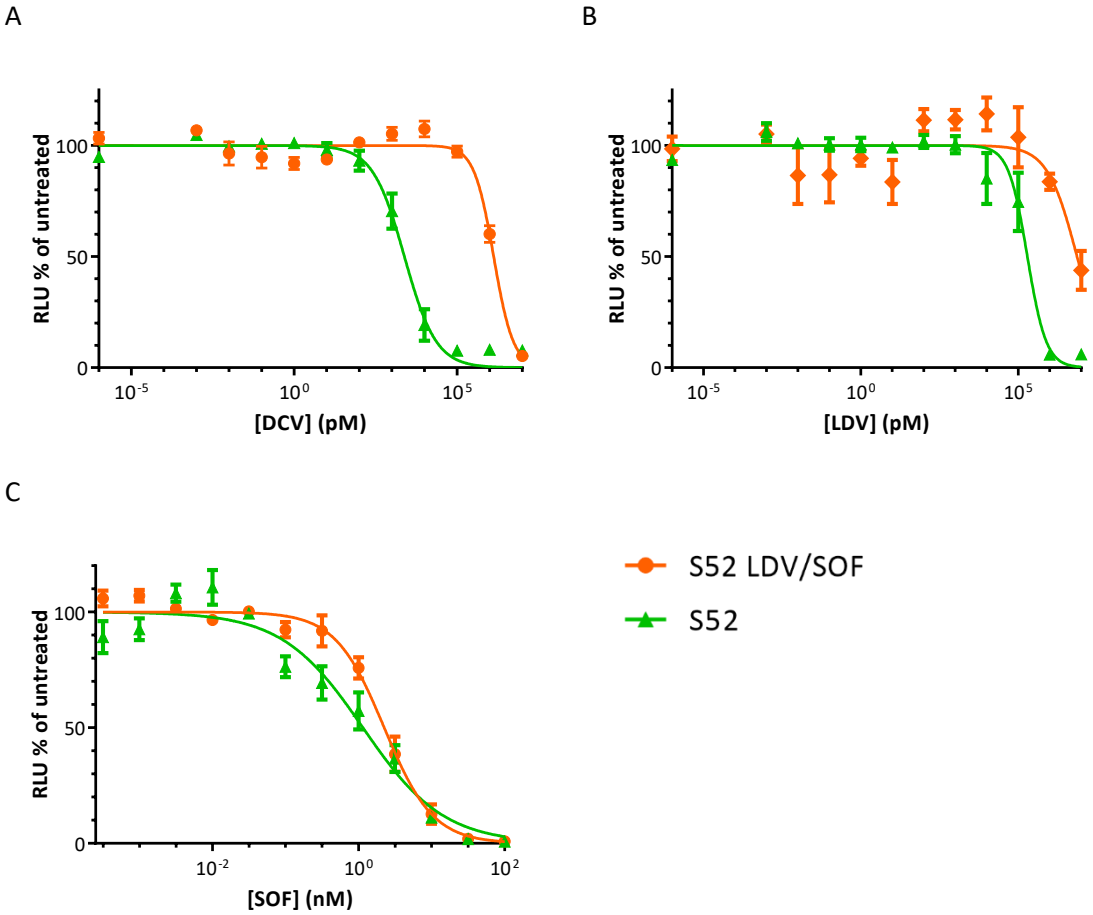

Figure 4-17. Selection of S52 SGR harbouring cells with LDV/SOF generates a population which are more resistant to NS5A and NS5B inhibitors. S52 SGR harbouring cells were treated with 100x the calculated EC_{50} of LDV (17.2 µM) and SOF (440 nM) for 48 hours in the absence of G418 to allow resistant mutations to emerge before G418 selection was reintroduced. Surviving cells were pooled into a polyclonal population and termed S52 LDV/SOF. $8x10^3$ of these cells were seeded in white 96-well plates and treated with the indicated concentrations of DCV (A), LDV (B), SOF (C) for 48 hours before being harvested for luciferase assay. RLU values were expressed as percentages relative to a DMSO vehicle control. Error bars show the standard error of the mean of three experimental repeats.

	DCV	LDV	SOF
EC_{50}	1.33 μM	7.4 μM	2.2 nM
Fold over wild-type	700	43	2

Table 4-4. Comparison of calculated EC_{50} values for S52 SOF/LDV SGR harbouring cell lines. Fold changes to two significant figures.

As shown in Table 4-4 there is a shift in EC_{50} of 700-fold for DCV but only 43-fold for LDV and 2-fold for SOF. It is surprising that the EC_{50} after selection should not exceed the concentration which was used for selection, considering that these cells are maintained in 100-fold the wild-type EC_{50} concentrations. It is likely for LDV that the effect upon the double-resistant SGR at the highest concentration is linked to toxicity of the compound –LDV is associated with cytotoxicity at the highest concentration and is also affected by solubility in culture medium at these concentrations.

4.2.2.10 Analysis of sensitivity of HCV SGRs to VEL

During the course of this project a second-generation NS5A inhibitor (Lawitz et al., 2015), Velpatasvir (VEL) was licenced. VEL has been described as pan-genotypic with a higher barrier to resistance and so these reports were investigated using the assays detailed in this chapter. As shown in Figure 4-18 and Table 4-5 VEL was more effective against Con1 SGR than S52 and DCV-resistant S52 both in stable replication and transient replication assays. The DCV-resistant S52 was also resistant to VEL.

SGR/cell line		VEL (transient)	VEL (stable)
Con1	EC_{50}		0.21 pM
	Fold over Con1		
JFH-1	EC_{50}	17.57 pM	0.64 pM
	Fold over Con1		3.1
S52	EC_{50}	0.079 pM	76.5 pM
	Fold over Con1		370
S52 DCV/Y93H	EC_{50}	2.92 nM	6.24 nM
	Fold over Con1		30,000
	Fold over wild-type	37,000	82

Table 4-5. Comparison of calculated EC_{50} values of VEL HCV SGR and SGR harbouring cell lines. Fold changes to two significant figures.

A

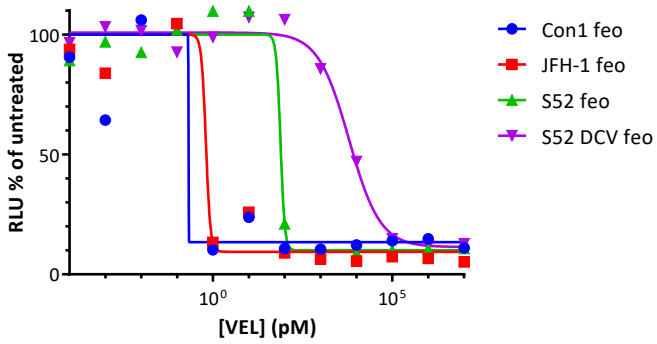

B

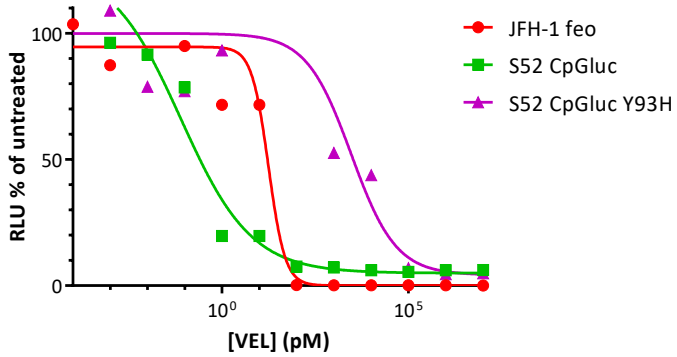

Figure 4-18. S52 SGR is more resistant to VEL than other genotypes. $8x10^3$ of the indicated cell lines were seeded in white 96-well plates and treated with the indicated concentrations of VEL for 48 hours before being harvested for luciferase assay (A). $8x10^3$ of VSEC cells electroporated with the indicated SGRs were seeded in white, 96-well plates and treated at 4 hpe (JFH-1) or 24 hpe (S52, S52 Y93H) with the indicated concentrations of VEL for 72 hours before being harvested for luciferase assay. Relative light units were expressed relative to a 0.25% DMSO vehicle control. EC_{50} values were calculated using Graphpad Prism 7 software

The concentration-response curves for each compound consist of an initial plateau, where concentration is too low for any effect to be observed, a linear portion within which the EC_{50} lies, and a second plateau, in which the concentrations are higher than that which exerted its maximum effect. This second plateau usually reaches a baseline number of relative light units, usually around 100 RLU. However, the second plateau of the VEL concentration-response curve to measure sensitivity of S52 and S52 DCV-resistant SGR did not reach this baseline level, and instead reached a plateau of several thousand RLU, as shown in Figure 4-19.

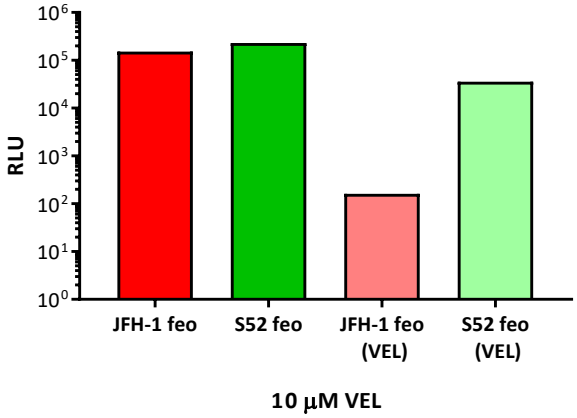

Figure 4-19. Higher concentrations of VEL do not eradicate replication of S52. Bar chart shows the average luciferase activity in SGR harbouring cells treated with 10 μM VEL for 48 hours.

This effect seems to be unique to the S52 SGR harbouring cells. S52 SGR harbouring cells do indeed have a higher luciferase activity than their JFH-1 counterparts, however the difference in RLU at this highest concentration of VEL is 200-fold between S52 and JFH-1 SGR harbouring cells, and the difference between untreated RLU values for these same cells is 1.5-fold. It is not known why such an effect occurs when S52 SGR harbouring cells are treated. In contrast, the S52 SGR is highly sensitive to VEL compared to DCV and LDV, when EC_{50} is calculated.

4.2.3 Investigation of the emergence of NS5A inhibitor resistance

Clinical studies of NS5A inhibitor efficacy usually investigate RASs (RAS) in patients who have failed therapy. Those in GT3 patients associated with the highest degree of resistance, and correlate with treatment response, are Y93H and L31V (section 1.3.2.3). However, the link is not causative: patients with a pre-existing RAS may go on to achieve SVR, and patients who do not present with a pre-existing RAS may go on to fail treatment and develop RAS in the relapse or rebound virus sequences. Thus, the relationship between RAS and treatment response is not fully known.

4.2.3.1 Comparison of replication of Y93H and wild-type S52 by colony formation assay

To investigate this, a colony formation experiment was carried out. 2μg of RNA transcribed from S52 neo wild-type and Y93H were electroporated into Huh7.5 cells and selected with

G418 for three weeks. Surviving colonies were fixed and counted and this data is shown in Figure 4-20.

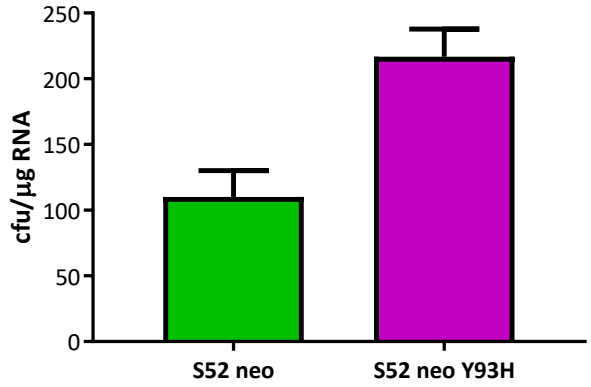

Figure 4-20. S52 neo Y93H replication can be quantified by colony formation assay, and shows no fitness cost. 2 µg of the indicated RNAs were electroporated into Huh7.5 cells and seeded at a density of $1x10^5$ in a 6-well plate. 48 hours after electroporation the cells were selected with 50ng/mL G418 for three weeks, re-treating with G418 every 48 hours. Following selection, colonies were fixed and stained with 10% PFA in crystal violet, then counted manually and expressed as colony forming units per µg RNA electroporated.

As the data show the fitness cost of the transient Y93H mutation was not apparent in this system. Indeed, colony formation efficiency is higher than for wild-type.

4.2.3.2 Investigation of the effect of pre-existing RAS upon development of DCV resistance

The consensus of *in vitro* data is that RAS such as Y93H confer high levels of resistance upon SGRs of all GTs. However, the role of RAS in treatment response is not clear as, upon treatment, they can arise *de novo* or expand from pre-existing low frequencies within patient sequences (Kai et al., 2017). The pre-existence of a RAS within a patient is associated with a decreased likelihood of achieving SVR, but patients with a RAS can eradicate the virus and those without can fail without a RAS being detected. The colony formation assay outlined in Figure 4-20 was then used to explore the effect of pre-existing RAS on the colony-formation efficiency of S52 in the presence of DCV. Huh7.5 cells were electroporated with different ratios of wild-type and Y93H S52 neo RNA and selected with G418 to quantify colony formation efficiency.

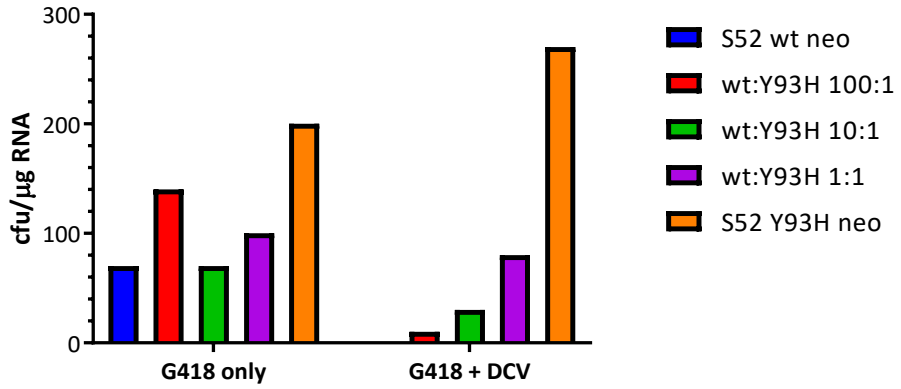

Figure 4-21. Pre-existence of a RAS strongly correlates with colony formation efficiency in the presence of DCV. 2 µg of the indicated RNAs at the indicated ratios were electroporated into Huh7.5 cells and seeded at a density of $1x10^5$ in a 6-well plate. 48 hours after electroporation the cells were selected with 50ng/mL G418 for three weeks, re-treating with G418 every 48 hours. Following selection, colonies were fixed and stained with 10% PFA in crystal violet, then counted manually and expressed as colony forming units per 100 ng RNA electroporated.

The result of a preliminary experiment is shown in Figure 4-21. This experiment is highly variable but there is a clear association between abundance of a RAS and the capacity to replicate in the presence of DCV. Indeed, there may be an increase in the colony-formation efficiency of Y93H SGR in the presence of DCV compared to the absence, though this requires verification.

4.2.4 Epidemiological analysis of resistance

The initial focus of this project was to investigate NS5A inhibitor resistance in sequences derived from clinical samples obtained from GT3-infected patients. The strategy was to establish transient replication of the S52 feo SGR then use this system to develop a shuttle construct with a pair of unique restriction sites flanking the NS5A coding region. Once constructed, NS5A sequences from clinical samples could then be amplified by PCR using a pair of primers to insert the respective restriction sites at either end. These PCR products could then be ligated into the shuttle construct and the resulting chimera SGR plasmid DNA propagated as a mixture to maintain the quasispecies of NS5A sequences which existed within the patient. This strategy would lead to the construction of a set of chimera SGRs, one for

each original patient sample, in which the variability of NS5A exists as a mixture. The purpose of this would then be to select resistant sequences from this mixture using DCV treatment and identify patterns of RAS which emerged using sequencing. However, the work to establish transient replication exceeded its expected timescale and the experiment could not be completed. This section details the initial work to construct the transiently-replicating shuttle construct and optimise the amplification of NS5A from clinical samples.

4.2.4.1 Construction of the S52 shuttle construct

The S52 SGR already contains a unique PsiI restriction site at the 3' end of NS5A; it was modified to insert a silent Bsu36I restriction site at the 5' end. However, it has been shown that the S2204I culture-adaptive mutation in the LCS-I of NS5A is essential for replication of this SGR and such a mutation cannot be assumed to be present in the clinical sequences. Thus, a second unique site was introduced within the LCS-I downstream of the S2204I mutation site: PspXI. Since the low CpG/UpA reporter which was used to replace the feo cassette contains a Bsu36I restriction site, this was removed silently by site-directed mutagenesis (with care taken to maintain the CpG and UpA dinucleotide frequency). The resulting SGR with CpGluc, A1672V culture-adaptive mutation and unique restriction sites flanking NS5A domain I was labelled S52t, for transiently-replicating S52 (Figure 4-22).

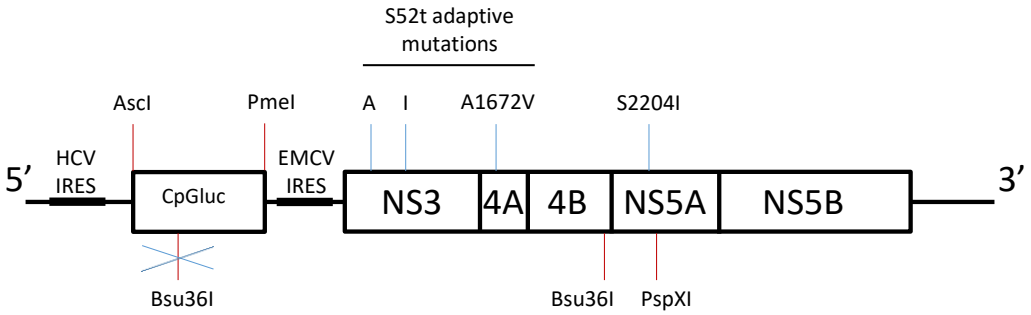

Figure 4-22. Diagram of the S52t SGR. Features of the SGR are labelled: CpGluc (low CpG/UpA luciferase) and HCV non-structural proteins (NS3, NS4A, NS4B, NS5A, NS5B). CAS (T1056A, T1429I, A1672V) labelled with blue lines, restriction sites labelled with red lines; the site of the second Bsu36I site which was removed by site-directed mutagenesis is denoted by a crossed-out red line.

Since the experimental strategy involved subcloning and expanding the chimera SGR DNA as a mixture, individual bacterial colonies would not be screened as part of the ligation. Hence, there was concern that any religation of vector would result in the inclusion of wild-type SGR

sequences which would skew the results of the experiment. To prevent this from occurring a short stuffer fragment of 20 nucleotides was designed to be ligated into the shuttle construct in place of NS5A domain I; this would be the vector used for insertion of amplified patient sequences. This was termed S52t-SF (stuffer fragment). Any religated vector within the mixture would be inconsequential since the lack of NS5A domain I should render the SGR replication-incompetent.

The respective replication capacities of S52t and S52t-SF were verified. All modifications to the SGR were silent in terms of the amino acid coding sequence and the CpG/UpA dinucleotide frequency of the reporter, however RNA structures are known to be important to the virus and so replication of the modified S52t SGR was assayed. Figure 4-23 shows that the S52t replicated to similar levels to the S52 CpGluc A1672V SGR, which contains the additional Bsu36I site within the luciferase gene and lacks the PspXI restriction site within the LCS-I. In addition the S25t-SF, which contains the stuffer fragment in place of NS5A domain I, was unable to replicate.

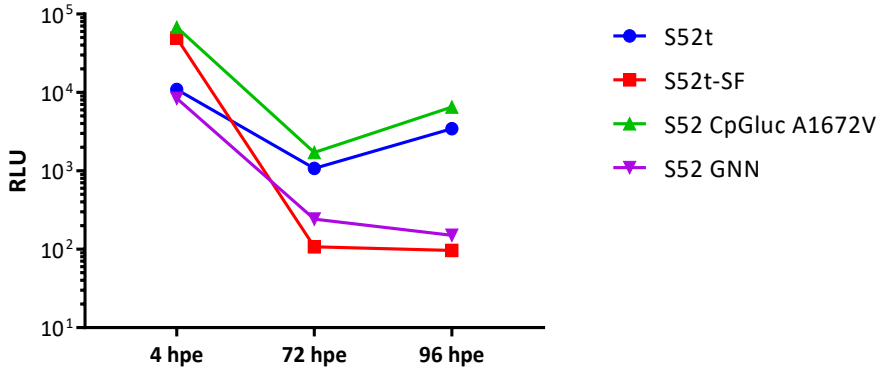

Figure 4-23. S52t, containing the modifications required for insertion of NS5A coding regions from clinical samples, is capable of transient replication. 2 µg of the indicated RNAs were electroporated into VSEC cells and harvested for luciferase assay at the indicated time points.

4.2.4.2 Patient sample information

The samples obtained were from the HCV Research UK Biobank and were from patients with chronic HCV GT3 enrolled in the NHS EAP. The samples selected were from patients who failed to respond to DCV treatment; patients treated with LDV were not selected due to the lower efficacy of this drug against GT3. 7 sets of paired samples were received, taken at baseline and

at time of relapse for each patient. In addition, samples from ten patients were received who achieved SVR – initially the purpose of these samples was for optimisation of the amplification protocol since they are more abundant than the 6 pairs of relapse samples which were vital for the experiment once the parameters were optimised. However during the course of the experiment it was expected that the SVR samples might provide a valuable control, with the potential for differences to be identified which could at least partially explain the response rates between the two sets of patients. The SVR samples were also supplied at a range of different viral loads, to provide the opportunity to identify the limit of amplification. A summary of the information for each sample is provided in Table 4-6 and Table 4-7.

Patient key (last four digits)	**Sample barcode (last four digits)**	**Sample type**	**Viral load (IU/mL)**
4309	1984	Baseline	$1.25X10^6$
	1980	Relapse	$4.96X10^5$
	1977	Relapse	$4.96X10^5$
1844	1973	Baseline	$1.59X10^6$
	1978	Relapse	$1.29X10^6$
1447	1983	Baseline	$7.76X10^5$
	1974	Relapse	$5.63X10^5$
8810	1982	Baseline	$4.91X10^5$
	1976	Relapse	$1.48X10^4$
0925	1971	Baseline	$2.99X10^5$
	1979	Relapse	$1.67X10^5$
4471	1972	Baseline	$1.88X10^5$
	1981	Relapse	$3.05X10^2$
1785	1970	Baseline	$4.52X10^4$
	1985	Relapse	$2.93X10^2$
	1975	Relapse	$2.93X10^2$

Table 4-6. Clinical samples received from the HCVRUK biobank for the epidemiological study: Nonresponder group.

Patient key (last four digits)	Sample barcode (last four digits)	Sample type	Viral load (IU/mL)
6456	1935	SVR	$5.61X10^6$
4447	1934	SVR	$1.20X10^6$
7307	1933	SVR	$6.63X10^5$
2355	1932	SVR	$2.47X10^5$
1703	1931	SVR	$6.00X10^4$
4221	1930	SVR	$2.00X10^4$
7980	1929	SVR	$1.63X10^4$
6115	1928	SVR	$8.20X10^3$
6264	1927	SVR	$7.91X10^3$
7228	1926	SVR	$4.57X10^3$

Table 4-7. Clinical samples received from the HCVRUK biobank for the epidemiological study: SVR group.

4.2.4.3 Amplification of NS5A sequences

I initially designed primers to contain ambiguous bases to reflect the variability of the locations at which the restriction sites would need to be introduced. GT3 sequences from the Los Alamos HCV database (Kuiken et al., 2005) were used for primer design. These were tested against plasmid DNA of Con1, JFH-1 and S52 SGR and a no-template control to confirm specificity. As shown in Figure 4-24 there was a single band which resolved at the appropriate size of NS5A domain I.

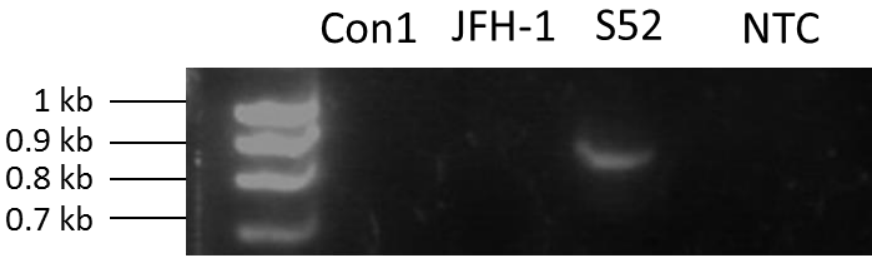

Figure 4-24. NS5A domain I can be amplified from plasmid DNA using degenerate primers. Plasmid DNA of Con1, JFH-1 and S52 SGR was amplified by PCR and resolved on 1% agarose gel.

However, when these primers were used to amplify NS5A from cDNA reverse-transcribed from RNA extracted from the patient sample in the SVR group with the highest viral load, no bands were visible. To address this the primers were redesigned to remove the ambiguous bases. Although this would likely bias the amplification of certain sequences, this was considered an acceptable risk, compared to failure of amplification. Nested PCR amplification was repeated using these redesigned primers and a weak band was visible when the PCR products were resolved. The reproducibility of this was poor in that on some occasions no amplification was visible. A representative gel of a successful amplification is shown in Figure 4-25.

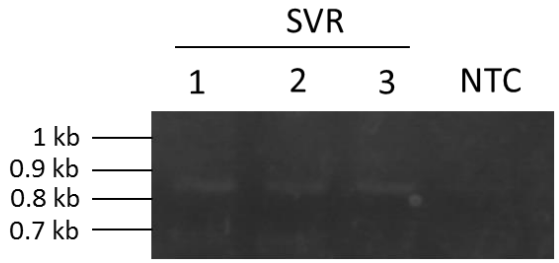

Figure 4-25. NS5A domain I can be amplified by PCR from patient samples. RNA was extracted from clinical samples using the QIAmp viral RNA kit and reverse-transcribed to cDNA using a gene-specific reverse primer. cDNA was amplified by nested PCR and resolved on 1% agarose gel. SVR 1, 2 and 3 refer to three high viral load samples from the SVR patient group.

To improve the reproducibility and the yield of amplified DNA the addition of magnesium chloride ($MgCl_2$) was investigated. It was found that the addition of $MgCl_2$ to the second (nested) PCR reaction greatly improves the yield of the DNA fragment, as well as the reproducibility. A representative gel is shown in Figure 4-26.

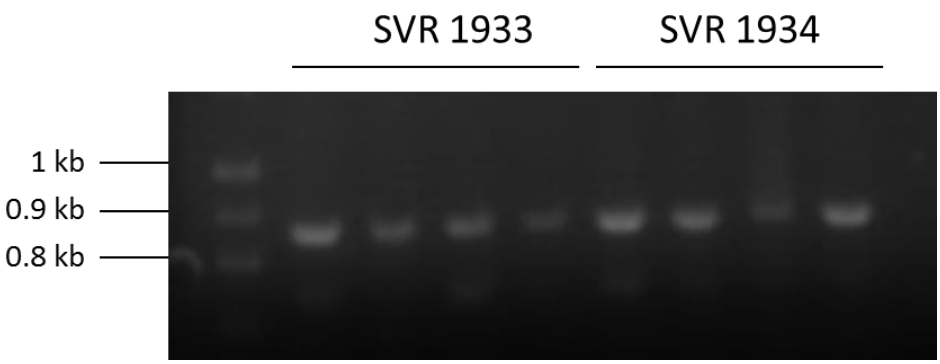

Figure 4-26. Amplification of NS5A domain I from patient samples was optimised. RNA was extracted from clinical samples using the QIAmp viral RNA kit and reverse-transcribed to cDNA using a gene-specific reverse primer. cDNA was amplified by nested PCR and resolved on 1% agarose gel. SVR 1933 and 1934 refer to two high viral load samples from the SVR patient group, of which four replicate PCR reactions are shown.

In this experiment four reactions were pooled to give a higher amount of cDNA which was then precipitated with ethanol. DNA preparations were then digested with Bsu36I and PspXI alongside the S52t-SF plasmid for subcloning, shown in Figure 4-27. Unfortunately the resulting ligation was not successful as the bacterial cultures which grew on the selection plate did not contain the correct plasmid when screened. More work is needed to optimise the ligation and propagation of the chimera plasmid DNA.

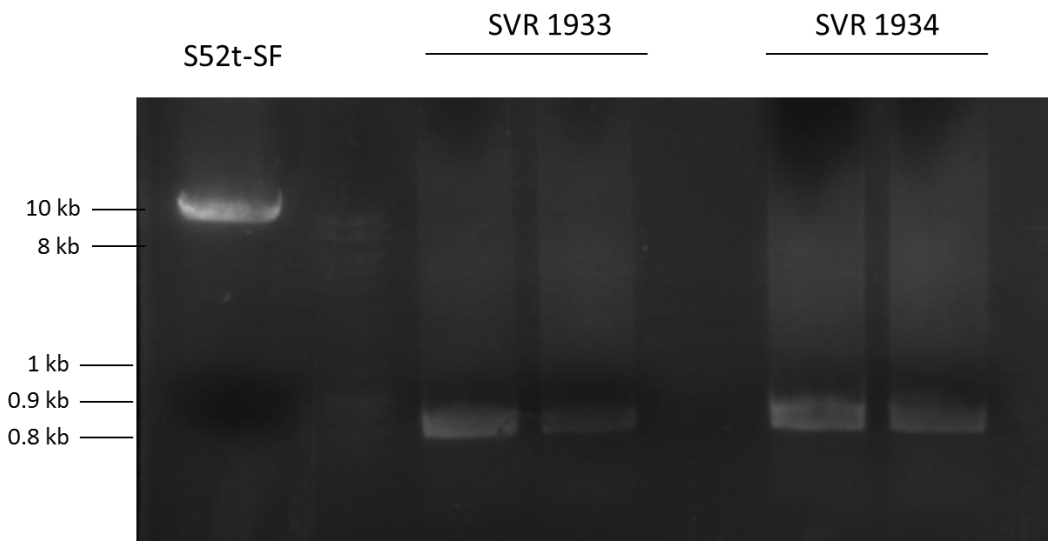

Figure 4-27. S52t-SF and NS5A domain I fragments amplified from patient samples resolve at the correct molecular weights after restriction digest. 5 µg of S52t-SF plasmid DNA was digested with 10 units each of Bsu36I and PspXI. The pooled and precipitated NS5A fragments amplified from SVR samples 1933 and 1934 was digested with 5 units of each of the aforementioned restriction enzymes. Digested DNA was resolved on 0.7% agarose gel**.**

4.3 Discussion

Across all different culture systems and clinical trials, GT3 is less sensitive to DAAs of all classes, to a greater or lesser extent. NS5A inhibitors are significantly less effective against GT3 and even those reported to have pangenotypic potency such as VEL are subject to the same trend. Interestingly, this work has shown that VEL treatment does not completely eradicate replication of a GT3 SGR, even at very high concentrations. The EC_{50} calculated supports the claim of VEL as pan-genotypic, though selected DCV resistance also confers resistance to VEL, and the inhibition of VEL never exceeds 90%. This is potentially linked to solubility at the highest concentration used, though this does not explain the lack of such a phenomenon in JFH-1 treatment experiments and the lack of a complete effect upon replication above EC_{90}. It would be surprising to observe that VEL is subject to such solubility issues that it cannot be used above EC_{90}. It would be interesting to select resistance with this inhibitor in the same fashion as that carried out for DCV.

It was also observed that DCV is much more effective against transient replication of S52 than stable replication, which concurs with what is already known about the mechanism of action of DCV and NS5A inhibitors. DCV is proposed to bind at the dimer interface of an NS5A homodimer and stabilise the structure, inhibiting the switch between replication and assembly that NS5A is thought to effect (Ascher et al., 2015; Barakat et al., 2015; Lambert et al., 2014). It is also hypothesised to bind to a precursor of NS4B and NS5A before the two are cleaved (Qiu et al., 2011) which requires the drug to be present at the point of translation of the genome. Such a difference in the efficacy of the drug on different stages of replication must partially explain why resistance is so readily acquired. If the initial effect of the drug is on assembly of virus, and later on RNA replication, then continuing replication in the short term provides opportunity for RAS to arise.

Selection of resistance is also associated with significant shifts in EC_{50} for all NS5A inhibitors. The introduction of a common RAS Y93H which is associated with a lesser response to NS5A inhibitors in clinical trials showed the same phenotype and in most cases increased the EC_{50} to the same concentrations, if not higher, than those calculated for stable SGR harbouring cells which were selected with DCV. These SGRs which have undergone resistance selection as a forward genetic approach also contain a mixture of sequences at L31; a linkage of L31V and Y93H is associated with much higher levels of resistance *in vitro* than either substitution alone. That this phenotype was not evident in the S52 DCV-selected SGR harbouring cells is

potentially due to the mixture of sequences at each of these positions. A complete substitution of L31V and Y93H is likely to further increase resistance to DCV.

A difference was identified in the fitness cost of NS5A inhibitor resistance in GT3. In *in vitro* studies using different genotypes a fitness cost of resistance has been widely reported. It is to be expected that mutation at the proposed dimer interface site should have an effect on the normal functioning of the protein. Interestingly, a study of resistance to the NS5A inhibitor Elbasvir identified a fitness cost phenotype which was less apparent in GT3 (Liu et al., 2015). In addition, the persistence of RAS at long-term follow-up in patients who failed treatment has been demonstrated. Accordingly, such a fitness cost was only observed during transient replication and not stable. This was evident in luciferase reporter activity, NS5A protein expression and SGR RNA level, as well as persistence of the RAS in the prolonged absence of selection pressure. . The reason for this is not likely to simply be due to a mixture of wild-type and resistant sequences within the cell, since the fitness cost phenotype was not observed in the colony formation assay. This observation was also reported by Scheel and colleagues; the fitness cost to Y93H in GT3 at 3 days is lost by days 5 and 7 (Scheel et al., 2011).

A potential reason for this is that NS5A develops further stabilising mutations which do not directly contribute to resistance, however no such mutations within NS5A domain I were identified. NS5A domain I was the primary focus: NS5A domain I is highly structured and is likely to form multi-order structures made up of repeating homodimers (Sun et al., 2015). It is possible that such a mutation may exist in other non-structural proteins which interact with NS5A such as NS4B, but it is not likely because not every NS5A dimer within the repeating structure will interact with a molecule of NS4B – in fact only those at the periphery will form such an interaction. In addition, transient replication of SGR RNA extracted from S52 DCV SGR harbouring cells is subject to the same fitness cost as transiently-replicating S52 SGR. If genetic compensation was solely responsible for the differential phenotype between the two systems, then the yet unidentified resistance-stabilising mutations would confer wild-type replication levels on the S52 DCV RNA. This was not so, indicating another factor involved.

This work also demonstrated that the effect is not likely to be solely due to a transcomplementation effect of persistent replication upon newly-initiated replication. NS5A is proposed to control the switch between genome replication and assembly, linked to hyperphosphorylation of the protein and a conformational change of the homodimer, with one of the functions of NS5A being to deliver virus genomes to sites of assembly to associate with core and package into new virus particles. It is feasible that a mutation at the dimer

interface should have a more pronounced phenotype early in replication, with such a fitness cost overcome by the time replication has already been established. This is, however, not likely to be solely the reason for the difference in phenotype: How, then, would resistance spread to other cells? Persistence of the RAS despite fitness cost may be a consequence of both genetic compensation and a complementation effect of persistence upon early replication. It may be possible that K41R, being the only non-synonymous change in NS5A domain I which was not directly resistance-associated, is still involved, but in a transcomplementation role. The linkage of K41R and Y93H is lethal to replication but they may not necessarily exist on the same genome strand, although this would mean that resistance does not readily spread to other cells.

This work investigated the difference between emergence of RAS and pre-existence within a population. RAS are common in the untreated population (Suzuki et al., 2012; Paolucci et al., 2013; Patiño-Galindo et al., 2016) and it is known that the presence of a RAS at baseline correlates with treatment response, with patients having a RAS before treatment being less likely to respond. However RAS are just as likely to emerge on-treatment and are equally likely to affect treatment response (Kai et al., 2017). *In vitro* the presence of a RAS as a mixed sequence (mimicking the quasispecies of an infected individual) before selection with DCV strongly effects the ability of the SGR mixture to replicate in the presence of the drug, however there are clearly other factors which affect treatment response *in vivo* which complicate the issue, such as BMI, presence of clinical signs of cirrhosis or non-hepatic disease, and some demographic factors including age, gender and race. Testing for RAS before treatment will not necessarily allow prediction of patients who will respond to therapy, although it may identify a group of patients who would likely benefit from longer treatment, or the addition of RBV, as current recommendations for a new combination therapy of Elbasvir (NS5A) and Grazoprevir (NS3) state for GT1a (Bruchfeld et al., 2017).

This project sought initially to perform these experiments using chimera SGRs containing NS5A from clinical samples, as an epidemiological and functional study. An amplification protocol has been established which is sensitive and reproducible, and the tools to construct these chimera SGRs and screen them have been developed. Further work is necessary to optimise the digestion and ligation steps in this protocol. Once completed, patient sequences in S52 will provide clinical context to this work and may be able to shed light on the complicated relationship between resistance-associated variation and treatment response.

Chapter 5: Evaluation of Genotype-specific differences in the perturbation of lipid metabolism pathways by hepatitis C virus

5.1 Introduction

It has been widely shown that GT3 infection is associated with severe hepatic steatosis that is not associated with other risk factors such as BMI. This steatosis in GT3 patients correlates with HCV RNA level in the liver and disappears completely upon achieving SVR (Mihm et al., 1997; Rubbia-Brandt et al., 2004; Abid et al., 2005; Nkontchou et al., 2011). Indeed, GT3 core causes a greater degree of lipid accumulation than core from other genotypes, (Abid et al., 2005; Jhaveri et al., 2009) and core domain 3 is sufficient to induce lipid accumulation (Jhaveri et al., 2009). A series of studies using clinical material has shown correlative associations between GT3 infection and lipid metabolism perturbation: GT3 infection is associated with an increase in hepatic miR-122, a modifier of hepatic lipid metabolism (Oliveira et al., 2016); It is also associated with an increase in gluconeogenic genes, contributing to type 2 diabetes observed in HCV patients (Sheikh et al., 2015); and a polymorphism in Microsomal Triglyceride Transfer protein (MTP) is associated with more severe steatosis in GT3 patients (Zampino et al., 2008). However, greater understanding of the biochemical basis of GT3-specific lipid accumulation may identify pathways to exploit for therapeutic purposes, to treat the pathogenesis of infection in addition to the virus itself.

5.2 Results

GT3 replication systems developed in chapter 3 allow us to investigate pathways which are linked to the steatosis seen in patients, which is more severe and causes quicker progression to cirrhosis and further disease states. The hypothesis to be tested was that the NS3-5B non-structural proteins play a role in steatosis, following observations that non-structural proteins play roles in the organisation of the membranous web and recruitment of lipoproteins; and induction of autophagy (Egger et al., 2002; Eyre et al., 2014). Transient replication of S52 was not sufficiently high to cause discernible effects on lipid metabolism pathways so a range of experiments were performed using SGR harbouring cells

5.2.1 Comparison of lipid accumulation and rearrangement in genotype 3

5.2.1.1 Comparison of lipid distribution by immunofluorescence

Intracellular lipids are known to be upregulated in HCV infected and SGR-transfected cells *in vitro*. Lipid content and distribution were compared between Con1, JFH-1 and S52 SGR harbouring cells, and naïve Huh7.5 cells. NS5A was detected by indirect immunofluorescence as previously described and total lipids were identified using 594 nm BODIPY labelling. The data in Figure 5-1 show three individual cells for each cell type. It is clear that these polyclonal populations show marked differences in both NS5A and lipid distribution. It might be expected that some degree of lipid accumulation occurs in the S52 SGR harbouring cells, however there is no clear difference in lipid distribution between naïve cells and S52; indeed, the SGR harbouring cell line with the most striking difference in lipid distribution is that containing Con1, which is a GT1b sequence. GT1b is not associated with hepatic steatosis in the absence of other risk factors such as high BMI. In addition to this it seems from this data that a negative correlation can be observed between NS5A and lipid immunofluorescence intensity.

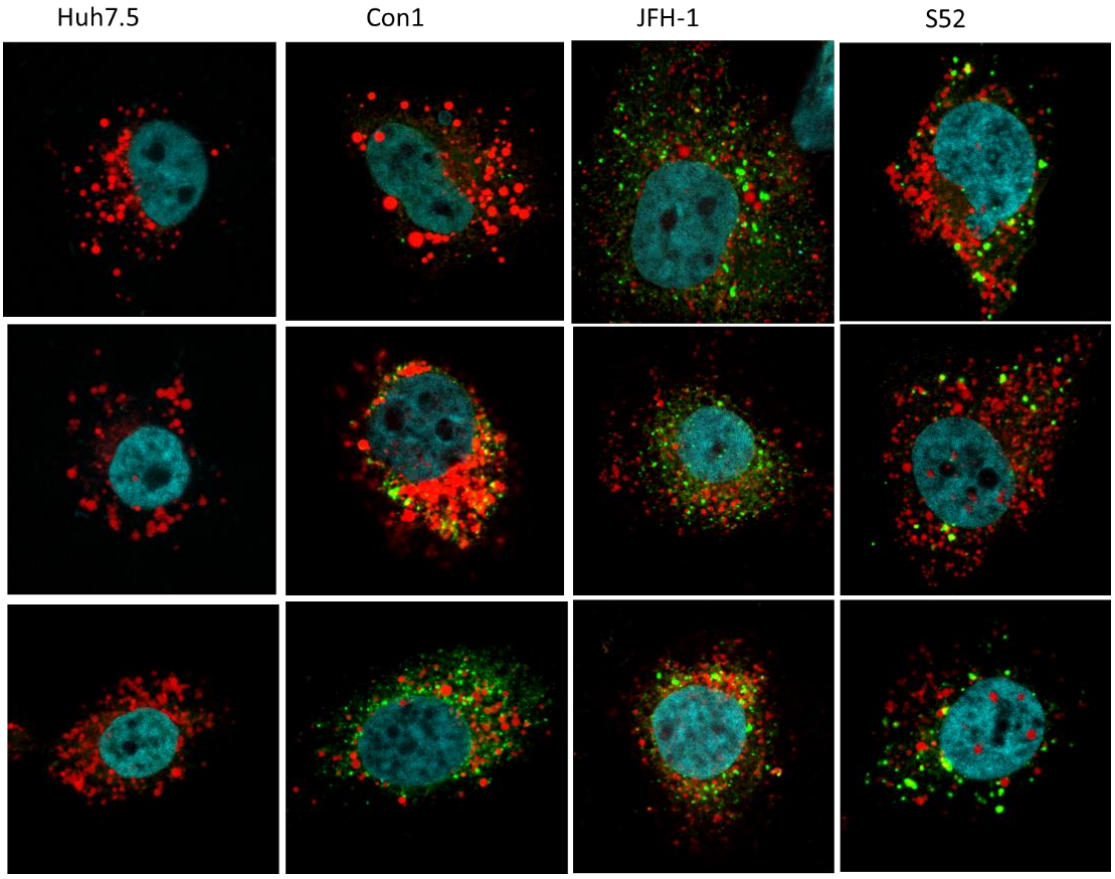

Figure 5-1. S52 SGR harbouring cells do not have a higher intensity of lipid fluorescence than other genotypes. S52 and S52 DCV SGR-harbouring cells were immunostained for NS5A (green) using a sheep polyclonal anti-NS5A serum, and stained for lipids using BODIPY-594 and nuclei using DAPI. Multiple images shown for each cell type**.**

Lipid accumulation has been proposed to be mediated by core. Hence, it was investigated whether the lack of any discernible difference in lipid fluorescence intensity and distribution between the genotypes was due to the absence of core protein in the SGR harbouring cells. To address this, an experiment was carried out using the S52 chimera virus. Huh7.5 cells infected with JFH-1 or S52 GERA virus (see chapter 3 – the S52 virus is a chimera of 5' UTR to NS5A of S52 and NS5B to 3' UTR of JFH-1) were imaged for NS5A and lipids; the images are shown in Figure 5-2. The fluorescence images are the same shown in Figure 3-16. As the data show, there is an unusual pattern of lipid fluorescence visible in the S52-infected cell, which appears to be a redistribution rather than accumulation. Due to extremely low infectivity of the S52 virus supernatant it was not possible to explore this further within this experiment, though it may be a promising avenue to explore. NS5A immunofluorescence intensity in the S52-

infected cell was also significantly lower than for JFH-1 – the parameters for imaging NS5A within the S52-infected cell had to be increased before NS5A punctae were visible which makes comparison of the two unrealiable.

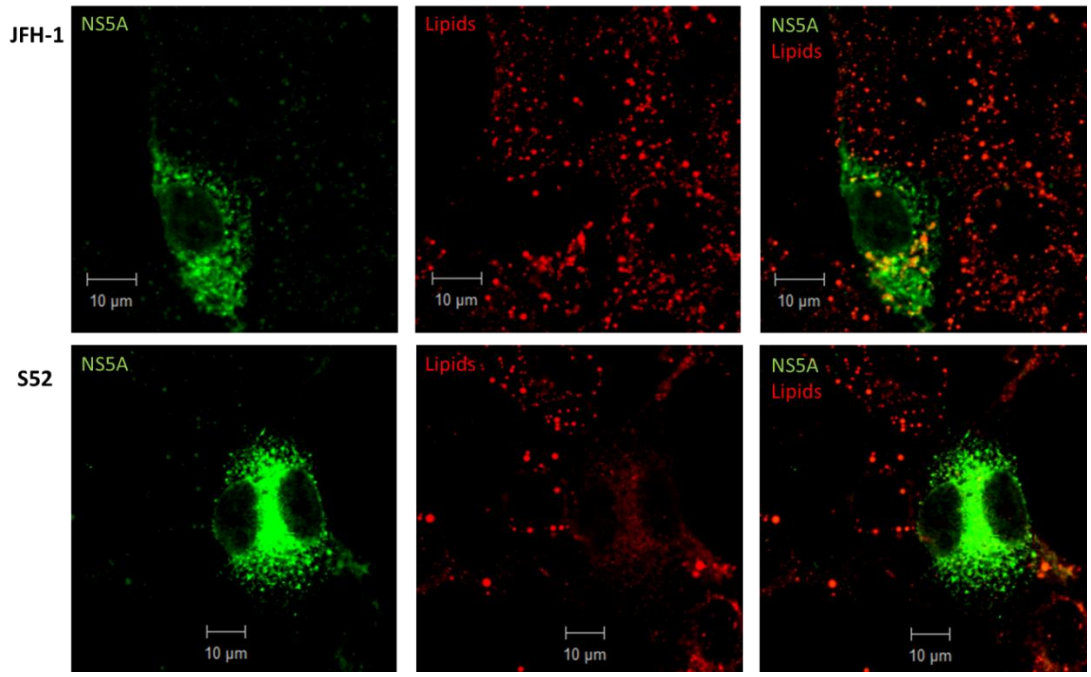

Figure 5-2. S52 virus-infected cells have a distinct rearrangement of lipids. Huh7.5 cells were infected at a MOI of 1 with S52 GERA virus supernatant for 48h, fixed and immunostained for NS5A (green) using a sheep polyclonal anti-NS5A serum, BODIPY 594 (red) and nuclei using DAPI

5.2.1.2 Comparison of total lipid content using flow cytometry

The difference in lipid content between S52 and other SGR harbouring cells was not quantifiable, therefore to investigate the subtle differences between them the total lipid content within SGR harbouring cells was quantified, and compared to NS5A content between each cell line, using flow cytometry. JFH-1, S52 SGR harbouring cells and Huh7.5 cells were fixed and stained in suspension with anti-NS5A serum and BODIPY, before being analysed in a flow cytometer, shown in Figure 5-3.

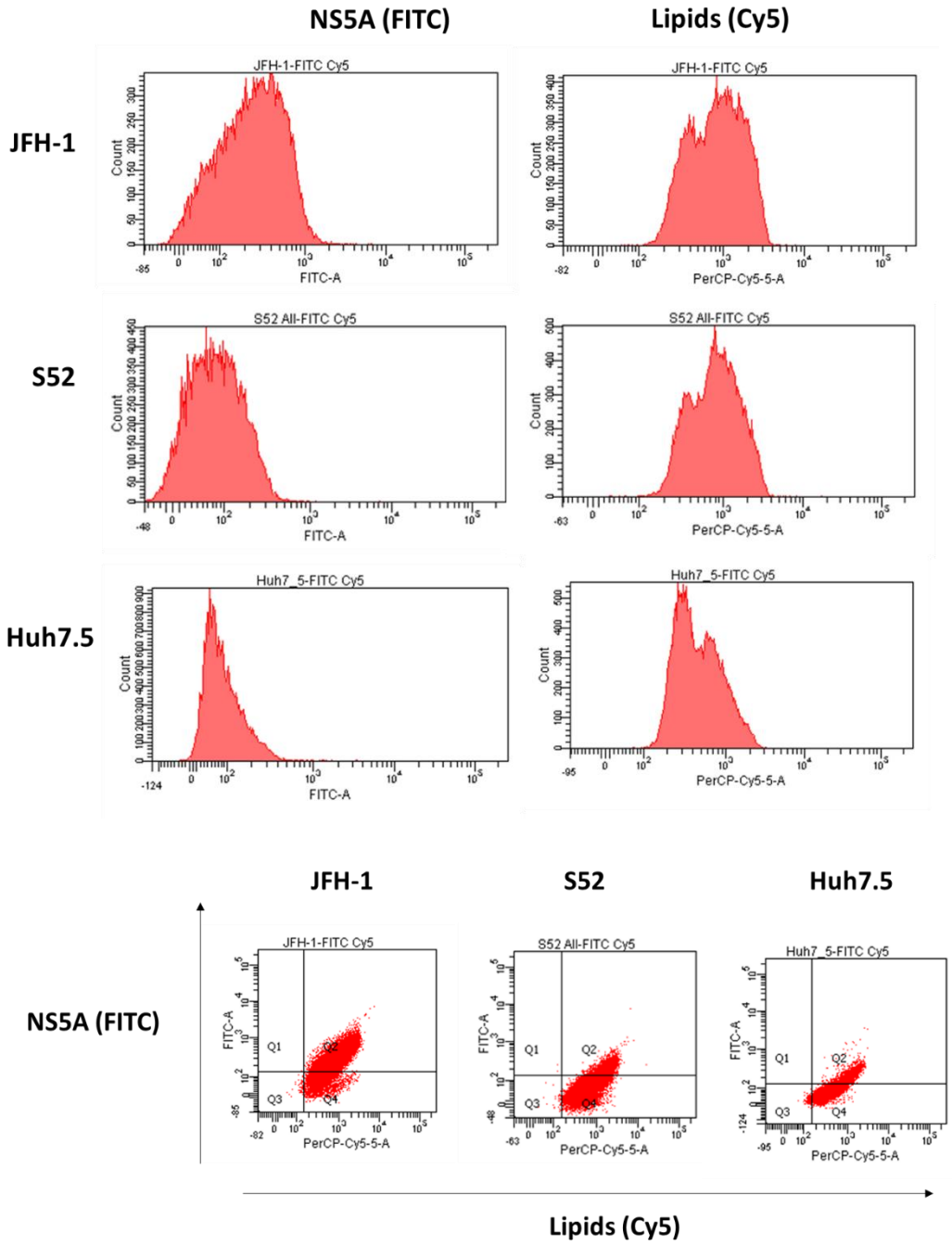

Figure 5-3. S52 SGR harbouring cells have a similar lipid content to JFH-1, and lower NS5A. JFH-1, S52 SGR harbouring and Huh7.5 cells were fixed and analysed for NS5A content and total lipid using anti-NS5A serum and BODIPY respectively. Stained cells were analysed alongside unstained and monostained controls for gating and optimisation of sensitivity parameters using a BD LSR Fortessa flow cytometer and analysed using DiVa6 software.

	JFH-1		S52		Huh7.5	
	# events	% of events	# events	% of events	# events	% of events
Q1 (high NS5A, low lipid)	24	0.1	3	0	2	0
Q2 (high NS5A and lipid)	18,928	72.8	5,848	26.0	4,089	19.7
Q3 (negative for both)	825	3.2	449	2.0	289	1.4
Q4 (high lipid, low NS5A)	6,238	24.0	16,224	72.0	16,349	78.9
Total events	26,015		22,524		20,729	
Total events gated	20,000	76.9	20,000	88.0	20,000	96.5

Table 5-1. Quantification of flow cytometry data from Figure 5-3.

Interestingly there is an increase in lipid content between Huh7.5 and SGR-harbouring cells, in that the histograms in Figure 5-3 show that the distribution is towards higher lipid content in the SGR-harbouring cells, but no clear difference between JFH-1 and S52. In addition, the level of quantified NS5A intensity is much lower in the S52 cells. There is evidence of a separate population with lower NS5A content in the JFH-1 cells. It is not known whether these cells are suboptimally fixed or stained, or whether there is indeed a population with lower NS5A content. In contrast to the immunofluorescence images showing that the highest number and size of lipid droplets seems to be in cells with fewer and smaller NS5A punctate structures, the flow cytometry data show a clear correlation between NS5A and lipid content.

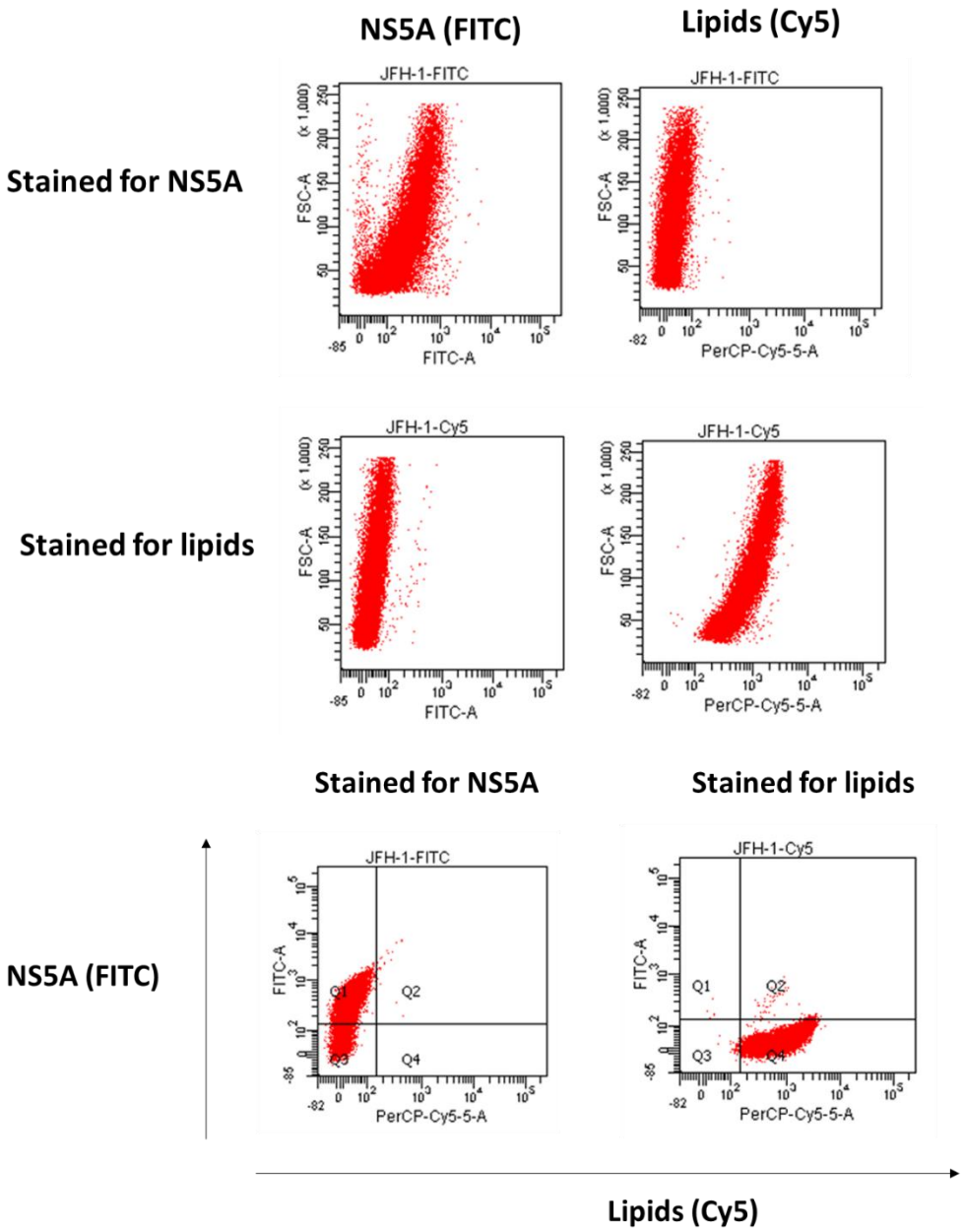

Figure 5-4. Bleed-through of signal between channels during flow cytometry analysis was addressed. JFH-1 SGR harbouring cells were fixed in 4% paraformaldehyde and permeabilised with 0.1% Triton-X 100 prior to analysis for NS5A or total lipid content using anti-NS5A serum or BODIPY respectively on a BD LSR Fortessa flow cytometer.

Analysis of this data required computational correction for a bleed-through of signal between channels. As shown in Figure 5-4 there is a FITC signal (corresponding to NS5A) in the cells stained with BODIPY only, and a Cy5 signal (corresponding to BODIPY) in the cells stained with NS5A only. To address this, two different approaches were considered to reduce the overlap

of the signal: The use of a lipid-imaging molecule with a higher wavelength than the 594 nm BODIPY; or the use of a secondary antibody for NS5A with a lower wavelength than the AlexaFluor 488 secondary antibody used thus far.

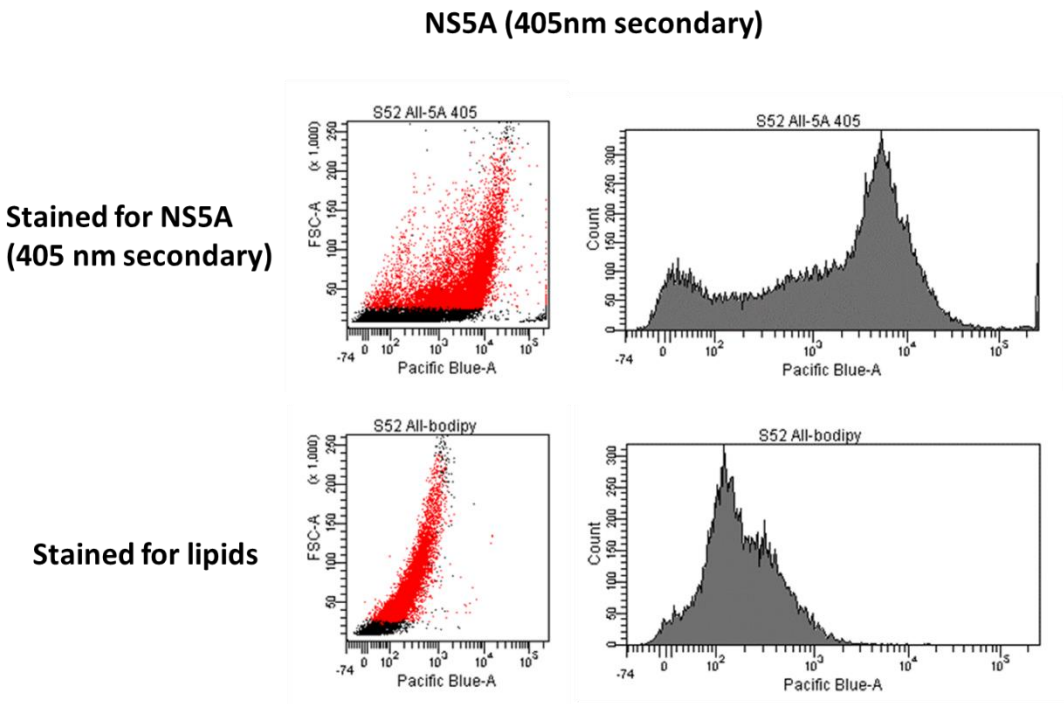

Figure 5-5. Alternative 405 nm secondary antibody for NS5A is not suitable for flow cytometry. S52 SGR harbouring cells, alongside Huh7.5 cells, were fixed in 4% paraformaldehyde and permeabilised with 0.1% Triton-X 100 before being analysed for NS5A using anti-NS5A serum and AlexaFluor 405 nm secondary antibody. Stained cells were analysed alongside unstained controls for gating and optimisation of sensitivity parameters using a BD LSR Fortessa flow cytometer and analysed using DiVa6 software.

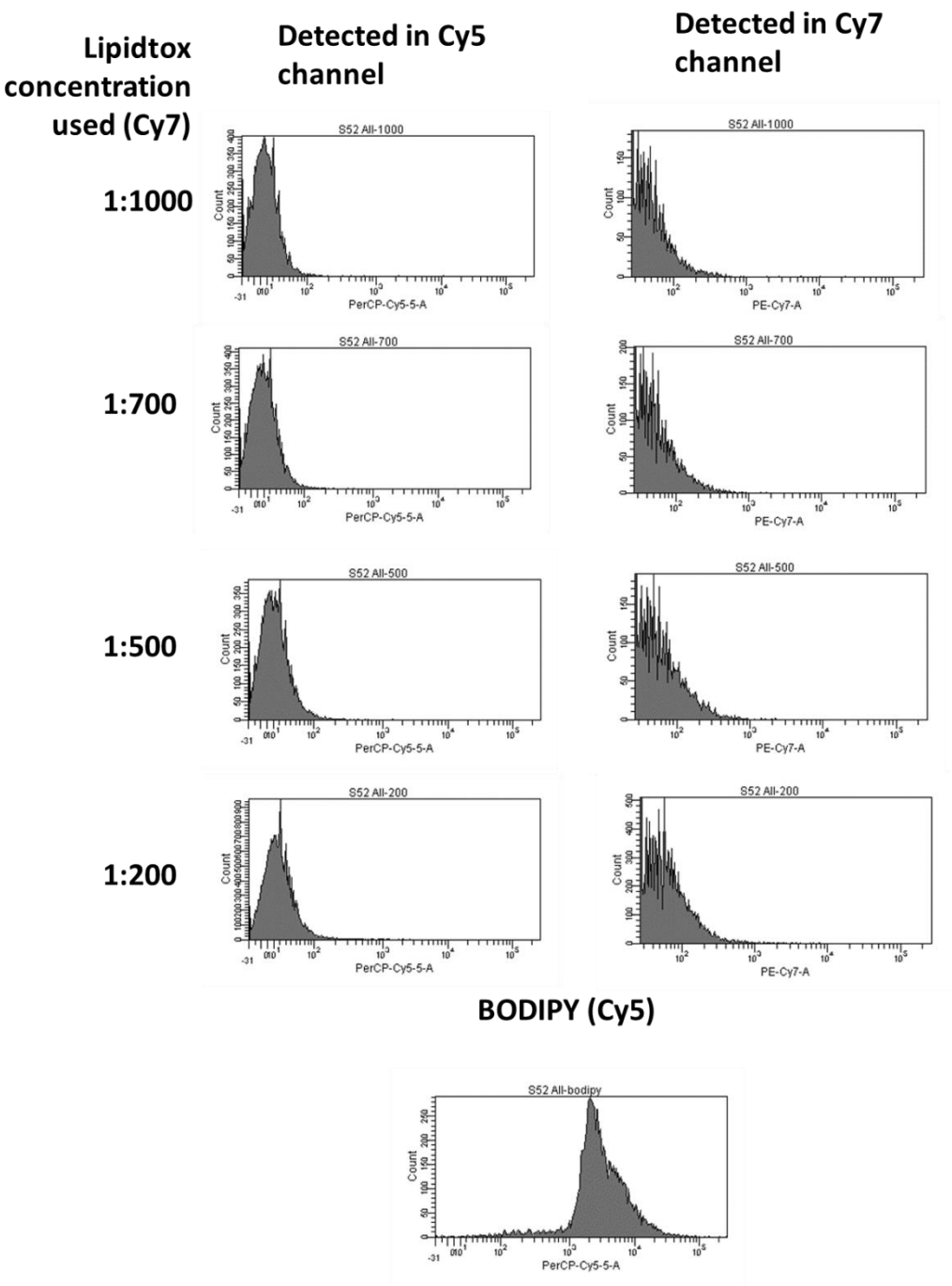

Figure 5-6. Lipidtox lipid dye cannot be analysed by flow cytometry. S52 SGR harbouring cells, alongside Huh7.5 cells, were fixed in 4% paraformaldehyde and permeabilised with 0.1% Triton-X 100 before being analysed for lipids using LipidTox or BODIPY. Stained cells were analysed alongside unstained controls for gating and optimisation of sensitivity parameters using a BD LSR Fortessa flow cytometer and analysed using DiVa6 software.

Figure 5-5 shows the analysis of NS5A stained with a 405 nm secondary antibody. As the histograms show there is not sufficient uniformity of the signal, and there is also substantial crossover of signal from lipid imaging into the Pacific Blue channel. Figure 5-6 shows that, at concentrations up to 1:200 the flow cytometry instrument was not able to detect the Lipidtox signal in the Cy7 channel. These data show that these options are not suitable for the purposes of this experiment.

5.2.2 Comparison of basal and activated AMPK

5.2.2.1 Comparison of AMPK activation in SGR harbouring cells

Previous work from this laboratory (Mankouri et al., 2010) has shown that HCV inhibits activity of adenosine monophosphate (AMP)-activated protein kinase, AMPK, the energy sensor of the cell. This blocks the ability of the kinase to downregulate lipid synthesis to maintain energy production over energy consumption. This may result in an upregulation of total lipids, adding to the enrichment of lipids at sites of assembly. This work was reproduced and the GT3 SGR harbouring cells were applied to the assay.

To explore whether the effect exerted by HCV on AMPK might be different depending on genotype, cells harbouring Con1, JFH-1 and S52 SGR and Huh7.5 cells were treated for 48h with metformin, an activator of AMPK. AMPK activation was measured using antibodies to Threonine 172 (T172)-phosphorylated AMPK and Serine 79 (S79) phosphorylated Acetyl CoA Carboxylase (ACC), a substrate of AMPK. Cells were serum-starved for 24h before treatment as being in a state of starvation accentuates the induction of AMPK, making any effects on the SGR and downstream ACC more readily apparent. As shown in Figure 5-7 there is a decrease in both untreated and metformin-upregulated phosphorylation of both AMPK and ACC in S52 harbouring cells compared to JFH-1 harbouring cells. The level of phosphorylated AMPK and ACC in S52 SGR harbouring cells treated with 10 mM is approximately equal to that within JFH-1 harbouring cells before metformin treatment. However, an increased amount compared to both JFH-1 and S52 should have been observed in Huh7.5 cells both basally and following metformin treatment, which was not the case. Treatment with metformin upregulated phosphorylated AMPK and ACC in all three cell lines though, interestingly, the level of activation in S52 harbouring cell lines is lower than for JFH-1.

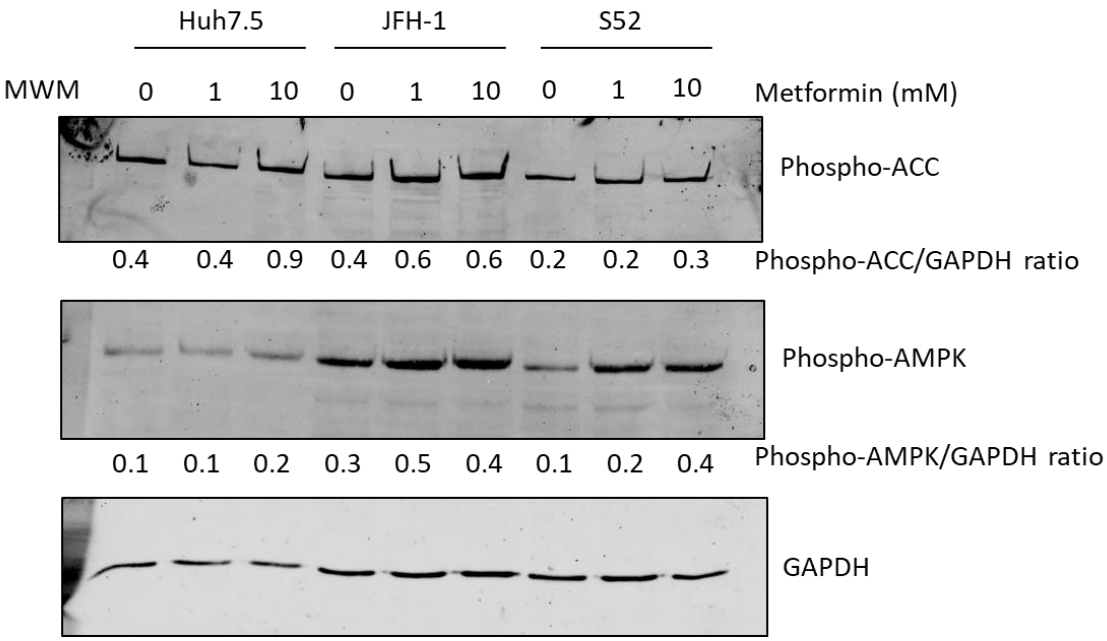

Figure 5-7. Metformin activates AMPK by phosphorylation in SGR harbouring cells to a lesser extent in S52 harbouring cells than JFH-1. Huh7.5, JFH-1 and S52 SGR harbouring cells were serum-starved for 24h before being treated with the indicated concentrations of metformin for 48h. Cells were then lysed in PLB supplemented with protease and phosphatase inhibitors for immunoblot analysis of phosphorylated ACC and AMPK, with GAPDH loading control**.**

The effect of metformin treatment on SGR replication was also explored. AMPK activation was shown in the study to have a negative effect on SGR replication (Mankouri et al., 2010). Given that there seems to be a difference in AMPK activation levels between GT2 and GT3 cells it should be expected that a differential effect on replication should also occur. Accordingly, there was a greater decrease in replication of S52 compared to JFH-1, indicating that the S52 cells are more sensitive to the effects of AMPK activation.

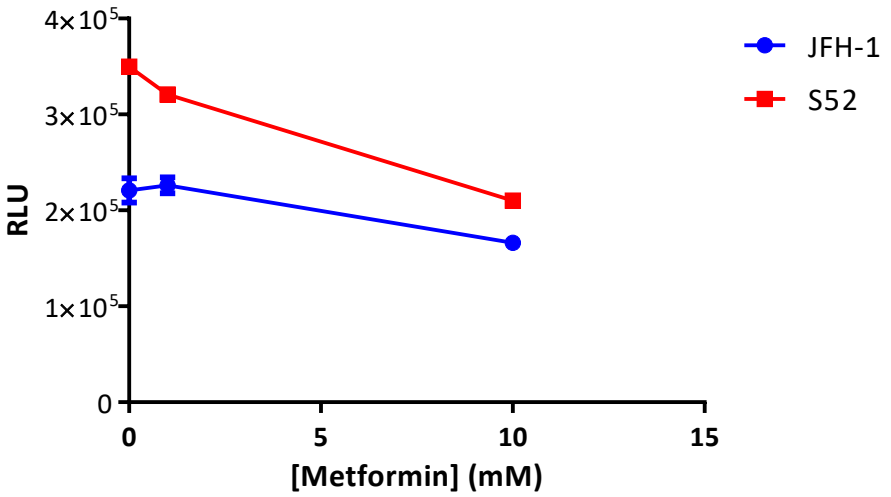

Figure 5-8. Metformin attenuates S52 SGR replication to a greater degree than JFH-1. The indicated SGR harbouring cells were serum starved for 24h prior to treatment with the indicated concentrations of metformin for 48h. Cells were harvested for luciferase and data show luciferase quantification in equal quantities of cell lysate**.**

5.2.2.2 AMPK activation in virus-infected cells

This observation was validated using the chimera S52 virus. Huh7.5 cells were either infected with S52 virus supernatant or electroporated with S52 virus RNA. Due to the poor yields of S52 virus it was not possible to conduct experiments at a higher MOI and there is little evidence of infection, and no evidence of a difference in AMPK activation (Figure 5-9). However, analysis of AMPK activation in virus-electroporated cells (Figure 5-10) concurs with the data generated using SGR harbouring cells.

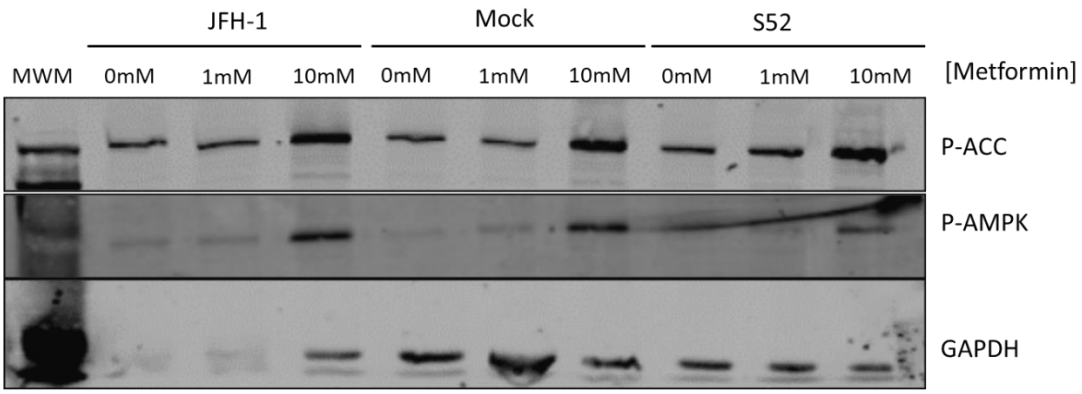

Figure 5-9. Metformin activates AMPK in S52-infected cells at lower levels compared to JFH-1-infected and uninfected cells. Huh7.5 cells were seeded in 6-well plates and infected for 48h with DMEM (mock), JFH-1 or S52 virus supernatants at an estimated MOI of 1. Virus inoculum was then aspirated and cells were serum-starved for 24h prior to treatment with the indicated concentrations of metformin for a further 48h. Cells were then prepared for immunoblot as described in chapter 2 and immunoblotted for phosphorylated ACC, AMPK and GAPDH.

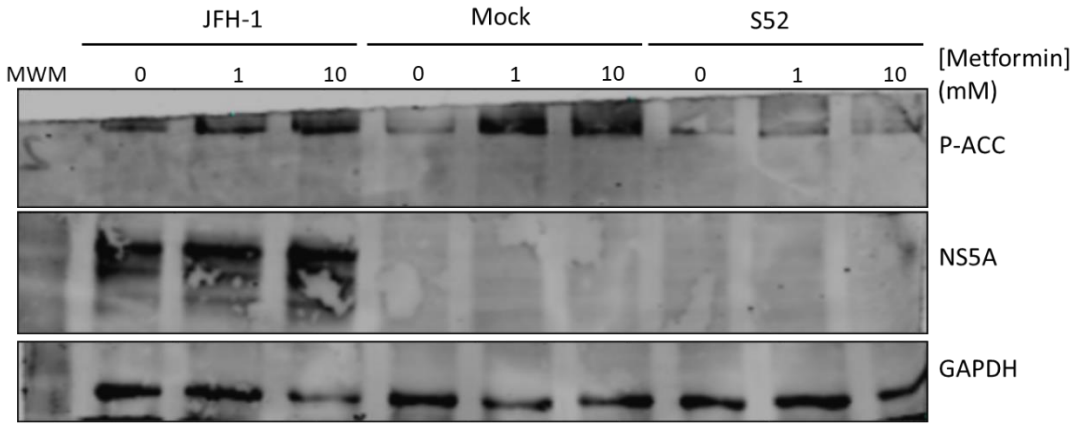

Figure 5-10. Metformin activates AMPK in S52-electroporated cells at lower levels compared to JFH-1-electroporated and mock-electroporated cells. Huh7.5 cells were electroporated with JFH-1, JFH-1 GND (mock) or S52 virus RNA and seeded in 6-well plates before being serum starved for 24h and treated with the indicated concentrations of metformin for a further 48h. Cells were then prepared for immunoblot as described in chapter 2 and immunoblotted for phosphorylated ACC, NS5A and GAPDH.

As Figure 5-10 shows, phosphorylated ACC levels (used as a surrogate for AMPK activation level) are higher in mock-electroporated cells than in HCV-electroporated, and both untreated and treated phosphorylated ACC is lower in S52-infected cells than JFH-1. This further indicates that S52 downregulation of AMPK is stronger than JFH-1. Due to low levels of replication, NS5A protein in S52-electroporated cells and released virus could not be detected. This is not likely to be related to the experiment, however it prevented the measurement of the effect of metformin treatment on infectious virus replication or release.

5.2.2.3 Investigation of additional AMPK activators

It was considered that a different AMPK activator might produce a more potent result that can be further explored. Recently a more specific AMPK activator known as compound #991 has been identified (Xiao et al., 2013). It is proposed to increase AMPK activity by both increasing allosteric activation of AMPK by phosphorylation at T172 and by protecting against dephosphorylation at this same residue.

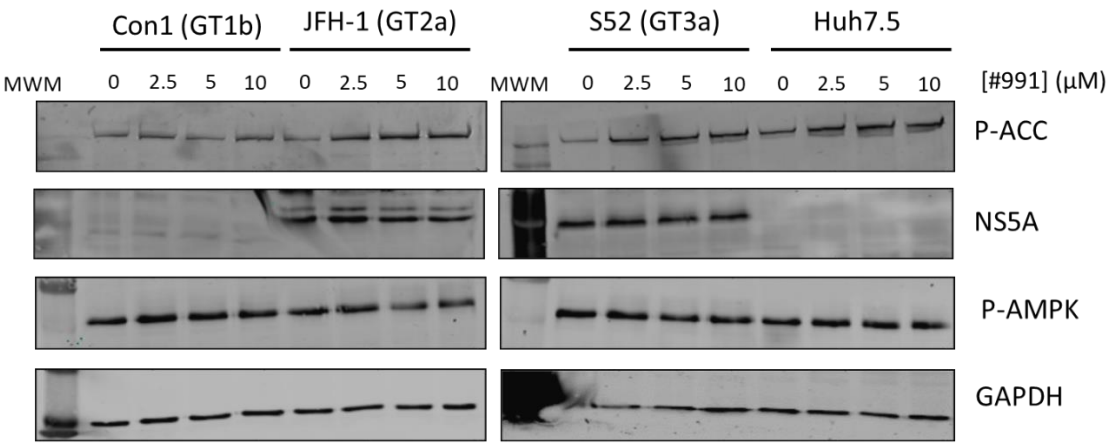

Figure 5-11. Compound #991 activates AMPK in SGR harbouring cells. Huh7.5 cells harbouring HCV SGRs and control Huh7.5 cells were seeded in 6-well plates, serum-starved for 24h and treated with the indicated concentrations of #991 for 48h. Cells were then harvested for immunoblot as described and blotted for phosphorylated ACC and AMPK, NS5A and GAPDH.

SGR harbouring cells and Huh7.5 cells were serum starved and treated as described previously. Immunoblots for phosphorylated ACC and AMPK as well as NS5A and GAPDH are shown in Figure 5-11. As the data show, there is an effect on phosphorylated ACC after 48h at concentrations of #991 above 2.5 mM. In addition, there is a greater level of activation in

Huh7.5 cells compared to the SGR-harbouring cells, though levels in S52 and JFH-1 cells are broadly similar, and Con1 has the lowest levels of activation. However, there is no effect on AMPK at any concentration, though untreated AMPK activation seems to be much higher than observed previously. It is of note that the solvent for #991 is DMSO whilst the solvent for metformin is water; there may be a higher AMPK activation signal than was observed for the previous experiments due to effects of the DMSO vehicle (Mhatre et al., 1983; Syed et al., 2013).

There was, in addition, no effect on the levels of NS5A detected by immunoblot in S52 and JFH-1 SGR harbouring cells (none was detected in Con1 harbouring cells throughout the experiment), which possibly indicated that little or no effect on replication was observed. To investigate this further, luciferase activity was measured in cells treated with #991. It would be expected that #991 treatment reduced replication of the SGRs similar to the effect seen for metformin, albeit to a lesser extent considering that it has a less pronounced effect on AMPK and ACC. Interestingly, as shown in Figure 5-12, there was no effect on JFH-1 replication and a slight increase in luciferase in Con1 and S52 SGR harbouring cells. This may be an effect on cell viability, since AMPK activation increases the available energy for the cell, however the RLU values shown are normalised by protein, so are not due to an increase in the cell number.

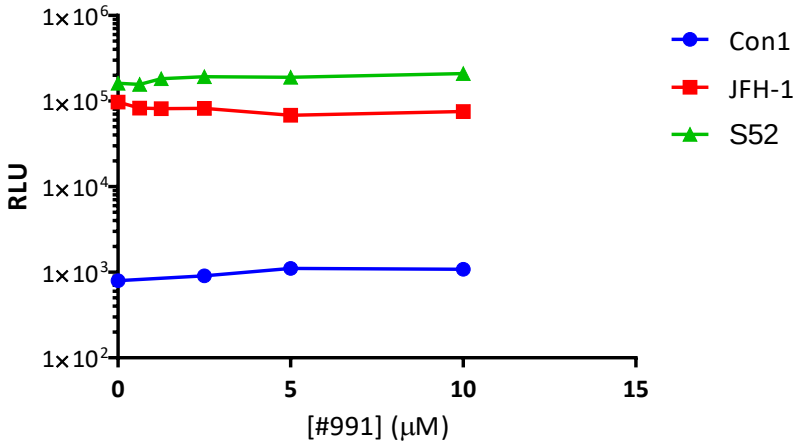

Figure 5-12. #991 does not noticeably affect replication of HCV SGRs. Con1, JFH-1, S52 SGR harbouring cells and Huh7.5 cells were seeded in 6-well plates, serum-starved for 24h and treated with the indicated concentrations of #991 for 48h. Cells were then harvested **for** luciferase assay in PLB as described. Luciferase activity was measured and normalised to total protein by BCA assay.

It was considered that the effect may be more transient in nature, and may be lost by the 48-hour time point at which cells are harvested for luciferase and immunoblot. To address this, a time course experiment was performed. Personal communication with David Carling stated that the compound is active immediately; luciferase activity was therefore assayed as a read-out of replication at a range of 5 minutes to 24h treatment with 10 µM #991.

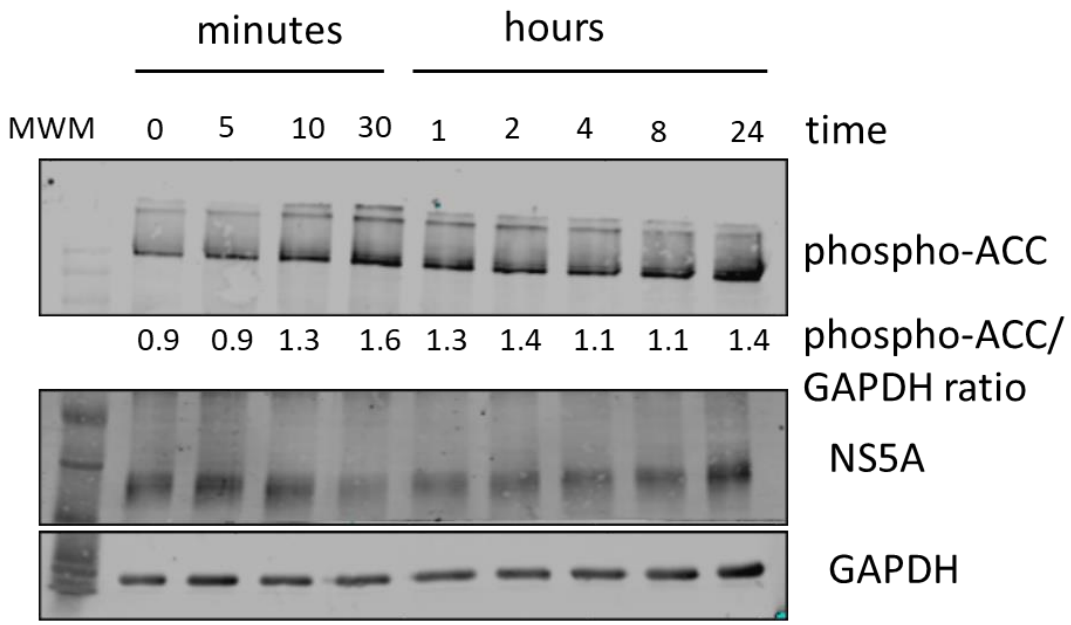

Figure 5-13. #991 activates AMPK in a transient fashion with an optimal treatment duration of 30 minutes. S52 SGR harbouring cells were seeded in 24-well plates, serum starved for 24h and treated with 10µM #991 for the indicated time points. Cells were then harvested for immunoblot as described and blotted for phosphorylated ACC, NS5A and GAPDH.

The immunoblots for NS5A and phosphorylated ACC are shown in Figure 5-13. The blots show a modest upregulation in phosphorylated ACC from 10-30 minutes after treatment. Interestingly this seems to decrease before reaching peak activation at 24h. The NS5A signal by immunoblot is not strong but there does indeed seem to be a decrease by 30 minutes and, in agreement with the hypothesis that the effect of this compound is transient, the effect is lost by 24h after treatment. The data also show that #991 does not seem to be as potent an activator of AMPK in my hands than was reported. In light of this, #991 was deemed unfeasible for these experiments.

5.3 Discussion

This chapter documents the application of the S52 SGR harbouring cells which were described in chapter 3 to other aspects of HCV biology. It is well known that GT3 is unique among HCV isolates in its direct pathogenesis in the form of hepatic steatosis. The established dogma states that HCV infection causes immune activation leading to cell death and tissue damage, which is repaired as fibrotic tissue. Over time this leads to cirrhosis and, ultimately, transformation of hepatocytes or hepatic progenitors and HCC. However, GT3 infection, and the associated steatosis, leads to quicker progression through disease states to fibrosis and HCC than other genotypes as well as a lower life expectancy. There are differences in the relationship between this genotype and the host cell which are not comprehensively studied.

No increase in total lipid content was observed in S52 SGR harbouring cells by flow cytometry, and a clear difference in lipid distribution or intensity was not observed by fluorescence. There was, however, a marked difference in the distribution of lipids in a cell which was infected with infectious S52 virus, which is consistent with the knowledge that lipid accumulation requires the presence of the core protein, which the SGR lacks. Due to experimental constraints this was not explored further, but a valid experiment would be to subject S52 infected cells to flow cytometry to investigate differences in total lipid content. There is also a clear need to validate the observation of an unusual lipid distribution in S52 infected cells which would be easier with a more infectious virus such as DBN3a (Ramirez et al., 2016). Published studies which document an upregulation of total lipids and the size of lipid droplets in cells show a vastly different pattern of lipid distribution to that which is reported in this chapter, however these studies mostly use core in isolation, with the exception of the S310 virus (Kim et al., 2014). The pattern of lipid distribution observed in S52-infected cells, although seemingly of a lesser intensity than the surrounding uninfected cells does show a greater number of lipid droplets. This lipid signal correlates with the intensity of NS5A, which could highlight an earlier stage of replication compared to the images shown of cells infected with S310. Also of note is the observation that NS5A and lipids seem to colocalise, which was explored by Galli and colleagues, who found that, in GT3, NS5A seems to be associated with the ER rather than lipid droplets (Galli et al., 2013).

This work highlighted a potential difference in the effect upon AMPK activation, which HCV downregulates to protect lipid biosynthesis pathways, amongst others, to allow enrichment of lipids at sites of replication and assembly (Mankouri et al., 2010). It is curious that virus infection, that most likely generates an energy deficit within the cell, should perturb a pathway

which exists to increase energy production, but HCV infection was also shown to increase lipid oxidation as well as synthesis (Diamond et al., 2010) which provides evidence that homeostasis is maintained to some extent in the presence of metabolism perturbation by the virus. This work presents preliminary evidence that the downregulation of AMPK by HCV GT3a is different to JFH-1, which was reproduced in infectious virus experiments. GT3 may exert a different level of control upon AMPK, as evidenced by the lower levels of activation by metformin treatment compared to JFH-1; GT3 is also more sensitive to the effects of AMPK activation, as evidenced by the greater degree of inhibition of replication after metformin treatment. It is interesting to note that GT3 seems to be more sensitive even to the lesser degree of AMPK activation observed in cells harbouring a GT3 SGR. Differential regulation of AMPK and its downstream effector proteins such ACC may contribute to lipid accumulation leading to steatosis in the livers of GT3 infected patients.

However, when Con1 (GT1b) was introduced into these experiments, it became evident that the differences observed may not be unique to S52. Instead it seems that the outlier in these experiments is JFH-1, which is consistent with the growing body of data that JFH-1 is distinctive amongst HCV isolates and SGRs in aspect such as its outstanding replication capacity and non-reliance on culture adaptation (Kato et al., 2003). JFH-1 replication is also unaffected by the expression of SEC14L2, a lipid binding factor which allows cells to support higher levels of HCV replication (discussed in chapter 3) (Saeed et al., 2015). The genotype difference which has been identified here may provide a candidate for further study as to how different genotypes of HCV affect the host, though this may turn out not to be contributing factors in the direct pathogenesis of GT3.

Better understanding of the pathogenesis of HCV and specifically GT3 may highlight areas for therapeutic development to target the effects of the virus upon the host in addition to direct targeting of the virus by DAAs. Such treatment of the consequences of HCV infection may increase health-related quality of life during treatment and hence increase adherence to treatment.

Chapter 6: General discussion

Development and refinement of all classes of DAAs for different genotypes has relied upon the advances of the SGR system (Ortega-Prieto and Dorner, 2016). Initial identification of NS5A inhibitors beginning with DCV utilised a high-throughput screen using replicon cell lines, generating hits compounds which were explored in depth and enhanced using SAR (Gao et al., 2009). Screening of these compounds against GT3 required the transient replication of chimeric SGRs comprising sequences from two different genotype isolates, which were used to investigate baseline efficacies as well as fold resistance changes of RAS (section 1.3.2.3). The key limitation of chimera SGRs stems from the inability to model interactions between NS proteins in a genotype-specific manner – the interaction between NS5A and NS4B, for instance, is vital to the formation of the membranous web (Egger et al., 2002; Eyre et al., 2014). NS5A rarely functions in isolation and the efficacy of a compound at inhibiting the functions which rely on such interactions cannot be effectively measured in chimera systems where a single NS protein is expressed in isolation in a high-replicative backbone.

The establishment of virus chimeras which consist of almost complete genotype uniformity was a major breakthrough in this regard (Scheel et al., 2011; Gottwein et al., 2013; Yi-Ping Li et al., 2014), as was the report of a full-GT3 SGR in the form of the S52 SGR (Saeed et al., 2012), though these are hindered by a lack of efficient replication capacity. This thesis documents a significant improvement on the S52 SGR which increases transient replication to that which exceeds input translation at an earlier timepoint than previously reported Yu et al., 2013). This allowed investigation into the differential sensitivities of different classes of DAA in a full-GT3 system; this is especially novel for NS5B inhibitors, though this work does not focus on this class of DAA. The majority of genotype chimeras retain an NS5B coding region and 3' UTR from an isolate capable of much greater levels of replication.

However, these improvements to the S52 SGR come at a cost of requiring additional modification of the SGR and substantial modification to the host cell environment. It can be argued that the inclusion of the low CpG/UpA luciferase gene represents a step towards a more relevant system, since it removes the immunological reaction to the insect-derived luciferase gene (Tulloch et al., 2014). Conversely, the necessity of further impairing the host cell environment by exploiting a mutation in an innate immune sensing pathway, RIG-I, and the expression of the PIV5 V protein to further attenuate the immune response to the SGR, is not an attractive solution to the problem, and invalidates the use of this SGR in any studies which may involve an immunological effect (Foy et al., 2005; Sumpter et al., 2005; Andrus et al., 2011; Poole et al., 2002).

Moreover the selection of cells with puromycin, and especially G418, will have further abnormal effects on the host cell, which may impact the interpretation of results (Yallop and Svendsen, 2001). In addition, G418 has been shown to negatively impact HCV replication (Ariza-Mateos et al., 2016). The combination of the two transgenes, V protein and SEC14L2 in a single lentiviral vector will improve this issue substantially, allowing the use of G418 as a resistance marker to cease (suggested in chapter 3.3 above). In a similar note, a further potential use for this system could be to select stable replication of SGRs which do not replicate in any other system; This allows the approach of culture adaptation and identification of CAS which resulted in transient replication of S52 SGR (and mirrors the approach initially used by the authors of the study which reported the Con1 SGR) (Lohmann et al., 1999) to be used for developing new SGRs for other genotypes and potentially related viruses such as EqHV.

The SGR-harbouring cells were treated with DAAs to eradicate the SGR in a similar experiment to the work which led to the panel of cells with higher permissibility to HCV replication which are commonly used, namely Huh7.5, Huh7.5.1 and lunet cells (Blight et al., 2002; Zhong et al., 2005; Yu et al., 2013). In each of these cases selection of SGR-harbouring cells had an unintended effect upon the host cell, to dampen the innate immune response (Foy et al., 2005; Sumpter et al., 2005). The S52-eradicated cells did not support replication of the wild-type SGR, though they may support replication of the adapted and reporter-optimised S52 SGR. This would eliminate such problems with the effects of selection drug upon the cells, though any change which increased permissibility to replication may well involve further immune attenuation, which therefore does not eliminate this issue.

This system was used to explore the differences in the emergence of resistance in a GT3-specific cell culture system and to investigate an observation that could help to explain the unprecedented propensity of GT3 to develop and maintain resistance to NS5A inhibitors. However, it is not known if these phenomena are GT3-specific or are a hallmark of HCV, in which case a worthwhile experiment would be to repeat these experiments alongside a comparator of Con1, JFH-1 or both to investigate if the differences in sensitivity of each genotype can be partially explained by these observations. In addition, different RAS are reported to have different effects depending on genotype (Table 1-3, Table 1-4, Table 1-5 and references therein) which is likely to impact the results of this work.

Investigation of the nature of genotype differences is of great importance in the improvement of treatment guidance. The relationship between RAS and treatment response is complicated,

with a correlation observed in clinical trials but a direct causative link not established despite the substantial differences observed *in vitro* by single point mutations which are readily introduced by the replicase machinery of the virus (Poveda et al., 2014; Cento et al., 2015; Chayama and Hayes, 2015). *In vitro*, a RAS always develops when an SGR is selected with a concentration of NS5A inhibitor which is not sufficient to completely inhibit replication, and a RAS engineered into an SGR by site-directed mutagenesis can completely abolish efficacy of the compound at concentrations which are not toxic and are practical for laboratory use. However, patients with a RAS at baseline can respond to treatment and achieve SVR and, similarly patients without a detectable RAS can fail treatment and have a detectable RAS at the point of breakthrough or relapse. The exploration of the origins of resistance in all genotypes may provide information to better tailor the treatment regimen prescribed or the structure of new drugs in development. Specifically, the proposed experiment to use sequences from clinical isolates in a full-GT3 shuttle vector may provide further information as to the role of RAS at baseline and the relationship of these with other residues which may not be directly resistance-associated.

This work has revealed a fascinating observation about the phenotype of RAS in GT3. The data presented show that there is a discrepancy between replication fitness of a single Y93H point mutant at different stages of replication, though the nature of this difference was not elucidated. However, the two hypotheses which were explored: genetic compensation which stabilises the resistant NS5A protein; or an ability of NS5A to overcome the fitness cost once replication has already been established; may still play a role in the fitness cost of resistance, or lack thereof for constituent replication. The presence of compensatory mutations in other non-structural proteins may provide a part of the effect, with the smaller degree of fitness cost being more readily overcome once replication is established. It was intended to combine the experiments used to investigate these two hypotheses: namely, the next step of the process was to assess the replication capacity of the SGR-harbouring cell RNA, in which a defect can be observed between S52 wild-type and S52 DCV cell RNA, in the neo SGR-harbouring cells. In parallel the full NS3-5B region would be explored by NGS to identify any other substitutions which were not found by PCR sequencing and screen them in the same method used for K41R and the combination experiment described above. It is unlikely, though not impossible, that the compensatory mutations should reside without NS5A and exert their effect in the form of a protein-protein interaction.

The NHS EAP has allowed the treatment of a small number of patients each year who are at risk of death or irreparable damage from HCV infection during the following 12 months (Cheung et al., 2016; Foster et al., 2016). This compassionate use programme has allowed the investigation of the efficacy of DAAs in extremely ill patients as well as monitoring the prognosis of such high-risk patients in the event of achieving SVR. However, this and other cohort studies (Younossi et al., 2014; Steinebrunner et al., 2015) have reported that the efficacy of DAAs is much higher when administered to patients who do not have such severe disease and, in addition, the deleterious effects of HCV infection are not necessarily reversed once SVR is achieved and may be accelerated for an unknown reason (Cheung et al., 2016; Conti et al., 2016; Reig et al., 2016; Strazzulla et al., 2016; Jakobsen et al., 2017). This is of concern for GT3, following extensive observation that GT3-infected patients have a higher incidence of hepatic steatosis which correlates with HCV RNA (Mihm et al., 1997; Rubbia-Brandt et al., 2000; Rubbia-Brandt et al., 2004) and is apparent in the absence of other risk factors for NASH. Though studies have shown that the successful treatment of HCV GT3 leads to the reversal of GT3-related hepatic steatosis (Rubbia-Brandt et al., 2004), these patients are at risk of quicker disease progression and have a higher incidence of HCC (Nkontchou et al., 2011). It was recently reported that the risk of HCC in patients with severe cirrhosis does not decrease after DAA treatment (Conti et al., 2016; Reig et al., 2016; Strazzulla et al., 2016), indicating that the cellular changes leading to transformation of hepatocytes or hepatic progenitors are already in place, and disease progression will continue in a proportion of patients regardless of the eradication of the virus. It is of crucial importance, then, to identify the molecular causes of GT3-related hepatic steatosis to identify patients who are likely to progress much quicker than others, and to slow the pathogenic effects by treatment of the modification of these pathways to maintain the healthy state in which DAAs are substantially more effective.

This work has identified two potential avenues for exploration, in addition to those already reported. Previous work has demonstrated that GT3 core expression causes higher lipid accumulation, GT3-infected cells have lower levels of PPARα RNA (responsible for glucose metabolism) (Abid et al., 2005), and higher levels of miR-122, the hepatotropic miRNA which is essential for HCV replication and exerts a post-transcriptional control on lipid metabolism (Esau et al., 2006; Oliveira et al., 2016). This work may form the basis of studies to add to this list a differential regulation of AMPK by GT3 and a difference in the level of autophagy induction, which increases the pool of double- and multi-membrane vesicles for replication complex formation, and has links to fatty liver disease *in vivo* (Linya Wang et al., 2015; Tanaka

et al., 2016). It is likely that the mechanism of lipid accumulation leading to hepatic steatosis in GT3-infected patient liver tissue is not attributable to a single cause, and instead is a combination of smaller changes which contribute to a more severe disease state than each would be capable individually. Refined GT3 culture techniques may also permit the identification of other genotype differences unrelated to hepatic steatosis or NS5A inhibitor resistance which, in the absence of robust experimental systems, are currently unknown.

References

Abe, H., Ochi, H., Maekawa, T., Hayes, C.N., Tsuge, M., Miki, D., Mitsui, F., Hiraga, N., Imamura, M., Takahashi, S., Ohishi, W., Arihiro, K., Kubo, M., Nakamura, Y. and Chayama, K. 2010. Common variation of IL28 affects gamma-GTP levels and inflammation of the liver in chronically infected hepatitis C virus patients. *Journal of Hepatology*. **53**(3),pp.439–443.

Abenavoli, L., Masarone, M., Peta, V., Milic, N., Kobyliak, N., Rouabhia, S. and Persico, M. 2014. Insulin resistance and liver steatosis in chronic hepatitis C infection genotype 3. *World Journal of Gastroenterology*. **20**(41),p.15233.

Abid, K., Pazienza, V., de Gottardi, A., Rubbia-Brandt, L., Conne, B., Pugnale, P., Rossi, C., Mangia, A. and Negro, F. 2005. An in vitro model of hepatitis C virus genotype 3a-associated triglycerides accumulation. *Journal of hepatology*. **42**(5),pp.744–51.

Agapov, E. V, Reed, K.E. and Rice, C.M. 1999. Use of the vaccinia virus/t7 expression system for studying HCV protein processing. *Methods in molecular medicine*. **19**,pp.303–14.

Agnello, V., Abel, G., Elfahal, M., Knight, G.B. and Zhang, Q.X. 1999. Hepatitis C virus and other flaviviridae viruses enter cells via low density lipoprotein receptor. *Proceedings of the National Academy of Sciences of the United States of America*. **96**(22),pp.12766–71.

Akamatsu, S., Hayes, C.N., Ochi, H., Uchida, T., Kan, H., Murakami, E., Abe, H., Tsuge, M., Miki, D., Akiyama, R., Hiraga, N., Imamura, M., Aikata, H., Kawaoka, T., Kawakami, Y. and Chayama, K. 2015. Association between variants in the interferon lambda 4 locus and substitutions in the hepatitis C virus non-structural protein 5A. *Journal of hepatology*. **63**(3),pp.554–63.

Akuta, N., Suzuki, F., Hirakawa, M., Kawamura, Y., Sezaki, H., Suzuki, Y., Hosaka, T., Kobayashi, M., Kobayashi, M., Saitoh, S., Arase, Y., Ikeda, K., Chayama, K., Nakamura, Y. and Kumada, H. 2012. Amino Acid Substitution in HCV Core/NS5A Region and Genetic Variation Near <i>IL28B</i> Gene Affect Treatment Efficacy to Interferon plus Ribavirin Combination Therapy. *Intervirology*. **55**(3),pp.231–241.

Akuta, N., Suzuki, F., Kawamura, Y., Yatsuji, H., Sezaki, H., Suzuki, Y., Hosaka, T., Kobayashi, M., Kobayashi, M., Arase, Y., Ikeda, K. and Kumada, H. 2007. Predictors of viral kinetics to peginterferon plus ribavirin combination therapy in Japanese patients infected with hepatitis C virus genotype 1b. *Journal of Medical Virology*. **79**(11),pp.1686–1695.

Aligeti, M., Roder, A. and Horner, S.M. 2015. Cooperation between the Hepatitis C Virus p7 and NS5B Proteins Enhances Virion Infectivity. J.-H. J. Ou, ed. *Journal of virology*. **89**(22),pp.11523–33.

Alvisi, G., Madan, V. and Bartenschlager, R. 2011. Hepatitis C virus and host cell lipids: an intimate connection. *RNA Biol*. **8**(2),pp.258–269.

Amako, Y., Igloi, Z., Mankouri, J., Kazlauskas, A., Saksela, K., Dallas, M., Peers, C. and Harris, M. 2013. Hepatitis C virus NS5A inhibits mixed lineage kinase 3 to block apoptosis. *The Journal of biological chemistry*. **288**(34),pp.24753–63.

Amako, Y., Munakata, T., Kohara, M., Siddiqui, A., Peers, C. and Harris, M. 2015. Hepatitis C virus attenuates mitochondrial lipid β-oxidation by downregulating mitochondrial trifunctional-protein expression. M. S. Diamond, ed. *Journal of virology*. **89**(8),pp.4092–

101.

Ampuero, J., Romero-Gómez, M. and Reddy, K.R. 2014. Review article: HCV genotype 3 – the new treatment challenge. *Alimentary pharmacology & therapeutics*. **39**(7),pp.686–98.

Andrus, L., Marukian, S., Jones, C.T., Catanese, M.T., Sheahan, T.P., Schoggins, J.W., Barry, W.T., Dustin, L.B., Trehan, K., Ploss, A., Bhatia, S.N. and Rice, C.M. 2011. Expression of paramyxovirus V proteins promotes replication and spread of hepatitis C virus in cultures of primary human fetal liver cells. *Hepatology*. **54**(6),pp.1901–1912.

Appel, N., Herian, U. and Bartenschlager, R. 2005. Efficient Rescue of Hepatitis C Virus RNA Replication by trans-Complementation with Nonstructural Protein 5A. *Journal of Virology*. **79**(2),pp.896–909.

Appel, N., Pietschmann, T. and Bartenschlager, R. 2005. Mutational analysis of hepatitis C virus nonstructural protein 5A: potential role of differential phosphorylation in RNA replication and identification of a genetically flexible domain. *Journal of virology*. **79**(5),pp.3187–94.

Appel, N., Zayas, M., Miller, S., Krijnse-Locker, J., Schaller, T., Friebe, P., Kallis, S., Engel, U. and Bartenschlager, R. 2008. Essential role of domain III of nonstructural protein 5A for hepatitis C virus infectious particle assembly. D. Moradpour, ed. *PLoS pathogens*. **4**(3),p.e1000035.

Ariza-Mateos, A., Díaz-Toledano, R., Block, T.M., Prieto-Vega, S., Birk, A. and Gómez, J. 2016. Geneticin Stabilizes the Open Conformation of the 5′ Region of Hepatitis C Virus RNA and Inhibits Viral Replication. *Antimicrobial Agents and Chemotherapy*. **60**(2),pp.925–935.

Ascher, D.B., Wielens, J., Nero, T.L., Doughty, L., Morton, C.J. and Parker, M.W. 2015. Potent hepatitis C inhibitors bind directly to NS5A and reduce its affinity for RNA. *Scientific Reports*. **4**(1),p.4765.

Atkinson, N.J., Witteveldt, J., Evans, D.J. and Simmonds, P. 2014. The influence of CpG and UpA dinucleotide frequencies on RNA virus replication and characterization of the innate cellular pathways underlying virus attenuation and enhanced replication. *Nucleic acids research*. **42**(7),pp.4527–45.

Aydin, C., Mukherjee, S., Hanson, A.M., Frick, D.N. and Schiffer, C.A. 2013. The interdomain interface in bifunctional enzyme protein 3/4A (NS3/4A) regulates protease and helicase activities. *Protein Science*. **22**(12),pp.1786–1798.

Banerjee, D. and Reddy, K.R. 2016. Review article: safety and tolerability of direct-acting anti-viral agents in the new era of hepatitis C therapy. *Alimentary Pharmacology & Therapeutics*. **43**(6),pp.674–696.

Barakat, K.H., Anwar-Mohamed, A., Tuszynski, J.A., Robins, M.J., Tyrrell, D.L. and Houghton, M. 2015. A Refined Model of the HCV NS5A protein bound to daclatasvir explains drug-resistant mutations and activity against divergent genotypes. *Journal of chemical information and modeling*. **55**(2),pp.362–73.

Barba, G., Harper, F., Harada, T., Kohara, M., Goulinet, S., Matsuura, Y., Eder, G., Schaff, Z., Chapman, M.J., Miyamura, T. and Bréchot, C. 1997. Hepatitis C virus core protein shows a cytoplasmic localization and associates to cellular lipid storage droplets. *Proceedings of the National Academy of Sciences of the United States of America*. **94**(4),pp.1200–5.

Bartenschlager, R., Ahlborn-Laake, L., Mous, J. and Jacobsen, H. 1994. Kinetic and structural analyses of hepatitis C virus polyprotein processing. *Journal of virology*. **68**(8),pp.5045–

55.

Bartenschlager, R., Lohmann, V., Wilkinson, T. and Koch, J.O. 1995. Complex formation between the NS3 serine-type proteinase of the hepatitis C virus and NS4A and its importance for polyprotein maturation. *Journal of virology*. **69**(12),pp.7519–28.

Bartosch, B., Dubuisson, J. and Cosset, F.-L. 2003. Infectious hepatitis C virus pseudo-particles containing functional E1-E2 envelope protein complexes. *The Journal of experimental medicine*. **197**(5),pp.633–42.

Bassendine, M.F., Nielsen, S.U., Bridge, S.H., Felmlee, D.J., Sheridan, D.A., Packard, C.J. and Neely, R.D. 2017. Hepatitis C virus and atherosclerosis: A legacy after virologic cure? *Clinics and research in hepatology and gastroenterology*. **41**(1),pp.25–30.

Behrens, S.E., Tomei, L. and De Francesco, R. 1996. Identification and properties of the RNA-dependent RNA polymerase of hepatitis C virus. *The EMBO journal*. **15**(1),pp.12–22.

Benedicto, I., Gondar, V., Molina-Jiménez, F., García-Buey, L., López-Cabrera, M., Gastaminza, P. and Majano, P.L. 2015. Clathrin Mediates Infectious Hepatitis C Virus Particle Egress R. W. Doms, ed. *Journal of Virology*. **89**(8),pp.4180–4190.

Bentham, M.J., Foster, T.L., McCormick, C. and Griffin, S. 2013. Mutations in hepatitis C virus p7 reduce both the egress and infectivity of assembled particles via impaired proton channel function. *The Journal of general virology*. **94**(Pt 10),pp.2236–48.

Bittar, C., Jardim, A.C.G., Yamasaki, L.H., de Queiróz, A.T., Carareto, C.M., Pinho, J.R.R., de Carvalho-Mello, I.M.V. and Rahal, P. 2010. Genetic diversity of NS5A protein from hepatitis C virus genotype 3a and its relationship to therapy response. *BMC Infectious Diseases*. **10**(1),p.36.

Blight, K.J., McKeating, J.A. and Rice, C.M. 2002. Highly permissive cell lines for subgenomic and genomic hepatitis C virus RNA replication. *Journal of virology*. **76**(24),pp.13001–14.

Boson, B., Denolly, S., Turlure, F., Chamot, C., Dreux, M. and Cosset, F.-L. 2017. Daclatasvir Prevents Hepatitis C Virus Infectivity by Blocking Transfer of the Viral Genome to Assembly Sites. *Gastroenterology*. **152**(4),p.895–907.e14.

Boson, B., Granio, O., Bartenschlager, R. and Cosset, F.-L. 2011. A concerted action of hepatitis C virus p7 and nonstructural protein 2 regulates core localization at the endoplasmic reticulum and virus assembly. A. Pekosz, ed. *PLoS pathogens*. **7**(7),p.e1002144.

Boulant, S., Douglas, M.W., Moody, L., Budkowska, A., Targett-Adams, P. and McLauchlan, J. 2008. Hepatitis C virus core protein induces lipid droplet redistribution in a microtubule- and dynein-dependent manner. *Traffic (Copenhagen, Denmark)*. **9**(8),pp.1268–82.

Brazzoli, M., Bianchi, A., Filippini, S., Weiner, A., Zhu, Q., Pizza, M. and Crotta, S. 2008. CD81 Is a Central Regulator of Cellular Events Required for Hepatitis C Virus Infection of Human Hepatocytes. *Journal of Virology*. **82**(17),pp.8316–8329.

Bruchfeld, A., Roth, D., Martin, P., Nelson, D.R., Pol, S., Londoño, M.-C., Monsour, H., Silva, M., Hwang, P., Arduino, J.-M., Robertson, M., Nguyen, B.-Y., Wahl, J., Barr, E. and Greaves, W. 2017. Elbasvir plus grazoprevir in patients with hepatitis C virus infection and stage 4-5 chronic kidney disease: clinical, virological, and health-related quality-of-life outcomes from a phase 3, multicentre, randomised, double-blind, placebo-controlled trial. *The lancet. Gastroenterology & hepatology*. **2**(8),pp.585–594.

Bukh, J. 2012. Animal models for the study of hepatitis C virus infection and related liver

disease. *Gastroenterology*. **142**(6),p.1279–1287.e3.

Bukh, J. 2016. The history of hepatitis C virus (HCV): Basic research reveals unique features in phylogeny, evolution and the viral life cycle with new perspectives for epidemic control. *Journal of hepatology*. **65**(1 Suppl),pp.S2–S21.

Bukh, J., Purcell, R.H. and Miller, R.H. 1993. At least 12 genotypes of hepatitis C virus predicted by sequence analysis of the putative E1 gene of isolates collected worldwide. *Proceedings of the National Academy of Sciences of the United States of America*. **90**(17),pp.8234–8.

Butt, A.A., Ren, Y., Marks, K., Shaikh, O.S. and Sherman, K.E. 2017. Do directly acting antiviral agents for HCV increase the risk of hepatic decompensation and decline in renal function? Results from ERCHIVES. *Alimentary Pharmacology & Therapeutics*. **45**(1),pp.150–159.

Camus, G., Xu, S., Han, B., Lu, J., Dvory-Sobol, H., Yu, M., Cheng, G., Miller, M.D., Doehle, B.P. and Mo, H. 2018. Establishment of robust HCV genotype 4d, 5a, and 6a replicon systems. *Virology*. **514**,pp.134–141.

Caronia, S., Taylor, K., Pagliaro, L., Carr, C., Palazzo, U., Petrik, J., O'Rahilly, S., Shore, S., Tom, B.D. and Alexander, G.J. 1999. Further evidence for an association between non-insulin-dependent diabetes mellitus and chronic hepatitis C virus infection. *Hepatology (Baltimore, Md.)*. **30**(4),pp.1059–63.

Carrère-Kremer, S., Montpellier-Pala, C., Cocquerel, L., Wychowski, C., Penin, F. and Dubuisson, J. 2002. Subcellular localization and topology of the p7 polypeptide of hepatitis C virus. *Journal of virology*. **76**(8),pp.3720–30.

Cavalcante, L.N. and Lyra, A.C. 2015. Predictive factors associated with hepatitis C antiviral therapy response. *World Journal of Hepatology*. **7**(12),p.1617.

Cento, V., Chevaliez, S. and Perno, C.F. 2015. Resistance to direct-acting antiviral agents: clinical utility and significance. *Current opinion in HIV and AIDS*. **10**(5),pp.381–9.

Chan, D.P.C., Sun, H.-Y., Wong, H.T.H., Lee, S.-S. and Hung, C.-C. 2016. Sexually acquired hepatitis C virus infection: a review. *International Journal of Infectious Diseases*. **49**,pp.47–58.

Chayama, K. and Hayes, C. 2015. HCV Drug Resistance Challenges in Japan: The Role of Pre-Existing Variants and Emerging Resistant Strains in Direct Acting Antiviral Therapy. *Viruses*. **7**(10),pp.5328–5342.

Chen, Y.-L., Jeng, Y.-M., Chang, C.-N., Lee, H.-J., Hsu, H.-C., Lai, P.-L. and Yuan, R.-H. 2014. TERT promoter mutation in resectable hepatocellular carcinomas: A strong association with hepatitis C infection and absence of hepatitis B infection. *International Journal of Surgery*. **12**(7),pp.659–665.

Cheng, G., Tian, Y., Doehle, B., Peng, B., Corsa, A., Lee, Y.-J., Gong, R., Yu, M., Han, B., Xu, S., Dvory-Sobol, H., Perron, M., Xu, Y., Mo, H., Pagratis, N., Link, J.O. and Delaney, W. 2016. In Vitro Antiviral Activity and Resistance Profile Characterization of the Hepatitis C Virus NS5A Inhibitor Ledipasvir. *Antimicrobial agents and chemotherapy*. **60**(3),pp.1847–1853.

Cheng, J.C., Chang, M.F. and Chang, S.C. 1999. Specific interaction between the hepatitis C virus NS5B RNA polymerase and the 3' end of the viral RNA. *Journal of virology*. **73**(8),pp.7044–9.

Cheng, L., Zhang, Y., Nan, Y. and Qiao, L. 2015. Induced pluripotent stem cells (iPSCs) in the

modeling of hepatitis C virus infection. *Current stem cell research & therapy*. **10**(3),pp.216–9.

Cheung, M.C.M., Walker, A.J., Hudson, B.E., Verma, S., McLauchlan, J., Mutimer, D.J., Brown, A., Gelson, W.T.H., MacDonald, D.C., Agarwal, K., Foster, G.R., Irving, W.L. and HCV Research UK 2016. Outcomes after successful direct-acting antiviral therapy for patients with chronic hepatitis C and decompensated cirrhosis. *Journal of Hepatology*. **65**(4),pp.741–747.

Cho, N.-J., Dvory-Sobol, H., Lee, C., Cho, S.-J., Bryson, P., Masek, M., Elazar, M., Frank, C.W. and Glenn, J.S. 2010. Identification of a Class of HCV Inhibitors Directed Against the Nonstructural Protein NS4B. *Science Translational Medicine*. **2**(15),p.15ra6-15ra6.

Chong, W.M., Hsu, S.-C., Kao, W.-T., Lo, C.-W., Lee, K.-Y., Shao, J.-S., Chen, Y.-H., Chang, J., Chen, S.S.-L. and Yu, M.-J. 2016. Phosphoproteomics Identified an NS5A Phosphorylation Site Involved in Hepatitis C Virus Replication. *The Journal of biological chemistry*. **291**(8),pp.3918–31.

Choo, Q.L., Weiner, A.J., Overby, L.R., Kuo, G., Houghton, M. and Bradley, D.W. 1990. Hepatitis C virus: the major causative agent of viral non-A, non-B hepatitis. *British medical bulletin*. **46**(2),pp.423–41.

Choudhary, M.C., Natarajan, V., Pandey, P., Gupta, E., Sharma, S., Tripathi, R., Kumar, M.S., Kazim, S.N. and Sarin, S.K. 2014. Identification of Indian sub-continent as hotspot for HCV genotype 3a origin by Bayesian evolutionary reconstruction. *Infection, Genetics and Evolution*. **28**,pp.87–94.

Chukkapalli, V., Berger, K.L., Kelly, S.M., Thomas, M., Deiters, A. and Randall, G. 2015. Daclatasvir inhibits hepatitis C virus NS5A motility and hyper-accumulation of phosphoinositides. *Virology*. **476**,pp.168–79.

Clarke, D., Griffin, S., Beales, L., Gelais, C.S., Burgess, S., Harris, M. and Rowlands, D. 2006. Evidence for the formation of a heptameric ion channel complex by the hepatitis C virus p7 protein in vitro. *The Journal of biological chemistry*. **281**(48),pp.37057–68.

Colpitts, C.C. and Baumert, T.F. 2016. Hepatitis C virus cell entry: a target for novel antiviral strategies to address limitations of direct acting antivirals. *Hepatology International*. **10**(5),pp.741–748.

Conti, F., Buonfiglioli, F., Scuteri, A., Crespi, C., Bolondi, L., Caraceni, P., Foschi, F.G., Lenzi, M., Mazzella, G., Verucchi, G., Andreone, P. and Brillanti, S. 2016. Early occurrence and recurrence of hepatocellular carcinoma in HCV-related cirrhosis treated with direct-acting antivirals. *Journal of Hepatology*. **65**(4),pp.727–733.

Curry, M.P., O'Leary, J.G., Bzowej, N., Muir, A.J., Korenblat, K.M., Fenkel, J.M., Reddy, K.R., Lawitz, E., Flamm, S.L., Schiano, T., Teperman, L., Fontana, R., Schiff, E., Fried, M., Doehle, B., An, D., McNally, J., Osinusi, A., Brainard, D.M., McHutchison, J.G., Brown, R.S., Charlton, M. and ASTRAL-4 Investigators 2015. Sofosbuvir and Velpatasvir for HCV in Patients with Decompensated Cirrhosis. *The New England journal of medicine*. **373**(27),pp.2618–28.

Diamond, D.L., Syder, A.J., Jacobs, J.M., Sorensen, C.M., Walters, K.-A., Proll, S.C., McDermott, J.E., Gritsenko, M.A., Zhang, Q., Zhao, R., Metz, T.O., Camp, D.G., Waters, K.M., Smith, R.D., Rice, C.M. and Katze, M.G. 2010. Temporal proteome and lipidome profiles reveal hepatitis C virus-associated reprogramming of hepatocellular metabolism and

bioenergetics. G. G. Luo, ed. *PLoS pathogens*. **6**(1),p.e1000719.

Ding, S.C., Kohlway, A.S. and Pyle, A.M. 2011. Unmasking the active helicase conformation of nonstructural protein 3 from hepatitis C virus. *Journal of virology*. **85**(9),pp.4343–53.

Douglas, M.W. and George, J. 2009. Molecular mechanisms of insulin resistance in chronic hepatitis C. *World journal of gastroenterology*. **15**(35),pp.4356–64.

Dreux, M. and Chisari, F. V. 2011. Impact of the Autophagy Machinery on Hepatitis C Virus Infection. *Viruses*. **3**(12),pp.1342–1357.

Drummer, H.E., Boo, I. and Poumbourios, P. 2007. Mutagenesis of a conserved fusion peptide-like motif and membrane-proximal heptad-repeat region of hepatitis C virus glycoprotein E1. *The Journal of general virology*. **88**(Pt 4),pp.1144–8.

Dumoulin, F.L., von dem Bussche, A., Li, J., Khamzina, L., Wands, J.R., Sauerbruch, T. and Spengler, U. 2003. Hepatitis C virus NS2 protein inhibits gene expression from different cellular and viral promoters in hepatic and nonhepatic cell lines. *Virology*. **305**(2),pp.260–6.

Egger, D., Wölk, B., Gosert, R., Bianchi, L., Blum, H.E., Moradpour, D. and Bienz, K. 2002. Expression of hepatitis C virus proteins induces distinct membrane alterations including a candidate viral replication complex. *Journal of virology*. **76**(12),pp.5974–84.

Eggert, D., Rösch, K., Reimer, R. and Herker, E. 2014. Visualization and Analysis of Hepatitis C Virus Structural Proteins at Lipid Droplets by Super-Resolution Microscopy M. Yi, ed. *PLoS ONE*. **9**(7),p.e102511.

El-Shamy, A., Nagano-Fujii, M., Sasase, N., Imoto, S., Kim, S. and Hotta, H. 2008. Sequence variation in hepatitis C virus nonstructural protein 5A predicts clinical outcome of pegylated interferon/ribavirin combination therapy. *Hepatology*. **48**(1),pp.38–47.

Elbaz, T., El-Kassas, M. and Esmat, G. 2015. New era for management of chronic hepatitis C virus using direct antiviral agents: A review. *Journal of advanced research*. **6**(3),pp.301–10.

Elgharably, A., Gomaa, A.I., Crossey, M.M., Norsworthy, P.J., Waked, I. and Taylor-Robinson, S.D. 2017. Hepatitis C in Egypt - past, present, and future. *International journal of general medicine*. **10**,pp.1–6.

Eltahla, A.A., Leung, P., Pirozyan, M.R., Rodrigo, C., Grebely, J., Applegate, T., Maher, L., Luciani, F., Lloyd, A.R. and Bull, R.A. 2017. Dynamic evolution of hepatitis C virus resistance-associated substitutions in the absence of antiviral treatment. *Scientific reports*. **7**,p.41719.

England, C.G., Ehlerding, E.B. and Cai, W. 2016. NanoLuc: A Small Luciferase Is Brightening Up the Field of Bioluminescence. *Bioconjugate Chemistry*. **27**(5),pp.1175–1187.

Enomoto, H., Bando, Y., Nakamura, H., Nishiguchi, S. and Koga, M. 2015. Liver fibrosis markers of nonalcoholic steatohepatitis. *World Journal of Gastroenterology*. **21**(24),p.7427.

Enomoto, N., Sakuma, I., Asahina, Y., Kurosaki, M., Murakami, T., Yamamoto, C., Ogura, Y., Izumi, N., Marumo, F. and Sato, C. 1996. Mutations in the nonstructural protein 5A gene and response to interferon in patients with chronic hepatitis C virus 1b infection. *The New England journal of medicine*. **334**(2),pp.77–81.

Esau, C., Davis, S., Murray, S.F., Yu, X.X., Pandey, S.K., Pear, M., Watts, L., Booten, S.L., Graham,

M., McKay, R., Subramaniam, A., Propp, S., Lollo, B.A., Freier, S., Bennett, C.F., Bhanot, S. and Monia, B.P. 2006. miR-122 regulation of lipid metabolism revealed by in vivo antisense targeting. *Cell metabolism*. **3**(2),pp.87–98.

Eyre, N.S., Fiches, G.N., Aloia, A.L., Helbig, K.J., McCartney, E.M., McErlean, C.S.P., Li, K., Aggarwal, A., Turville, S.G. and Beard, M.R. 2014. Dynamic Imaging of the Hepatitis C Virus NS5A Protein during a Productive Infection. *Journal of Virology*. **88**(7),pp.3636–3652.

Eyre, N.S., Hampton-Smith, R.J., Aloia, A.L., Eddes, J.S., Simpson, K.J., Hoffmann, P. and Beard, M.R. 2016. Phosphorylation of NS5A Serine-235 is essential to hepatitis C virus RNA replication and normal replication compartment formation. *Virology*. **491**,pp.27–44.

Failla, C., Tomei, L. and De Francesco, R. 1994. Both NS3 and NS4A are required for proteolytic processing of hepatitis C virus nonstructural proteins. *Journal of virology*. **68**(6),pp.3753–60.

Falcón, V., Acosta-Rivero, N., González, S., Dueñas-Carrera, S., Martinez-Donato, G., Menéndez, I., Garateix, R., Silva, J.A., Acosta, E. and Kourı, J. 2017. Ultrastructural and biochemical basis for hepatitis C virus morphogenesis. *Virus Genes*. **53**(2),pp.151–164.

Fanning, L.J. 2002. The Irish paradigm on the natural progression of hepatitis C virus infection: an investigation in a homogeneous patient population infected with HCV 1b (review). *International journal of molecular medicine*. **9**(2),pp.179–84.

Farci, P., Shimoda, A., Wong, D., Cabezon, T., De Gioannis, D., Strazzera, A., Shimizu, Y., Shapiro, M., Alter, H.J. and Purcell, R.H. 1996. Prevention of hepatitis C virus infection in chimpanzees by hyperimmune serum against the hypervariable region 1 of the envelope 2 protein. *Proceedings of the National Academy of Sciences of the United States of America*. **93**(26),pp.15394–9.

Farquhar, M.J., Hu, K., Harris, H.J., Davis, C., Brimacombe, C.L., Fletcher, S.J., Baumert, T.F., Rappoport, J.Z., Balfe, P. and McKeating, J.A. 2012. Hepatitis C virus induces CD81 and claudin-1 endocytosis. *Journal of virology*. **86**(8),pp.4305–16.

Foster, G.R., Afdhal, N., Roberts, S.K., Bräu, N., Gane, E.J., Pianko, S., Lawitz, E., Thompson, A., Shiffman, M.L., Cooper, C., Towner, W.J., Conway, B., Ruane, P., Bourlière, M., Asselah, T., Berg, T., Zeuzem, S., Rosenberg, W., Agarwal, K., Stedman, C.A.M., Mo, H., Dvory-Sobol, H., Han, L., Wang, J., McNally, J., Osinusi, A., Brainard, D.M., McHutchison, J.G., Mazzotta, F., Tran, T.T., Gordon, S.C., Patel, K., Reau, N., Mangia, A., Sulkowski, M., ASTRAL-2 Investigators and ASTRAL-3 Investigators 2015. Sofosbuvir and Velpatasvir for HCV Genotype 2 and 3 Infection. *New England Journal of Medicine*. **373**(27),pp.2608–2617.

Foster, G.R., Irving, W.L., Cheung, M.C.M., Walker, A.J., Hudson, B.E., Verma, S., McLauchlan, J., Mutimer, D.J., Brown, A., Gelson, W.T.H., MacDonald, D.C., Agarwal, K. and HCV Research, UK 2016. Impact of direct acting antiviral therapy in patients with chronic hepatitis C and decompensated cirrhosis. *Journal of hepatology*. **64**(6),pp.1224–31.

Foster, T.L., Belyaeva, T., Stonehouse, N.J., Pearson, A.R. and Harris, M. 2010. All Three Domains of the Hepatitis C Virus Nonstructural NS5A Protein Contribute to RNA Binding. *Journal of Virology*. **84**(18),pp.9267–9277.

Foster, T.L., Thompson, G.S., Kalverda, A.P., Kankanala, J., Bentham, M., Wetherill, L.F., Thompson, J., Barker, A.M., Clarke, D., Noerenberg, M., Pearson, A.R., Rowlands, D.J., Homans, S.W., Harris, M., Foster, R. and Griffin, S. 2014. Structure-guided design affirms

inhibitors of hepatitis C virus p7 as a viable class of antivirals targeting virion release. *Hepatology (Baltimore, Md.)*. **59**(2),pp.408–22.

Foy, E., Li, K., Sumpter, R., Loo, Y.-M., Johnson, C.L., Wang, C., Fish, P.M., Yoneyama, M., Fujita, T., Lemon, S.M. and Gale, M. 2005. Control of antiviral defenses through hepatitis C virus disruption of retinoic acid-inducible gene-I signaling. *Proceedings of the National Academy of Sciences of the United States of America*. **102**(8),pp.2986–91.

Frangeul, L., Cresta, P., Perrin, M., Lunel, F., Opolon, P., Agut, H. and Huraux, J.M. 1998. Mutations in NS5A region of hepatitis C virus genome correlate with presence of NS5A antibodies and response to interferon therapy for most common European hepatitis C virus genotypes. *Hepatology (Baltimore, Md.)*. **28**(6),pp.1674–9.

Fridell, R.A., Qiu, D., Wang, C., Valera, L. and Gao, M. 2010. Resistance analysis of the hepatitis C virus NS5A inhibitor BMS-790052 in an in vitro replicon system. *Antimicrobial agents and chemotherapy*. **54**(9),pp.3641–50.

Fridell, R.A., Wang, C., Sun, J.-H., O'Boyle, D.R., Nower, P., Valera, L., Qiu, D., Roberts, S., Huang, X., Kienzle, B., Bifano, M., Nettles, R.E. and Gao, M. 2011. Genotypic and phenotypic analysis of variants resistant to hepatitis C virus nonstructural protein 5A replication complex inhibitor BMS-790052 in Humans: In Vitro and In Vivo Correlations. *Hepatology*. **54**(6),pp.1924–1935.

Fukuhara, T., Taketomi, A., Motomura, T., Okano, S., Ninomiya, A., Abe, T., Uchiyama, H., Soejima, Y., Shirabe, K., Matsuura, Y. and Maehara, Y. 2010. Variants in IL28B in Liver Recipients and Donors Correlate With Response to Peg-Interferon and Ribavirin Therapy for Recurrent Hepatitis C. *Gastroenterology*. **139**(5),p.1577–1585.e3.

Galli, A., Scheel, T.K.H., Prentoe, J.C., Mikkelsen, L.S., Gottwein, J.M. and Bukh, J. 2013. Analysis of hepatitis C virus core/NS5A protein co-localization using novel cell culture systems expressing core-NS2 and NS5A of genotypes 1-7. *Journal of General Virology*. **94**(Pt_10),pp.2221–2235.

Gane, E.J., Hyland, R.H., An, D., Svarovskaia, E., Pang, P.S., Brainard, D. and Stedman, C.A. 2015. Efficacy of ledipasvir and sofosbuvir, with or without ribavirin, for 12 weeks in patients with HCV genotype 3 or 6 infection. *Gastroenterology*. **149**(6),p.1454–1461.e1.

Gao, M., Nettles, R.E., Belema, M., Snyder, L.B., Nguyen, V.N., Fridell, R.A., Serrano-Wu, M.H., Langley, D.R., Sun, J.-H., O'Boyle II, D.R., Lemm, J.A., Wang, C., Knipe, J.O., Chien, C., Colonno, R.J., Grasela, D.M., Meanwell, N.A. and Hamann, L.G. 2010. Chemical genetics strategy identifies an HCV NS5A inhibitor with a potent clinical effect. *Nature*. **465**(7294),pp.96–100.

Gao, M., O'Boyle, D.R. and Roberts, S. 2016. HCV NS5A replication complex inhibitors. *Current opinion in pharmacology*. **30**,pp.151–157.

García-Mediavilla, M.V., Pisonero-Vaquero, S., Lima-Cabello, E., Benedicto, I., Majano, P.L., Jorquera, F., González-Gallego, J. and Sánchez-Campos, S. 2012. Liver X receptor α-mediated regulation of lipogenesis by core and NS5A proteins contributes to HCV-induced liver steatosis and HCV replication. *Laboratory investigation; a journal of technical methods and pathology*. **92**(8),pp.1191–202.

Gastaldi, G., Goossens, N., Clément, S. and Negro, F. 2017. Current level of evidence on causal association between hepatitis C virus and type 2 diabetes: A review. *Journal of advanced research*. **8**(2),pp.149–159.

Gastaminza, P., Dryden, K.A., Boyd, B., Wood, M.R., Law, M., Yeager, M. and Chisari, F. V 2010. Ultrastructural and biophysical characterization of hepatitis C virus particles produced in cell culture. *Journal of virology*. **84**(21),pp.10999–1009.

Gauthiez, E., Habfast-Robertson, I., Rüeger, S., Kutalik, Z., Aubert, V., Berg, T., Cerny, A., Gorgievski, M., George, J., Heim, M.H., Malinverni, R., Moradpour, D., Müllhaupt, B., Negro, F., Semela, D., Semmo, N., Villard, J., Bibert, S., Bochud, P.-Y. and Swiss Hepatitis C Cohort Study 2017. A systematic review and meta-analysis of HCV clearance. *Liver international : official journal of the International Association for the Study of the Liver*.

Ge, D., Fellay, J., Thompson, A.J., Simon, J.S., Shianna, K. V., Urban, T.J., Heinzen, E.L., Qiu, P., Bertelsen, A.H., Muir, A.J., Sulkowski, M., McHutchison, J.G. and Goldstein, D.B. 2009. Genetic variation in IL28B predicts hepatitis C treatment-induced viral clearance. *Nature*. **461**(7262),pp.399–401.

Ghany, M.G., Strader, D.B., Thomas, D.L., Seeff, L.B. and American Association for the Study of Liver Diseases 2009. Diagnosis, management, and treatment of hepatitis C: An update. *Hepatology*. **49**(4),pp.1335–1374.

Goonawardane, N., Gebhardt, A., Bartlett, C., Pichlmair, A. and Harris, M. 2017. Phosphorylation of serine 225 in hepatitis C virus NS5A regulates protein-protein interactions. *Journal of virology*.,p.JVI.00805-17.

Götte, M. and Feld, J.J. 2016. Direct-acting antiviral agents for hepatitis C: structural and mechanistic insights. *Nature reviews. Gastroenterology & hepatology*. **13**(6),pp.338–51.

Gottwein, J.M., Jensen, S.B., Li, Y.-P., Ghanem, L., Scheel, T.K.H., Serre, S.B.N., Mikkelsen, L. and Bukh, J. 2013. Combination Treatment with Hepatitis C Virus Protease and NS5A Inhibitors Is Effective against Recombinant Genotype 1a, 2a, and 3a Viruses. *Antimicrobial Agents and Chemotherapy*. **57**(3),pp.1291–1303.

Gottwein, J.M., Scheel, T.K.H., Callendret, B., Li, Y.P., Eccleston, H.B., Engle, R.E., Govindarajan, S., Satterfield, W., Purcell, R.H., Walker, C.M. and Bukh, J. 2010. Novel Infectious cDNA Clones of Hepatitis C Virus Genotype 3a (Strain S52) and 4a (Strain ED43): Genetic Analyses and In Vivo Pathogenesis Studies. *Journal of Virology*. **84**(10),pp.5277–5293.

Gottwein, J.M., Scheel, T.K.H., Hoegh, A.M., Lademann, J.B., Eugen–Olsen, J., Lisby, G. and Bukh, J. 2007. Robust Hepatitis C Genotype 3a Cell Culture Releasing Adapted Intergenotypic 3a/2a (S52/JFH1) Viruses. *Gastroenterology*. **133**(5),pp.1614–1626.

Gouklani, H., Bull, R.A., Beyer, C., Coulibaly, F., Gowans, E.J., Drummer, H.E., Netter, H.J., White, P.A. and Haqshenas, G. 2012. Hepatitis C virus nonstructural protein 5B is involved in virus morphogenesis. *Journal of virology*. **86**(9),pp.5080–8.

Gouttenoire, J., Castet, V., Montserret, R., Arora, N., Raussens, V., Ruysschaert, J.-M., Diesis, E., Blum, H.E., Penin, F. and Moradpour, D. 2009. Identification of a Novel Determinant for Membrane Association in Hepatitis C Virus Nonstructural Protein 4B. *Journal of Virology*. **83**(12),pp.6257–6268.

Grakoui, A., McCourt, D.W., Wychowski, C., Feinstone, S.M. and Rice, C.M. 1993. A second hepatitis C virus-encoded proteinase. *Proceedings of the National Academy of Sciences of the United States of America*. **90**(22),pp.10583–7.

Grassi, G., Di Caprio, G., Fimia, G.M., Ippolito, G., Tripodi, M. and Alonzi, T. 2016. Hepatitis C virus relies on lipoproteins for its life cycle. *World Journal of Gastroenterology*. **22**(6),p.1953.

Griffin, S. 2010. Inhibition of HCV p7 as a therapeutic target. *Current opinion in investigational drugs (London, England : 2000)*. **11**(2),pp.175–81.

Griffin, S., Clarke, D., McCormick, C., Rowlands, D. and Harris, M. 2005. Signal Peptide Cleavage and Internal Targeting Signals Direct the Hepatitis C Virus p7 Protein to Distinct Intracellular Membranes. *Journal of Virology*. **79**(24),pp.15525–15536.

Griffin, S.D.C., Beales, L.P., Clarke, D.S., Worsfold, O., Evans, S.D., Jaeger, J., Harris, M.P.G. and Rowlands, D.J. 2003. The p7 protein of hepatitis C virus forms an ion channel that is blocked by the antiviral drug, Amantadine. *FEBS letters*. **535**(1–3),pp.34–8.

Gu, M. and Rice, C.M. 2016. The Spring α-Helix Coordinates Multiple Modes of HCV (Hepatitis C Virus) NS3 Helicase Action. *The Journal of biological chemistry*. **291**(28),pp.14499–509.

Guedj, J., Dahari, H., Rong, L., Sansone, N.D., Nettles, R.E., Cotler, S.J., Layden, T.J., Uprichard, S.L. and Perelson, A.S. 2013. Modeling shows that the NS5A inhibitor daclatasvir has two modes of action and yields a shorter estimate of the hepatitis C virus half-life. *Proceedings of the National Academy of Sciences of the United States of America*. **110**(10),pp.3991–6.

Guo, X., Wang, S., Qiu, Z.-G., Dou, Y.-L., Liu, W.-L., Yang, D., Shen, Z.-Q., Chen, Z.-L., Wang, J.-F., Zhang, B.-, Wang, X.-W., Guo, X.-F., Zhang, X.-L., Jin, M. and Li, J.-W. 2017. Efficient replication of blood borne Hepatitis C Virus in human fetal liver stem cells. *Hepatology*.

Gürtler, L.G. and Eberle, J. 2017. Aspects on the history of transmission and favor of distribution of viruses by iatrogenic action: perhaps an example of a paradigm of the worldwide spread of HIV. *Medical microbiology and immunology*. **206**(4),pp.287–293.

Haqshenas, G. 2012. The conserved lysine 151 of HCV NS5B modulates viral genome replication and infectious virus production. *Journal of Viral Hepatitis*. **19**(12),pp.862–866.

Haqshenas, G., Mackenzie, J.M., Dong, X. and Gowans, E.J. 2007. Hepatitis C virus p7 protein is localized in the endoplasmic reticulum when it is encoded by a replication-competent genome. *The Journal of general virology*. **88**(Pt 1),pp.134–42.

Harak, C., Meyrath, M., Romero-Brey, I., Schenk, C., Gondeau, C., Schult, P., Esser-Nobis, K., Saeed, M., Neddermann, P., Schnitzler, P., Gotthardt, D., Perez-del-Pulgar, S., Neumann-Haefelin, C., Thimme, R., Meuleman, P., Vondran, F.W.R., Francesco, R. De, Rice, C.M., Bartenschlager, R. and Lohmann, V. 2016. Tuning a cellular lipid kinase activity adapts hepatitis C virus to replication in cell culture. *Nature Microbiology*. **2**,p.16247.

He, B., Paterson, R.G., Stock, N., Durbin, J.E., Durbin, R.K., Goodbourn, S., Randall, R.E. and Lamb, R.A. 2002. Recovery of paramyxovirus simian virus 5 with a V protein lacking the conserved cysteine-rich domain: the multifunctional V protein blocks both interferon-beta induction and interferon signaling. *Virology*. **303**(1),pp.15–32.

He, Y., Weng, L., Li, R., Li, L., Toyoda, T. and Zhong, J. 2012. The N-terminal helix α0 of hepatitis C virus NS3 protein dictates the subcellular localization and stability of NS3/NS4A complex. *Virology*. **422**(2),pp.214–223.

Hernandez, D., Zhou, N., Ueland, J., Monikowski, A. and McPhee, F. 2013. Natural prevalence of NS5A polymorphisms in subjects infected with hepatitis C virus genotype 3 and their effects on the antiviral activity of NS5A inhibitors. *Journal of Clinical Virology*. **57**(1),pp.13–18.

Hijikata, M., Kato, N., Ootsuyama, Y., Nakagawa, M. and Shimotohno, K. 1991. Gene mapping

of the putative structural region of the hepatitis C virus genome by in vitro processing analysis. *Proceedings of the National Academy of Sciences of the United States of America*. **88**(13),pp.5547–51.

Hijikata, M., Mizushima, H., Akagi, T., Mori, S., Kakiuchi, N., Kato, N., Tanaka, T., Kimura, K. and Shimotohno, K. 1993. Two distinct proteinase activities required for the processing of a putative nonstructural precursor protein of hepatitis C virus. *Journal of virology*. **67**(8),pp.4665–75.

Hoornenborg, E., Achterbergh, R.C.A., Schim van der Loeff, M.F., Davidovich, U., Hogewoning, A., de Vries, H.J.C., Schinkel, J., Prins, M., van de Laar, T.J.W. and Amsterdam PrEP Project team in the HIV Transmission Elimination AMsterdam Initiative, MOSAIC study group 2017. MSM starting preexposure prophylaxis are at risk of hepatitis C virus infection. *AIDS*. **31**(11),pp.1603–1610.

Horton, J.D., Goldstein, J.L. and Brown, M.S. 2002. SREBPs: activators of the complete program of cholesterol and fatty acid synthesis in the liver. *The Journal of clinical investigation*. **109**(9),pp.1125–31.

Hsu, M., Zhang, J., Flint, M., Logvinoff, C., Cheng-Mayer, C., Rice, C.M. and McKeating, J.A. 2003. Hepatitis C virus glycoproteins mediate pH-dependent cell entry of pseudotyped retroviral particles. *Proceedings of the National Academy of Sciences of the United States of America*. **100**(12),pp.7271–6.

Hu, B., Li, S., Zhang, Z., Xie, S., Hu, Y., Huang, X. and Zheng, Y. 2016. HCV NS4B targets Scribble for proteasome-mediated degradation to facilitate cell transformation. *Tumour biology : the journal of the International Society for Oncodevelopmental Biology and Medicine*. **37**(9),pp.12387–12396.

Hughes, M., Gretton, S., Shelton, H., Brown, D.D., McCormick, C.J., Angus, A.G.N., Patel, A.H., Griffin, S. and Harris, M. 2009. A conserved proline between domains II and III of hepatitis C virus NS5A influences both RNA replication and virus assembly. *Journal of virology*. **83**(20),pp.10788–96.

Hughes, M., Griffin, S. and Harris, M. 2009. Domain III of NS5A contributes to both RNA replication and assembly of hepatitis C virus particles. *The Journal of general virology*. **90**(Pt 6),pp.1329–34.

Hwang, L.-H., Hsieh, C.-L., Yen, A., Chung, Y.-L. and Chen, D.S. 1998. Involvement of the 5' Proximal Coding Sequences of Hepatitis C Virus with Internal Initiation of Viral Translation. *Biochemical and Biophysical Research Communications*. **252**(2),pp.455–460.

Igloi, Z., Kazlauskas, A., Saksela, K., Macdonald, A., Mankouri, J. and Harris, M. 2015. Hepatitis C virus NS5A protein blocks epidermal growth factor receptor degradation via a proline motif- dependent interaction. *The Journal of general virology*. **96**(8),pp.2133–44.

Ishizaka, N., Ishizaka, Y., Takahashi, E., Tooda, E. ichi, Hashimoto, H., Nagai, R. and Yamakado, M. 2002. Association between hepatitis C virus seropositivity, carotid-artery plaque, and intima-media thickening. *Lancet (London, England)*. **359**(9301),pp.133–5.

Ivanov, A. V., Smirnova, O.A., Ivanova, O.N., Masalova, O. V., Kochetkov, S.N. and Isaguliants, M.G. 2011. Hepatitis C Virus Proteins Activate NRF2/ARE Pathway by Distinct ROS-Dependent and Independent Mechanisms in HUH7 Cells R. Jhaveri, ed. *PLoS ONE*. **6**(9),p.e24957.

Jacobson, I.M., Gordon, S.C., Kowdley, K. V., Yoshida, E.M., Rodriguez-Torres, M., Sulkowski,

M.S., Shiffman, M.L., Lawitz, E., Everson, G., Bennett, M., Schiff, E., Al-Assi, M.T., Subramanian, G.M., An, D., Lin, M., McNally, J., Brainard, D., Symonds, W.T., McHutchison, J.G., Patel, K., Feld, J., Pianko, S., Nelson, D.R., POSITRON Study and FUSION Study 2013. Sofosbuvir for Hepatitis C Genotype 2 or 3 in Patients without Treatment Options. *New England Journal of Medicine*. **368**(20),pp.1867–1877.

Jakobsen, J.C., Nielsen, E.E., Feinberg, J., Katakam, K.K., Fobian, K., Hauser, G., Poropat, G., Djurisic, S., Weiss, K.H., Bjelakovic, M., Bjelakovic, G., Klingenberg, S.L., Liu, J.P., Nikolova, D., Koretz, R.L. and Gluud, C. 2017. Direct-acting antivirals for chronic hepatitis C *In*: J. C. Jakobsen, ed. *Cochrane Database of Systematic Reviews* [Online]. Chichester, UK: John Wiley & Sons, Ltd, p. CD012143.

Jennings, T., Chen, Y., Sikora, D. and Harrison, M. 2008. RNA unwinding activity of the hepatitis C virus NS3 helicase is modulated by the NS5B polymerase. *Biochemistry*.

Jhaveri, R., Qiang, G. and Diehl, A.M. 2009. Domain 3 of Hepatitis C Virus Core Protein Is Sufficient for Intracellular Lipid Accumulation. *The Journal of Infectious Diseases*. **200**(11),pp.1781–1788.

Jirasko, V., Montserret, R., Lee, J.Y., Gouttenoire, J., Moradpour, D., Penin, F. and Bartenschlager, R. 2010. Structural and functional studies of nonstructural protein 2 of the hepatitis C virus reveal its key role as organizer of virion assembly. M. S. Diamond, ed. *PLoS pathogens*. **6**(12),p.e1001233.

Johnson, S.W., Thompson, D.K. and Raccor, B. 2017. Hepatitis C Virus-Genotype 3: Update on Current and Emergent Therapeutic Interventions. *Current Infectious Disease Reports*. **19**(6),p.22.

Jones, C.T., Murray, C.L., Eastman, D.K., Tassello, J. and Rice, C.M. 2007. Hepatitis C Virus p7 and NS2 Proteins Are Essential for Production of Infectious Virus. *Journal of Virology*. **81**(16),pp.8374–8383.

Jopling, C.L., Yi, M., Lancaster, A.M., Lemon, S.M. and Sarnow, P. 2005. Modulation of hepatitis C virus RNA abundance by a liver-specific MicroRNA. *Science (New York, N.Y.)*. **309**(5740),pp.1577–81.

Kadjbaf, D., Keshvari, M., Alavian, S.M., Pouryasin, A., Behnava, B., Salimi, S., Mehrnoush, L., Karimi Elizee, P. and Sharafi, H. 2016. The Prevalence of Hepatitis C Virus Core Amino Acid 70 Substitution and Genotypes of Polymorphisms Near the IFNL3 Gene in Iranian Patients With Chronic Hepatitis C. *Hepatitis monthly*. **16**(6),p.e37011.

Kai, Y., Hikita, H., Morishita, N., Murai, K., Nakabori, T., Iio, S., Hagiwara, H., Imai, Y., Tamura, S., Tsutsui, S., Naito, M., Nishiuchi, M., Kondo, Y., Kato, T., Suemizu, H., Yamada, R., Oze, T., Yakushijin, T., Hiramatsu, N., Sakamori, R., Tatsumi, T. and Takehara, T. 2017. Baseline quasispecies selection and novel mutations contribute to emerging resistance-associated substitutions in hepatitis C virus after direct-acting antiviral treatment. *Scientific reports*. **7**,p.41660.

Kannan, R.P., Hensley, L.L., Evers, L.E., Lemon, S.M. and McGivern, D.R. 2011. Hepatitis C virus infection causes cell cycle arrest at the level of initiation of mitosis. *Journal of virology*. **85**(16),pp.7989–8001.

Kato, T., Date, T., Miyamoto, M., Furusaka, A., Tokushige, K., Mizokami, M. and Wakita, T. 2003. Efficient replication of the genotype 2a hepatitis C virus subgenomic replicon. *Gastroenterology*. **125**(6),pp.1808–17.

Katsarou, K., Lavdas, A.A., Tsitoura, P., Serti, E., Markoulatos, P., Mavromara, P. and Georgopoulou, U. 2010. Endocytosis of hepatitis C virus non-enveloped capsid-like particles induces MAPK–ERK1/2 signaling events. *Cellular and Molecular Life Sciences*. **67**(14),pp.2491–2506.

Kelly, L., Badhan, A., Roberts, G.C., Mbisa, J.L. and Harris, M. 2017. Manipulation of both virus- and cell-specific factors is required for robust transient replication of a hepatitis C virus genotype 3a sub-genomic replicon. *Journal of General Virology*. **98**(10),pp.2495–2506.

Kim, J.L., Morgenstern, K.A., Griffith, J.P., Dwyer, M.D., Thomson, J.A., Murcko, M.A., Lin, C. and Caron, P.R. 1998. Hepatitis C virus NS3 RNA helicase domain with a bound oligonucleotide: the crystal structure provides insights into the mode of unwinding. *Structure (London, England : 1993)*. **6**(1),pp.89–100.

Kim, J.L., Morgenstern, K.A., Lin, C., Fox, T., Dwyer, M.D., Landro, J.A., Chambers, S.P., Markland, W., Lepre, C.A., O'Malley, E.T., Harbeson, S.L., Rice, C.M., Murcko, M.A., Caron, P.R. and Thomson, J.A. 1996. Crystal structure of the hepatitis C virus NS3 protease domain complexed with a synthetic NS4A cofactor peptide. *Cell*. **87**(2),pp.343–55.

Kim, K., Kim, K.H., Ha, E., Park, J.Y., Sakamoto, N. and Cheong, J. 2009. Hepatitis C virus NS5A protein increases hepatic lipid accumulation via induction of activation and expression of PPARgamma. *FEBS Letters*. **583**(17),pp.2720–2726.

Kim, S., Date, T., Yokokawa, H., Kono, T., Aizaki, H., Maurel, P., Gondeau, C. and Wakita, T. 2014. Development of hepatitis C virus genotype 3a cell culture system. *Hepatology (Baltimore, Md.)*. **60**(6),pp.1838–50.

Kirby, B.J., Symonds, W.T., Kearney, B.P. and Mathias, A.A. 2015. Pharmacokinetic, Pharmacodynamic, and Drug-Interaction Profile of the Hepatitis C Virus NS5B Polymerase Inhibitor Sofosbuvir. *Clinical pharmacokinetics*. **54**(7),pp.677–90.

Knolle, P.A., Kremp, S., Höhler, T., Krummenauer, F., Schirmacher, P. and Gerken, G. 1998. Viral and host factors in the prediction of response to interferon-alpha therapy in chronic hepatitis C after long-term follow-up. *Journal of viral hepatitis*. **5**(6),pp.399–406.

Koike, K. 2007. Hepatitis C virus contributes to hepatocarcinogenesis by modulating metabolic and intracellular signaling pathways. *Journal of Gastroenterology and Hepatology*. **22**(s1),pp.S108–S111.

Kolykhalov, A.A., Feinstone, S.M. and Rice, C.M. 1996. Identification of a highly conserved sequence element at the 3' terminus of hepatitis C virus genome RNA. *Journal of virology*. **70**(6),pp.3363–71.

Kuiken, C., Yusim, K., Boykin, L. and Richardson, R. 2005. The Los Alamos hepatitis C sequence database. *Bioinformatics*. **21**(3),pp.379–384.

Kylefjord, H., Danielsson, A., Sedig, S., Belda, O., Wiktelius, D., Vrang, L. and Targett-Adams, P. 2014. Transient replication of a hepatitis C virus genotype 1b replicon chimera encoding NS5A-5B from genotype 3a. *Journal of virological methods*. **195**,pp.156–63.

Kyono, K., Miyashiro, M. and Taguchi, I. 2002. Human eukaryotic initiation factor 4AII associates with hepatitis C virus NS5B protein in vitro. *Biochemical and biophysical research communications*. **292**(3),pp.659–66.

Lambert, S.M., Langley, D.R., Garnett, J.A., Angell, R., Hedgethorne, K., Meanwell, N.A. and Matthews, S.J. 2014. The crystal structure of NS5A domain 1 from genotype 1a reveals

new clues to the mechanism of action for dimeric HCV inhibitors. *Protein science : a publication of the Protein Society*. **23**(6),pp.723–34.

Lanford, R.E., Guerra, B. and Lee, H. 2006. Hepatitis C virus genotype 1b chimeric replicon containing genotype 3 NS5A domain. *Virology*. **355**(2),pp.192–202.

Lawitz, E., Freilich, B., Link, J., German, P., Mo, H., Han, L., Brainard, D.M., McNally, J., Marbury, T. and Rodriguez-Torres, M. 2015. A phase 1, randomized, dose-ranging study of GS-5816, a once-daily NS5A inhibitor, in patients with genotype 1-4 hepatitis C virus. *Journal of Viral Hepatitis*. **22**(12),pp.1011–1019.

Lee, C., Ma, H., Hang, J.Q., Leveque, V., Sklan, E.H., Elazar, M., Klumpp, K. and Glenn, J.S. 2011. The hepatitis C virus NS5A inhibitor (BMS-790052) alters the subcellular localization of the NS5A non-structural viral protein. *Virology*. **414**(1),pp.10–18.

Lee, K.-Y., Chen, Y.-H., Hsu, S.-C. and Yu, M.-J. 2016. Phosphorylation of Serine 235 of the Hepatitis C Virus Non-Structural Protein NS5A by Multiple Kinases. Y.-S. Ho, ed. *PloS one*. **11**(11),p.e0166763.

Lemm, J.A., O'Boyle, D., Liu, M., Nower, P.T., Colonno, R., Deshpande, M.S., Snyder, L.B., Martin, S.W., St. Laurent, D.R., Serrano-Wu, M.H., Romine, J.L., Meanwell, N.A. and Gao, M. 2010. Identification of Hepatitis C Virus NS5A Inhibitors. *Journal of Virology*. **84**(1),pp.482–491.

Leroy, V., Angus, P., Bronowicki, J.-P., Dore, G.J., Hezode, C., Pianko, S., Pol, S., Stuart, K., Tse, E., McPhee, F., Bhore, R., Jimenez-Exposito, M.J. and Thompson, A.J. 2016. Daclatasvir, sofosbuvir, and ribavirin for hepatitis C virus genotype 3 and advanced liver disease: A randomized phase III study (ALLY-3+). *Hepatology*. **63**(5),pp.1430–1441.

Lesburg, C.A., Cable, M.B., Ferrari, E., Hong, Z., Mannarino, A.F. and Weber, P.C. 1999. Crystal structure of the RNA-dependent RNA polymerase from hepatitis C virus reveals a fully encircled active site. *Nature structural biology*. **6**(10),pp.937–43.

Li, C., Lu, L., Murphy, D.G., Negro, F. and Okamoto, H. 2014. Origin of hepatitis C virus genotype 3 in Africa as estimated through an evolutionary analysis of the full-length genomes of nine subtypes, including the newly sequenced 3d and 3e. *The Journal of general virology*. **95**(Pt 8),pp.1677–88.

Li, H.-C., Ma, H.-C., Yang, C.-H. and Lo, S.-Y. 2014. Production and pathogenicity of hepatitis C virus core gene products. *World journal of gastroenterology*. **20**(23),pp.7104–22.

Li, H.-F., Huang, C.-H., Ai, L.-S., Chuang, C.-K. and Chen, S.S.L. 2009. Mutagenesis of the fusion peptide-like domain of hepatitis C virus E1 glycoprotein: involvement in cell fusion and virus entry. *Journal of biomedical science*. **16**(1),p.89.

Li, S., Yu, X., Guo, Y. and Kong, L. 2012. Interaction networks of hepatitis C virus NS4B: implications for antiviral therapy. *Cellular microbiology*. **14**(7),pp.994–1002.

Li, Y.-P., Ramirez, S., Humes, D., Jensen, S.B., Gottwein, J.M. and Bukh, J. 2014. Differential sensitivity of 5'UTR-NS5A recombinants of hepatitis C virus genotypes 1-6 to protease and NS5A inhibitors. *Gastroenterology*. **146**(3),p.812–821.e4.

Lindenbach, B.D., Evans, M.J., Syder, A.J., Wölk, B., Tellinghuisen, T.L., Liu, C.C., Maruyama, T., Hynes, R.O., Burton, D.R., McKeating, J.A. and Rice, C.M. 2005. Complete replication of hepatitis C virus in cell culture. *Science (New York, N.Y.)*. **309**(5734),pp.623–6.

Lindenbach, B.D. and Rice, C.M. 2013. The ins and outs of hepatitis C virus entry and assembly.

Nature reviews. Microbiology. **11**(10),pp.688–700.

Link, J.O., Taylor, J.G., Xu, L., Mitchell, M., Guo, H., Liu, H., Kato, D., Kirschberg, T., Sun, J., Squires, N., Parrish, J., Keller, T., Yang, Z.-Y., Yang, C., Matles, M., Wang, Y., Wang, K., Cheng, G., Tian, Y., Mogalian, E., Mondou, E., Cornpropst, M., Perry, J. and Desai, M.C. 2014. Discovery of ledipasvir (GS-5885): a potent, once-daily oral NS5A inhibitor for the treatment of hepatitis C virus infection. *Journal of medicinal chemistry*. **57**(5),pp.2033–46.

Liu, R., Curry, S., McMonagle, P., Yeh, W.W., Ludmerer, S.W., Jumes, P.A., Marshall, W.L., Kong, S., Ingravallo, P., Black, S., Pak, I., DiNubile, M.J. and Howe, A.Y.M. 2015. Susceptibilities of genotype 1a, 1b, and 3 hepatitis C virus variants to the NS5A inhibitor elbasvir. *Antimicrobial agents and chemotherapy*. **59**(11),pp.6922–9.

Lohmann, V., Körner, F., Herian, U. and Bartenschlager, R. 1997. Biochemical properties of hepatitis C virus NS5B RNA-dependent RNA polymerase and identification of amino acid sequence motifs essential for enzymatic activity. *Journal of virology*. **71**(11),pp.8416–28.

Lohmann, V., Körner, F., Koch, J., Herian, U., Theilmann, L. and Bartenschlager, R. 1999. Replication of subgenomic hepatitis C virus RNAs in a hepatoma cell line. *Science (New York, N.Y.)*. **285**(5424),pp.110–3.

Lourenço, S., Costa, F., Débarges, B., Andrieu, T. and Cahour, A. 2008. Hepatitis C virus internal ribosome entry site-mediated translation is stimulated by cis-acting RNA elements and trans-acting viral factors. *The FEBS journal*. **275**(16),pp.4179–97.

Love, R.A., Brodsky, O., Hickey, M.J., Wells, P.A. and Cronin, C.N. 2009. Crystal structure of a novel dimeric form of NS5A domain I protein from hepatitis C virus. *Journal of virology*. **83**(9),pp.4395–403.

Lu, J., Xiang, Y., Tao, W., Li, Q., Wang, N., Gao, Y., Xiang, X., Xie, Q. and Zhong, J. 2014. A Novel Strategy To Develop a Robust Infectious Hepatitis C Virus Cell Culture System Directly from a Clinical Isolate. *Journal of Virology*. **88**(3),pp.1484–1491.

Lu, L.L., Puri, M., Horvath, C.M. and Sen, G.C. 2008. Select paramyxoviral V proteins inhibit IRF3 activation by acting as alternative substrates for inhibitor of kappaB kinase epsilon (IKKe)/TBK1. *The Journal of biological chemistry*. **283**(21),pp.14269–76.

Lu, W., Lo, S., Chen, M., Wu, K., Fung, Y.K.T. and Ou, J. 1999. Activation of p53 Tumor Suppressor by Hepatitis C Virus Core Protein. *Virology*. **264**(1),pp.134–141.

de Lucas, S., Bartolome, J. and Carreno, V. 2005. Hepatitis C virus core protein down-regulates transcription of interferon-induced antiviral genes. *The Journal of infectious diseases*. **191**(1),pp.93–9.

Lukavsky, P.J. 2009. Structure and function of HCV IRES domains. *Virus Research*. **139**(2),pp.166–171.

Luke, G., Escuin, H., De Felipe, P. and Ryan, M. 2010. 2A to the fore - research, technology and applications. *Biotechnology & genetic engineering reviews*. **26**,pp.223–60.

Lupberger, J., Zeisel, M.B., Xiao, F., Thumann, C., Fofana, I., Zona, L., Davis, C., Mee, C.J., Turek, M., Gorke, S., Royer, C., Fischer, B., Zahid, M.N., Lavillette, D., Fresquet, J., Cosset, F.-L., Rothenberg, S.M., Pietschmann, T., Patel, A.H., Pessaux, P., Doffoël, M., Raffelsberger, W., Poch, O., McKeating, J.A., Brino, L. and Baumert, T.F. 2011. EGFR and EphA2 are host factors for hepatitis C virus entry and possible targets for antiviral therapy. *Nature medicine*. **17**(5),pp.589–95.

Ma, Y., Anantpadma, M., Timpe, J.M., Shanmugam, S., Singh, S.M., Lemon, S.M. and Yi, M. 2011. Hepatitis C Virus NS2 Protein Serves as a Scaffold for Virus Assembly by Interacting with both Structural and Nonstructural Proteins. *Journal of Virology*. **85**(1),pp.86–97.

MacArthur, K.L., Wu, C.H. and Wu, G.Y. 2012. Animal models for the study of hepatitis C virus infection and replication. *World journal of gastroenterology*. **18**(23),pp.2909–13.

Machida, K., Tsukamoto, H., Mkrtchyan, H., Duan, L., Dynnyk, A., Liu, H.M., Asahina, K., Govindarajan, S., Ray, R., Ou, J.-H.J., Seki, E., Deshaies, R., Miyake, K. and Lai, M.M.-C. 2009. Toll-like receptor 4 mediates synergism between alcohol and HCV in hepatic oncogenesis involving stem cell marker Nanog. *Proceedings of the National Academy of Sciences of the United States of America*. **106**(5),pp.1548–53.

Madan, V. and Bartenschlager, R. 2015. Structural and Functional Properties of the Hepatitis C Virus p7 Viroporin. *Viruses*. **7**(8),pp.4461–81.

Magiorkinis, G., Magiorkinis, E., Paraskevis, D., Ho, S.Y.W., Shapiro, B., Pybus, O.G., Allain, J.-P. and Hatzakis, A. 2009. The global spread of hepatitis C virus 1a and 1b: a phylodynamic and phylogeographic analysis. A. Y. Kim, ed. *PLoS medicine*. **6**(12),p.e1000198.

Manickam, C. and Reeves, R.K. 2014. Modeling HCV disease in animals: virology, immunology and pathogenesis of HCV and GBV-B infections. *Frontiers in microbiology*. **5**,p.690.

Mankouri, J., Tedbury, P.R., Gretton, S., Hughes, M.E., Griffin, S.D.C., Dallas, M.L., Green, K.A., Hardie, D.G., Peers, C. and Harris, M. 2010. Enhanced hepatitis C virus genome replication and lipid accumulation mediated by inhibition of AMP-activated protein kinase. *Proceedings of the National Academy of Sciences of the United States of America*. **107**(25),pp.11549–54.

Manns, M.P., McHutchison, J.G., Gordon, S.C., Rustgi, V.K., Shiffman, M., Reindollar, R., Goodman, Z.D., Koury, K., Ling, M. and Albrecht, J.K. 2001. Peginterferon alfa-2b plus ribavirin compared with interferon alfa-2b plus ribavirin for initial treatment of chronic hepatitis C: a randomised trial. *Lancet (London, England)*. **358**(9286),pp.958–65.

Mansoor, A., Ali, L., Sabah, N., Hashmi, A.H., Khan, M.H., Kazmi, S.A.R., Ahmad, N., Siddiqi, S. and Khan, K.M. 2013. Study of PKRBD in HCV genotype 3a infected patients in response to interferon therapy in Pakistani population. *Virology Journal*. **10**(1),p.352.

Mantry, P.S. and Pathak, L. 2016. Dasabuvir (ABT333) for the treatment of chronic HCV genotype I: a new face of cure, an expert review. *Expert review of anti-infective therapy*. **14**(2),pp.157–65.

Manzano-Robleda, M.C., Ornelas-Arroyo, V., Barrientos-Gutiérrez, T., Méndez-Sánchez, N., Uribe, M. and Chávez-Tapia, N.C. 2015. Boceprevir and telaprevir for chronic genotype 1 hepatitis C virus infection. A systematic review and meta-analysis. *Ann Hepatol*. **14**(1),pp.46–57.

Martell, M., Esteban, J.I., Quer, J., Genescà, J., Weiner, A., Esteban, R., Guardia, J. and Gómez, J. 1992. Hepatitis C virus (HCV) circulates as a population of different but closely related genomes: quasispecies nature of HCV genome distribution. *Journal of virology*. **66**(5),pp.3225–9.

Masaki, T., Suzuki, R., Murakami, K., Aizaki, H., Ishii, K., Murayama, A., Date, T., Matsuura, Y., Miyamura, T., Wakita, T. and Suzuki, T. 2008. Interaction of Hepatitis C Virus Nonstructural Protein 5A with Core Protein Is Critical for the Production of Infectious Virus Particles. *Journal of Virology*. **82**(16),pp.7964–7976.

May, S., Ngui, S.L., Collins, S., Lattimore, S., Ramsay, M., Tedder, R.S. and Ijaz, S. 2015. Molecular epidemiology of newly acquired hepatitis C infections in England 2008-2011: genotype, phylogeny and mutation analysis. *Journal of clinical virology : the official publication of the Pan American Society for Clinical Virology*. **64**,pp.6–11.

McCauley, J.A. and Rudd, M.T. 2016. Hepatitis C virus NS3/4a protease inhibitors. *Current opinion in pharmacology*. **30**,pp.84–92.

McGivern, D.R., Masaki, T., Williford, S., Ingravallo, P., Feng, Z., Lahser, F., Asante-Appiah, E., Neddermann, P., De Francesco, R., Howe, A.Y. and Lemon, S.M. 2014. Kinetic analyses reveal potent and early blockade of hepatitis C virus assembly by NS5A inhibitors. *Gastroenterology*. **147**(2),p.453–62.e7.

McKechnie, V.M., Mills, P.R. and McCruden, E.A. 2000. The NS5a gene of hepatitis C virus in patients treated with interferon-alpha. *Journal of medical virology*. **60**(4),pp.367–78.

McMahon, H.T. and Gallop, J.L. 2005. Membrane curvature and mechanisms of dynamic cell membrane remodelling. *Nature*. **438**(7068),pp.590–596.

Meola, A., Tarr, A.W., England, P., Meredith, L.W., McClure, C.P., Foung, S.K.H., McKeating, J.A., Ball, J.K., Rey, F.A. and Krey, T. 2015. Structural flexibility of a conserved antigenic region in hepatitis C virus glycoprotein E2 recognized by broadly neutralizing antibodies. J.-H. J. Ou, ed. *Journal of virology*. **89**(4),pp.2170–81.

Merz, A., Long, G., Hiet, M.-S., Brügger, B., Chlanda, P., Andre, P., Wieland, F., Krijnse-Locker, J. and Bartenschlager, R. 2011. Biochemical and morphological properties of hepatitis C virus particles and determination of their lipidome. *The Journal of biological chemistry*. **286**(4),pp.3018–32.

Messina, J.P., Humphreys, I., Flaxman, A., Brown, A., Cooke, G.S., Pybus, O.G. and Barnes, E. 2015. Global distribution and prevalence of hepatitis C virus genotypes. *Hepatology*. **61**(1),pp.77–87.

Mhatre, S.S., Chetty, K.G. and Pradhan, D.S. 1983. Uncoupling of oxidative phosphorylation in rat liver mitochondria following the administration of dimethyl sulphoxide. *Biochemical and Biophysical Research Communications*. **110**(1),pp.325–331.

Mihm, S., Fayyazi, A., Hartmann, H. and Ramadori, G. 1997. Analysis of histopathological manifestations of chronic hepatitis C virus infection with respect to virus genotype. *Hepatology*. **25**(3),pp.735–739.

Miura, M., Maekawa, S., Sato, M., Komatsu, N., Tatsumi, A., Takano, S., Amemiya, F., Nakayama, Y., Inoue, T., Sakamoto, M. and Enomoto, N. 2014. Deep sequencing analysis of variants resistant to the non-structural 5A inhibitor daclatasvir in patients with genotype 1b hepatitis C virus infection. *Hepatology research : the official journal of the Japan Society of Hepatology*. **44**(14),pp.E360-7.

Mokhtari, M., Basirkazeruni, H. and Rostami, M. 2017. The Correlation between Different Risk Factors of Hepatitis C and Different Genotypes. *Advanced Biomedical Research*. **6**(1),p.45.

Molina, J.-M., Orkin, C., Iser, D.M., Zamora, F.-X., Nelson, M., Stephan, C., Massetto, B., Gaggar, A., Ni, L., Svarovskaia, E., Brainard, D., Subramanian, G.M., McHutchison, J.G., Puoti, M., Rockstroh, J.K. and PHOTON-2 study team 2015. Sofosbuvir plus ribavirin for treatment of hepatitis C virus in patients co-infected with HIV (PHOTON-2): a multicentre, open-label, non-randomised, phase 3 study. *The Lancet*. **385**(9973),pp.1098–1106.

Moreno, C., Berg, T., Tanwandee, T., Thongsawat, S., Van Vlierberghe, H., Zeuzem, S., Lenz, O., Peeters, M., Sekar, V. and De Smedt, G. 2012. Antiviral activity of TMC435 monotherapy in patients infected with HCV genotypes 2-6: TMC435-C202, a phase IIa, open-label study. *Journal of hepatology*. **56**(6),pp.1247–53.

Murayama, A., Sugiyama, N., Suzuki, R., Moriyama, M., Nakamura, N., Mochizuki, H., Wakita, T. and Kato, T. 2017. Amino Acid Mutations in the NS4A Region of Hepatitis C Virus Contribute to Viral Replication and Infectious Virus Production M. S. Diamond, ed. *Journal of Virology*. **91**(4),pp.e02124-16.

Nakatsuka, K., Atsukawa, M., Shimizu, M., Takahashi, H. and Kawamoto, C. 2015. Ribavirin contributes to eradicate hepatitis C virus through polarization of T helper 1/2 cell balance into T helper 1 dominance. *World journal of hepatology*. **7**(25),pp.2590–6.

Nelson, D.R., Cooper, J.N., Lalezari, J.P., Lawitz, E., Pockros, P.J., Gitlin, N., Freilich, B.F., Younes, Z.H., Harlan, W., Ghalib, R., Oguchi, G., Thuluvath, P.J., Ortiz-Lasanta, G., Rabinovitz, M., Bernstein, D., Bennett, M., Hawkins, T., Ravendhran, N., Sheikh, A.M., Varunok, P., Kowdley, K. V., Hennicken, D., McPhee, F., Rana, K., Hughes, E.A. and ALLY-3 Study Team 2015. All-oral 12-week treatment with daclatasvir plus sofosbuvir in patients with hepatitis C virus genotype 3 infection: ALLY-3 phase III study. *Hepatology*. **61**(4),pp.1127–1135.

Nettles, J.H., Stanton, R.A., Broyde, J., Amblard, F., Zhang, H., Zhou, L., Shi, J., McBrayer, T.R., Whitaker, T., Coats, S.J., Kohler, J.J. and Schinazi, R.F. 2014. Asymmetric binding to NS5A by daclatasvir (BMS-790052) and analogs suggests two novel modes of HCV inhibition. *Journal of medicinal chemistry*. **57**(23),pp.10031–43.

Nitta, S., Asahina, Y., Matsuda, M., Yamada, N., Sugiyama, R., Masaki, T., Suzuki, R., Kato, N., Watanabe, M., Wakita, T. and Kato, T. 2016. Effects of Resistance-Associated NS5A Mutations in Hepatitis C Virus on Viral Production and Susceptibility to Antiviral Reagents. *Scientific Reports*. **6**(1),p.34652.

Nkontchou, G., Ziol, M., Aout, M., Lhabadie, M., Baazia, Y., Mahmoudi, A., Roulot, D., Ganne-Carrie, N., Grando-Lemaire, V., Trinchet, J.-C., Gordien, E., Vicaut, E., Baghad, I. and Beaugrand, M. 2011. HCV genotype 3 is associated with a higher hepatocellular carcinoma incidence in patients with ongoing viral C cirrhosis. *Journal of Viral Hepatitis*. **18**(10),pp.e516–e522.

O'Boyle, D.R., Nower, P.T., Gao, M., Fridell, R., Wang, C., Hewawasam, P., Lopez, O., Tu, Y., Meanwell, N.A., Belema, M., Roberts, S.B., Cockett, M. and Sun, J.-H. 2016. Synergistic Activity of Combined NS5A Inhibitors. *Antimicrobial Agents and Chemotherapy*. **60**(3),pp.1573–1583.

O'Boyle Ii, D.R., Sun, J.-H., Nower, P.T., Lemm, J.A., Fridell, R.A., Wang, C., Romine, J.L., Belema, M., Nguyen, V.N., Laurent, D.R.S., Serrano-Wu, M., Snyder, L.B., Meanwell, N.A., Langley, D.R. and Gao, M. 2013. Characterizations of HCV NS5A replication complex inhibitors. *Virology*. **444**(1–2),pp.343–54.

Okada, S., Ishii, H., Nose, H., Okusaka, T., Kyogoku, A., Yoshimori, M. and Wakabayashi, K. 1997. Evidence for increased somatic cell mutations in patients with hepatocellular carcinoma. *Carcinogenesis*. **18**(2),pp.445–9.

Oliveira, K.G., Malta, F.M., Nastri, A.C.S.S., Widman, A., Faria, P.L., Santana, R.A.F., Alves, V.A.F., Carrilho, F.J. and Pinho, J.R.R. 2016. Increased hepatic expression of miRNA-122 in patients infected with HCV genotype 3. *Medical microbiology and immunology*.

205(2),pp.111–7.

Ortega-Prieto, A.M. and Dorner, M. 2016. The expanding toolbox for hepatitis C virus research. *Journal of viral hepatitis*. **23**(5),pp.320–9.

Pal, S., Polyak, S.J., Bano, N., Qiu, W.C., Carithers, R.L., Shuhart, M., Gretch, D.R. and Das, A. 2010. Hepatitis C virus induces oxidative stress, DNA damage and modulates the DNA repair enzyme NEIL1. *Journal of gastroenterology and hepatology*. **25**(3),pp.627–34.

Paolucci, S., Fiorina, L., Mariani, B., Gulminetti, R., Novati, S., Barbarini, G., Bruno, R. and Baldanti, F. 2013. Naturally occurring resistance mutations to inhibitors of HCV NS5A region and NS5B polymerase in DAA treatment-naïve patients. *Virology journal*. **10**(1),p.355.

Park, C.-Y., Jun, H.-J., Wakita, T., Cheong, J.H. and Hwang, S.B. 2009. Hepatitis C Virus Nonstructural 4B Protein Modulates Sterol Regulatory Element-binding Protein Signaling via the AKT Pathway. *Journal of Biological Chemistry*. **284**(14),pp.9237–9246.

Parvaiz, F., Manzoor, S., Iqbal, J., McRae, S., Javed, F., Ahmed, Q.L. and Waris, G. 2014. Hepatitis C virus nonstructural protein 5A favors upregulation of gluconeogenic and lipogenic gene expression leading towards insulin resistance: a metabolic syndrome. *Archives of Virology*. **159**(5),pp.1017–1025.

Pascu, M., Martus, P., Höhne, M., Wiedenmann, B., Hopf, U., Schreier, E. and Berg, T. 2004. Sustained virological response in hepatitis C virus type 1b infected patients is predicted by the number of mutations within the NS5A-ISDR: a meta-analysis focused on geographical differences. *Gut*. **53**(9),pp.1345–1351.

Patiño-Galindo, J.Á., Salvatierra, K., González-Candelas, F. and López-Labrador, F.X. 2016. Comprehensive Screening for Naturally Occurring Hepatitis C Virus Resistance to Direct-Acting Antivirals in the NS3, NS5A, and NS5B Genes in Worldwide Isolates of Viral Genotypes 1 to 6. *Antimicrobial agents and chemotherapy*. **60**(4),pp.2402–16.

Pawlotsky, J.-M. 2016. Hepatitis C Virus Resistance to Direct-Acting Antiviral Drugs in Interferon-Free Regimens. *Gastroenterology*. **151**(1),pp.70–86.

Pawlotsky, J.-M. 2013. Treatment of chronic hepatitis C: current and future. *Current topics in microbiology and immunology*. **369**,pp.321–42.

Pawlotsky, J.M., Tsakiris, L., Roudot-Thoraval, F., Pellet, C., Stuyver, L., Duval, J. and Dhumeaux, D. 1995. Relationship between hepatitis C virus genotypes and sources of infection in patients with chronic hepatitis C. *The Journal of infectious diseases*. **171**(6),pp.1607–10.

Peiffer, K.-H., Sommer, L., Susser, S., Vermehren, J., Herrmann, E., Döring, M., Dietz, J., Perner, D., Berkowski, C., Zeuzem, S. and Sarrazin, C. 2016. Interferon lambda 4 genotypes and resistance-associated variants in patients infected with hepatitis C virus genotypes 1 and 3. *Hepatology*. **63**(1),pp.63–73.

Petruzziello, A., Marigliano, S., Loquercio, G., Cozzolino, A. and Cacciapuoti, C. 2016. Global epidemiology of hepatitis C virus infection: An up-date of the distribution and circulation of hepatitis C virus genotypes. *World Journal of Gastroenterology*. **22**(34),p.7824.

Petta, S. 2017. Hepatitis C virus and cardiovascular: A review. *Journal of advanced research*. **8**(2),pp.161–168.

Pezzuto, F., Izzo, F., Buonaguro, L., Annunziata, C., Tatangelo, F., Botti, G., Buonaguro, F.M. and Tornesello, M.L. 2016. Tumor specific mutations in TERT promoter and CTNNB1 gene in

hepatitis B and hepatitis C related hepatocellular carcinoma. *Oncotarget*. **7**(34),pp.54253–54262.

Pfaender, S., Cavalleri, J.M. V, Walter, S., Doerrbecker, J., Campana, B., Brown, R.J.P., Burbelo, P.D., Postel, A., Hahn, K., Anggakusuma, Riebesehl, N., Baumgärtner, W., Becher, P., Heim, M.H., Pietschmann, T., Feige, K. and Steinmann, E. 2015. Clinical course of infection and viral tissue tropism of hepatitis C virus-like nonprimate hepaciviruses in horses. *Hepatology (Baltimore, Md.)*. **61**(2),pp.447–59.

Pietschmann, T., Kaul, A., Koutsoudakis, G., Shavinskaya, A., Kallis, S., Steinmann, E., Abid, K., Negro, F., Dreux, M., Cosset, F.-L. and Bartenschlager, R. 2006. Construction and characterization of infectious intragenotypic and intergenotypic hepatitis C virus chimeras. *Proceedings of the National Academy of Sciences of the United States of America*. **103**(19),pp.7408–13.

Pileri, P., Uematsu, Y., Campagnoli, S., Galli, G., Falugi, F., Petracca, R., Weiner, A.J., Houghton, M., Rosa, D., Grandi, G. and Abrignani, S. 1998. Binding of hepatitis C virus to CD81. *Science (New York, N.Y.)*. **282**(5390),pp.938–41.

Pol, S., Corouge, M. and Vallet-Pichard, A. 2016. Daclatasvir-sofosbuvir combination therapy with or without ribavirin for hepatitis C virus infection: from the clinical trials to real life. *Hepatic medicine : evidence and research*. **8**,pp.21–6.

Poole, E., He, B., Lamb, R.A., Randall, R.E. and Goodbourn, S. 2002. The V proteins of simian virus 5 and other paramyxoviruses inhibit induction of interferon-beta. *Virology*. **303**(1),pp.33–46.

Poordad, F., Schiff, E.R., Vierling, J.M., Landis, C., Fontana, R.J., Yang, R., McPhee, F., Hughes, E.A., Noviello, S. and Swenson, E.S. 2016. Daclatasvir with sofosbuvir and ribavirin for hepatitis C virus infection with advanced cirrhosis or post-liver transplantation recurrence. *Hepatology (Baltimore, Md.)*. **63**(5),pp.1493–505.

Popescu, C.-I., Riva, L., Vlaicu, O., Farhat, R., Rouillé, Y. and Dubuisson, J. 2014. Hepatitis C Virus Life Cycle and Lipid Metabolism. *Biology*. **3**(4),pp.892–921.

Poveda, E., Wyles, D.L., Mena, A., Pedreira, J.D., Castro-Iglesias, A. and Cachay, E. 2014. Update on hepatitis C virus resistance to direct-acting antiviral agents. *Antiviral research*. **108**,pp.181–91.

Powdrill, M.H., Tchesnokov, E.P., Kozak, R.A., Russell, R.S., Martin, R., Svarovskaia, E.S., Mo, H., Kouyos, R.D. and Gotte, M. 2011. Contribution of a mutational bias in hepatitis C virus replication to the genetic barrier in the development of drug resistance. *Proceedings of the National Academy of Sciences*. **108**(51),pp.20509–20513.

Premoli, C. and Aghemo, A. 2016. Directly acting antivirals against hepatitis C virus: mechanisms of action and impact of resistant associated variants. *Minerva gastroenterologica e dietologica*. **62**(1),pp.76–87.

Pybus, O.G., Cochrane, A., Holmes, E.C. and Simmonds, P. 2005. The hepatitis C virus epidemic among injecting drug users. *Infection, Genetics and Evolution*. **5**(2),pp.131–139.

Qadri, I., Choudhury, M., Rahman, S.M., Knotts, T.A., Janssen, R.C., Schaack, J., Iwahashi, M., Puljak, L., Simon, F.R., Kilic, G., Fitz, J.G. and Friedman, J.E. 2012. Increased Phosphoenolpyruvate Carboxykinase Gene Expression and Steatosis during Hepatitis C Virus Subgenome Replication. *Journal of Biological Chemistry*. **287**(44),pp.37340–37351.

Qashqari, H., Al-Mars, A., Chaudhary, A., Abuzenadah, A., Damanhouri, G., Alqahtani, M., Mahmoud, M., El Sayed Zaki, M., Fatima, K. and Qadri, I. 2013. Understanding the molecular mechanism(s) of hepatitis C virus (HCV) induced interferon resistance. *Infection, genetics and evolution : journal of molecular epidemiology and evolutionary genetics in infectious diseases*. **19**,pp.113–9.

Qiu, D., Lemm, J.A., O'Boyle, D.R., Sun, J.-H., Nower, P.T., Nguyen, V., Hamann, L.G., Snyder, L.B., Deon, D.H., Ruediger, E., Meanwell, N.A., Belema, M., Gao, M. and Fridell, R.A. 2011. The effects of NS5A inhibitors on NS5A phosphorylation, polyprotein processing and localization. *Journal of General Virology*. **92**(11),pp.2502–2511.

Rajyaguru, S., Yang, H., Martin, R., Miller, M.D. and Mo, H. 2013. Development and characterization of a replicon-based phenotypic assay for assessing HCV NS4B from clinical isolates. *Antiviral research*. **100**(2),pp.328–36.

Ramirez, S., Mikkelsen, L.S., Gottwein, J.M. and Bukh, J. 2016. Robust HCV Genotype 3a Infectious Cell Culture System Permits Identification of Escape Variants With Resistance to Sofosbuvir. *Gastroenterology*. **151**(5),p.973–985.e2.

Rauch, A., Kutalik, Z., Descombes, P., Cai, T., Di Iulio, J., Mueller, T., Bochud, M., Battegay, M., Bernasconi, E., Borovicka, J., Colombo, S., Cerny, A., Dufour, J.-F., Furrer, H., Günthard, H.F., Heim, M., Hirschel, B., Malinverni, R., Moradpour, D., Müllhaupt, B., Witteck, A., Beckmann, J.S., Berg, T., Bergmann, S., Negro, F., Telenti, A., Bochud, P.-Y., Swiss Hepatitis C Cohort Study and Swiss HIV Cohort Study 2010. Genetic variation in IL28B is associated with chronic hepatitis C and treatment failure: a genome-wide association study. *Gastroenterology*. **138**(4),pp.1338–45, 1345–7.

Reig, M., Mariño, Z., Perelló, C., Iñarrairaegui, M., Ribeiro, A., Lens, S., Díaz, A., Vilana, R., Darnell, A., Varela, M., Sangro, B., Calleja, J.L., Forns, X. and Bruix, J. 2016. Unexpected high rate of early tumor recurrence in patients with HCV-related HCC undergoing interferon-free therapy. *Journal of Hepatology*. **65**(4),pp.719–726.

Reiss, S., Rebhan, I., Backes, P., Romero-Brey, I., Erfle, H., Matula, P., Kaderali, L., Poenisch, M., Blankenburg, H., Hiet, M.-S., Longerich, T., Diehl, S., Ramirez, F., Balla, T., Rohr, K., Kaul, A., Bühler, S., Pepperkok, R., Lengauer, T., Albrecht, M., Eils, R., Schirmacher, P., Lohmann, V. and Bartenschlager, R. 2011. Recruitment and activation of a lipid kinase by hepatitis C virus NS5A is essential for integrity of the membranous replication compartment. *Cell host & microbe*. **9**(1),pp.32–45.

Research, C. for D.E. and 2015. U.S. Food and Drug Administration. Hepatitis C Treatments Viekira Pak and Technivie: Drug Safety Communication - Risk of Serious Liver Injury. *Safety Alerts for Human Medical Products. US Food and Drug Administration.*

Reuter, G., Maza, N., Pankovics, P. and Boros, A. 2014. Non-primate hepacivirus infection with apparent hepatitis in a horse - Short communication. *Acta veterinaria Hungarica*. **62**(3),pp.422–7.

Rice, C.M. 2011. New insights into HCV replication: potential antiviral targets. *Topics in antiviral medicine*. **19**(3),pp.117–20.

Rogers, D.W., Lee, C.H., Pound, D.C., Kumar, S., Cummings, O.W. and Lumeng, L. 1992. Hepatitis C virus does not cause nonalcoholic steatohepatitis. *Digestive diseases and sciences*. **37**(11),pp.1644–7.

Rojas, Á., del Campo, J.A., Maraver, M., Aparcero, R., García-Valdecasas, M., Diago, M.,

Carmona, I., Andrade, R.J., Solà, R. and Romero-Gómez, M. 2014. Hepatitis C virus infection alters lipid metabolism depending on IL28B polymorphism and viral genotype and modulates gene expression in vivo and in vitro. *Journal of viral hepatitis*. **21**(1),pp.19–24.

Romero-Brey, I., Merz, A., Chiramel, A., Lee, J.-Y., Chlanda, P., Haselman, U., Santarella-Mellwig, R., Habermann, A., Hoppe, S., Kallis, S., Walther, P., Antony, C., Krijnse-Locker, J. and Bartenschlager, R. 2012. Three-dimensional architecture and biogenesis of membrane structures associated with hepatitis C virus replication. G. G. Luo, ed. *PLoS pathogens*. **8**(12),p.e1003056.

Ross-Thriepland, D., Amako, Y. and Harris, M. 2013. The C terminus of NS5A domain II is a key determinant of hepatitis C virus genome replication, but is not required for virion assembly and release. *The Journal of general virology*. **94**(Pt 5),pp.1009–18.

Ross-Thriepland, D. and Harris, M. 2014. Insights into the complexity and functionality of hepatitis C virus NS5A phosphorylation. *Journal of virology*. **88**(3),pp.1421–32.

Ross-Thriepland, D., Mankouri, J. and Harris, M. 2015. Serine phosphorylation of the hepatitis C virus NS5A protein controls the establishment of replication complexes. M. S. Diamond, ed. *Journal of virology*. **89**(6),pp.3123–35.

Rubbia-Brandt, L., Fabris, P., Paganin, S., Leandro, G., Male, P.-J., Giostra, E., Carlotto, A., Bozzola, L., Smedile, A. and Negro, F. 2004. Steatosis affects chronic hepatitis C progression in a genotype specific way. *Gut*. **53**(3),pp.406–12.

Rubbia-Brandt, L., Quadri, R., Abid, K., Giostra, E., Malé, P.J., Mentha, G., Spahr, L., Zarski, J.P., Borisch, B., Hadengue, A. and Negro, F. 2000. Hepatocyte steatosis is a cytopathic effect of hepatitis C virus genotype 3. *Journal of hepatology*. **33**(1),pp.106–15.

Saeed, M., Andreo, U., Chung, H.-Y., Espiritu, C., Branch, A.D., Silva, J.M. and Rice, C.M. 2015. SEC14L2 enables pan-genotype HCV replication in cell culture. *Nature*. **524**(7566),pp.471–5.

Saeed, M., Gondeau, C., Hmwe, S., Yokokawa, H., Date, T., Suzuki, T., Kato, T., Maurel, P. and Wakita, T. 2013. Replication of Hepatitis C Virus Genotype 3a in Cultured Cells. *Gastroenterology*. **144**(1),p.56–58.e7.

Saeed, M., Scheel, T.K.H., Gottwein, J.M., Marukian, S., Dustin, L.B., Bukh, J. and Rice, C.M. 2012. Efficient replication of genotype 3a and 4a hepatitis C virus replicons in human hepatoma cells. *Antimicrobial agents and chemotherapy*. **56**(10),pp.5365–73.

Salloum, S., Wang, H., Ferguson, C., Parton, R.G. and Tai, A.W. 2013. Rab18 binds to hepatitis C virus NS5A and promotes interaction between sites of viral replication and lipid droplets. G. Luo, ed. *PLoS pathogens*. **9**(8),p.e1003513.

Santolini, E., Migliaccio, G. and La Monica, N. 1994. Biosynthesis and biochemical properties of the hepatitis C virus core protein. *Journal of virology*. **68**(6),pp.3631–41.

Sato, Y., Kato, J., Takimoto, R., Takada, K., Kawano, Y., Miyanishi, K., Kobune, M., Sato, Y., Takayama, T., Matunaga, T. and Niitsu, Y. 2006. Hepatitis C virus core protein promotes proliferation of human hepatoma cells through enhancement of transforming growth factor alpha expression via activation of nuclear factor-kappaB. *Gut*. **55**(12),pp.1801–8.

Scarselli, E., Ansuini, H., Cerino, R., Roccasecca, R.M., Acali, S., Filocamo, G., Traboni, C., Nicosia, A., Cortese, R. and Vitelli, A. 2002. The human scavenger receptor class B type I is

a novel candidate receptor for the hepatitis C virus. *The EMBO journal*. **21**(19),pp.5017–25.

Scheel, T.K.H., Gottwein, J.M., Mikkelsen, L.S., Jensen, T.B. and Bukh, J. 2011. Recombinant HCV Variants With NS5A From Genotypes 1–7 Have Different Sensitivities to an NS5A Inhibitor but Not Interferon-α. *Gastroenterology*. **140**(3),p.1032–1042.e6.

Seeff, L.B. 2009. The history of the 'natural history' of hepatitis C (1968-2009) *In*: *Liver International*., pp. 89–99.

Seo, Y.L., Heo, S. and Jang, K.L. 2015. Hepatitis C virus core protein overcomes H2O2-induced apoptosis by downregulating p14 expression via DNA methylation. *The Journal of general virology*. **96**(Pt 4),pp.822–32.

Sesmero, E. and Thorpe, I.F. 2015. Using the Hepatitis C Virus RNA-Dependent RNA Polymerase as a Model to Understand Viral Polymerase Structure, Function and Dynamics. *Viruses*. **7**(7),pp.3974–94.

Shatskaya, G.S. and Dmitrieva, T.M. 2013. Structural organization of viral RNA-dependent RNA polymerases. *Biochemistry (Moscow)*. **78**(3),pp.231–235.

Sheikh, T.I., Adam, T. and Qadri, I. 2015. Upregulated hepatic expression of mitochondrial PEPCK triggers initial gluconeogenic reactions in the HCV-3 patients. *Asian Pacific journal of tropical medicine*. **8**(8),pp.618–23.

Sheldon, J., Beach, N.M., Moreno, E., Gallego, I., Piñeiro, D., Martínez-Salas, E., Gregori, J., Quer, J., Esteban, J.I., Rice, C.M., Domingo, E. and Perales, C. 2014. Increased replicative fitness can lead to decreased drug sensitivity of hepatitis C virus. *Journal of virology*. **88**(20),pp.12098–111.

Sherman, A.C. and Sherman, K.E. 2015. Extrahepatic manifestations of hepatitis C infection: navigating CHASM. *Current HIV/AIDS reports*. **12**(3),pp.353–61.

Shimoike, T., Mimori, S., Tani, H., Matsuura, Y. and Miyamura, T. 1999. Interaction of hepatitis C virus core protein with viral sense RNA and suppression of its translation. *Journal of virology*. **73**(12),pp.9718–25.

Shimotohno, K., Tanji, Y., Hirowatari, Y., Komoda, Y., Kato, N. and Hijikata, M. 1995. Processing of the hepatitis C virus precursor protein. *Journal of hepatology*. **22**(1 Suppl),pp.87–92.

Smirnova, O.A., Ivanova, O.N., Mukhtarov, F.S., Tunitskaya, V.L., Jansons, J., Isaguliants, M.G., Kochetkov, S.N. and Ivanov, A. V. 2016. Analysis of the domains of hepatitis C virus core and NS5A proteins that activate the NRF2/are cascade. *Acta Naturae*. **8**(3),pp.123–127.

Smith, D.B., Bukh, J., Kuiken, C., Muerhoff, A.S., Rice, C.M., Stapleton, J.T. and Simmonds, P. 2014. Expanded classification of hepatitis C virus into 7 genotypes and 67 subtypes: Updated criteria and genotype assignment web resource. *Hepatology*. **59**(1),pp.318–327.

Stapleford, K.A. and Lindenbach, B.D. 2011. Hepatitis C virus NS2 coordinates virus particle assembly through physical interactions with the E1-E2 glycoprotein and NS3-NS4A enzyme complexes. *Journal of virology*. **85**(4),pp.1706–17.

Steinebrunner, N., Sprinzl, M.F., Zimmermann, T., Wörns, M.A., Zimmerer, T., Galle, P.R., Stremmel, W., Eisenbach, C., Stein, K., Antoni, C., Schattenberg, J.M. and Pathil, A. 2015. Early virological response may predict treatment response in sofosbuvir-based combination therapy of chronic hepatitis c in a multi-center "real-life" cohort. *BMC gastroenterology*. **15**(1),p.97.

Steinmann, E., Penin, F., Kallis, S., Patel, A.H., Bartenschlager, R. and Pietschmann, T. 2007. Hepatitis C virus p7 protein is crucial for assembly and release of infectious virions. *PLoS pathogens*. **3**(7),p.e103.

Stewart, H., Bingham, R.J., White, S.J., Dykeman, E.C., Zothner, C., Tuplin, A.K., Stockley, P.G., Twarock, R. and Harris, M. 2016. Identification of novel RNA secondary structures within the hepatitis C virus genome reveals a cooperative involvement in genome packaging. *Scientific reports*. **6**(1),p.22952.

Strazzulla, A., Maria Rita Iemmolo, R., Carbone, E., Concetta Postorino, M., Mazzitelli, M., De Santis, M., Di Benedetto, F., Maria Cristiani, C., Costa, C., Pisani, V. and Torti, C. 2016. The Risk of Hepatocellular Carcinoma After Directly Acting Antivirals for Hepatitis C Virus Treatment in Liver Transplanted Patients: Is It Real? *Hepatitis Monthly*. **16**(11),p.e41933.

Street, A., Macdonald, A., Crowder, K. and Harris, M. 2004. The Hepatitis C virus NS5A protein activates a phosphoinositide 3-kinase-dependent survival signaling cascade. *The Journal of biological chemistry*. **279**(13),pp.12232–41.

Street, A., Macdonald, A., McCormick, C. and Harris, M. 2005. Hepatitis C Virus NS5A-Mediated Activation of Phosphoinositide 3-Kinase Results in Stabilization of Cellular -Catenin and Stimulation of -Catenin-Responsive Transcription. *Journal of Virology*. **79**(8),pp.5006–5016.

Sulkowski, M.S., Jacobson, I.M. and Nelson, D.R. 2014. Daclatasvir plus Sofosbuvir for HCV Infection. *New England Journal of Medicine*. **370**(16),pp.1560–1561.

Sulkowski, M.S., Naggie, S., Lalezari, J., Fessel, W.J., Mounzer, K., Shuhart, M., Luetkemeyer, A.F., Asmuth, D., Gaggar, A., Ni, L., Svarovskaia, E., Brainard, D.M., Symonds, W.T., Subramanian, G.M., McHutchison, J.G., Rodriguez-Torres, M. and Dieterich, D. 2014. Sofosbuvir and Ribavirin for Hepatitis C in Patients With HIV Coinfection. *JAMA : the journal of the American Medical Association*. **312**(4),pp.353–61.

Sumpter, R., Loo, Y.-M., Foy, E., Li, K., Yoneyama, M., Fujita, T., Lemon, S.M. and Gale, M. 2005. Regulating intracellular antiviral defense and permissiveness to hepatitis C virus RNA replication through a cellular RNA helicase, RIG-I. *Journal of virology*. **79**(5),pp.2689–99.

Sun, J.-H., O'Boyle II, D.R., Fridell, R.A., Langley, D.R., Wang, C., Roberts, S.B., Nower, P., Johnson, B.M., Moulin, F., Nophsker, M.J., Wang, Y.-K., Liu, M., Rigat, K., Tu, Y., Hewawasam, P., Kadow, J., Meanwell, N.A., Cockett, M., Lemm, J.A., Kramer, M., Belema, M. and Gao, M. 2015. Resensitizing daclatasvir-resistant hepatitis C variants by allosteric modulation of NS5A. *Nature*. **527**(7577),pp.245–248.

Sun, J.-H., O'Boyle II, D.R., Zhang, Y., Wang, C., Nower, P., Valera, L., Roberts, S., Nettles, R.E., Fridell, R.A. and Gao, M. 2012. Impact of a baseline polymorphism on the emergence of resistance to the hepatitis C virus nonstructural protein 5a replication complex inhibitor, BMS-790052. *Hepatology*. **55**(6),pp.1692–1699.

Suzuki, F., Sezaki, H., Akuta, N., Suzuki, Y., Seko, Y., Kawamura, Y., Hosaka, T., Kobayashi, M., Saito, S., Arase, Y., Ikeda, K., Kobayashi, M., Mineta, R., Watahiki, S., Miyakawa, Y. and Kumada, H. 2012. Prevalence of hepatitis C virus variants resistant to NS3 protease inhibitors or the NS5A inhibitor (BMS-790052) in hepatitis patients with genotype 1b. *Journal of Clinical Virology*. **54**(4),pp.352–354.

Syed, G.H., Khan, M., Yang, S. and Siddiqui, A. 2017. Hepatitis C Virus Lipoviroparticles Assemble in the Endoplasmic Reticulum (ER) and Bud off from the ER to the Golgi

Compartment in COPII Vesicles J.-H. J. Ou, ed. *Journal of Virology*. **91**(15),pp.e00499-17.

Syed, M., Skonberg, C. and Hansen, S.H. 2013. Effect of some organic solvents on oxidative phosphorylation in rat liver mitochondria: Choice of organic solvents. *Toxicology in Vitro*. **27**(8),pp.2135–2141.

Taherkhani, R. and Farshadpour, F. 2017. Global elimination of hepatitis C virus infection: Progresses and the remaining challenges. *World J Hepatol*. **9**(33),pp.1239–1252.

Takacs, C.N., Andreo, U., Belote, R.L., Pulupa, J., Scull, M.A., Gleason, C.E., Rice, C.M. and Simon, S.M. 2017. Green fluorescent protein-tagged apolipoprotein E: A useful marker for the study of hepatic lipoprotein egress. *Traffic (Copenhagen, Denmark)*. **18**(3),pp.192–204.

Takeda, H., Takai, A., Inuzuka, T. and Marusawa, H. 2017. Genetic basis of hepatitis virus-associated hepatocellular carcinoma: linkage between infection, inflammation, and tumorigenesis. *Journal of Gastroenterology*. **52**(1),pp.26–38.

Takeuchi, T., Katsume, A., Tanaka, T., Abe, A., Inoue, K., Tsukiyama-Kohara, K., Kawaguchi, R., Tanaka, S. and Kohara, M. 1999. Real-time detection system for quantification of hepatitis C virus genome. *Gastroenterology*. **116**(3),pp.636–42.

Tanaka, S., Hikita, H., Tatsumi, T., Sakamori, R., Nozaki, Y., Sakane, S., Shiode, Y., Nakabori, T., Saito, Y., Hiramatsu, N., Tabata, K., Kawabata, T., Hamasaki, M., Eguchi, H., Nagano, H., Yoshimori, T. and Takehara, T. 2016. Rubicon inhibits autophagy and accelerates hepatocyte apoptosis and lipid accumulation in nonalcoholic fatty liver disease in mice. *Hepatology*. **64**(6),pp.1994–2014.

Tanaka, T., Kato, N., Cho, M.J. and Shimotohno, K. 1995. A novel sequence found at the 3' terminus of hepatitis C virus genome. *Biochemical and biophysical research communications*. **215**(2),pp.744–9.

Tanaka, T., Kato, N., Cho, M.J., Sugiyama, K. and Shimotohno, K. 1996. Structure of the 3' terminus of the hepatitis C virus genome. *Journal of virology*. **70**(5),pp.3307–12.

Tanaka, Y., Shimoike, T., Ishii, K., Suzuki, R., Suzuki, T., Ushijima, H., Matsuura, Y. and Miyamura, T. 2000. Selective Binding of Hepatitis C Virus Core Protein to Synthetic Oligonucleotides Corresponding to the 5' Untranslated Region of the Viral Genome. *Virology*. **270**(1),pp.229–236.

Tang, S., Collier, A.J. and Elliott, R.M. 1999. Alterations to both the primary and predicted secondary structure of stem-loop IIIc of the hepatitis C virus 1b 5' untranslated region (5'UTR) lead to mutants severely defective in translation which cannot be complemented in trans by the wild-type 5'UTR sequence. *Journal of virology*. **73**(3),pp.2359–64.

Targett-Adams, P., Graham, E.J.S., Middleton, J., Palmer, A., Shaw, S.M., Lavender, H., Brain, P., Tran, T.D., Jones, L.H., Wakenhut, F., Stammen, B., Pryde, D., Pickford, C. and Westby, M. 2011. Small Molecules Targeting Hepatitis C Virus-Encoded NS5A Cause Subcellular Redistribution of Their Target: Insights into Compound Modes of Action. *Journal of Virology*. **85**(13),pp.6353–6368.

Tarr, A., Khera, T., Hueging, K., Sheldon, J., Steinmann, E., Pietschmann, T. and Brown, R. 2015. Genetic Diversity Underlying the Envelope Glycoproteins of Hepatitis C Virus: Structural and Functional Consequences and the Implications for Vaccine Design. *Viruses*. **7**(7),pp.3995–4046.

Tedbury, P., Welbourn, S., Pause, A., King, B., Griffin, S. and Harris, M. 2011. The subcellular localization of the hepatitis C virus non-structural protein NS2 is regulated by an ion channel-independent function of the p7 protein. *Journal of General Virology*. **92**(4),pp.819–830.

Tellinghuisen, T.L., Marcotrigiano, J., Gorbalenya, A.E. and Rice, C.M. 2004. The NS5A protein of hepatitis C virus is a zinc metalloprotein. *The Journal of biological chemistry*. **279**(47),pp.48576–87.

Tesfaye, A., Stift, J., Maric, D., Cui, Q., Dienes, H.-P. and Feinstone, S.M. 2013. Chimeric Mouse Model for the Infection of Hepatitis B and C Viruses R. Ray, ed. *PLoS ONE*. **8**(10),p.e77298.

Thomas, E., Ghany, M.G. and Liang, T.J. 2012. The Application and Mechanism of Action of Ribavirin in Therapy of Hepatitis C. *Antiviral Chemistry and Chemotherapy*. **23**(1),pp.1–12.

Thomson, E., Ip, C.L.C., Badhan, A., Christiansen, M.T., Adamson, W., Ansari, M.A., Bibby, D., Breuer, J., Brown, A., Bowden, R., Bryant, J., Bonsall, D., Da Silva Filipe, A., Hinds, C., Hudson, E., Klenerman, P., Lythgow, K., Mbisa, J.L., McLauchlan, J., Myers, R., Piazza, P., Roy, S., Trebes, A., Sreenu, V.B., Witteveldt, J., STOP-HCV Consortium, E., Barnes, E. and Simmonds, P. 2016. Comparison of Next-Generation Sequencing Technologies for Comprehensive Assessment of Full-Length Hepatitis C Viral Genomes. M. J. Loeffelholz, ed. *Journal of clinical microbiology*. **54**(10),pp.2470–84.

Thrift, A.P., El-Serag, H.B. and Kanwal, F. 2017. Global epidemiology and burden of HCV infection and HCV-related disease. *Nature reviews. Gastroenterology & hepatology*. **14**(2),pp.122–132.

Tong, W.-Y., Nagano-Fujii, M., Hidajat, R., Deng, L., Takigawa, Y. and Hotta, H. 2002. Physical interaction between hepatitis C virus NS4B protein and CREB-RP/ATF6β. *Biochemical and Biophysical Research Communications*. **299**(3),pp.366–372.

Tovo, P.-A., Calitri, C., Scolfaro, C., Gabiano, C. and Garazzino, S. 2016. Vertically acquired hepatitis C virus infection: Correlates of transmission and disease progression. *World Journal of Gastroenterology*. **22**(4),p.1382.

Tripathi, L.P., Kambara, H., Chen, Y.-A., Nishimura, Y., Moriishi, K., Okamoto, T., Morita, E., Abe, T., Mori, Y., Matsuura, Y. and Mizuguchi, K. 2013. Understanding the biological context of NS5A-host interactions in HCV infection: a network-based approach. *Journal of proteome research*. **12**(6),pp.2537–51.

Tsukiyama-Kohara, K., Iizuka, N., Kohara, M. and Nomoto, A. 1992. Internal ribosome entry site within hepatitis C virus RNA. *Journal of virology*. **66**(3),pp.1476–83.

Tsutsumi, T., Suzuki, T., Moriya, K., Shintani, Y., Fujie, H., Miyoshi, H., Matsuura, Y., Koike, K. and Miyamura, T. 2003. Hepatitis C virus core protein activates ERK and p38 MAPK in cooperation with ethanol in transgenic mice. *Hepatology*. **38**(4),pp.820–828.

Tulloch, F., Atkinson, N.J., Evans, D.J., Ryan, M.D. and Simmonds, P. 2014. RNA virus attenuation by codon pair deoptimisation is an artefact of increases in CpG/UpA dinucleotide frequencies. *eLife*. **3**,p.e04531.

Uchida, Y., Kouyama, J.-I., Naiki, K., Sugawara, K., Ando, S., Nakao, M., Motoya, D., Inao, M., Imai, Y., Nakayama, N. and Mochida, S. 2016. Significance of variants associated with resistance to NS5A inhibitors in Japanese patients with genotype 1b hepatitis C virus infection as evaluated using cycling-probe real-time PCR combined with direct sequencing. *Journal of gastroenterology*. **51**(3),pp.260–70.

Ventura, G.T., Costa, E.C.B. da, Capaccia, A.M. and Mohana-Borges, R. 2014. pH-dependent conformational changes in the HCV NS3 protein modulate its ATPase and helicase activities. X. Zhou, ed. *PloS one*. **9**(12),p.e115941.

Vercauteren, K., de Jong, Y.P. and Meuleman, P. 2014. HCV animal models and liver disease. *Journal of hepatology*. **61**(1 Suppl),pp.S26-33.

Vercauteren, K., Mesalam, A.A., Leroux-Roels, G. and Meuleman, P. 2014. Impact of lipids and lipoproteins on hepatitis C virus infection and virus neutralization. *World journal of gastroenterology*. **20**(43),pp.15975–91.

Vince, B., Hill, J.M., Lawitz, E.J., O'Riordan, W., Webster, L.R., Gruener, D.M., Mofsen, R.S., Murillo, A., Donovan, E., Chen, J., McCarville, J.F., Sullivan-Bólyai, J.Z., Mayers, D. and Zhou, X.-J. 2014. A randomized, double-blind, multiple-dose study of the pan-genotypic NS5A inhibitor samatasvir in patients infected with hepatitis C virus genotype 1, 2, 3 or 4. *Journal of hepatology*. **60**(5),pp.920–7.

Vitvitski, L., Trepo, C., Prince, A.M. and Brotman, B. 1979. Detection of virus-associated antigen in serum and liver of patients with non-A non-B hepatitis. *Lancet*. **2**(8155),pp.1263–1267.

Vogt, D.A., Camus, G., Herker, E., Webster, B.R., Tsou, C.-L., Greene, W.C., Yen, T.-S.B. and Ott, M. 2013. Lipid droplet-binding protein TIP47 regulates hepatitis C Virus RNA replication through interaction with the viral NS5A protein. A. Siddiqui, ed. *PLoS pathogens*. **9**(4),p.e1003302.

Wakita, T., Pietschmann, T., Kato, T., Date, T., Miyamoto, M., Zhao, Z., Murthy, K., Habermann, A., Kräusslich, H.-G., Mizokami, M., Bartenschlager, R. and Liang, T.J. 2005. Production of infectious hepatitis C virus in tissue culture from a cloned viral genome. *Nature medicine*. **11**(7),pp.791–6.

Walker, A., Siemann, H., Groten, S., Ross, R.S., Scherbaum, N. and Timm, J. 2015. Natural prevalence of resistance-associated variants in hepatitis C virus NS5A in genotype 3a-infected people who inject drugs in Germany. *Journal of clinical virology : the official publication of the Pan American Society for Clinical Virology*. **70**,pp.43–5.

Walker, C.M. 1997. Comparative features of hepatitis C virus infection in humans and chimpanzees. *Springer seminars in immunopathology*. **19**(1),pp.85–98.

Wang, A., Thurmond, S., Islas, L., Hui, K. and Hai, R. 2017. Zika virus genome biology and molecular pathogenesis. *Emerging Microbes & Infections*. **6**(3),p.e13.

Wang, C., Huang, H., Valera, L., Sun, J.-H., O'Boyle, D.R., Nower, P.T., Jia, L., Qiu, D., Huang, X., Altaf, A., Gao, M. and Fridell, R.A. 2012. Hepatitis C Virus RNA Elimination and Development of Resistance in Replicon Cells Treated with BMS-790052. *Antimicrobial Agents and Chemotherapy*. **56**(3),pp.1350–1358.

Wang, C., Valera, L., Jia, L., Kirk, M.J., Gao, M. and Fridell, R.A. 2013. In Vitro Activity of Daclatasvir on Hepatitis C Virus Genotype 3 NS5A. *Antimicrobial Agents and Chemotherapy*. **57**(1),pp.611–613.

Wang, L., Tian, Y. and Ou, J.J. 2015. HCV Induces the Expression of Rubicon and UVRAG to Temporally Regulate the Maturation of Autophagosomes and Viral Replication G. G. Luo, ed. *PLOS Pathogens*. **11**(3),p.e1004764.

Wang, W.-T., Tsai, T.-Y., Chao, C.-H., Lai, B.-Y. and Wu Lee, Y.-H. 2015. Y-Box Binding Protein 1 Stabilizes Hepatitis C Virus NS5A via Phosphorylation-Mediated Interaction with NS5A To

Regulate Viral Propagation. J.-H. J. Ou, ed. *Journal of virology*. **89**(22),pp.11584–602.

Waris, G., Felmlee, D.J., Negro, F. and Siddiqui, A. 2007. Hepatitis C virus induces proteolytic cleavage of sterol regulatory element binding proteins and stimulates their phosphorylation via oxidative stress. *Journal of virology*. **81**(15),pp.8122–30.

Welbourn, S. and Pause, A. 2007. The hepatitis C virus NS2/3 protease. *Current issues in molecular biology*. **9**(1),pp.63–9.

Welsch, C., Albrecht, M., Maydt, J., Herrmann, E., Welker, M.W., Sarrazin, C., Scheidig, A., Lengauer, T. and Zeuzem, S. 2007. Structural and functional comparison of the non-structural protein 4B in flaviviridae. *Journal of molecular graphics & modelling*. **26**(2),pp.546–57.

Wilson, J.A. and Huys, A. 2013. miR-122 promotion of the hepatitis C virus life cycle: sound in the silence. *Wiley interdisciplinary reviews. RNA*. **4**(6),pp.665–76.

Witteveldt, J., Martin-Gans, M. and Simmonds, P. 2016. Enhancement of the Replication of Hepatitis C Virus Replicons of Genotypes 1 to 4 by Manipulation of CpG and UpA Dinucleotide Frequencies and Use of Cell Lines Expressing SECL14L2 for Antiviral Resistance Testing. *Antimicrobial agents and chemotherapy*. **60**(5),pp.2981–92.

Wose Kinge, C.N., Espiritu, C., Prabdial-Sing, N., Sithebe, N.P., Saeed, M. and Rice, C.M. 2014. Hepatitis C Virus Genotype 5a Subgenomic Replicons for Evaluation of Direct-Acting Antiviral Agents. *Antimicrobial Agents and Chemotherapy*. **58**(9),pp.5386–5394.

Wozniak, A.L., Griffin, S., Rowlands, D., Harris, M., Yi, M., Lemon, S.M. and Weinman, S.A. 2010. Intracellular proton conductance of the hepatitis C virus p7 protein and its contribution to infectious virus production. C. M. Rice, ed. *PLoS pathogens*. **6**(9),p.e1001087.

Wyles, D.L., Ruane, P.J., Sulkowski, M.S., Dieterich, D., Luetkemeyer, A., Morgan, T.R., Sherman, K.E., Dretler, R., Fishbein, D., Gathe, J.C., Henn, S., Hinestrosa, F., Huynh, C., McDonald, C., Mills, A., Overton, E.T., Ramgopal, M., Rashbaum, B., Ray, G., Scarsella, A., Yozviak, J., McPhee, F., Liu, Z., Hughes, E., Yin, P.D., Noviello, S., Ackerman, P. and ALLY-2 Investigators 2015. Daclatasvir plus Sofosbuvir for HCV in Patients Coinfected with HIV-1. *The New England journal of medicine*. **373**(8),pp.714–25.

Xiao, B., Sanders, M.J., Carmena, D., Bright, N.J., Haire, L.F., Underwood, E., Patel, B.R., Heath, R.B., Walker, P.A., Hallen, S., Giordanetto, F., Martin, S.R., Carling, D. and Gamblin, S.J. 2013. Structural basis of AMPK regulation by small molecule activators. *Nature communications*. **4**,p.3017.

Yallop, C.A. and Svendsen, I. 2001. The effects of G418 on the growth and metabolism of recombinant mammalian cell lines. *Cytotechnology*. **35**(2),pp.101–14.

Yamashita, J., Yoshimasa, T., Arai, H., Hiraoka, J., Takaya, K., Miyamoto, Y., Ogawa, Y., Itoh, H. and Nakao, K. 1998. Identification of cis-elements of the human endothelin-A receptor gene and inhibition of the gene expression by the decoy strategy. *The Journal of biological chemistry*. **273**(26),pp.15993–9.

Yan, Y., He, Y., Boson, B., Wang, X., Cosset, F.-L. and Zhong, J. 2017. A Point Mutation in the N-Terminal Amphipathic Helix α0 in NS3 Promotes Hepatitis C Virus Assembly by Altering Core Localization to the Endoplasmic Reticulum and Facilitating Virus Budding. M. S. Diamond, ed. *Journal of virology*. **91**(6),pp.e02399-16.

Yang, Y.-M. and Choi, E.J. 2017. Efficacy and safety outcomes of sofosbuvir-based treatment regimens for hepatitis C virus-infected patients with or without cirrhosis from phase III clinical trials. *Therapeutics and Clinical Risk Management*. **Volume 13**,pp.477–497.

Yokozaki, S., Katano, Y., Hayashi, K., Ishigami, M., Itoh, A., Hirooka, Y., Nakano, I. and Goto, H. 2011. Mutations in two PKR-binding domains in chronic hepatitis C of genotype 3a and correlation with viral loads and interferon responsiveness. *Journal of medical virology*. **83**(10),pp.1727–32.

Yoshimi, S., Imamura, M., Murakami, E., Hiraga, N., Tsuge, M., Kawakami, Y., Aikata, H., Abe, H., Hayes, C.N., Sasaki, T., Ochi, H. and Chayama, K. 2015. Long term persistence of NS5A inhibitor-resistant hepatitis C virus in patients who failed daclatasvir and asunaprevir therapy. *Journal of medical virology*. **87**(11),pp.1913–20.

Younossi, Z.M., Stepanova, M., Nader, F., Lam, B. and Hunt, S. 2015. The patient's journey with chronic hepatitis C from interferon plus ribavirin to interferon- and ribavirin-free regimens: a study of health-related quality of life. *Alimentary pharmacology & therapeutics*. **42**(3),pp.286–95.

Younossi, Z.M., Stepanova, M., Zeuzem, S., Dusheiko, G., Esteban, R., Hezode, C., Reesink, H.W., Weiland, O., Nader, F. and Hunt, S.L. 2014. Patient-reported outcomes assessment in chronic hepatitis C treated with sofosbuvir and ribavirin: the VALENCE study. *Journal of hepatology*. **61**(2),pp.228–34.

Yu, M.-L. 2017. Hepatitis C treatment from 'response-guided' to 'resource-guided' therapy in the transition era from interferon-containing to interferon-free regimens. *Journal of Gastroenterology and Hepatology*. **32**(8),pp.1436–1442.

Yu, M., Corsa, A.C., Xu, S., Peng, B., Gong, R., Lee, Y.-J., Chan, K., Mo, H., Delaney, W. and Cheng, G. 2013. In vitro efficacy of approved and experimental antivirals against novel genotype 3 hepatitis C virus subgenomic replicons. *Antiviral research*. **100**(2),pp.439–45.

Yu, M., Peng, B., Chan, K., Gong, R., Yang, H., Delaney, W. and Cheng, G. 2014. Robust and Persistent Replication of the Genotype 6a Hepatitis C Virus Replicon in Cell Culture. *Antimicrobial Agents and Chemotherapy*. **58**(5),pp.2638–2646.

Zampino, R., Ingrosso, D., Durante-Mangoni, E., Capasso, R., Tripodi, M.-F., Restivo, L., Zappia, V., Ruggiero, G. and Adinolfi, L.E. 2008. Microsomal triglyceride transfer protein (MTP) -493G/T gene polymorphism contributes to fat liver accumulation in HCV genotype 3 infected patients. *Journal of viral hepatitis*. **15**(10),pp.740–6.

Zeng, Q.-L., Zhang, J.-Y., Zhang, Z., Wang, L.-F. and Wang, F.-S. 2013. Sofosbuvir and ABT-450: Terminator of hepatitis C virus? *World Journal of Gastroenterology*. **19**(21),p.3199.

Zeuzem, S., Dusheiko, G.M., Salupere, R., Mangia, A., Flisiak, R., Hyland, R.H., Illeperuma, A., Svarovskaia, E., Brainard, D.M., Symonds, W.T., Subramanian, G.M., McHutchison, J.G., Weiland, O., Reesink, H.W., Ferenci, P., Hézode, C., Esteban, R. and VALENCE Investigators 2014. Sofosbuvir and Ribavirin in HCV Genotypes 2 and 3. *New England Journal of Medicine*. **370**(21),pp.1993–2001.

Zhong, J., Gastaminza, P., Cheng, G., Kapadia, S., Kato, T., Burton, D.R., Wieland, S.F., Uprichard, S.L., Wakita, T. and Chisari, F. V. 2005. Robust hepatitis C virus infection in vitro. *Proceedings of the National Academy of Sciences*. **102**(26),pp.9294–9299.

Zhou, J.-J., Chen, R.-F., Deng, X.-G., Zhou, Y., Ye, X., Yu, M., Tang, J., He, X.-Y., Cheng, D., Zeng, B., Zhou, Q. and Li, Z. 2014. Hepatitis C virus core protein regulates NANOG expression via

the stat3 pathway. *FEBS letters*. **588**(4),pp.566–73.

Zhou, J.-J., Meng, Z., Zhou, Y., Cheng, D., Ye, H.-L., Zhou, Q.-B., Deng, X.-G. and Chen, R.-F. 2016. Hepatitis C virus core protein regulates OCT4 expression and promotes cell cycle progression in hepatocellular carcinoma. *Oncology Reports*.

Zona, L., Lupberger, J., Sidahmed-Adrar, N., Thumann, C., Harris, H.J., Barnes, A., Florentin, J., Tawar, R.G., Xiao, F., Turek, M., Durand, S.C., Duong, F.H.T., Heim, M.H., Cosset, F.-L., Hirsch, I., Samuel, D., Brino, L., Zeisel, M.B., Le Naour, F., McKeating, J.A. and Baumert, T.F. 2013. HRas signal transduction promotes hepatitis C virus cell entry by triggering assembly of the host tetraspanin receptor complex. *Cell host & microbe*. **13**(3),pp.302–13.